

GENE THERAPY FOR PULMONARY ARTERIAL
HYPERTENSION WITH BONE MORPHOGENETIC
PROTEIN RECEPTOR TYPE-2 MODULATION VIA
ENGINEERED ENDOTHELIAL PROGENITOR CELLS
OR A TARGETED ADENO-VIRAL CONSTRUCT:
CHANGES IN SMAD AND NON-SMAD SIGNALLING
CONTRIBUTED TO AMELIORATION OF DISEASE

BY

REBECCA L HARPER

A thesis submitted in fulfilment of
DOCTOR OF PHILOSOPHY

in the



THE UNIVERSITY
of ADELAIDE

Discipline of Medicine, School of Medicine,
Faculty of Health Sciences,
University of Adelaide

January 2016

To my love, Ninh.

And to all the rural kids who dare to look beyond the horizon.

ABSTRACT

Pulmonary arterial hypertension (PAH) is a rare but devastating disease and despite available therapeutics, survival remains at 3-5 years. Reduced expression of the bone morphogenetic protein receptor type 2 (BMPR2) is causally linked to hereditary, idiopathic and secondary forms of PAH. Thus, we proposed that up-regulation of BMPR2 may be therapeutic. As proof of concept, we've previously attenuated PAH in animal models through BMPR2 targeted gene delivery using Adenoviral (Ad) vectors. However, further understanding of the cell signalling mechanisms involved, as well as overcoming limitations with viral vector approaches is required to progress this approach to the clinic. Endothelial progenitor cells (EPCs) may be the key to avoiding the shortcomings of Ad-vector technology. EPCs are important for angiogenesis as well as tissue repair and have been shown to have altered function and abundance in patients with PAH. Manipulating these cells may be an alternate means to up-regulate BMPR2 in lungs affected by PAH, thereby avoiding some of the limitations of viral gene delivery techniques and enabling easier clinical translation.

Herein, I confirmed disease reversal in the rat monocrotaline (MCT)-induced PAH model following targeted gene delivery of BMPR2 to the pulmonary vascular endothelium and assessed the relevant BMPR2 mediated Smad pathways in whole lung tissue, 10 days following treatment. Microarray technology was utilised to identify any novel molecular targets, with results from this indicating that a peak Smad signalling effect was missed at this 10 day time-point. However, the microarray did indicate potential changes in BMPR2 mediated non-Smad signalling. PAH reversal was then assessed 2 days following targeted gene delivery of BMPR2 to the pul-

monary endothelium and further assessment of BMPR2 mediated Smad and non-Smad pathways were analysed in the subsequent whole lung tissue.

Moving towards a more clinically applicable therapy, cell therapy using *ex vivo* engineered EPCs to deliver BMPR2 to the pulmonary endothelium was investigated in the rat MCT-induced PAH model. To do this, the technique to isolate and culture rat bone marrow derived EPCs (r-EPCs) was developed. Successful transduction of these cells to over-express BMPR2 was optimised and these now engineered cells were used as a vehicle to deliver BMPR2 to the pulmonary vasculature via intravenous injection into rats with MCT-induced PAH. Amelioration of PAH was confirmed 10 days following the cell therapy treatment and subsequent protein analysis of BMPR2 mediated Smad pathways in the whole lung tissue saw changes activated Smad1/5/8.

The development of new therapies for PAH is critical. BMPR2 modulation is a novel therapeutic strategy which addresses the well known underlying pathology of BMPR2 deficiency that occurs not only in hereditary PH, but secondary PH and most PAH animal models. The success of our highly novel pre-clinical BMPR2 cell therapy may lead the way for further development of other BMPR2 therapies, as well as give significant insight into the pathophysiology of this devastating disease.

DECLARATION

I certify that this work contains no material which has been accepted for the award of any other degree or diploma in my name, in any university or other tertiary institution and, to the best of my knowledge and belief, contains no material previously published or written by another person, except where due reference has been made in the text. In addition, I certify that no part of this work will, in the future, be used in a submission in my name, for any other degree or diploma in any university or other tertiary institution without the prior approval of the University of Adelaide and where applicable, any partner institution responsible for the joint-award of this degree.

I give consent to this copy of my thesis when deposited in the University Library, being made available for loan and photocopying, subject to the provisions of the Copyright Act 1968. The author acknowledges that copyright of published works contained within this thesis resides with the copyright holder(s) of those works. I also give permission for the digital version of my thesis to be made available on the web, via the University's digital research repository, the Library Search and also through web search engines, unless permission has been granted by the University to restrict access for a period of time.

Rebecca L Harper,

July 25, 2016

ACKNOWLEDGEMENTS

To have the privilege of undertaking and completing a PhD in medicine was not a goal I imagined to be possible for myself. There have been many instrumental people who have contributed to the success of this work, of whom I am eternally grateful and would like to particularly mention.

Firstly, thank you to my supervisor Prof. Paul Reynolds, who is responsible for giving me the opportunity to pursue a dream I didn't ever think I was capable of. For empowering me to voice my ideas and giving me the freedom to explore all possibilities. For always having time, when in reality, you had no time to give at all. Thank you for instilling in me the importance of scientific rigour and for teaching me the value of small details and hard work. Your humble nature and quiet determination inspires me everyday and I will forever be grateful that I've had the privilege to have you as a mentor.

I would also like to acknowledge and thank my second supervisor A/Prof. Claudine Bonder. I'm very grateful for your positive nature and easy going approach. At times it lifted me to a higher level of motivation and confidence. You are a shining example of who I aspire to be, both professionally and personally.

To all my colleagues at the Lung Research Laboratory, past and present, in particular Dr Ann Reynolds who taught me all the technical skills to complete this work, and who has become a very dear friend of mine. Your support and advice throughout my PhD studies has been invaluable.

A special thanks to my family who have all been very supportive in many different ways. You have always supported me tremendously in every endeavour and I will forever be grateful for that.

I would like to thank Aesha and Kallan for the perspective they gave me when they entered my life, for teaching me what is important and for being the most wonderful kids anyone could hope to have.

To my darling Ninha, thank you for instilling patience in me, for inspiring me to be better everyday just by being who you are. Thank you for always lifting me up and never pulling me down. For being a selfless and strong pillar for me to depend on always. Thank you for motivating me during the tough times and for enabling me to be assertive and to have confidence in my capabilities. Thank you for being the greatest friend I could ever wish for and giving me a renewed sense of life.

PUBLICATIONS

JOURNAL ARTICLES

Accepted

1. R L Harper, A M Reynolds and P N Reynolds, *Changes in Smad Signalling Leads to Amelioration of PAH Following Gene Delivery of BMPR2* , accepted *Respirology*, September, 2015.
2. F Feng, R L Harper and P N Reynolds, *BMPR-2 gene delivery reduces mutation-related PAH and counteracts TGF β mediated pulmonary cell signalling*, accepted *Respirology*, September, 2015.

In preparation

1. R L Harper, C S Bonder and P N Reynolds, *Endothelial Progenitor Cells Over-expressing BMPR2 Ameliorates PAH in A Rat MCT Model*.
2. R L Harper, C S Bonder and P N Reynolds, *Biodistribution of Engineered Endothelial Progenitor Cells Following Intravenous Injection into Rats*.
3. R L Harper, C S Bonder and P N Reynolds, *Identification of Novel Therapy Targets following a Microarray Study of rat lungs from a disease reversal model of MCT-induced PAH*.

CONFERENCE PRESENTATIONS

1. R L Harper and P N Reynolds, *Smad and Non Smad Signalling in PAH Following BMPR2 Gene Delivery*, presented as a poster presentation at the 2015 ATS Annual Scientific Meeting, Denver, CO, May 2015
2. R L Harper and P N Reynolds, *Up-regulation of BMPR2 in Rat Derived Endothelial Progenitor Cells Leads to the Attenuation of PAH in a MCT Rat Model*, presented as a poster presentation at the 2015 ATS Annual Scientific Meeting, Denver, CO, May 2015.

Recipient of ATS Scholarship

3. R L Harper and P N Reynolds, *BMPR2 Replacement Therapy via In Situ Gene Delivery or Engineered Endothelial Cells Alleviates PAH in a Rat Model*, presented as a poster presentation at the 2015 American Society of Gene and Cell Therapy, Annual Scientific Meeting, New Orleans, LO, May 2015.
4. R L Harper and P N Reynolds, *BMPR2 Upregulation Via in situ Gene Delivery or Via Engineered Endothelial Progenitor Cells Alleviates Pulmonary Arterial Hypertension (PAH) in a Rat Model*, presented as an oral presentation at the 2015 TSANZ, Annual Scientific Meeting, Gold Coast, QLD, May 2015.

Winner of the Ann Woolcock Young Investigator of the Year

5. R L Harper and P N Reynolds, *Identification of Novel Cellular Signalling Pathways Following Gene Delivery of Bone Morphogenetic Protein Receptor Type-2: A Microarray Study*, presented as an oral presentation at the 2014 TSANZ Annual Scientific Meeting, Adelaide, April, 2014.
6. R L Harper and P N Reynolds, *Identification of Novel Cellular Signalling Pathways Following Gene Delivery of Bone Morphogenetic Protein Receptor*

- Type-2: A Microarray Study*, presented as an oral presentation at the 2014 TSANZ Annual Scientific Meeting, Adelaide, April, 2014.
7. R L Harper, C S Bonder and P N Reynolds, *Isolation and Characterisation of a Defined Populations of Endothelial Progenitor Cells from the Left Ventricle: A Pilot Study*, presented as a poster presentation at the 2014 TSANZ Annual Scientific Meeting, Adelaide, April, 2014.
 8. R L Harper, A M Reynolds and P N Reynolds, *BMPR2 Gene Delivery Shifts Intracellular Smad Activation Profile*, presented as a poster presentation at the 2012 European Respiratory Society Annual Congress, Vienna, September, 2012.
 9. R L Harper, A M Reynolds and P R Reynolds, *Changes in Smad Signalling Leads To Amelioration of PAH Following Gene Delivery of Bone Morphogenetic Protein Receptor Type 2*, *Am J Respir Crit Care Med*, vol. 185, pg. A6517, 2012. Presented as an oral presentation at the 2012 ATS Annual Conference, San Francisco, 2012.
 10. R L Harper, A M Reynolds and P R Reynolds, *Gene Delivery of Bone Morphogenetic Protein Receptor Type 2 Ameliorates PAH via Changes in Smad Signalling*, in proceedings of Respiriology, vol 17, pg. 19, 2012. Presented as an oral presentation at the TSANZ Annual Scientific Meeting, Canberra, 2012
 11. R L Harper, A M Reynolds and P R Reynolds, *Amelioration Of PAH Following Gene Delivery Of BMPR2 Via Changes in Smad Signalling*, in proceedings of Respiriology, vol 17, pg. 19, 2012. Poster presented at the South Australian Cardiovascular Research Forum, 2012.
 12. S Pradeepan, R Harper, A Thornton, S Johnston and H Greville, *β -Blocker Usage by Patients Referred For Lung Function Testing: An Observational Study*, in proceedings of Respiriology, vol. 16, pg. TP-155, 2011.

13. R Harper, S Johnston and A Thornton, *Six Minute Walk Test: Compliance with ATS Guidelines*, in proceedings *Respirology*, vol. 15:1, pg. A8, March, 2010. Poster presented at Australian and New Zealand Society of Respiratory Science (ANZSRS) Annual Scientific Meeting, Brisbane, March, 2010.
14. R Harper, P Roger, S Johnston and A Thornton, *15 Years of Inter-Laboratory Quality Control*, in proceedings, *Respirology*, vol. 14:1, pg. A5, April, 2009. Poster presented at Australian and New Zealand Society of Respiratory Science (ANZSRS) Annual Scientific Meeting, Darwin, April, 2009.

INVITED PRESENTATIONS

1. Japanese Respiratory Society, ASM, Tokyo. April, 2015.
2. Asia Pacific Respiratory Society, ASM, Kuala Lumpur. December, 2015.

AWARDS AND SCHOLARSHIPS

1. **Ann Woolcock Young Investigator of the Year 2015**, Thoracic Society of Australia and New Zealand.
A single prestigious annual award open to both Australia and New Zealand.
2. **Asia Pacific Young Investigator Award 2015**, Asia Pacific Respiratory Society.
A single award open to all nations in the Asia Pacific region to represent the region at the Japanese Respiratory Society, ASM, Tokyo.

3. **South Australia/ NT Branch, Young Investigator of the Year 2015**, Thoracic Society of Australia and New Zealand.
A single annual award open to candidates from South Australia and Northern Territory.
4. **Abstract Scholarship 2015**, Pulmonary Circulation Committee, American Thoracic Society.
A \$500 award given to outstanding ATS ASM submissions.
5. **Dawes Top-up Scholarship. 2013-2015**.
\$5,000 pa scholarship, selected by the Royal Adelaide Hospital Research Committee.
6. **Lions Medical Research Foundation Top-up Scholarship. 2012-2015**.
One of three \$10,000 pa scholarships for PhD projects, selected by the Lions Medical Foundation.
7. **Australian Postgraduate Award 2012-2015**.
Scholarships awarded to top honours students to undertake their PhD.
8. **Scicchitano Award 2012**.
Annual \$5,000 award given to outstanding research in the field of Thoracic Medicine.

CONTENTS

Dedication	iii
Abstract	iv
Declaration	vi
Acknowledgements	vii
Publications	viii
List of Figures	xxi
List of Tables	xxvi
Acronyms	xxvii
I INTRODUCTION	1
1 PULMONARY ARTERIAL HYPERTENSION	2
1.1 Classification	4
2 PULMONARY ARTERIES IN THE LUNG	8
2.1 Overview	8
2.1.1 Anatomy	8
2.1.2 Histology	11
2.1.3 Physiology	13
2.2 Right Heart	14
2.2.1 Right Ventricle Anatomy	15
2.2.2 Right Ventricle Histology	15
2.2.3 Right Ventricle Physiology	15
2.3 Endothelial Cells and Blood Vessels	17
2.4 Endothelial Cells and Vascular Disease	19
3 DISEASE PATHOGENESIS	21
3.1 Overview	21
3.2 Plexiform Lesions	24

3.2.1	Molecular Changes	25
3.3	Inflammation	25
3.4	Disrupted Cellular Function	26
3.4.1	Endothelial Cell Dysfunction	26
3.4.2	Smooth Muscle Cell Dysfunction	27
3.5	Gene Mutation in PAH	28
4	BONE MORPHOGENETIC PROTEIN RECEPTOR TYPE 2	30
4.1	Overview	30
4.2	Genomic Information and Receptor Structure	32
4.3	Bone Morphogenetic Proteins	33
4.4	Smad Signalling Pathway	34
4.5	Non-Smad Signalling Pathway	37
4.6	Mutations in the BMPR2 gene	38
5	EXPERIMENTAL MODELS OF PAH	42
5.1	Overview	42
5.2	Monocrotaline Model	44
5.3	Chronic Hypoxia Model	45
5.4	Sugen-5416/ Hypoxia Model	46
5.5	Transgenic Mouse Models	47
5.6	Summary	50
6	TREATMENT	51
6.1	Overview	51
6.2	Current Treatments	52
6.2.1	Calcium Channel Blockers	52
6.2.2	Endothelin-Receptor Antagonists	54
6.2.3	Prostacyclin Therapy	55
6.2.4	Phosphodiesterase-5 Inhibitors	56
6.2.5	Combination Therapy	56
6.3	Emerging Treatments	57
6.3.1	Riociguat	57

6.3.2	FK506(Tacrolimus)	57
6.3.3	Cell Therapy	58
7	GENE THERAPY	60
7.1	Overview	60
7.2	Viral Vectors	62
7.2.1	Adenovirus	62
7.2.2	Retrovirus	64
7.2.3	Adeno-associated Virus	64
7.3	Non-viral Vectors	67
7.4	Gene Therapy and PAH	67
7.4.1	BMPR2 Replacement Therapy	68
8	CONCLUSION	69
II	GENERAL METHODOLOGY	71
9	METHODS AND MATERIALS	72
9.1	Cell Culture	72
9.2	Adenoviral Vector Preparation	72
9.2.1	Virus Amplification	72
9.2.2	Cesium Chloride Purification of Virus	73
9.2.3	Particle and Infectious Titre	74
9.3	Rat derived EPC Isolation and Characterisation	75
9.3.1	Extraction, Isolation and Culture of Rat derived EPCs	75
9.3.2	Rat derived EPC characterisation	76
9.3.3	Flow Cytometry	76
9.3.4	Rat derived EPC AdCMVGFP Transduction Studies	77
9.3.5	Rat derived EPC Transduction with AdCMVBMPR2myc	77
9.3.6	Analysis of AdCMVBMPR2myc Transduction in r-EPCS	78
9.4	Physiological Studies	78
9.4.1	Construction of Fab-9B9: ACE Targeted Gene Delivery Conjugate	78

9.4.2	Validation of ACE Targeted Gene Delivery <i>in vitro</i> via Luciferase Assay	79
9.4.3	Validation of ACE Targeted Gene Delivery <i>in vivo</i> via Luciferase Assay	79
9.4.4	Animals	80
9.4.5	Bio-Distribution Studies of Rat derived EPCs in Sprague-Dawley Rats	80
9.4.6	Protein Analysis: 1 hour post BMPR2-EPC injection	81
9.4.7	Rat Monocrotaline Model	82
9.4.8	AdBMPR2 Studies: 2 and 10-day time-points	82
9.4.9	AdBMPR2-EPC Studies: 10-day Time-point	84
9.5	Animal Tissue Processing and Analysis	85
9.5.1	Tissue Extraction and Preparation	85
9.5.2	Smad and Non-Smad Pathway Analysis	86
9.5.3	RNA extraction	87
9.6	Microarray Studies	87
9.6.1	Ingenuity Pathway Analysis	88
9.7	Statistical analysis	88
III	RESULTS	89
10	BMPR2 MEDIATED SMAD SIGNALLING ANALYSIS	90
10.1	Overview	90
10.2	Amelioration of PAH: 10 days following AdBMPR2 treatment	96
10.3	Activation of Smad pathways was inconclusive 10-days following AdBMPR2 treatment	97
10.4	Reduction in right ventricular hypertrophy in MCT-induced PAH rats only 2 days post AdBMPR2 treatment	101
10.5	Activation of Smad1/5/8: 2 days following AdBMPR2 treatment	103
10.6	Effect on Smad3 activation: 2 days following AdBMPR2 treatment	104

10.7	Discussion and Conclusions	106
11	MICROARRAY STUDIES	110
11.1	Overview	110
11.2	Gene expression profiles differ between treatment groups	112
11.3	Preliminary Analysis	114
11.4	Ingenuity Pathway Analysis: main summary	116
11.5	Non-Smad pathways identified in the pathway analysis	118
11.6	Discussion and Conclusions	122
12	NON-SMAD SIGNALLING PROFILES ARE ALTERED FOLLOWING BMPR2 MODULATION	126
12.1	Overview	126
12.2	PI ₃ K is significantly increased 2 days following AdBMPR2 treatment	127
12.3	De-activation of p38 MAPK: 2 days following AdBMPR2 treat- ment	128
12.4	Discussion and Conclusions	130
13	GENE THERAPY USING ENDOTHELIAL PROGENITOR CELLS	134
13.1	Overview	134
13.2	Isolation and characterisation of rat derived EPCs	137
13.2.1	Morphological Assessment	137
13.2.2	Flow cytometric analysis	139
13.3	Efficient transduction of rat derived EPCs	139
13.3.1	AdCMVGFP	139
13.3.2	AdCMVLuc	140
13.4	Successful BMPR2 Up-regulation in Rat Derived EPCs	141
13.5	Discussion and Conclusion	143
14	AMELIORATION OF PAH FOLLOWING BMPR2 DELIVERY VIA AUG- MENTED <i>ex vivo</i> RAT DERIVED EPCS	147
14.1	Overview	147
14.2	Bio-distribution of Rat derived EPCs	150

14.2.1	<i>In vivo</i> Luciferase Peak Signalling Time-curve	150
14.2.2	R-EPCs home to the lung following IV injection	152
14.3	BMPR2 up-regulation 1 h following BMPR2-EPC treatment	153
14.4	Activation of the Smad1/5/8 pathway 1 h following BMPR2-EPC treatment	155
14.5	BMPR2 Augmented Rat derived EPCs ameliorates PAH in the rat MCT model	156
14.6	Comparison of AdBMPR2 treatment with BMPR2-EPCs treatment: FI 10-days following treatment	158
14.7	Discussion and Conclusions	160
15	SMAD SIGNALLING PROFILES ARE ALTERED FOLLOWING BMPR2 MODULATED EX VIVO EPC DELIVERY	164
15.1	Overview	164
15.2	BMPR2 expression is increased 10-days following EPC and BMPR2-EPC treatment	165
15.3	Activation of the Smad1/5/8 pathway 10-days following BMPR2-EPC treatment	166
15.4	Decrease in activated Smad3 10-days following BMPR2-EPC treatment	167
15.5	Discussion and Conclusions	169
IV	CONCLUSIONS AND FUTURE WORK	173
16	CONCLUSIONS	174
16.1	Conclusions	174
16.2	Future Work	183
	Appendices	188
A	ACE TARGETING	189
A.1	ACE Targeting <i>in vitro</i> Results	189
A.2	ACE Targeting <i>in vivo</i> Results	189
B	MICROARRAY	191

B.1	Bioanalyzer Results	191
B.2	Sample list of significant genes from MCT Only vs MCT + AdBMPR2Fab-9B9 comparison	194
C	HUMAN EPCS	196
C.1	Human derived Endothelial Progenitor Cells	196
C.1.1	Isolation, Culture and Characterisation of h-EPCs from the peripheral blood	196
C.1.2	Transduction of h-EPCs with AdCMVGFP	198
C.1.3	Transduction of h-EPCs with AdCMVBMPR2myc	200
	BIBLIOGRAPHY	201

LIST OF FIGURES

Figure 1	A Kaplan-Meier plot of survival for patients with PAH over 3 years	2
Figure 2	Anatomy and histology of the pulmonary arteries . .	10
Figure 3	Changes in cell composition as blood vessels progress in size	12
Figure 4	Pulmonary circulation and the systemic circuit	14
Figure 5	Anatomy of the heart	16
Figure 6	Cross section of a normal rat heart and a rat heart with right ventricular hypertrophy	17
Figure 7	Schematic demonstrating the role of endothelial cells in blood vessels	19
Figure 8	Disease pathogenesis of PAH	23
Figure 9	Converging factors of PAH pathogenesis	24
Figure 10	Role of inflammation in PAH	27
Figure 11	TGF- β Super-family of Receptors	31
Figure 12	BMPR2 chromosome and gene with germline mutations for PAH	32
Figure 13	BMPR2 receptor	33
Figure 14	BMPR2 mediated Smad1/5/8 signalling pathway . .	35
Figure 15	TGF- β mediated Smad2/3 signalling pathway	36
Figure 16	BMPR2 mediated non-Smad signalling pathway . . .	37
Figure 17	TGF- β mediated non-Smad signalling pathways . . .	38
Figure 18	Mechanism of Truncating and Missense mutations in the BMPR2 gene	40
Figure 19	A Kaplan-Meier plot of the disease Severity of Truncating vs Missense mutations over time	41

Figure 20	Targeted molecular pathways and actions of current approved PAH therapies	52
Figure 21	Updated PAH evidence based treatment algorithm . .	53
Figure 22	Mechanism of adenovirus, adeno-associated virus and retrovirus entering the cell and integrating their DNA	66
Figure 23	Cesium chloride centrifugation purification method .	74
Figure 24	Tissue culture infectious dose TCID ₅₀ Assay	75
Figure 25	Placement of left and right heart catheters for hemodynamic assessment	84
Figure 26	Example of hemodynamic pressure traces taken from a healthy rat	92
Figure 27	Up-regulation of BMPR2 mediated Smad _{1/5/8} and down-regulation of pSmad ₃ following BMPR2 transduction of HMVEC-LBI	95
Figure 28	Hemodynamic assessment of MCT-induced PAH following AdBMPR2Fab-9B9 treatment	98
Figure 29	Consistency of animal health at the time of hemodynamic analysis	99
Figure 30	Immunoblot proetin analysis of BMPR2 mediated Smad _{1/5/8} signalling pathway in whole rat lung 10-days following AdBMPR2 treatment	100
Figure 31	Immunoblot protein analysis of TGF- β mediated Smad _{2/3} dependent signalling pathway in whole rat lung 10-days following AdBMPR2 treatment	101
Figure 32	Reduction in right ventricular hypertrophy in MCT-induced PAH rats only 2 days post AdBMPR2Fab-9B9 treatment	102
Figure 33	Body weight of animals at the time of Fulton Index measurement	103

Figure 34	Immunoblot protein analysis of BMPR2 mediated Smad dependent signalling pathways in whole rat lung 10-days following AdBMPR2 treatment	104
Figure 35	Immunoblot protein analysis of TGF- β mediated Smad2/3 dependent signalling pathway in whole rat lung 10-days following AdBMPR2 treatment	105
Figure 36	Principle Component Analysis Graph of gene expression differences between each treatment group from the MCT-induced PAH: 10 days following AdBMPR2 treatment	114
Figure 37	Venn diagram of microarray results	115
Figure 38	ERK1/2 Network Map: a cell signalling network identified by the IPA analysis of the gene expression profile of rat lungs 10 days following AdBMPR2 treatment in MCT-induced PAH rats	119
Figure 39	MAPK Network map: a cell signalling network identified by the IPA analysis of the gene expression profile of rat lungs 10 days following AdBMPR2 treatment in MCT-induced PAH rats	120
Figure 40	eIF2 Network map: a cell signalling network identified by the IPA analysis of the gene expression profile of rat lungs 10 days following AdBMPR2 treatment in MCT-induced PAH rats	121
Figure 41	Immunoblot protein analysis of BMPR2 mediated non-Smad dependent PI3K signalling pathway	129
Figure 42	Immunoblot protein analysis of BMPR2 mediated non-Smad dependent p38 MAPK signalling pathway . . .	130
Figure 43	Phase contrast images of rat derived EPCs	138
Figure 44	Flow cytometric analysis of rat derived EPCs	140

Figure 45	Assessment of transduction efficiency of AdCMVGFP in r-EPCs	141
Figure 46	Luciferase activity following r-EPC transduction with AdCMVLuc	141
Figure 47	Immunoblot proetin analysis of BMPR2 expression in r-EPCs following AdBMPR2 transduciton	142
Figure 48	Immunoblot proetin analysis of myc expression in r-EPCs following AdBMPR2 transduciton	143
Figure 49	Luminescence time-curve in live rats post IV injection of AdTrackLuc transduced EPCs	151
Figure 50	Luminescence scanning of rats post IV injection of AdTrackLuc transduced r-EPCs	152
Figure 51	Quantification of luminescence scanning of rats post IV injection of AdTrackLuc transduced r-EPCs	153
Figure 52	Immunoblot protein analysis of BMPR2 in whole rat lungs 1 h following BMPR2-EPC treatment	154
Figure 53	Immunoblot protein analysis of the BMPR2 mediated Smad _{1/5/8} signalling pathway in whole rat lung 1 h following BMPR2-EPC treatment	155
Figure 54	Hemodynamic assessment of MCT-induced PAH following BMPR2-EPCs treatment	158
Figure 55	Consistency of animal health at the time of hemodynamic assessment	159
Figure 56	Fulton index measurement 10 days post BMPR2-EPC, EPC Only and AdBMPR2-Fab-9B9 treatments in SD rats with MCT induced PAH	160
Figure 57	Immunoblot protein analysis of BMPR2 expression in whole rat lung 10-days following BMPR2-EPCs treatment	166

Figure 58	Immunoblot protein analysis of BMPR2 mediated Smad1/5/8 signalling pathways in whole rat lung 10-days following BMPR2-EPC treatment	167
Figure 59	Immunoblot protein analysis of TGF- β mediated Smad3 signalling in whole rat lung 10-days following BMPR2-EPC treatment	168
Figure 60	Luciferase assay of CHO and CHO-2C2 cells to assess the targeting ability of Fab-9B9 fractions <i>in vitro</i> . . .	189
Figure 61	Luciferase assay of CHO and CHO-2C2 cells to assess the targeting ability of Fab-9B9 fractions <i>in vitro</i> . . .	190
Figure 62	Chosen samples for microarray. (A) MCT+AdTrackLucFab-9B9; (B) MCT+AdCMVBMPR2Fab-9B9	193
Figure 63	Example list of significant genes resulting from the microarray analysis	195
Figure 64	Isolation, culture and characterisation technique of h-EPC.	197
Figure 65	Phase contrast image and fluorescent image of h-EPCs	198
Figure 66	Flow cytometric analysis of h-EPCs derived from the left ventricle	199
Figure 67	Immunoblot image of BMPR2 up-regulation in h-EPCs following AdCMVBMPR2myc transduction	200

LIST OF TABLES

Table 1	Updated classification of pulmonary hypertension . . .	6
Table 2	Modified New York Heart Association functional classification scale	7
Table 3	Relevant animal models of Group 1 pulmonary hypertension	43
Table 4	Transgenic mouse models of PAH	49
Table 5	Raw hemodynamic data obtained 10 days following AdBMPR2 treatment	97
Table 6	False discovery rate report of microarray results from the MCT-induced PAH: 10 days following AdBMPR2 treatment	113
Table 7	IPA main summary of analysis	117
Table 8	Raw hemodynamic data obtained 10 days following AdBMPR2 treatment	157

ACRONYMS

Alpha-SM Actin	Alpha-Smooth Muscle Actin
5-HT	Hydroxytryptamine or Serotonin
5-HTT	Hydroxytryptamine (Serotonin) Transporter
6MWD	6 Minute Walk Distance
AAV	Adeno-associated Virus
ACE	Angiotensin Converting Enzyme
Ad	Adenovirus
ADA-SCID	Adenosine Deaminase Deficiency
ALK-5	Activin Receptor-Like Kinase-5
ALK	Activin-Like Receptor Kinase-1
ANG-1	Angiopoietin-1
APC	Antigen Presenting Cell
BMPR₂	Bone Morphogenetic Protein Receptor Type 2
BSA	Bovine Serum Albumin
cAMP	cyclic AMP
CAR	Coxsackie and Adenovirus Receptor
CCB	Calcium Channel Blockers
cGMP	cyclic Guanosine Monophosphate

CPE	Cytopathic Effect
CsCl	Cesium Chloride
CXCL ₁₀	CXC-chemokine Ligand 10
DMEM	Dulbecco's Modeified Eagle Medium
EC	Endothelial Cell
ECM	Extracellular Matrix
EGF	Epidermal Growth Factor
EHS	Engelbreth-Holm-Swarm
eIF ₂	Eukaryotic Initiation Factor 2
EM	Electron Microscopy
EMA	European Medicine Agency
EMT	Epithelial to Mesenchymal Transition
EndoMT	Endothelial to Mesenchymal Transition
ENG	Endoglin
EPC	Endothelial Progenitor Cell
ERA	Endothelin-Receptor Antagonists
ESC	Embryonic Stem Cells
ET ₁	Endothelin-1
ETA	Endothelin-1 A
ETB	Endothelin-1 B
FCS	Foetal Calf Serum

FDA	Food and Drug Administration
FDR	False Discovery Rate
FH Rats	Fawn-Hooded Rats
FI	Fulton Index
FKBP	FK506 Binding Protein
FLAP	5-lipoxygenase Activating Protein
GFP	Green Florescent Protein
HIF-1alpha	Hypoxia Inducible Factor -1alpha
HIF-1beta	Hypoxia Inducible Factor -1beta
HMVEC-L	Lung Derived Human Microvascular Endothelial Cell
HPAH	Hereditary Pulmonary Arterial Hypertension
HRQOL	Health Related Quality of Life
IPA	Ingenuity Pathway Analysis
IPAH	Idiopathic Pulmonary Arterial Hypertension
Luc	Luciferase
LV	Left Ventricle
MAPK	Mitogen Activated Protein Kinase
MBP	Myeloid Binding Protein
mcDNA	Minicircle DNA
MCP-1	Monocyte Chemoattractant Protein-1
MHD	Mad-homology Domain

mPAP	Mean Pulmonary Arterial Pressure
NHMRC	National Health and Medical Research Council
NMD	Nonsense Mediated Decay
NO	Nitric Oxide
NT-proBNP	N-terminal Prohormone of Brain Natriuretic Peptide
NYHA	New York Heart Association
p-Smad	Phosphorylated-Smad
PA	Pulmonary Artery
PAEC	Pulmonary Arterial Endothelial Cell
PAH	Pulmonary Arterial Hypertension
PASMC	Pulmonary Arterial Smooth Muscle Cell
PAWP	Pulmonary Arterial Wedge Pressure
PBS	Phosphate Buffered Solution
PCA	Principle Component Analysis
PDE-5	Phosphodiesterase-5
PDGF	Platelet-Derived Growth Factor
pDNA	Naked Plasmid DNA
PFU	Plaque Forming Units
PGI₂S	Prostacyclin Synthase
PH	Pulmonary Hypertension
PI₃K	Phosphoinositide 3-Kinase

PVR	Pulmonary Vascular Resistance
rEPCs	Rat Derived Endothelial Progenitor Cell
RHC	Right Heart Catheterisation
Rho	Ras Homologous
RIN	RNA Integrity Score
ROCK	Rho Kinase
RT	Room Temperature
RVOT	Right Ventricle Outflow Tract
S	Septum
SDF-1	Stromal Derived Factor-1
sGC	Soluable Guanylate Cyclase
SMAD	Some Mothers Against Decapentaplegic
SMC	Smooth Muscle Cell
SVC	Superior Vena Cava
TCID₅₀	Tissue Culture Infectious Dose 50
TGF	Transforming Growth Factor- β
TNS	Trypsin Neutralising Solution
Treg Cells	High Regulatory T Cells
V/Q	Ventilation and Perfusion
VEGF	Vascular Endothelial Growth Factor
WSPH	World Symposium on Pulmonary Hypertension

Part I

INTRODUCTION

PULMONARY ARTERIAL HYPERTENSION

Pulmonary arterial hypertension (PAH) is a rare, fatal disease caused by pulmonary vascular remodelling. It is defined as the sustained elevation of the mean pulmonary arterial pressure (mPAP), coupled with a normal mean capillary-wedge pressure (PAWP) and left end-diastolic pressure. The disease is characterised by the narrowing of the small pulmonary arteries due to the formation of plexiform lesions and intimal thickening as a result of abnormal endothelial and smooth muscle cell function. These pathological changes lead to the physiological changes of increased pulmonary vascular resistance, ventilation-perfusion mismatching and ultimately respiratory and right heart failure. Unfortunately, despite available therapeutics, survival remains at 54.9% at 3-5 years [Figure 1](#) [1].

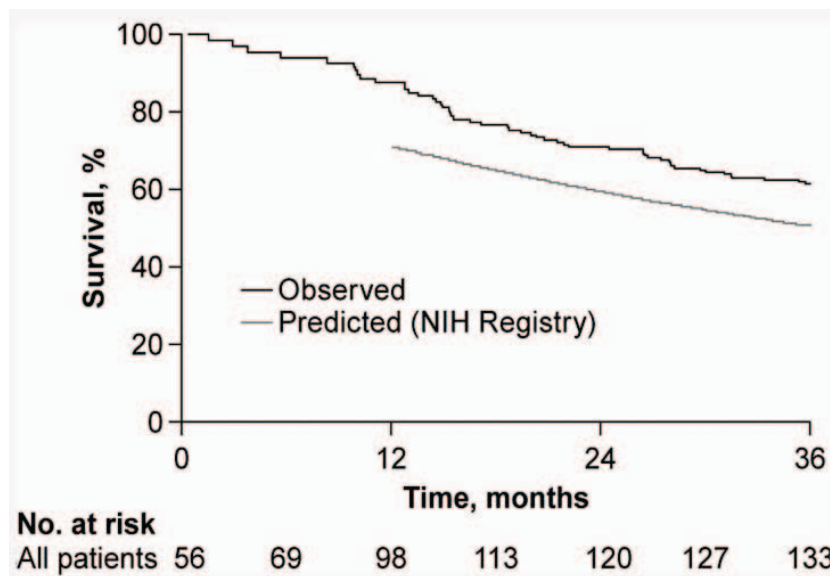


Figure 1: A Kaplan-Meier plot of survival for patients with PAH over 3 years. Showing both the 2010 observed percentage of survival (black line) and the predicted survival derived from the 1980 NIH-supported US registry (gray line) [1].

Incidence is variable across countries, however conservative estimates from the US registry (REVEAL), as well as French, Belgium, Chinese and Israeli registries place the incidence between 1.1 and 5.9 cases per million population [2]. Although PAH is rare, it is a costly disease. The latest reported health care costs for PAH in the US is \$116,681 (USD) per patient in the initial 12 months following diagnosis, and \$98,243 (USD) per patient in a 12 month follow-up period [3]. These high costs are due to the specialised resources required for diagnosis as well as ongoing medications, ambulance, inpatient occurrences and other ongoing medical costs such as oxygen therapy. However, economic costs are not the only deleterious effect of this disease. Quality of life for individuals with PAH is quite diminished. Patients experience severe shortness of breath, syncope and have very limited exercise capacity. Patients ultimately become limited in their ability to perform every-day tasks and in most cases, mobility is markedly restricted. Therefore, it is widely accepted that effective treatment is vital for this patient cohort.

PAH is characterised by increased pulmonary resistance due to the formation of plexiform lesions and intimal thickening in the distal pulmonary arteries, ultimately leading to respiratory and right heart failure. Current therapies exert vasodilatory effects and control cellular proliferation in pulmonary vessels; however this does not reverse the abnormal vascular remodelling that has already occurred. Changes in blood vessels are due to endothelial cellular hyperplasia as well as smooth muscle hypertrophy and intimal thickening. The precise mechanism of how this abnormal cellular behaviour occurs is largely unknown, however, importantly in the year 2000, mutations in the bone morphogenetic protein receptor type 2 (BMPR2) were found to be causally linked to PAH [4]. These mutations ultimately result in reduced function and expression of the receptor, and following this seminal discovery, it has been subsequently shown that BMPR2 function and

expression is reduced not only in patients who harbour a mutation, but in various primary and secondary forms of pulmonary hypertension (PH), as well as in commonly used animals models [1, 5]. Additionally, of those who harbour a mutation, disease penetrance is only 20%, suggesting the occurrence of a 'second hit' that triggers the PAH phenotype. This leads to the notion that perhaps a 'reversal trigger' is required to restore normal cell signalling processes for the reversal of the disease.

Despite an increasing awareness of PAH, diagnosis is still difficult due to the non-specific symptoms of breathlessness, syncope, lethargy, oedema, racing heart beat and chest pain. Additionally, symptoms may not manifest until significant progression of the disease has occurred, with many patients presenting with moderate to severe disease. This has a significant impact on patient prognosis, as there is a correlation between survival and early diagnosis [1, 6, 7].

1.1 CLASSIFICATION

Historically, PAH was designated as 'primary pulmonary hypertension,' however in 1998 at the second world symposium on PH, a more specific clinical classification was adopted to group different categories of PH according to their similar pathological findings, hemodynamic characteristics and management [8]. From this, five groups of PH were identified and PAH is Group 1 Table 1 [9]. This classification has since further been updated. The disease is defined as a sustained elevations of mPAP of ≥ 25 mmHg, coupled with a normal PAWP of ≤ 15 mmHg. Patient populations predominately lie in the idiopathic (IPAH) (87.5%), heritable (HPAH) (5.4%) and drug and toxin induced (7.1%) sub-groups [1] and due to an increase in research of this disease, there have been substantial changes to what was thought to be the common PAH phenotype in terms of age, sex, co-morbidities and

survival. Once thought to be a disease of young females, current registries show that mean age of diagnosis is between 50 ± 14 years and 65 ± 15 years and female predominance is now variable between registries and may not be present in elderly patients [10]. As the molecular and pathological understanding of PAH continues to grow, the sub-groups within Group 1 also continue to evolve to reflect this. At the latest world symposium on PH held in Nice, France in 2013, more sub-groups were added as well as recent genetic discoveries Table 1. Additionally, as a greater understanding of the genetic basis of PAH is occurring, the proportion of IPAH is decreasing, with the HPAH incidence increasing.

A functional classification system has been developed by the New York Heart Association (NYHA) Table 2. Following diagnosis, patients undergo functionality assessment and are placed in a NYHA Class. Patients in a higher NYHA class have reduced predicted survival. Independent predictors of survival are greater six minute walk test distance (6MWD), female gender and higher cardiac output [1]. Recently, patient-reported outcomes were assessed in the form of a questionnaire to assess health related quality of life (HRQOL) and there is a strong correlation between reported HRQOL and transplant-free survival [11].

UPDATED CLASSIFICATION OF PULMONARY HYPERTENSION

<p>1. Pulmonary arterial hypertension (PAH)</p> <p>1.1 Idiopathic PAH</p> <p>1.2 Heritable PAH</p> <p> 1.2.1 BMPR2</p> <p> 1.2.2 <i>ALK-1, ENG, SMAD9, CAV1, KCNK3</i></p> <p> 1.2.3 Unknown</p> <p>1.3 Drug and toxin induced</p> <p>1.4 Associated with:</p> <p> 1.4.1 Connective tissue disease</p> <p> 1.4.2 HIV infection</p> <p> 1.4.3 Portal hypertension</p> <p> 1.4.4 Congenital heart diseases</p> <p> 1.4.5 Schistosomiasis</p> <p><i>1' Pulmonary veno-occlusive disease and/ or pulmonary capillary hemangiomatosis</i></p> <p>1'' Persistent pulmonary hypertension of the newborn (PPHN)</p>
<p>2. Pulmonary hypertension due to left heart disease</p> <p> 2.1 Left ventricular systolic dysfunction</p> <p> 2.2 Left ventricular diastolic dysfunction</p> <p> 2.3 Valvular disease</p> <p> 2.4 <i>Congenital/ acquired left heart inflow/ outflow tract obstruction and congenital cardiomyopathies</i></p>
<p>3. Pulmonary hypertension due to lung diseases and/ or hypoxia</p> <p> 3.1 Chronic obstructive pulmonary disease</p> <p> 3.2 Interstitial lung disease</p> <p> 3.3 other pulmonary diseases with mixed restrictive and obstructive pattern</p> <p> 3.4 Sleep-disordered breathing</p> <p> 3.5 Alveolar hypoventilation disorders</p> <p> 3.6 Chronic exposure to high altitude</p> <p> 3.7 Developmental lung diseases</p>
<p>4. Chronic thromboembolic pulmonary hypertension (CTEPH)</p>
<p>5. Pulmonary hypertension with unclear multi-factorial mechanisms</p> <p> 5.1 Hematologic disorders <i>chronic hemolytic anaemia</i>, myeloproliferative disorders, splenectomy</p> <p> 5.2 Systemic disorders, sarcoidosis, pulmonary histiocytosis, lymphangioleiomyomatosis</p> <p> 5.3 Metabolic disorders: glycogen storage disease, Gaucher disease, thyroid disorders</p> <p> 5.4 Others: tumoral obstruction, fibrosing mediastinitis, chronic renal failure, <i>segmental PH</i></p>

Table 1: Updated Classification of Pulmonary Hypertension from the 8th world symposium on PH, Nice, France, 2013 [9]. PAH Group 1 shown in bold. Modifications from previous WSPH in italics.

FUNCTIONAL CLASSIFICATION OF PAH	
Class	Description
Class I	PAH without a resulting limitation of physical activity. Ordinary physical activity does not cause undue dyspnoea or fatigue, chest pain, or near-syncope.
Class II	PAH resulting in a slight limitation of physical activity. The patient is comfortable at rest, but ordinary physical activity cause undue dyspnoea or fatigue, chest pain or near-syncope.
Class III	PAH resulting in a marked limitation of physical activity. The patient is comfortable at rest, but less than ordinary activity causes undue dyspnoea or fatigue, chest pain, or near-syncope.
Class IV	PAH resulting in an inability to carry out any physical activity without symptoms. The patient has signs of right heart failure. Dyspnoea, fatigue, or both may be present even at rest, and discomfort is increase by any physical activity.

Table 2: Functional classification scale modified from the New York Heart Association classification on cardiac disease. This is adapted from the World Symposium on PPH in Evian, France, 1998 [12].

PULMONARY ARTERIES IN THE LUNG

2.1 OVERVIEW

The vasculature is a highly adaptable and multifunctional system comprised of arteries, veins and capillaries. These rely on endothelial cells (ECs), which form the inner luminal surface of all blood vessels. The largest blood vessels (arteries and veins) have thick, tough walls comprising of loose connective tissue, smooth muscle cells (SMCs) and elastin fibres with a thin endothelial sheet lining the lumen. The presence of SMCs and connective tissue varies with the size of the blood vessel, however the endothelial lining always remains.

2.1.1 *Anatomy*

The main pulmonary artery (PA) or pulmonary trunk originates from the right ventricle where it conveys venous blood to the lungs [Figure 2](#). The vessel is approximately 5 cm long, 3 cm in diameter and divides into two branches, the right and left PAs of around equal size. The right PA branch runs horizontally to the right, posterior to the ascending aorta and superior vena cava (SVC), and anterior to the right bronchus, travelling to the root of the right lung where it divides into two branches. The lower and largest of these branches feeds the middle and lower lobes and the smaller upper branch feeds the upper lobe. The left branch of the PA passes horizontally anterior of the descending aorta and left bronchus to the root of the left lung where it divides into two branches, one for each lobe of the left lung [Figure 2](#). The branching patterns of the right and left PAs differ, however they mainly divide into truncal, lobar, segmental and sub-segmental

arteries and generally follow the branches of the bronchial tree. The arterial tree conventionally courses from the lung hilus to the peripheral pleural boarder. They comprise of 17 branch orders from the main pulmonary arteries with a diameter of 30 mm to more than 72 million order one arteries, which range in diameter from 10-15 μm [Figure 2](#) [13, 14]. In the periphery, the arteries form a bronchovascular bundle, involving PAs, alveolar and capillary tissue [Figure 2](#).

In the bronchovascular bundle, the adventitial surface of the vessel is tethered to the surface of the adjacent airway on one side and tethered to the alveolar septal networks on the other side [Figure 2](#) [13]. This close interaction is essential for efficient oxygen diffusion from the alveoli into the blood stream, which flows back to the left side of the heart and is then pumped around the body.

2.1.2 *Histology*

The adventitia (outer layer) of the PA is loosely comprised of an extracellular matrix including fibroblasts or other interstitial cells, a vasa vasorum (small network of blood vessels) and a neuronal network. Both elastin and collagen fibres comprise the outer lamina of the arterial wall and are continuous with the elastin and collagen fibres of the alveolar septal walls [16]. This continuum contributes to the overall stability of the lung in the distal areas. The composition of the arterial wall varies from the proximal artery trunk to the smallest distal extra-alveolar arteries. The largest PAs are mainly elastic, with short, thin elastin fibres interspersed with collagen and SMCs that form multiple layers of elastic lamina. These larger elastin arteries give rise to smaller muscularised vessels, with decreasing diameter resulting in a decrease of elastin layering, with a single internal and external elastic lamina. This layer fragments and eventually disappears in the muscular and non-muscular distal PAs. The composition of the arterial wall changes from muscular, to partially muscular and finally to non-muscular. This transition is due to the presence of SMCs, which decreases as the size of the vessel decreases, and thus the vessel becomes only partially muscular as the SMCs are replaced with intermediate cells. Finally, as the vessel becomes small enough to be non-muscular, it is largely made up of pericytes instead of SMCs. Partially muscular arteries can range in diameter from 35-228 μm and non-muscularised arteries can be as large as 120 μm [Figure 3](#) [13].

Throughout the arterial tree the intima (inner layer) is thin and consists of ECs lining the vessel lumen and sub-endothelial interstitium that extends to the internal elastic lamina. Intimal thickness ranges from 1% to 16% of the total wall thickness or approximately 15% of the wall area. The shape of the ECs change throughout the arterial tree. Proximal ECs are flat, spindle-

shaped with their long axis parallel to the flow path and are connected by well organised tight junctions which form a strong endothelial barrier. The integrity of this layer is critical to limit the transfer of fluid, proteins and other blood constituents into the interstitium. Tight junctions between ECs and SMCs are common in PAs. These heterocellular junctions are important for bi-directional signalling between these cells. Distal ECs are more rounded and relatively uniform in thickness.

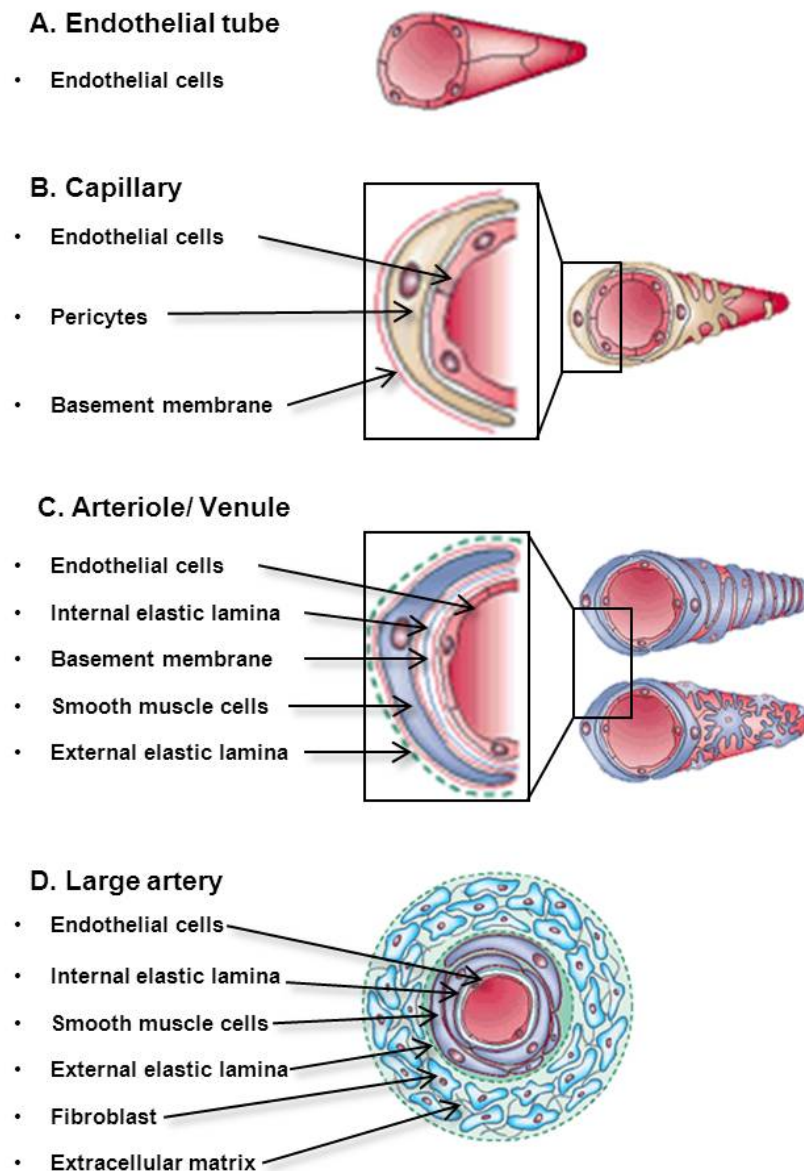


Figure 3: Changes in cell composition as blood vessels progress in size. From small (A) to large (D) blood vessels. A. Endothelial tube; B. Capillary; C. Arteriole or Venule; and D. Large artery. Schematic adapted from Jain *et al* [17].

2.1.3 *Physiology*

Normal pulmonary circulation is characterised by high flow, low pressure and low resistance. The PAs conduct venous blood from the right ventricle of the heart to the arterioles and capillary beds where oxygen is diffused across the alveolar wall into the circulating blood [Figure 4](#). The blood flows from the lungs back to the left ventricle of the heart via the pulmonary veins where it is then systemically pumped throughout the body via the aorta. Measurement of the mPAP, pulmonary vascular resistance (PVR) and cardiac output (CO) are important physiological indicators for abnormalities in pulmonary circulation. Normal mPAP at rest is 14.0 ± 3.3 mmHg, which is a value independent of sex and ethnicity, and should not be elevated above 20 mmHg [18]. PVR is calculated as the ratio of $(\text{mPAP}-\text{PAWP})/\text{CO}$ and in normal adults is 67 ± 23 dyne-sec-cm⁻⁵. CO is a measure of the volume of blood pumped by the heart per minute. This measurement indicates the function of the heart as well as the presence of other external forces, such as increased PVR, that may be restricting the stroke volume or heart rate.

Ventilation and perfusion (V/Q) across the lung is an important process and further to this, the ratio of ventilation to perfusion (V/Q ratio) is a reliable way of measuring the efficiency and adequacy of how well the air that reaches the alveoli is matched with the blood that reaches the capillary bed. When there is a V/Q mismatch, there is either an issue in the airways or in the PAs. A ventilation perfusion mismatch results in symptoms such as dyspnoea, syncope and exercise intolerance, all of which are hallmark symptoms of patients with PAH.

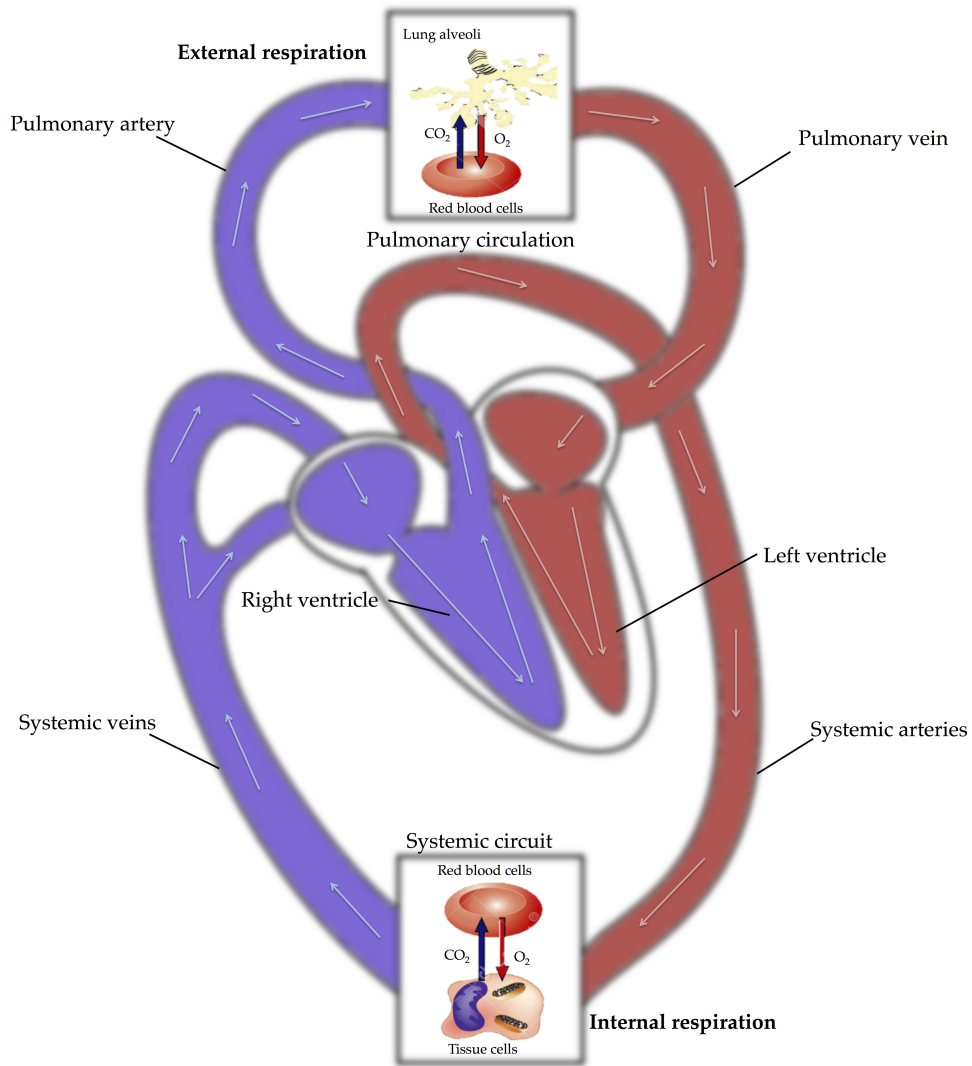


Figure 4: Circulation of blood from the right ventricle via pulmonary arteries, to the lung where oxygen from external respiration is diffused across the lung alveoli and taken up by the red blood cells in the blood. This oxygenated blood is then returned to the left ventricle via pulmonary veins and then pumped via the aorta to the systemic circuit and used in internal respiration. This process involves the release of oxygen from the red blood cells to the surrounding tissue cells.

2.2 RIGHT HEART

Pulmonary arterial hypertension is referred to as a 'right-sided' heart disease, and thus knowledge of the structure and function of the right ventricle (RV) is important in understanding the pathogenesis of PAH.

2.2.1 *Right Ventricle Anatomy*

The RV is a thin walled, asymmetrical structure which pushes venous blood at low pressure. Blood flows in through the tricuspid valve and exits through the right ventricular outflow tract (RVOT), a funnel of muscle that leads to the pulmonary valve. The RV is one of four chambers of the heart, it is adjacent to the more muscularised left ventricle, and has the right atrium attached at it's apex [Figure 5](#). The role of the RV is to pump oxygen depleted blood to the lungs.

2.2.2 *Right Ventricle Histology*

The heart consists of many cell types that all contribute to its structural, biochemical, electrical and mechanical properties. Sitting within the pericardial sac, the outer layer, the epicardium consists of cardiomyocytes and fibroblast precursors [19]. Cardiomyocytes form the muscular walls, called the myocardium, which is the bulk of the heart tissue. More than 50% of the cells in the heart are cardiac fibroblasts which also contribute to the myocardium. Within the myocardium, there are specialised cells such as pacemaker and Purkinje fibres which control the conduction system of the heart. The interior of the heart, the endocardium, consists of endothelial cells. These also form the interior lining of valves and blood vessels [Figure 5](#) [19].

2.2.3 *Right Ventricle Physiology*

The RV is designed to generate flow of deoxygenated blood (venous blood) to the lungs for gas exchange. At rest and under mild exercise, vascular pressure is very low (10-15 mmHg) and this is sufficient to drive the venous return through the pulmonary vasculature to the left ventricle without the

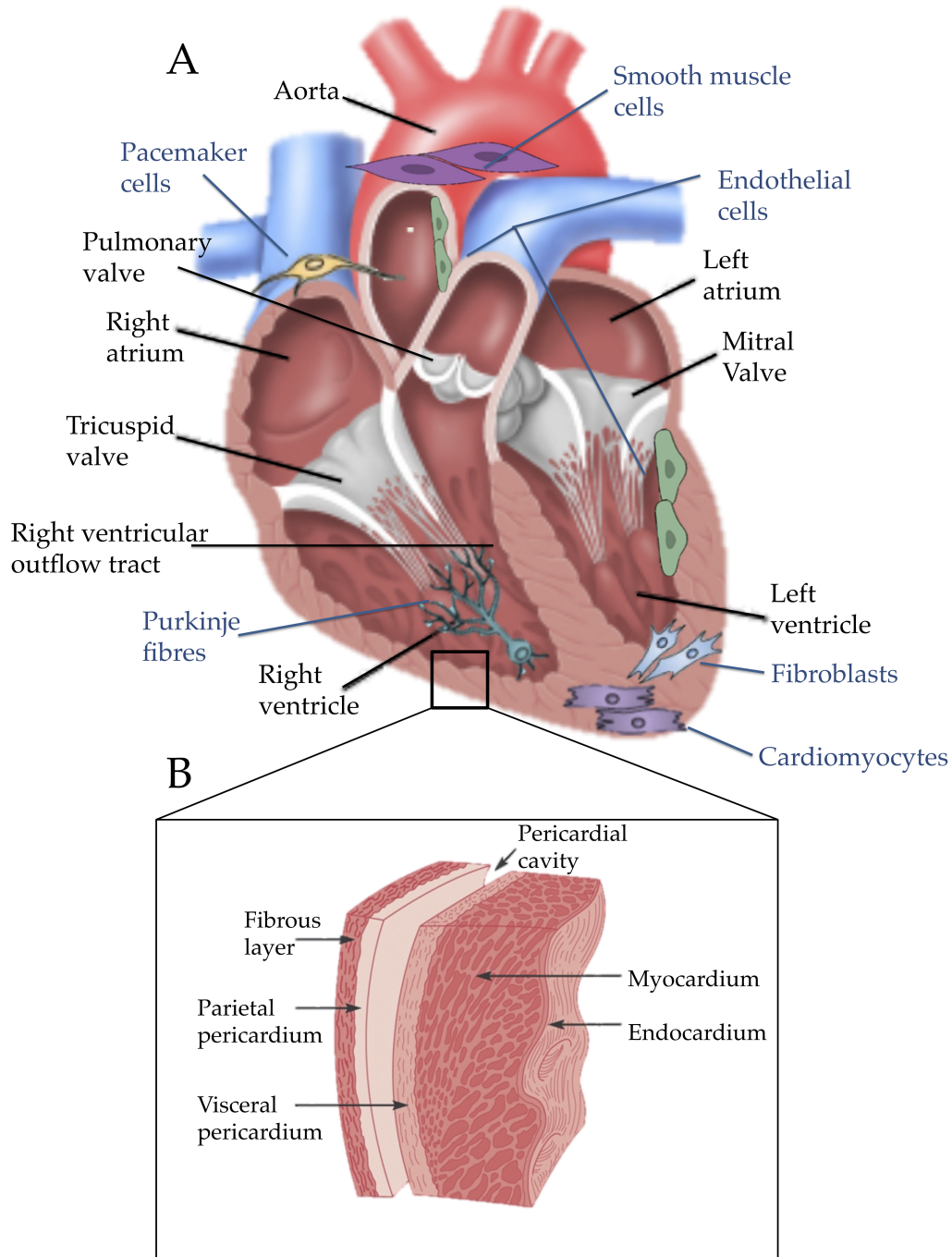


Figure 5: Anatomy of the heart. A. Main anatomical features of the heart including major cells types; and B. Cross section of the RV demonstrating the multiple layers that comprise the wall of the heart.

assistance of the RV pumping [20]. Therefore, the workload on the RV in normal conditions is quite low. When the PVR is elevated, the RV must alter its role and start pumping blood through the lungs and to do this, it must change its structure from thin walled to thick and muscularised, likened to

the LV [Figure 6](#). This process is called right ventricular hypertrophy (RVH) and is a process that occurs in PAH pathophysiology. This increase in size is to compensate for the increase in back pressure and workload needed to pump the venous blood through the pulmonary vasculature [\[20\]](#).

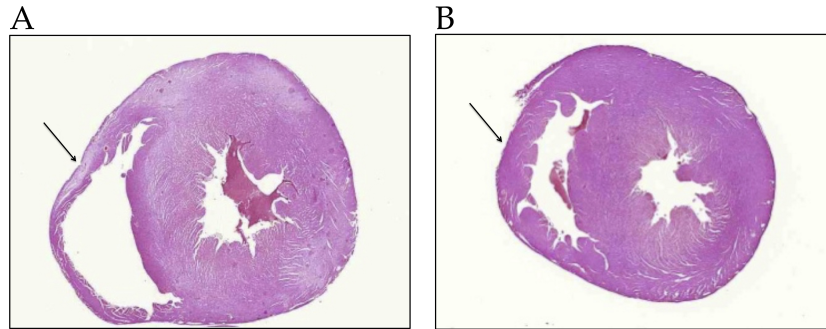


Figure 6: Cross section of a normal rat heart and a rat heart with right ventricular hypertrophy. A. Cross section of a heart from a healthy Sprague-Dawley rat, showing the thin right ventricle wall (arrow); and B. Cross section of a heart from a Sprague-Dawley rat with MCT-induced PAH, demonstrating the thick wall or the hypertrophy that occurs in the right ventricle (arrow) [\[21\]](#).

2.3 ENDOTHELIAL CELLS AND BLOOD VESSELS

The majority of the vasculature arises from the mesoderm, where small vessels comprising of EC precursors called angioblasts give rise to larger vessels such as the dorsal aorta and cardinal vein. The ECs actively recruit SMCs and pericytes for stability as the vessels become larger. This EC control continues as the vessel matures, particularly regulating the structure and formation of newer vessels. In adults, ECs replace themselves, proliferate and migrate to maintain the homeostasis of a vessel and also form new vessels. EC turnover can be slow, however, there can also be a period of rapid cell growth, which is aided by the presence of circulating precursor cells such as endothelial progenitor cells (EPCs) [\[22, 23, 24\]](#). These neo-vessels sprout as capillaries from existing vessels and continue to grow till they find another capillary, which allows them to join and the blood to start circulating. In an adult this process is termed angiogenesis [\[25, 23\]](#).

ECs have been shown to form tubes *in vitro* in Matrigel[®] (Corning Inc, Corning, NY, USA), which is a commercial product utilising a protein mixture secreted by Engelbreth-Holm-Swarm (HES) mouse carcinoma cells to promote tube formation. Thus, ECs have angiogenic potential in the absence of other surrounding cells and tissues [26]. In normal tissue, vascular growth is always balanced with nutrient demands of cells [17].

Endothelial cells form the inner lining of the vasculature from the largest arteries and heart tissue to the smallest capillary [25]. They have a remarkable capacity to adapt and change to varying environmental conditions to suit the requirements of their surroundings and also act as regulators for materials to pass in and out of the bloodstream. They enable the transit of leukocytes (monocytes and lymphocytes) from the blood stream to surrounding tissue [25]. Additionally, they are responsible for regulating thrombosis and thrombolysis, platelet adherence as well as modulating vascular tone and blood flow [23]. Importantly, there is also great phenotypic variation in ECs depending on where they lie in the vascular tree and whether they are arterial or venous. This gives rise to ECs with varying surface markers and also a diversity of responses to similar stimuli. Microvascular ECs, like those found in distal PAs, have been shown to have greater adhesion strength, unique mechanosensing properties, different organisation of signalling networks, high glycolytic influx and a discrete distribution of organelles when compared to ECs of the large PA (PAECs). These varied functions are retained when both cell populations are cultured *ex vivo* [27]. Importantly, the interaction between blood vessel ECs and lymphatic ECs is critical for controlling the distribution of antigens, antigen presenting cells (APC) and lymphocytes in the surrounding tissue [28]. Lymphatic ECs have unique cell-to-cell junctions for trafficking only certain molecules from the blood vessel into the lymph node and also form a barrier for the blood stream, stopping the diffusion of soluble molecules that arrive from the

lymph node. Thus, ECs create a dynamic life support system via an extensive vasculature system infiltrating into every region of the body [Figure 7](#).

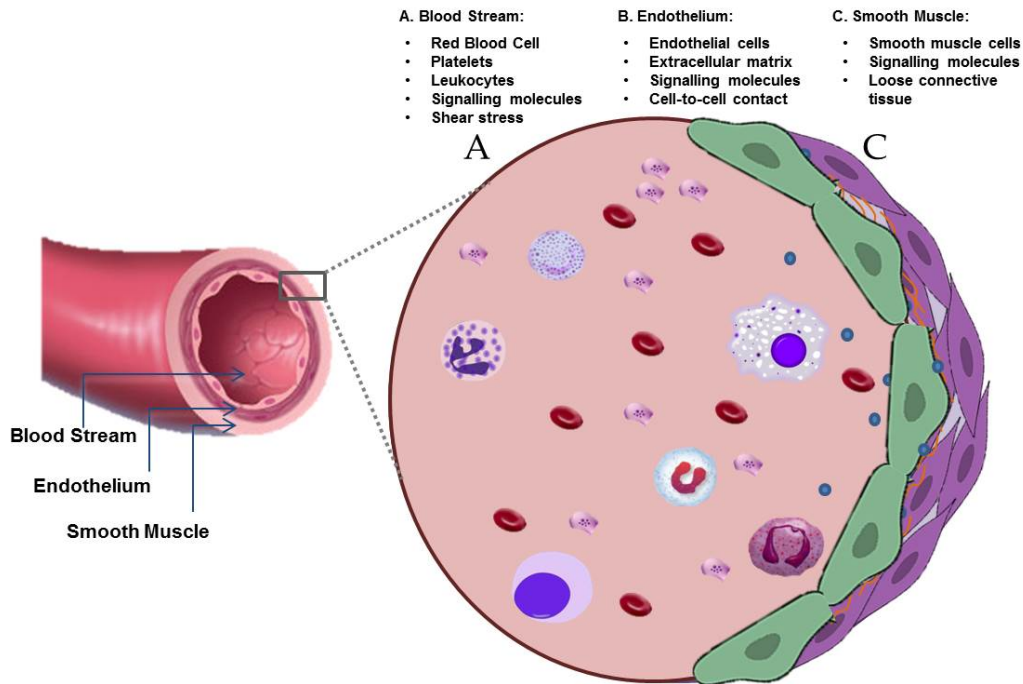


Figure 7: Schematic of a blood vessel showing the role of endothelial cells. A. Blood stream containing leukocytes such as lymphocytes, monocytes, eosinophils, neutrophils, basophils and macrophages; red blood cells, platelets and signalling molecules in an environment that causes shear stress on the luminal wall; B. Endothelium which comprises of a thin layer of endothelial cells that have cell-to-cell contact, tight-junctions for regulating the flow of molecules through the interstitium. Surrounded by an extracellular matrix (orange) with the presence of signalling molecules; and C. Smooth Muscle layer consisting of smooth muscle cells and loose connective tissue also with the presence of signalling molecules.

2.4 ENDOTHELIAL CELLS AND VASCULAR DISEASE

Endothelial cells are also recognised as contributors to disease pathologies. Abnormal stimulation, injury or uncontrolled proliferation of ECs contribute to the development of disease that are the biggest killers in the world: cancer and heart diseases such as atherosclerosis, hypertension, sepsis and inflammatory syndromes [23]. Generally in heart disease, the

organisation of ECs is chaotic and the resulting structure and size of vessel walls may be uneven, thus disrupting the equilibrium between vessels and cellular demands. Surface markers expressed by ECs are often abnormal, as well as the emission of signalling molecules from ECs. This can induce abnormal behaviour in surrounding cells such as SMCs and fibroblasts resulting in hyperplasia, hypertrophy, invasive lesions and fibrosis. All hallmark pathologies of PAH. Additionally, ECs have the potential to undertake endothelial-to-mesenchymal transition (EndoMT) [29, 30, 17, 23], where ECs differentiate to a mesenchymal phenotype, resulting in the loss of cell-to-cell adherence capacities and a gain in the ability to become more of an invasive cell type. This phenomenon has been associated with many vascular diseases such as cardiac and renal fibrosis, cancer, atherosclerosis and pulmonary hypertension [30, 31]. Importantly, EndoMT has been shown to be induced by $TGF\beta_1$ *in vitro* [29], a growth factor which is significantly elevated and driving vascular remodelling in PAH [32].

DISEASE PATHOGENESIS

3.1 OVERVIEW

In adults, the pathogenesis of PAH involves intimal hyperplasia and plexiform lesions in the distal PAs leading to occlusions and ultimately the destruction of the vessel. Medial remodelling also occurs with excessive SMC proliferation and extracellular matrix (ECM) remodelling [33, 34, 35]. Whilst research into the precise molecular pathology of the vascular remodelling in PAH is still ongoing, correlation between these changes with the altered hemodynamics seen in PAH occurred in the late 1940s to early 1950s [32]. Definitive pathological diagnosis of PAH relies on histopathological examination of pulmonary vascular walls, however, despite the greater use of cell-specific markers, these pathological advances do not correlate to more accurate or successful treatment regimes [32]. However, it is known that the extent of vascular remodelling does correlate to the severity of the disease [Figure 8](#) [35]. The presence of plexiform lesions accounts for most of the reduction in the luminal area, and this correlates to the more severe spectrum of the disease. Furthermore, the presence of fibrotic lesions in the ECM begins in moderate disease and whilst the eccentric arrangement of pulmonary arterial SMCs is a normal pathological feature in healthy individuals, this eccentric arrangement can thicken in PAH subjects as SMCs proliferate, and as the disease progresses the arrangement shows variation and concentric characteristics.

As demonstrated in the schema [Figure 9](#), the pathology seen in PAH can arise from varying triggers and causes, such as inflammation/infection, genetic mutations, drug/toxin and vascular injuries, metabolic abnormalities and altered hemodynamics and these do not manifest in isolation of one another. Interaction between these factors converge to constitute the complex pathogenesis of PAH [35].

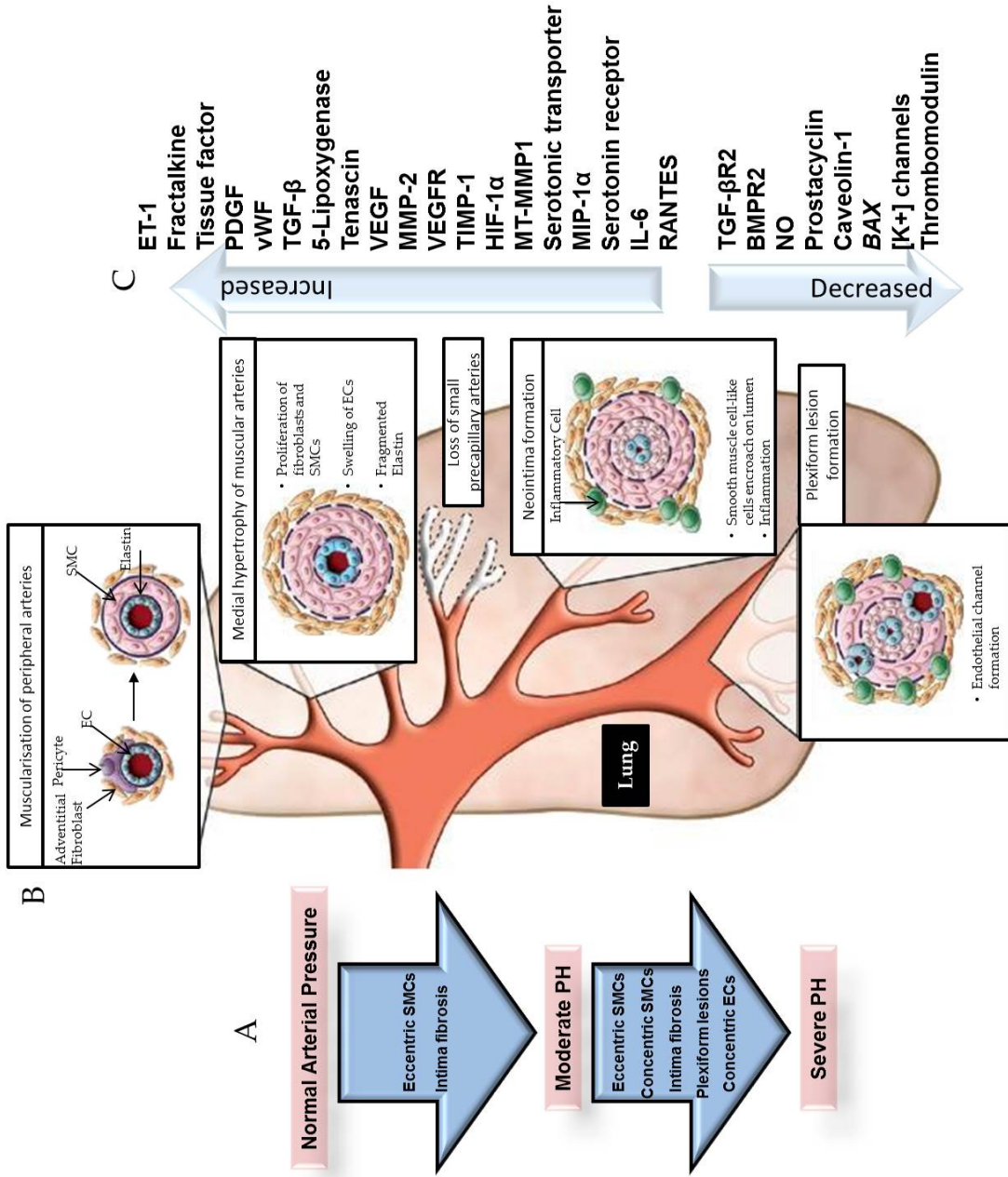


Figure 8: Incremental pathological changes that occur in PAH. A. Disease severity and the pathological changes occurring in the vessels as the severity increases; B. Disease progression; and C. Known mediators involved in PAH pathogenesis. Schematic adapted from Rabinovitch *et al* [35].

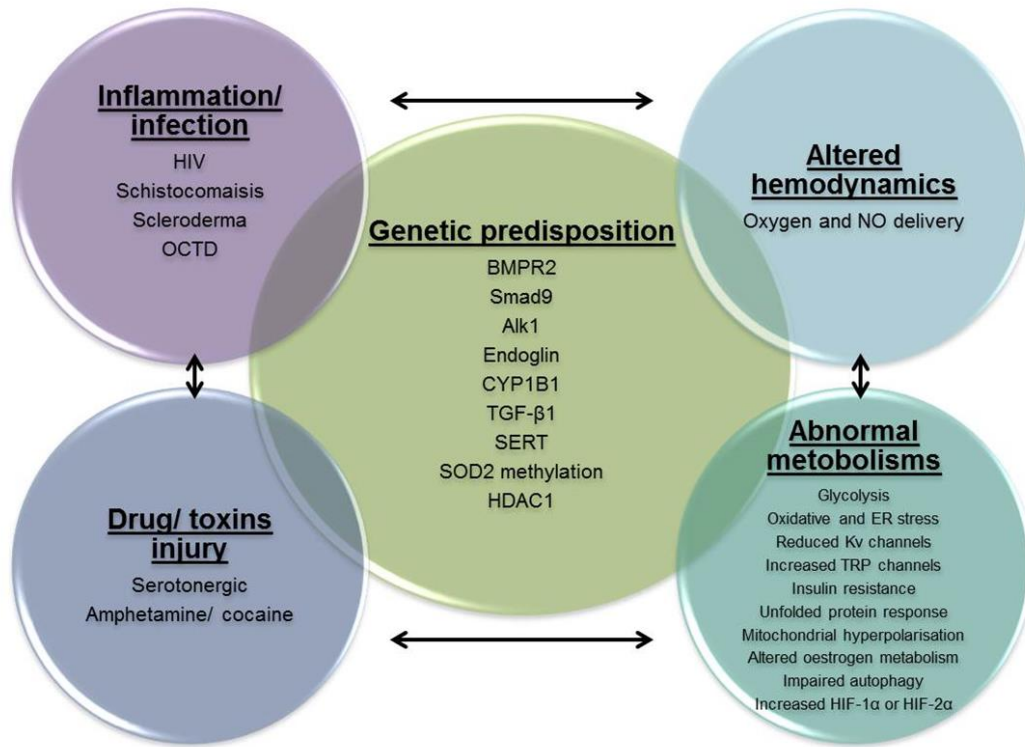


Figure 9: Converging factors of PAH pathogenesis. Inflammation/infection, genetic predisposition, drug/toxin induction, metabolic abnormalities and altered hemodynamics [35]

3.2 PLEXIFORM LESIONS

Plexiform lesions develop in PA branches of 50-300 μm in diameter in both primary and secondary PH and when present, bear a poorer prognosis [36]. These lesions arise from abnormal EC growth in the intra-luminal area, leading to occlusions and contributing to the observed elevation of pulmonary hemodynamics in these patient populations. EC growth in PAH is monoclonal, meaning that they're not proliferating, they are expansions of the same single cells, leading to the notion that these cells harbour genetic mutations. Thus, these lesions have been likened to tumour growth in cancer and SMC expansion within atherosclerotic plaques Figure 8 [37].

3.2.1 *Molecular Changes*

The development of plexiform lesions is thought to be related to abnormal EC growth, leading to uncontrolled angiogenesis [32]. This is due to the presence of VEGF, its receptors 1 (flt) and 2 (kdr) and hypoxia inducible factor-1 α and β (HIF-1), which are all mediators of new vessel formation. Importantly, ECs in plexiform lesions have significant phenotypic differences to normal ECs. Genetic mutations in TGF- β Receptor II (TGF- β RII) and *BAX* genes have been found in ECs from plexiform lesions demonstrating EC growth instability and apoptosis dysregulation [37]. Furthermore, important molecules for vascular homeostasis such as prostacyclin synthase (P12S) and NOS are reduced. However, ET-1, 5-lipoxygenase, 5-lipoxygenase activating protein (FLAP), are increased in these lesions [38, 32]. It has been reported that these lesions also lack BMP signalling, with the loss of Smad1/5/8 expression in the core of the lesion, allowing ECs in plexiform lesions to abnormally expand [Figure 8](#) [32]. Many of the angiogenic mediators found in plexiform lesions are commonly found in neoplasms [32, 35].

3.3 INFLAMMATION

Inflammatory cells such as dendritic cells, macrophages, T and B lymphocytes have been found to be present in and around plexiform lesions in PAH, and chemokines and cytokines play a significant role in the recruitment of these cells [Figure 10](#). Fractalkine, indirectly causes the up-regulation of the chemokine recruiter (CX₃CR₁) in circulating CD4⁺ and CD8⁺ lymphocytes, and has been shown to be elevated in PAH patients [39]. Stromal-derived factor-1 (SDF-1) and monocyte chemoattractant protein-1 (MCP-1) are also elevated in patient serum [35, 40]. RANTES or CCL5 is a known inflammatory mediator for vascular diseases such as glomeru-

lonephritis, Kawasaki disease and Takayasu's arteritis [41] and is thought to also play a role in PAH by inducing the release of endothelin (ET)-converting enzyme-1 and ET-1. These factors are derived from the endothelium exerting powerful control of vasoconstriction. RANTES mRNA expression has been found to be increased in lung samples of PAH patients [41]. Other chemokines such as CXC-ligand 10 (CXCL10) and CCL2 have also been shown to be increase in PAH patients compared to controls [42, 41, 43]. Additionally, increased concentrations of the pro-inflammatory cytokines: IL-1 and IL-6, have been reported in the plexiform lesions of lungs and patient serum. Animal models of PAH (hypoxia and MCT) have also been reported to have elevated levels of IL-6 [42].

3.4 DISRUPTED CELLULAR FUNCTION

3.4.1 *Endothelial Cell Dysfunction*

Uncontrolled EC proliferation is the key process of the pathological changes associated with PAH. Whilst, the precise mechanism is yet to be determined, EC dysfunction is suggested to start with excessive apoptosis leading to the emergence of apoptotic resistant ECs, which have the capacity to proliferate uncontrollably [44, 45, 32]. Factors that are present in plexiform lesions such as VEGF, ET-1 and survivin may contribute to the unchecked cell growth or suppression of apoptosis. The role of RhoA (*Ras homologous A*) in EC permeability, proliferation, migration and apoptosis may be another important component of the pathogenesis of PAH. The RhoA/Rho kinase (ROCK) pathway has been shown to be regulated in ECs and is also implicated in thrombin- and thromboxane A₂- induced platelet aggregation [46]. This uncontrolled angiogenesis due to EC dysfunction is on a background of many complex molecular processes that are occurring in the disease, such

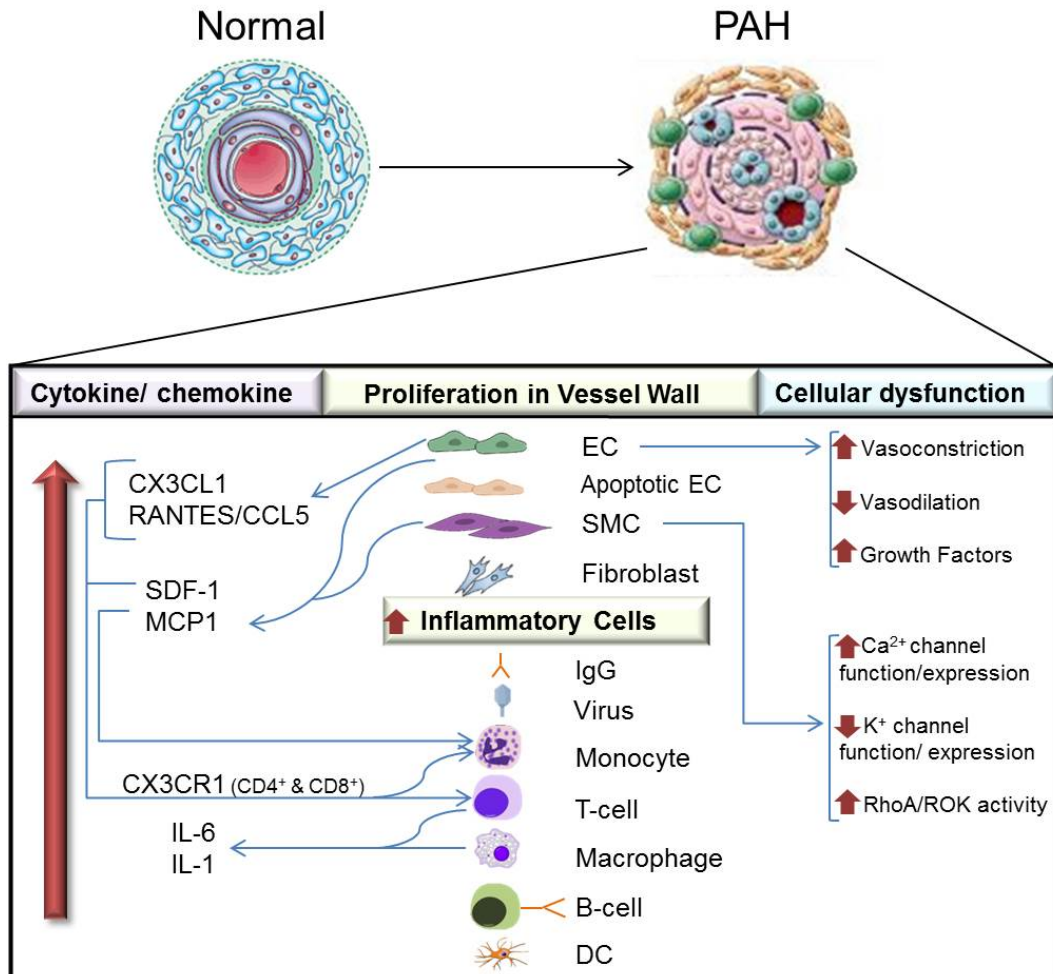


Figure 10: Chemokine/cytokines present in PAH and their interaction with endothelial cells, smooth muscle cells, fibroblasts and inflammatory cells: ultimately resulting in cellular dysfunction. Schematic adapted from Hassoun *et al* [41].

as inflammation, genetic predispositions, endothelial injury and abnormal metabolic function.

3.4.2 Smooth Muscle Cell Dysfunction

Muscularisation in the distal PAs associated with PAH is due to SMC hyperplasia and hypertrophy. Several molecular pathways have been attributed to this abnormal cellular behaviour. Over-expression of tyrosine kinase with immunoglobulin-like and EGF-like domains 2 (Tie2) receptors on ECs is matched with elevated levels of angiopoietin (ANG)-1, a glyco-

protein which activates Tie2, which in turn induces the release of hydroxytryptamine (serotonin) or (5-HT) that stimulates SMC proliferation [46]. PAH patients have significantly elevated levels of circulating 5-HT, as well as an over-expression of its receptor hydroxytryptamine (serotonin) transporter (5-HTT) on SMCs. In the alveolar duct, pericytes are differentiated into SMCs which subsequently proliferate [35]. Additionally, in the presence of platelet-derived growth factor (PDGF)-BB or TGF- β , ECs transdifferentiate into SMCs. Reduced release of NO by ECs seen in PAH contributes to the promotion of SMC proliferation, as NO is not only a vasodilator, but it also suppresses SMC proliferation [32].

SMC proliferation, migration and contraction are highly regulated by Ca^{2+} in the cytosol and itself is affected by the availability and/or functionality of K^{+} channels. Reduced K^{+} channels lead to a sustained increase of Ca^{+} , as seen in PAH patients compared to controls [46]. Additionally, the 'Warburg effect' which was originally described by Warburg in 1926 [47] has been associated with PAH. This is where a metabolic shift from oxidative phosphorylation to glycolysis occurs in tumours. This shift leads to a 'pseudo-hypoxic environment,' which suppresses the expression of Kv channels, directly leading to an increase in cytosolic K^{+} and Ca^{+} creating proliferative, apoptosis-resistant SMCs [46].

3.5 GENE MUTATION IN PAH

The genetic basis of PAH is becoming increasingly better understood and whilst mutations relating to PAH are now being discovered in many different genes, 80% of families with multiple cases of PAH have a mutation in BMPR2 [9]. The subsequent reduction of BMPR2 mediated signalling may be associated with an increase in TGF- β mediated signalling Chapter 4 [48]. Other mutations in the genes belonging to the TGF- β super-family are

activin-like receptor kinase-1 (ALK1) [49], endoglin (ENG) [50], and some mothers against decapentaplegic-9 (SMAD9) [51], which all together, make up 5% of mutations in HPAH. Additionally, other gene mutations have been recently identified: caveolin-1 (CAV1) [52] and potassium channel super family K member number-3 (KCNK3) [53].

4.1 OVERVIEW

BMPR2 is a member of the TGF- β super-family of receptors [Figure 11](#) and plays an important role in organogenesis, and also in adult tissue homeostasis and regeneration. Thus, this receptor can be found in most organ tissues. In the lung, it is expressed predominantly on the cellular membrane of the pulmonary vascular endothelium and to a lesser extent, pulmonary smooth muscle [\[46\]](#).

BMPR2 has a pivotal role in embryogenesis. BMPR2 ligands and downstream mediators such as Smad proteins have been shown to have an impact on normal embryonic development as they are required for neural crest induction, neural crest cell migration and spinal cord patterning [\[54, 55, 56\]](#). Additionally, BMPR2 signalling has a role in limb development and endochondral bone formation [\[57\]](#). Importantly, complete knock-out of BMPR2 in mice leads to early embryonic lethality at 9.5 days postcoitum, as these embryos failed to develop an organised structure or mesoderm [\[54\]](#).

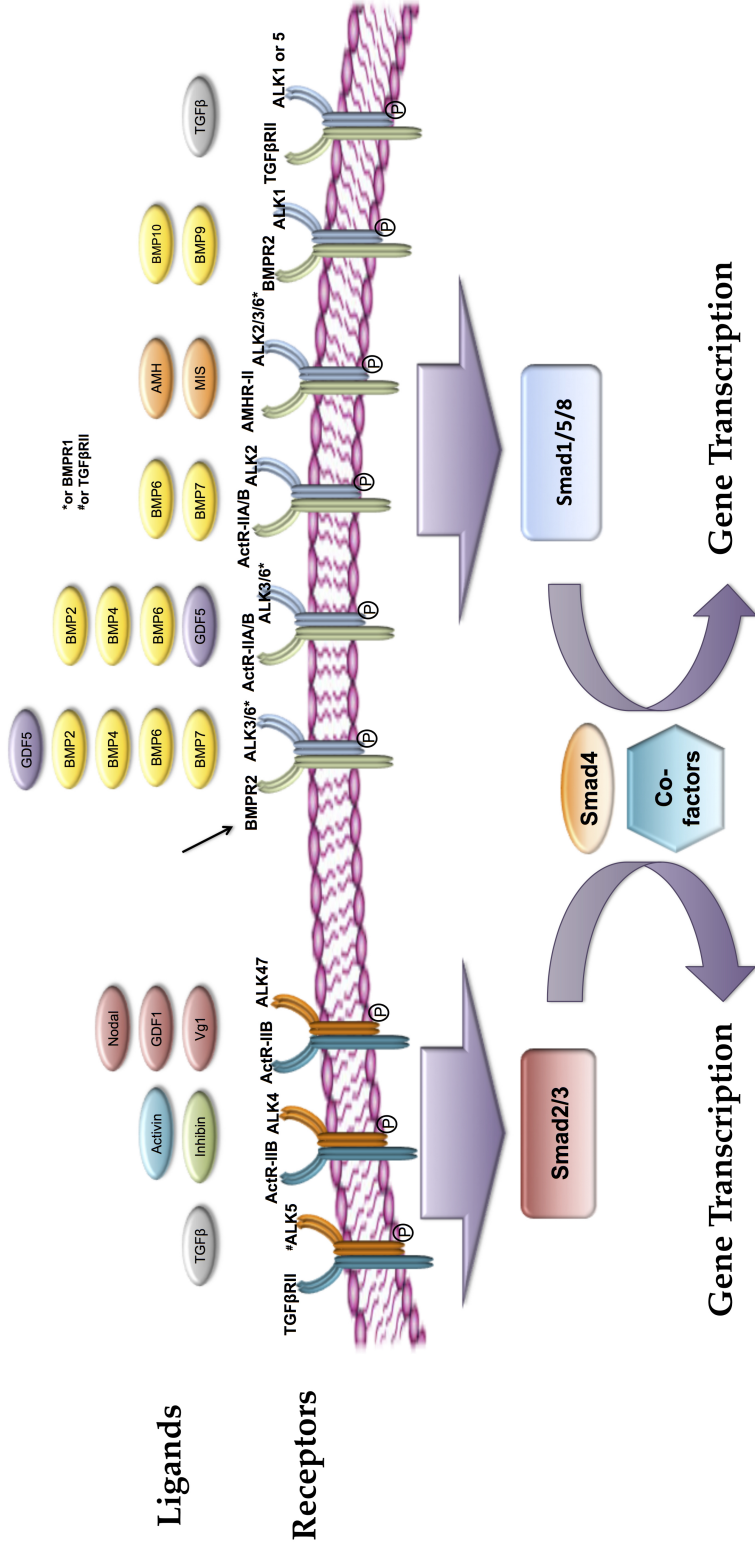


Figure 11: TGF-β super-family of receptors, their corresponding ligands and signalling pathways. Note: On the left is the TGF-β mediated Smad2/3 signalling pathway, and on the right is the BMPR2 (black arrow) mediated Smad1/5/8 signalling pathway. Adapted from Upton *et al* [58].

4.2 GENOMIC INFORMATION AND RECEPTOR STRUCTURE

The BMPR2 gene is mapped to the 3-cM region of chromosome 2q33 (locus *PPH1*) Figure 12 [4]. The gene has 13 exons and is over 180,000 base pairs in length, 98% of which are introns [59]. The transcript BMPR2 generates is a polypeptide of 1,038 amino acids, and the mature protein harbours four discrete domains Figure 13. The extracellular domain is encoded in exons 2 and 3, whilst the transmembrane domain is generated by exon 4 and the serine/threonine domains is encoded by exons 5 to 11 [60].

BMPR2 is a TGF- β type 2 serine/threonine kinase receptor and forms a heterodimeric complex with TGF- β type 1 receptors Figure 13 [61, 62]. Once on the cell membrane, the receptor interacts with specific ligands which activates a large variety of cellular signalling pathways Figure 11. Thus, the action of BMPR2 is quite diverse and complex.

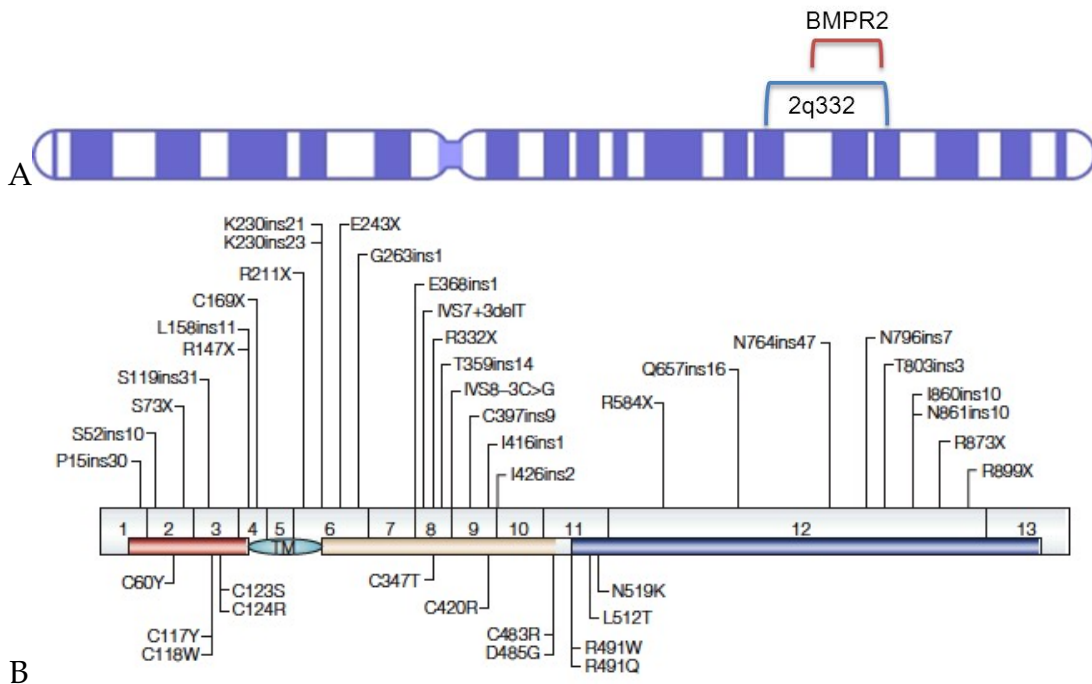


Figure 12: BMPR2 chromosome and gene with germline mutations for PAH. A. Chromosome 2, with the 2q33 and the BMPR2 regions indicated; and B. BMPR2 gene, with 13 exons and germline mutations for PAH indicated [63, 64].

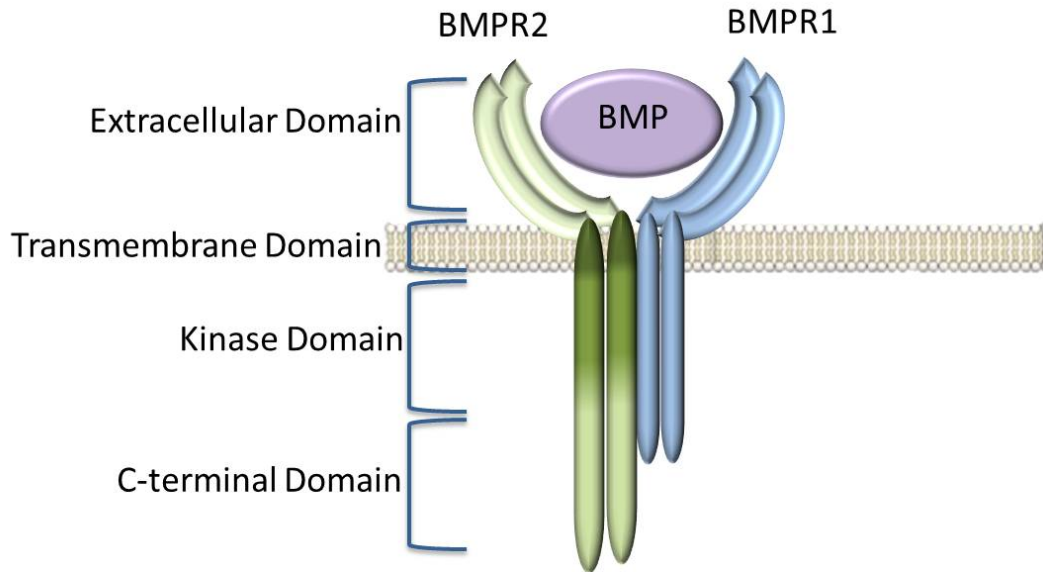


Figure 13: BMPR2 receptor including the four discrete domains: extracellular, transmembrane, kinase and C-terminal domains. BMPR2 forms a heterodimeric complex with BMPR1, and once together, BMP ligands have a high affinity to bind and activate the downstream pathways.

4.3 BONE MORPHOGENETIC PROTEINS

Bone morphogenetic proteins (BMPs) such as BMP2, BMP4, BMP7 and BMP9 act as ligands for BMPR2 [65]. Activation of BMPR2 by these ligands leads to the phosphorylation of Smad1/5/8 [Figure 14](#) and non-Smad molecules, including mitogen activated protein kinases (MAPK) such as ERK, p38 and PI3K [Figure 16](#). BMPs are all secreted as precursor proteins, where mature BMPs are obtained by proteolytic cleavage and exert their biological activity on many cells types including monocytes, endothelial, mesenchymal, epithelial and neuronal cells [66]. These ligands can bind to the type 1 receptor in the absence of the type 2, however when both receptor types are present the binding affinity is highly increased and is required for complete signal transduction [56].

4.4 SMAD SIGNALLING PATHWAY

There are three classes of Smad proteins: receptor-mediated Smads (R-Smads), common-mediator Smads (Co-Smads) and inhibitory Smads (I-Smads) [66]. R-Smads and I-Smads are expressed by most cell types, and in the absence of ligand binding, I-Smads are found predominately in the nucleus. R-Smads are phosphorylated by type 1 receptors, following BMP ligand binding. Once the BMP ligand binds to the receptor complex, R-Smads (Smad1, Smad5 and Smad8) are phosphorylated at the C terminus of the type 1 receptor. These Smad proteins (when activated) have a high affinity for the nuclear chaperone, Smad4 (Co-Smad). They form a complex that translocates to the nucleus, binding loosely to DNA and acting as transcription factors for target genes [Figure 14](#). Smad proteins are made up of 2 domains: MAD-homology domains 1 and 2 (MHD1 and MHD2) that are highly conserved at the N- and C-terminus respectively [67, 66]. These are joined by a 'linker' segment that is variable in length and amino acid sequence, and it is the interaction between this 'link' and the C-terminus of the type 1 receptor that leads to the phosphorylation and activation of the Smad proteins, resulting in a disruption of the auto-inhibitory relationship between MH1 and MH2. This allows Smad4 to bind to the activated Smad forming a multimeric complex, exposing a nuclear import signal and allowing the complex to translocate to the nucleus for transcriptional regulation [Figure 14](#) [56]. Inhibition of this pathway is mediated by Smad6/7, where upon ligand binding, these Smads are exported rapidly into the cytoplasm and are able to block R-Smad phosphorylation by the type 1 receptor through competitive inhibition. Additionally, Smad6 can inhibit the binding of Smad4 to the activated R-Smad [66, 67]. I-Smads can be induced through BMP7, TGF- β 1, activin, epidermal growth factor (EGF) and lamina shear stress [66].

TGF- β activates the Smad2/3 pathway via TGF- β receptors I and II [Figure 15](#). TGF- β is elevated in plexiform lesions as well as in the MCT induced PAH rat model [5]. Furthermore, inhibition of the TGF- β signalling pathway via the activin receptor-like kinase-5 (ALK-5) in the MCT model prevented development and progression of PAH [5].

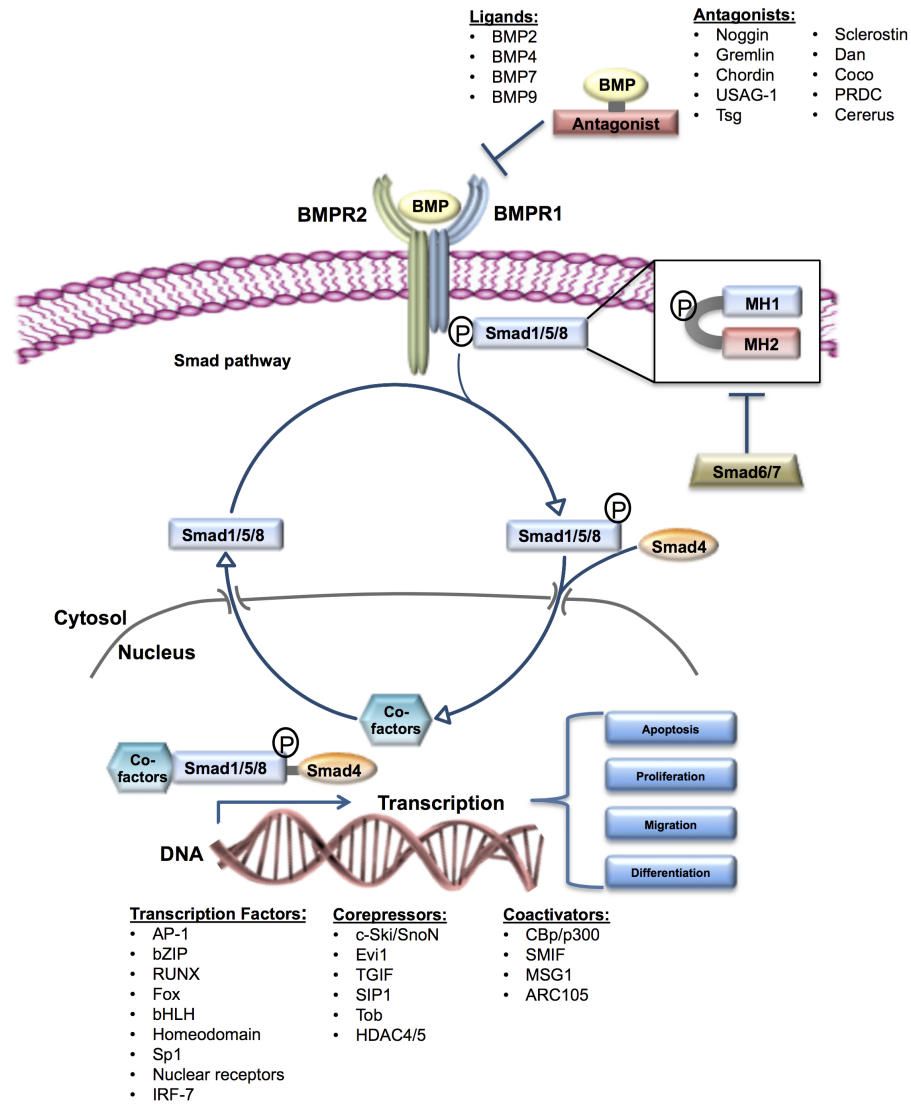
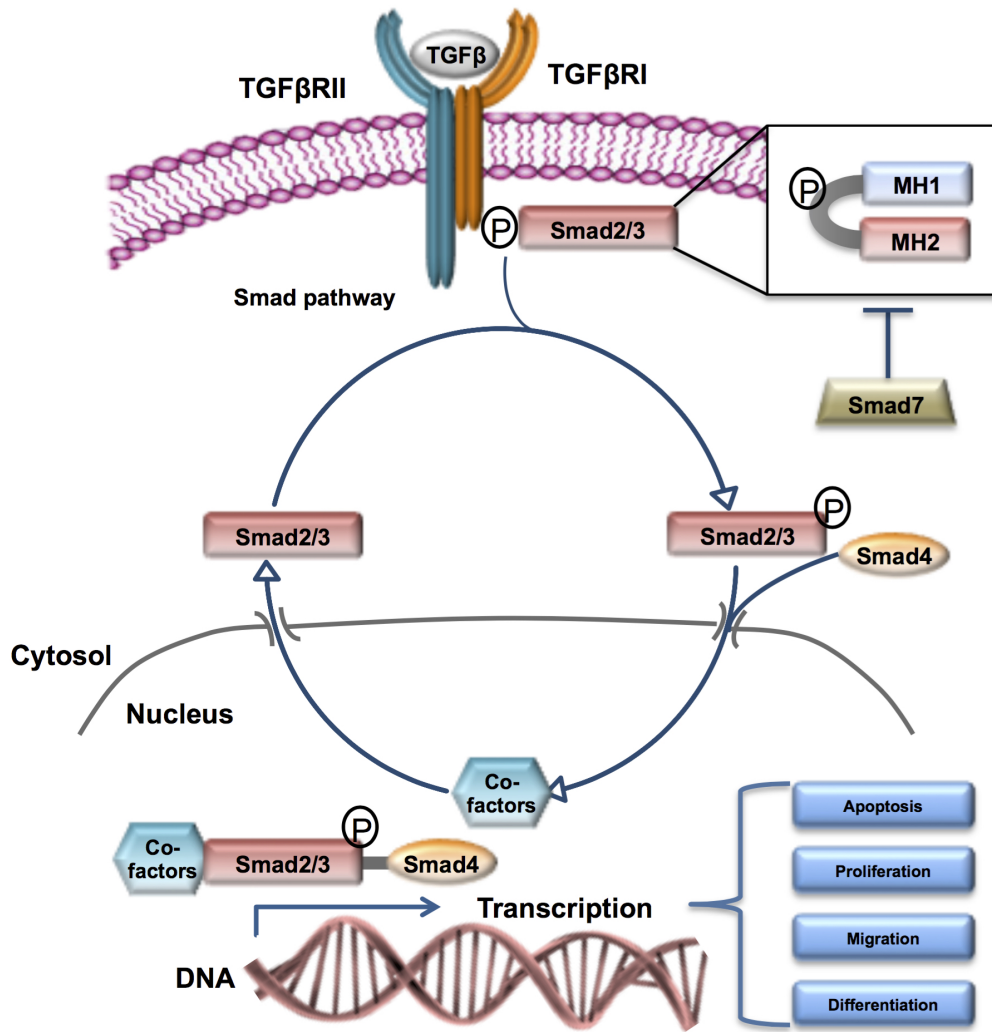


Figure 14: BMPR2 mediated Smad1/5/8 signalling pathway, including ligands and antagonists. Once the BMP ligand binds to the receptor complex, R-Smads (Smad1, Smad5 and Smad8) are phosphorylated at the C terminus of the type 1 receptor. These Smad proteins (when activated) have a high affinity for the nuclear chaperone, Smad4 (Co-Smad). They form a complex that translocates to the nucleus, binding loosely to DNA and acting as transcription factors for target genes, affecting cellular processes such as apoptosis, proliferation, migration and differentiation.



- | <u>Transcription Factors:</u> | <u>Corepressors:</u> | <u>Coactivators:</u> |
|---|--|--|
| <ul style="list-style-type: none"> • AP-1 • bZIP • RUNX • Fox • bHLH • Homeodomain • Sp1 • Nuclear receptors • IRF-7 | <ul style="list-style-type: none"> • c-Ski/SnoN • Evi1 • TGIF • SIP1 • Tob(BMP only) • HDAC4/5 | <ul style="list-style-type: none"> • CBp/p300 • SMIF • MSG1 • ARC105 |

Figure 15: TGF- β mediated Smad2/3 signalling pathway, where TGF- β RII and TGF- β RI are activated via TGF- β binding. This activates either Smad2 or 3, which is then complexed with Smad4 that acts as a nuclear chaperone. This complex is then joined by transcription factors that allow the whole complex to transcribe the gene of interest. This pathways controls cellular proliferation, migration, apoptosis and differentiation.

4.5 NON-SMAD SIGNALLING PATHWAY

BMPs can also activate non-Smad pathways, such as PI3K, MAP Kinases, ERK, AKT and Rho-like GTPases [67]. Specifically, BMP2 and BMP4 are known to activate TGF- β 1 activating kinase (TAK1), which controls the activation of the p38 MAPK pathway, small GTPases such as PI3K, and the ERK/ AKT pathways Figure 16 [66]. Importantly, non-Smad pathways are more generally known to be activated when TGF- β is the ligand Figure 17, and this can in turn can regulate Smad signalling pathways [67, 56, 68]. TGF- β mediated non-Smad signalling has been implicated in many molecular processes seen in PAH [48]. However, the exact interaction between receptors, ligands and these non-conical pathways needs to be further elucidated.

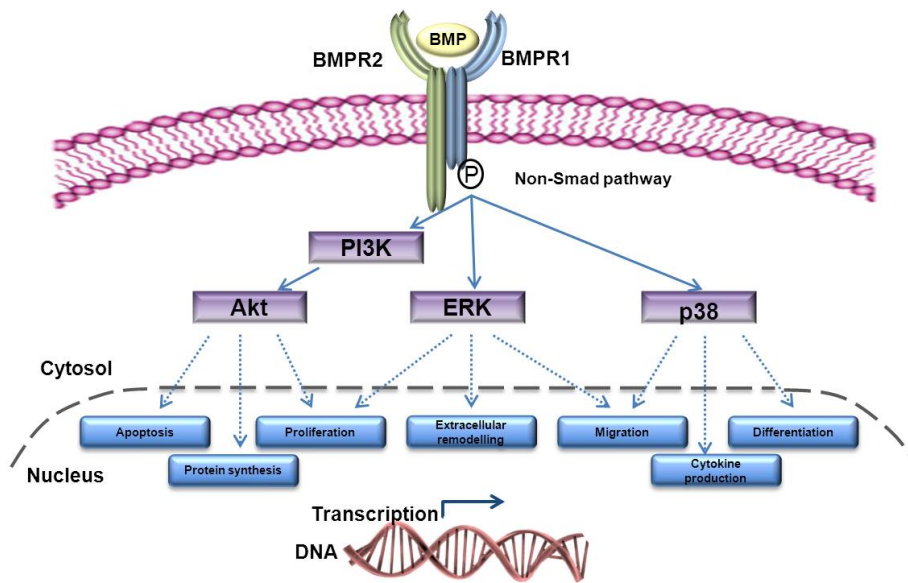


Figure 16: BMPR2 mediated non Smad signalling pathway, activated with the binding of certain BMP ligands which can activate a wide range of signalling proteins affecting a plethora of cellular behaviours.

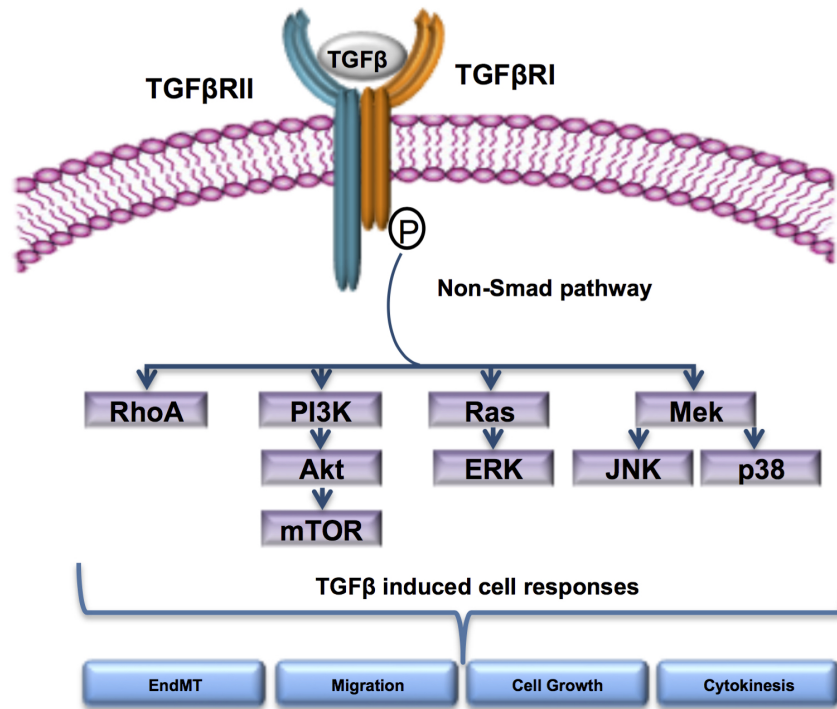


Figure 17: TGF- β mediated non-Smad signalling pathways. TGF β acts as the ligand to activate the TGF- β RII and TGF- β RI complex, which in turn activates a wide range of signalling molecules, instigating a plethora of cellular processes.

4.6 MUTATIONS IN THE BMPR2 GENE

Analysis of the types and occurrence of mutations in patients with HPAH, spanning many ethnic groups, age and gender is increasing. As genetic testing becomes more extensive, the number of sporadic or idiopathic cases decreases. BMPR2 mutations are heterozygous and patients with a mutation have reduced expression of the receptor, impacting Smad pathways [69]. There are two forms of BMPR2 mutation:

1. **Truncating**- where a mutant BMPR2 transcript is generated by a point mutation that produces a stop codon. This mutant mRNA is detected by cell mediated nonsense-mediated decay (NMD), which degrades the transcript, reducing the total amount of receptors on the cell membrane. This is termed 'haploinsufficiency' [Figure 18](#); and

2. **Missense**- where a nucleotide substitution occurs, which results in the incorrect amino acid being included in the polypeptide. This defective transcript escapes NMD, and thus mutated BMPR2 receptors are produced. These act as competitive inhibitors on the cell surface. This process is termed 'dominant negative' [Figure 18](#) [70].

Understanding the type of mutation is important, as this affects predicted survival. Patients with missense mutations have a lower survival rate compared to those with truncating mutations [Figure 19](#) [70]. Mutations are present in 80% of heritable and 11-40% of idiopathic cases [71, 72, 4, 69]. Despite this, only 10-20% of carriers of this mutation display the PAH phenotype. This suggests that a 'second hit,' in the form of environmental factors such as hypoxia or inflammation are required for the disease to manifest [73].

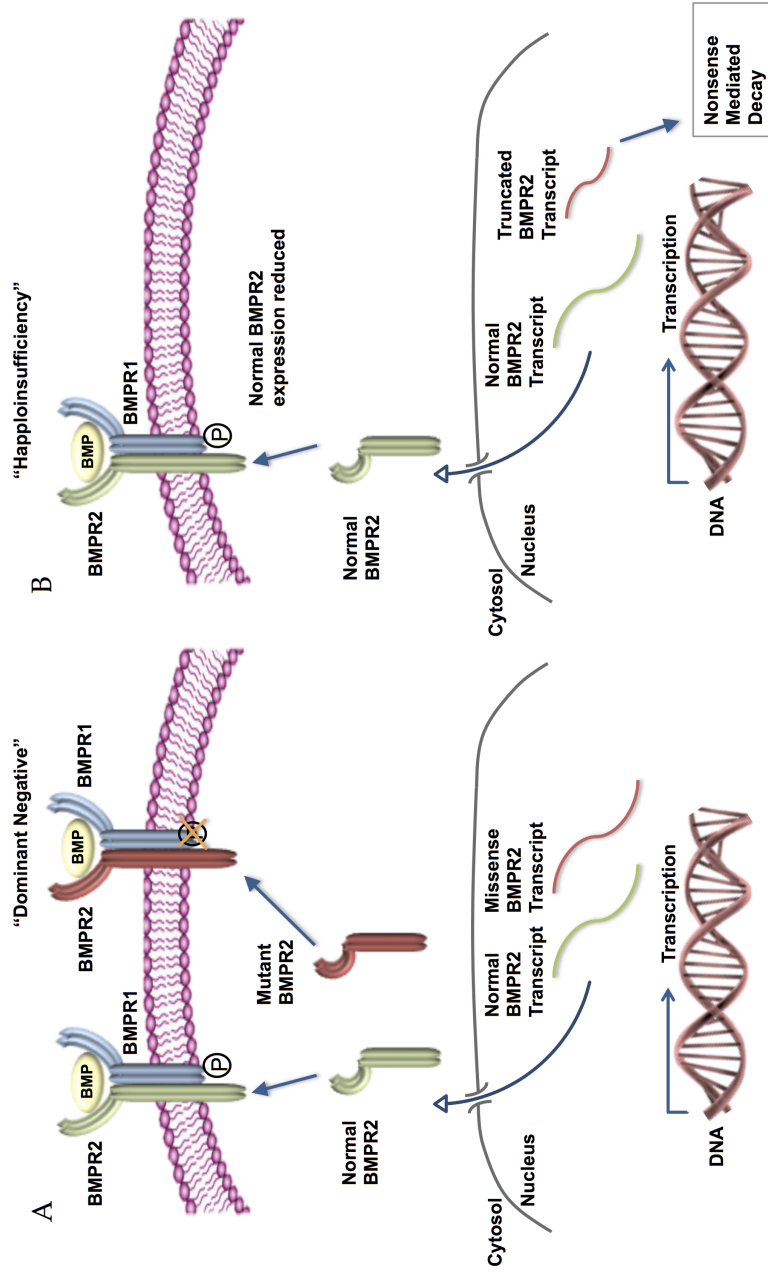


Figure 18: Mechanism of truncating and missense mutations in the BMPR2 gene. A. Missense mutation: where the mutant transcript does not get picked up as abnormal in the nucleus by 'nonsense mediated decay' (NMD), resulting in the mutated receptor sitting on the cell surface. Ligands are able to bind to the mutated receptor, however it cannot activate downstream pathways, causing a 'dominant negative' effect; and B. Truncating mutation: where the BMPR2 transcript is truncated, and picked up by NMD and destroyed. This leads to a reduced amount of BMPR2 expressed on the cell surface, called 'haploinsufficiency'.

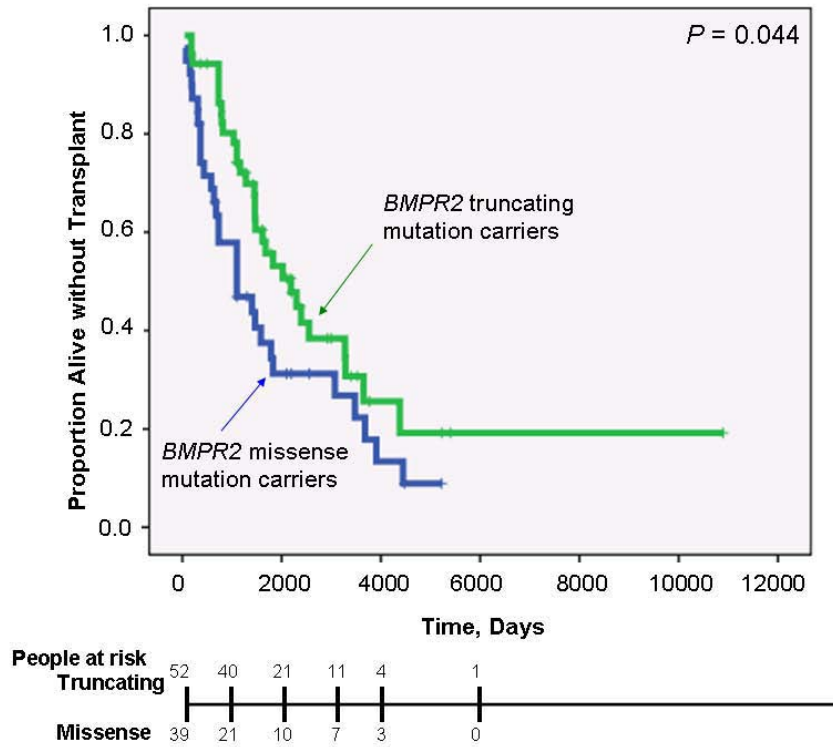


Figure 19: A Kaplan-Meier plot of the disease severity of truncating vs missense mutations over time. Severity is shown as proportion of patients that are alive without transplant. Missense mutation carriers (blue line) have worst survival compared to truncating mutation carriers (green line) [70].

EXPERIMENTAL MODELS OF PAH

5.1 OVERVIEW

Studying PAH in a clinical context is difficult. In human subjects, there is large histological diversity which arises from multiple, identifiable pathogenic stimuli [74] and due to the typical delayed diagnosis and severity of disease, subjects present with a low tolerance to invasive procedures. Because of this and to expedite research in this area, animal models of PAH are used to mimic the disease, and of these, rodent models are most robust. Larger animal models such as primates, dogs, sheep, rabbits and cows can be used, however they pose issues such as cost effectiveness, ethical considerations, slow disease progression and other problematic experimental practicalities relating to their size [74]. As in humans, PAH in animal models show pathological changes in the lung vasculature, however there is no 'one' perfect model, in fact, animals given multiple stimuli to induce disease tend to best mimic the diversity of pathological changes observed in human subjects [Table 3](#) [74].

RELEVANT ANIMAL MODELS OF GROUP 1 PULMONARY HYPERTENSION						
Animal Model	Method	Med. Hypertrophy	Plexiform Lesions	mPAP (mmHg)	RVH (mmHg)	Mortality
Human PAH	Spontaneous or Hereditary	Severe	Severe	30-60	Variable	30% at 3 yrs
MCT Rat	60-100 mg (SC) ±pneumonectomy	Severe	Mild	40-60	Moderate	100% at 2 mo
Chronic Hypoxia Rodent	10% O ₂ for 3-4 wks	Mild	None	30-40	Mild	Negligible
Sugen Hypoxia Rat	20 mg/kg of SU-5416 / 3 wks 10% O ₂	Moderate	Mild	40-60	Moderate	10% at 6 wks
Fawn-Hooded Rat	Hereditary	Moderate	None	30-50	Moderate	Up to 1 yr
BMPR2 Mutation Mice	↑ mutant BMPR2 alleles	Moderate	None	35-45	Mild	Stable up to 3 mo
ET _B Receptor Deficiency Rat	MCT SC to ET _B deficient rats	Mild	None	40-45	Mild	Stable up to 3 mo
Ang-1 Overexpression Rat	AAV-Ang-1 injected into RV outflow tract	Mild	None	30-40	Mild	Stable up to 3 mo
High fat diet to APO-E knockout Mice	Diet of high fat chow for 11 wks	Mild	Mild	20-30	Moderate	Stable up to 6 mo
MCT in Primates	60 mg/kg interscapularly 1/month for 4 mo	Mild	None	40-60	Mild	Stable up to 6 mo
Radiation Exposure to Whister Rat	Exposed to protons with shoot-through technique	Mild	None	25-35	Mild	Stable up to 2 mo
PA Banding Rodent	Main PA ligated with suture	Mild	None	Normal	Severe	Stable up to 12 wks
Aorta-caval Shunt Rodent	Needle advanced through abdominal aorta into IVC	Mild	None	25-35	Severe	Stable up to 12 wks
Brisket Disease Cattle	Cattle reared at 7,000 ft	Mild	None	60-80	Mild	Stable up to 6 mo

Table 3: Relevant animal models used to study Group 1 PH disease, including method of induction, disease pathology, hemodynamic characteristics and predicted mortality. Adapted from [74].

5.2 MONOCROTALINE MODEL

Monocrotaline is a toxic pyrrolizidine alkaloid taken from seeds of the plant *Crotalaria spectabilis*. Ingestion of MCT results in progressive development of PAH in many species of animals, however it is more commonly SC injected into rats. The mode of action involves converting MCT in the liver to dehydromonocrotaline by cytochrome P-450 enzyme CYP_{3A4}. At high doses, MCT can cause acute hepatic injury and at lower doses it exerts multiple effects on the pulmonary endothelium [74]. These effects include the induction of DNA damage [75], abnormal NO signalling and activation of proliferative factors [76], resulting in vascular leakage, adventitial oedema, as well as medial hypertrophy and obliteration of small PAs (20-100 μm) [74, 77]. Additionally, MCT can cause cell-cycle arrest in ECs, glial cells, pneumocytes and hepatocytes, as well as accumulate in erythrocytes. Platelet-mediated thrombosis and systemic inflammation is also observed in this model, with the latter thought to play a critical role in the initial stages of the disease [75, 74].

Vascular changes, initially seen in the pulmonary endothelium, are observed as early as 4 days post SC injection of MCT, with abnormal SMC proliferation and migration occurring around 8 days [77, 74]. Obliteration and medial hypertrophy of PAs occurs at around 2 weeks, and this is coupled with changes in hemodynamics, such as increased RVSP and mPAP as well as right ventricular hypertrophy [77, 75, 74]. This model does develop vascular lesions, however contrary to human disease, they are not plexiform in nature. However, there are overlapping molecular changes in the MCT-induced PAH model with human PAH. Importantly, Long *et al* have shown that the rat MCT-induced PAH model has reduced BMPR2 expression and increased TGF β expression at 21 days post injection [5].

MCT animal models have limitations, such as the development of myocarditis in some animals, damage to airways, lack of plexiform lesions and the non-applicability of MCT in mice [78]. Additionally, it has been documented that MCT-induced PAH is easily reversed due to its acute nature [79].

Nevertheless, the MCT-induced model of PAH is regarded as a simple, efficient and effective model where severe PAH gradually develops [79]. It has been extensively used to study PAH pathogenesis and is yet to be replaced by a more effective model, despite the growing popularity of the Sugen hypoxia model. [74].

5.3 CHRONIC HYPOXIA MODEL

Chronic hypoxia is an animal model that is largely used for Group 3 PH [Table 1](#), however, due to the activation of HIF- α in this model, it is used also for Group 1 PAH [74]. Once again, this model is commonly used in rodents, and is favoured due to its reproducibility within a selected animal strain, despite variability between species [79]. Animals are exposed to a hypoxic environment (10% O₂ for 3-4 weeks) either in a hypobaric or normobaric environment. Both of these environments yield similar PAH, though normobaric is most often used due to the noisy vacuum pump required for a hypobaric chamber [74]. This model is well tolerated and considered to be a less severe model compared to MCT, with the absence of right heart failure. The hallmark pathology of this model is medial hypertrophy of small PAs, which are normally non-muscularised and this is coupled with a rapid increase in cells with increased expression of α -smooth muscle actin (α -SM actin) [79]. Hemodynamic changes are largely due to this thickening of the small PAs causing increased PVR. Proliferation and migration of SMCs, pericytes, fibroblasts and mononuclear/ progenitor cells (mainly

mesenchymal cells) as well as EndoMT, contribute to an increase in medial and adventitial hypertrophy, and thickening of pre-capillary PAs in this model [79, 74]. Inflammation also has an important role, with the appearance of certain chemokine and cytokine receptors as precursors to the infiltration of inflammatory cells, as well as adhesions molecules and mesenchymal cells in vessel walls [80].

It should be noted that fawn-hooded (FH) rats spontaneously develop PAH which can be made more severe if exposed to hypoxia, with a great extent of vascular remodelling [79]. In this strain, PAH is heritable, occurring in 68% of both male and females [74]. Despite FH rats having similar molecular changes to human disease, such as an increase in ET-1 and NO, the rate of change is very slow and systemic hypertension occurs, which is not a feature of human disease.

Chronic hypoxia models have certain limitations. The model does not have severe obstructive remodelling nor does it feature vascular lesions as seen in the MCT and Sugén models. Hemodynamic changes are mild and RV failure is not present. Additionally, there are many more treatments that reverse the PAH in this model when compared to those that reverse PAH in the more severe MCT model [74]. Mice are not a good species to use with chronic hypoxia as there is only minimal vascular remodelling and increase in PA pressure [79]. When directly compared to the MCT model, there is more infrastructure, maintenance and cost involved in this model.

5.4 SUGEN-5416/ HYPOXIA MODEL

The sugén hypoxia rat model was developed by Taraseviciene-Stewart *et al* to better address the human disease pathology of hyperproliferative

ECs which infiltrate the PA lumen, a feature that is lacking in the chronic hypoxia and MCT models [79]. Sugen-5416 or 3-[(2,4-dimethylpyrrol-5-yl)methylidene]-indolin-2-one is a synthetic VEGFR-2 inhibitor, and when injected SC 3 times a week for 3 weeks into Sprague-Dawley (SD) rats that are concurrently exposed to hypoxia, severe PAH results [44]. The resultant changes in hemodynamic pressures are also coupled with EC death, SMC proliferation, obliteration of the arterial lumen by proliferating apoptotic-resistant ECs (a key feature of human disease) and eventually right heart failure [44]. The model is well tolerated with less death than the MCT model, despite PA pressures typically being more elevated [74]. Evaluation of this model showed pro-survival genes such as Bcl-2, Bcl-X and IGF-I were significantly decreased in lungs of the treated rats compared to untreated hypoxic rat lungs [44]. Remarkably, VEGFR-2 blockade only occurs in the lungs and was not systemic, however, when compared to human disease, lungs from this model only had four common gene expression profiles with lungs from human PAH subjects [81].

Limitations of this model include the absence of pro-inflammatory mediators such as mononuclear infiltrates into the perivascular region, and also the reliance on VEGFR-2 blockade, which has an unknown role in human PAH. Despite this, it is becoming widely used as a PAH model, and also has not demonstrated the same susceptibility to reversal as the MCT and hypoxia models [79]. Other advantages is that it is a comparatively cheap and simple to use.

5.5 TRANSGENIC MOUSE MODELS

There are many different transgenic models targeting a wide variety of mutations seen in human PAH [Table 4](#). The difficulty with using these models is that they only target one aspect of human PAH pathology, and whilst

similar pathogenic processes may occur as a consequence of manipulating a specific gene expression, the models are highly specific to one mutation, and are not applicable across the spectrum of human PAH pathogenesis. The most commonly used and developed models are the BMRP2 mutation models [Table 4](#).

TRANSGENIC MOUSE MODELS OF PAH			
Model	Method	PAH Severity	Mortality
Global Knockout Homozygous Mice	BMPR2 exons 4 and 5 are deleted globally	N/A	Death during gastrulation
Global Knockout Heterozygous Mice	BMPR2 exons 4 and 5 are deleted globally	Mild	Stable
Conditional Knockout Mice	loxP sequences flanking exons 4 and 5	Mild	Stable
BMPR2 Dominant Negative Mice	Mutant BMPR2 alleles are overexpressed in a tissue-specific and inducible manner	Moderate	Stable up to 3 mo
Short Hairpin (shRNA) BMPR2 Knockdown Mice	Silencing BMPR2 expression with shRNA	N/A	Stable up to 3 mo

Table 4: Relevant animals models used to study Group 1 PH disease, including method of induction, PAH severity and predicted mortality. Adapted from Ryan *et al* [74].

5.6 SUMMARY

There are many pre-clinical animal models available for Group 1 PH, however, there is no one perfect model currently available. Therefore, careful consideration must be taken when choosing the animal model to use. Important factors to consider are:

- Pathological similarities with human disease: inflammation, apoptosis resistant ECs and unchecked SMC proliferation;
- Vascular remodelling: plexiform lesions, right heart failure, medial and intimal thickening;
- Hemodynamic changes seen in human disease: increased PVR, mPAP, RVSP and RVH;
- Molecular changes present in human disease: decreased BMPR2 expression, increased TGF β and ID1 expression; and
- Cost, utility and reproducibility of the model

Despite the recognised limitations of animal models for PAH, they continue to provide valuable insight into molecular mechanisms of PAH as well as providing a good pre-clinical model for therapeutic investigation.

TREATMENT

6.1 OVERVIEW

Current therapies cause pulmonary vasodilation or inhibit pulmonary vasoconstriction with the aim of lowering PVR. However, there is no available treatment that either reverses the disease or stops its development indefinitely. There are 4 main groups of therapeutics currently in mainstream practice: calcium channel blockers (CCBs), prostanoids, endothelin receptor agonists and phosphodiesterase-5 (PDE-5) inhibitors [Figure 20](#).

The lung is a unique organ in that there is access via the vasculature and/or airways. Therefore, treatment options can be diverse, multi-factorial and possibly synergistic.

Currently, there is an evidence based treatment algorithm, published from the 5th World Symposium on PH, Nice, France, 2013 [83]. This was developed with 3 main areas:

1. General measures, supportive therapy, referral strategy, acute vasoreactivity testing, and chronic treatment with calcium channel blockers;
2. Initial therapy with PAH approved drugs; and
3. Assessment of clinical response to the initial therapy, combination therapy, balloon atrial septostomy and lung transplant

Treatment algorithms for PAH have evolved since the first proposed algorithm from the 2nd World Symposium of PH in Evian, France 1998. Unfortunately, the complexity of the algorithm has increased, reflecting the complex clinical presentations and responses to current treatments [Figure 21](#).

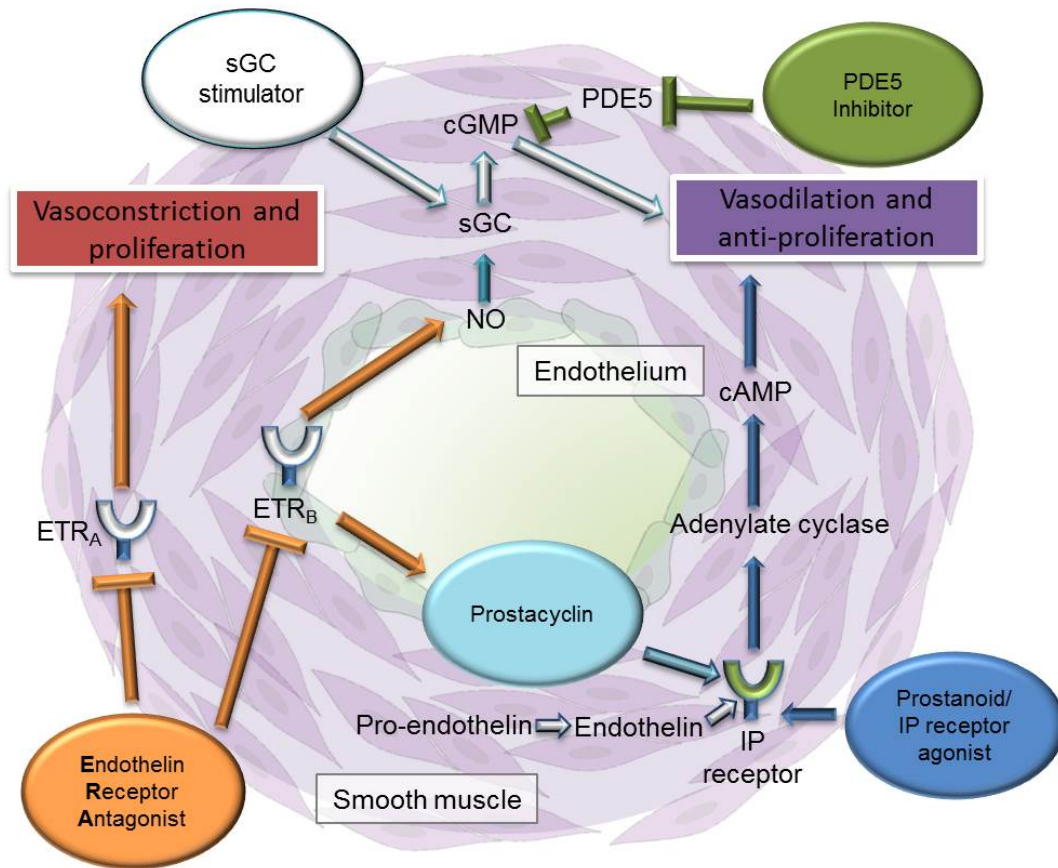


Figure 20: Targeted molecular pathways and actions of current approved PAH therapies. ERAs block the endothelin-1 (ET-1) production by ECs ET-1 exerts a direct vasoconstrictive effect via vascular SMC proliferation. Prostaglandin I₂ or prostacyclin is the main product of arachidonic acid, produced in the vascular endothelium. It induces the relaxation of SMCs by stimulating the production of cyclic AMP (cAMP), as well as exerting an inhibitory control over SMC proliferation. PDE-5 is a highly expressed enzyme by SMCs in the lungs. It is responsible for the metabolism of cyclic guanosine monophosphate (cGMP), which mediates vasodilation and anti-proliferative activities of SMC. Adapted from Humbert *et al* [82].

6.2 CURRENT TREATMENTS

6.2.1 Calcium Channel Blockers

Calcium channel blockers (CCBs) are a class of agents known to cause vasodilation through the relaxation of SMCs. This therapy however, has been shown to have limited effects. Effective changes are mainly seen in those patients that show vasoreactivity in their right heart catheterisation (RHC)

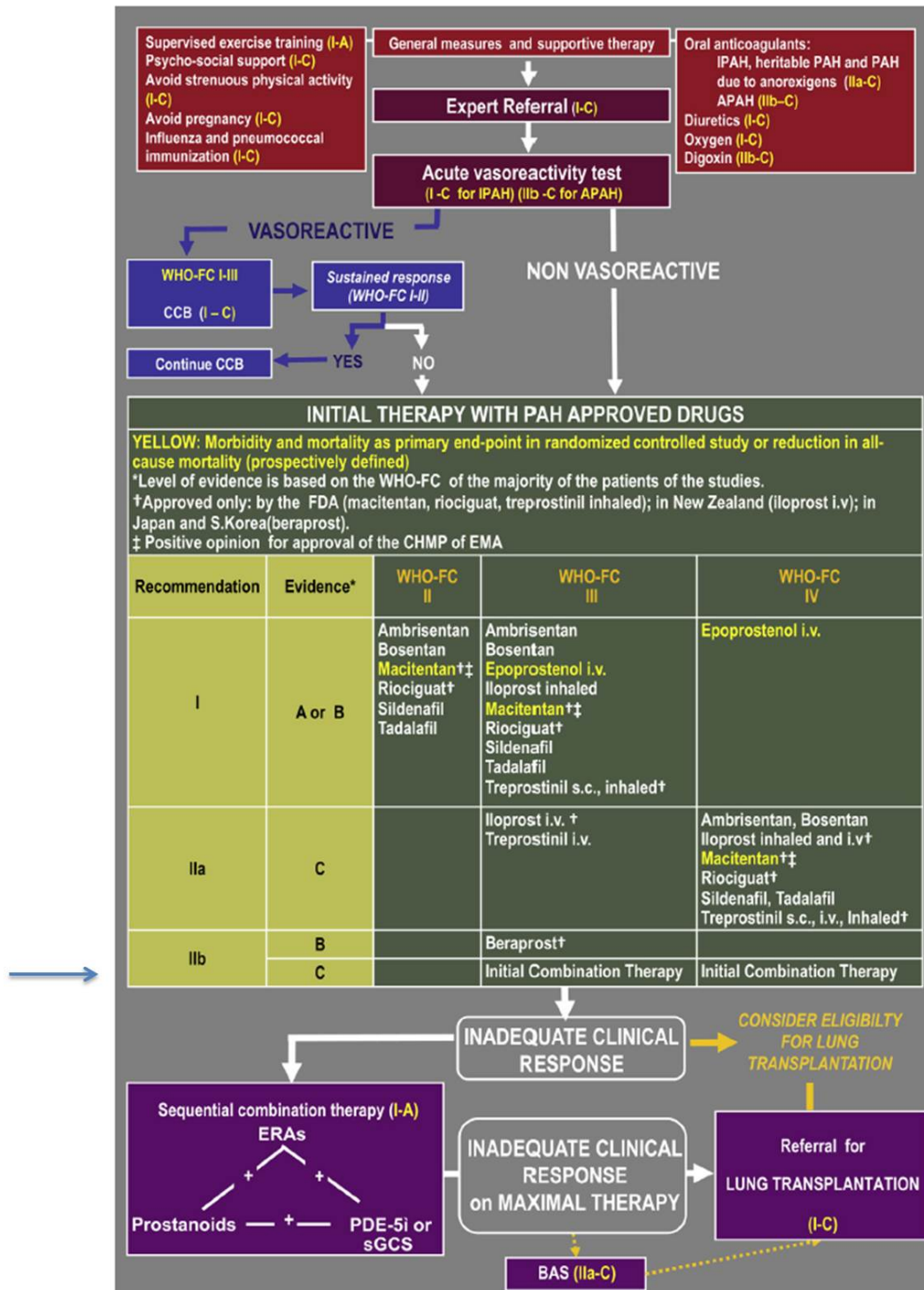


Figure 21: Updated PAH treatment algorithm from the 5th World Symposium on PH, Nice, France, 2013. Addition of combination therapy (blue arrow). Adapted from Galie *et al* [83, 84].

procedure [85, 12]. This procedure involves an acute vasodilator challenge with the use of short-acting agents such as intravenous prostacyclin, adeno-

sine or inhaled NO. Less than 10% of PAH patients show vasoreactivity and thus long-term CCB treatment is only useful in a small subset of PAH patients [86, 85].

6.2.2 Endothelin-Receptor Antagonists

Endothelin-receptor antagonists (ERAs) include: Bosentan, Sitaxsentan, Ambrisentan, Atrasentan, BQ-123, Zibotentan, Macitentan and Tezosentan.

Endothelin-1 (ET-1) is produced by ECs and exerts a direct vasoconstrictive effect via SMC proliferation. ET-1 is elevated in the plasma of PAH patients and also in the lungs [87]. It acts via two receptors, endothelin receptor A (ET_A), predominately expressed on vascular SMCs and endothelin receptor B (ET_B), which is expressed on ECs and to lesser extent, on vascular SMCs [Figure 20](#). ET_A induces the expression of certain adhesion molecules effecting an increase in SMC proliferation, inducing fibrosis and activating pro-inflammatory mediators, whilst ET_B induces NO and prostacyclin production by ECs and is responsible for ET-1 clearance from the lung. The dual receptor antagonist, Bosentan has been found to provide significant improvements in patients exercise capacity (6-minute walk distance (6MWD)) and hemodynamics after 12-16 weeks of treatment [88, 89]. Long-term (>4 years) Bosentan treatment has shown either an improvement or maintenance of NYHA Functional Class, with 20% of patients discontinuing due to adverse effects [90]. A disadvantage of Bosentan is the impact on the liver where the drug is metabolised, inducing an increase in hepatic amino-transferase, resulting in abnormal liver function. Nevertheless, survival with the use of Bosentan as a first line treatment in PAH increased from 69% to 96% in the first 12 months and 57% to 89% in the subsequent 24 months [91].

Selective ET_A treatments such as Sitaxsentan and Ambrisentan have been shown to provide functional and hemodynamic improvements in PAH patients [92, 93]. By selecting for ET_A, there should only be a blockade on the vasoconstrictive effects of this receptor with the ET-1 clearance and vasodilator effects of ET_B being maintained. This theoretical advantage has not translated into improved clinical outcomes, and these therapies have also shown to have adverse effects on liver function [92, 93].

6.2.3 Prostacyclin Therapy

Prostaglandin I₂ or prostacyclin is the main product of arachidonic acid metabolism, produced in the vascular endothelium. It induces the relaxation of SMCs by stimulating the production of cyclic AMP (cAMP), as well as exerting an inhibitory control over SMC proliferation [Figure 20](#) [94, 12]. Prostacyclin is also an inhibitor of platelet aggregation [95]. There are currently several different prostacyclin treatments available with varying methods of administration. Epoprotenol is an intravenous treatment developed and used since the 1980's [96]. This has shown functional and hemodynamic improvements, however the treatment is labour intensive and expensive. Treprostinil is a subcutaneously delivered drug which shows similar improvements to Epoprotenol, however the disadvantages of mode of delivery and half life is better with Treprostinil [12]. Beraprost is orally delivered and iloprost is an inhaled prostacyclin analogue, both exerting short-term hemodynamic effects after administration and thus requiring multiple daily doses. Both have shown improvements in patients 6MWD and iloprost is showing improvements in NYHA functional class assessment. Side-effects of these two therapies is a systemic vasodilation, syncope and cough [12].

6.2.4 *Phosphodiesterase-5 Inhibitors*

Phosphodiesterase-5 is a highly expressed enzyme by SMCs in the lungs. It is responsible for the metabolism of cyclic guanosine monophosphate (cGMP), which mediates vasodilation and anti-proliferative activities of SMCs [Figure 20](#). PDE-5 gene expression is increased in PAH, with elevated protein expression in SMCs and RV cardiomyocytes [97, 82]. Sildenafil is a PDE-5 inhibitor, preventing the breakdown of cGMP and thus enhancing its vasodilatory and anti-proliferative effects. Long-term trials evaluating Sildenafil, which was given orally 3 times a day, have shown positive results for PAH patients in their 6MWD as well showing hemodynamic and functional improvement in 46% of patients, with a 3 year survival of 79% [98]. Tadalafil is another PDE-5 inhibitor with a longer half-life allowing for once-only daily dosages, and has similar effects to sildenafil [82].

6.2.5 *Combination Therapy*

Combination therapy of all of the above-mentioned mono-therapies is emerging as a topical area of research. There are two options: sequential combinational therapy where patients are started on one therapy and as the effectiveness of that therapy either does not exist or deteriorates, then additional therapeutic options are introduced; and up front combination therapy where patients are started on a combination of therapies from the beginning of their treatment. The rationale behind combination therapy is by targeting more than one of the pathways there will be an enhanced or synergistic effect that will heighten the effectiveness of each therapy. Since the 5th World Symposium on Pulmonary Hypertension in 2013, sequential combinational therapy has become integrated into the treatment algorithm, following data from long-term trials and meta analyses [Figure 21](#) [99, 100, 101]. Up-front combinational therapy is largely based on

expert consensus, small studies and/ or retrospective studies [84]. However, a recently completed trial looking at upfront combinational therapy of ambrisentan and tildenafil for patients with PAH secondary to Scleroderma (SSc) demonstrated significant improvements in hemodynamics, RV structure and function and NYHA Functional Class [102].

6.3 EMERGING TREATMENTS

6.3.1 *Riociguat*

Riociguat is a soluble guanylate cyclase (sGC) stimulator. Its mode of action can be either dependent or independent of NO, both resulting in an increase of cGMP. The dependent pathway relies on riociguat sensitising sGC to endogenous NO through stabilising NO-sGC binding. The independent pathway is where sGC can be stimulated at a different binding site, without the presence of NO [103]. Riociguat is the first treatment to show efficacy in two PH disease pathologies, both PAH and chronic thromboembolic pulmonary hypertension (CTEPH) [104]. This treatment is now in its 3rd phase of clinical trials, with the first two showing promising results in 6MWD, PVR, N-terminal prohormone of brain natriuretic peptide (NT-proBNP), NYHA Functional Class, time to clinical worsening and Borg dyspnoea scale. Riociguat is now approved in the USA, Europe and several other countries for patients with Group I PAH in NYHA Functional Class II or III, and for the patients with inoperable CTEPH [82].

6.3.2 *FK506(Tacrolimus)*

FK506 or tacrolimus is an FDA approved macrolide antibiotic with immunosuppressant properties, typically used post transplant. Its mode of

action is through the inhibition of calcineurin phosphatase by binding to the immunophilin FK506 binding protein (FKBP), resulting in the inhibition of calcium-dependent events. These include: IL-2 gene transcription, NOS activation, cell de-granulation and apoptosis [105]. Tacrolimus is also a strong BMP activator by mimicking BMP4, and thus controlling ECs survival, enhancing tube formation and other functions which regulate angiogenesis [106]. When used at a low dose, Spiekerkoetter *et al* were able to show in both *in vitro* and *in vivo* PAH models that tacrolimus can not only halt disease processes in ECs, but also prevent the development of PAH in a rat sugen model [106]. Additionally, they were able to show that tacrolimus increased EC expression of ALK1 and endoglin [106]. Thus, in low doses, tacrolimus may be a useful treatment for PAH via its action in activating the BMPR2 pathway.

6.3.3 Cell Therapy

Cell therapy has emerged as a promising treatment for not only vascular diseases, but other diseases such as diabetes, kidney disease and degenerative eye disease. The application of cell therapy in PAH stems from the understanding that this disease not only manifests with EC and SMC dysfunction, but additionally, dysfunctional EPC and MSC populations contribute to PAH pathogenesis [107, 108]. Several studies have used EPCs, MSCs and even microvesicles from these cell populations, to treat PAH both in animal models of PAH and human PAH patients with varying success [109, 110, 111, 112, 113, 114, 115]. These cells can be used 'naked' or they may be altered to act as a vehicle to deliver a desired therapy, such as a gene or protein of interest [116]. The first clinical trial to use autologous EPC-based eNOS gene therapy was reported in June 2015, with positive findings in patient tolerance of the treatment, and positive short-time phys-

iological outcomes, such as increased exercise tolerance and hemodynamic improvements [115]. Clearly, further studies into the efficacy and mode of action of this therapy is needed, however, this may be a promising alternative to current therapies which don't reverse the pathological changes in PAH, and also offer a safer alternative to viral delivery of gene therapies by overcoming immunity issues.

GENE THERAPY

7.1 OVERVIEW

Gene therapy as defined by the National Health and Medical Research Council (NHMRC), Australian Government, as the 'treatment of inherited disease by the addition, insertion or replacement of normal gene or genes.' [117]. This rather narrow definition overlooks the application of gene therapy to non-inherited (i.e. acquired) diseases.

The European Medicine Agency (EMA) defines gene therapy medicinal products as fulfilling these following two characteristics (precluding vaccines for infectious diseases):

1. that 'it contains an active substance which contains or consists of a recombinant nucleic acid used in or administered to human beings with a view to regulating, repairing, replacing, adding or deleting a genetic sequence;' and
2. 'its therapeutic, prophylactic or diagnostic effect relates directly to the recombinant nucleic acid sequence it contains, or to the product of genetic expression of this sequence.' [118]

The US Food and Drug Administration (FDA) defines gene therapy as medicinal products 'that mediate their effects by transcription and/or translation of transferred genetic material and/or by integrating into the host genome and that are administered as nucleic acids, viruses, or genetically modified cells *in vivo* or transferred to cells *ex vivo* prior to administration to the recipient' [118].

Gene therapy can be broken down to two major areas: **somatic** and **germline**. Germline is a therapy that can be passed onto the next generation, whereas in somatic gene therapy the genetic material is inserted into a target cell, but cannot be inherited. As it stands, legislation in Australia, the US and Europe prohibit germline gene therapy.

The concept of gene therapy started to develop between 1928 and 1934 with the introduction of the 'transforming principle' by James Alloway in 1932, initiated by work undertaken by Frederick Griffith in 1928 [119, 120, 121]. By 1961, Howard Tamin discovered that specific genetic mutations can be inherited by viral transduction and quickly this concept gained momentum [122]. Waclaw Szybalski in 1962 was the first to document successful gene transfer in a bone marrow derived mammalian cell line (D98S) [123]. In this work, Szybalski demonstrated that a genetic defect in D98S cells can be restored by transferring functional DNA from D98S cells without the defect, and further to this, the restored gene was transferred to daughter cells. This concept was integral in the development of monoclonal antibodies [118]. Over the following decade, gene therapy as a field of study started to emerge. A proof-of-concept study of virus mediated gene transfer was published in 1968 by Rogers *et al* [124] and the first official gene transfer into humans was in 1989 [77]. The first approved gene therapy trial was in 1995, where 2 children with adenosine deaminase deficiency (ADA-SCID), a severe immunodeficiency disease, were given T lymphocytes that were modified *ex vivo* to express the normal gene for making adenosine deaminase [125]. The results of this trial were encouraging, and from this moment there was a boom in gene therapy programs until 1999, when the death of a patient was directly linked to the viral vector used for the treatment [118].

To-date, by far the most commonly treated disease by gene therapy is cancer (60%). More than 1800 approved clinical trials worldwide have been

conducted or are still ongoing, using adenoviral (Ad), retroviral vectors and naked plasmids as the most common mode of delivery [118].

Important characteristics for any gene therapy vector involves:

- the capacity to carry desired genes;
- being undetectable by the immune system;
- being non-inflammatory;
- the ability to express the necessary amount of protein to exert the desired effect;
- long-term expression (with the exception of cancer treatment); and
- being safely administered

7.2 VIRAL VECTORS

Viral vectors have been extensively used for gene therapy. Their utility in effective gene transfer to target cells stems from their capacity to package the desired gene into their genome. There are several different viral vectors including Ad, retroviral (including lentiviral) and adeno-associated viral (AAV) vectors.

7.2.1 *Adenovirus*

Adenoviruses (Ad) are non-enveloped (they do not possess an outer lipid membrane) viruses that are 60-90 nm in diameter. They were isolated in the 1950's from patients with respiratory diseases, and since then they have been isolated from many species with a huge diversity of serotypes that have been shown to infect humans [126]. Ads are the most widely used

vector in lung gene therapy, they can infect both quiescent and replicating cells, can be produced easily and have been shown to have 100% transduction efficiency in ECs [127, 128]. Ads contain linear double-stranded DNA and enter cells through receptor-mediated endocytosis, where the fibre knob domain binds to a coxsackie and adenovirus receptor (CAR), this in turn interacts with a secondary receptor (integrins) which triggers internalisation of the complex [Figure 22](#) [128, 126]. CAR is highly expressed on cell surfaces in different tissues, including the liver, which leads to sequestration of the virus to the liver following administration of the virus into the bloodstream [129]. This is in part due to Kupffer cells taking up the virus and degrading its DNA, as well as direct hepatocytes transduction. In recent years it has been discovered that hepatocyte transduction is largely mediated by an interaction between Ad capsid proteins and the coagulation factor X. This interaction mediates hepatic uptake. Inhibition of the interaction (for example, anticoagulants) reduces hepatic uptake. The presence of the hepatocytes has the potential to lead to hepato-toxicity, where there is an increase in the amount of hepatocytes in the bloodstream, resulting in transduction by these cells and potential 'off-target' effects of subsequent gene expression [129]. Nevertheless, there have been strategies to get around this tropism, such as bi-specific conjugates: where one end is specific for binding to the knob domain of the virus, masking the viral fibre from these cells, and the other end may be specific for a molecular target [129]. Additional advances in Ad vector technology have seen transgene expression increase from weeks to years, and fibre domains altered to express cell specific proteins, such as myeloid binding protein (MBP) [130]. Whilst these 'next generation' Ad vectors work towards greater efficacy and safety for this technology, there is still more work to be done. Immune reactions against the viral coat proteins remain an important hurdle, although this is on part being addressed by using new serotypes of Ads, including

those derived from apes, against which humans do not have pre-existing immunity.

7.2.2 *Retrovirus*

Retroviruses are enveloped single stranded RNA viruses, which adhere and penetrate directly through the cell membrane. This transfer is limited to cells with retrovirus-specific receptors [128]. Once the virus is taken up by the cell, it releases RNA, this is transformed into double-stranded DNA and is randomly integrated into the host cells genome [Figure 22](#). This allows pro-longed and stable transgene expression by that host cell. Whilst this may be more advantageous over Ad vectors, however, because of the randomness in which the DNA is inserted into the genome, there is a potential for insertional mutagenesis, as well as activation of oncogenes [128]. Additional disadvantages are that these viruses are difficult to produce, are unstable and can only be used in replicating cells.

A sub-category of retroviruses are Lentivirus, these are also single-stranded RNA and use the same mechanism to enter and replicate in cells [128]. However, they have a much more complex genome and can be used to transduce quiescent, non-replicating cells. Lentiviruses are emerging as a attractive platform for achieving long term transgene expression. Concerns still remain regarding insertional mutagenesis, although safety reports from early clinical trials are very encouraging [131, 132].

7.2.3 *Adeno-associated Virus*

Adeno-associated virus (AAVs) are single-stranded DNA vectors that are incapable of replicating on their own [133]. They are able to enter the cell by binding to cell surface receptors such as $\alpha v \beta_5$ integrin and FGFR1, where it

is internalised and transported to the nucleus [Figure 22](#). In the absence of a helper virus, AAVs can stably insert themselves into the q.13.4-ter arm of chromosome 19, where it enters a latent infection phase [\[128\]](#). The advantage of this is a lower risk of random insertional mutations. Furthermore, AAVs provoke less of an immune response than Ads, have a longer transgene expression period than Ads and are able to infect differentiated, undifferentiated, non-dividing and dividing cells [\[128\]](#). However, a disadvantage is that AAVs have been found to be less efficient in transducing cells, and they also have a small genome, making it difficult to package larger desired genes into the vector, such as *BMPR2*.

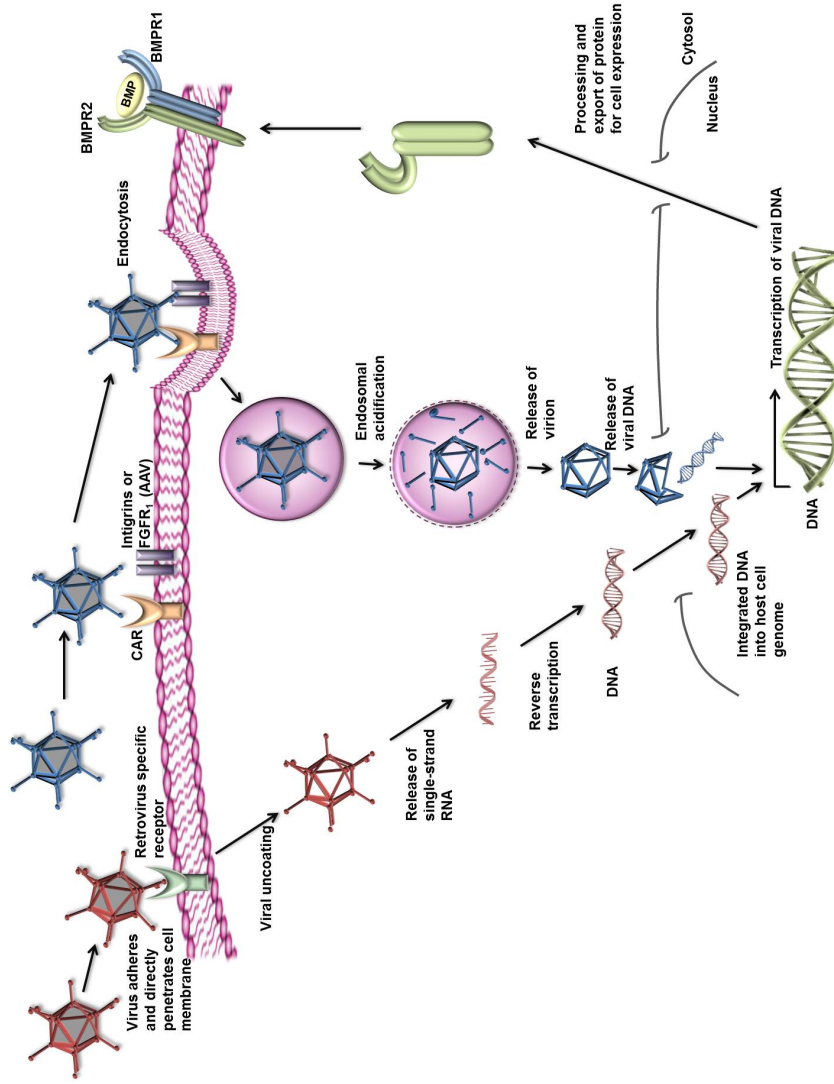


Figure 22: Mechanism of adenovirus, adeno-associated virus and retrovirus entering the cell and integrating their DNA. Adenovirus and adeno-associated virus (blue) utilise specific receptors to initiate the process of endocytosis, which allows these viruses to enter the cell and transport the packaged DNA for transcription in the nucleus. Whilst retroviruses (red) bind and penetrate directly through the cell membrane on cells which have retrovirus specific receptors. Once inside the cell, the virus releases its single-strand RNA in the cytosol, which undergoes reverse transcription to form DNA that then enters the nucleus for transcription.

7.3 NON-VIRAL VECTORS

The development of non-viral vectors for gene therapy was to avoid the known limitations of viral vectors such as host immune response, toxicity, and infections. Vectors include:

- Naked plasmid DNA (pDNA);
- Minicircle DNA (mcDNA);
- DNA and RNA oligonucleotides;
- DNA transposons; and
- Cell based gene transfer

Generally these non-viral vectors require a delivery method, for the DNA to enter the host genome. Additionally, these methods can also be used to increase transduction efficiency.

7.4 GENE THERAPY AND PAH

The lung is considered an ideal candidate for gene therapy. As mentioned above, the scope for varied delivery methods, the potential for combining these methods and also the range of lung diseases which gene therapy can target is wide. In particular, gene therapy for PAH is ideal for several reasons: firstly, it has been shown that inhalation of gases and mediations can affect the small pulmonary arteries; secondly, accessing the pulmonary arteries via the venous system is also advantageous [128]; and lastly, there are many different targets for therapy, including NO, BMPR2, CAV-1, ALK-1, ENG and BMP9. However, difficulty in targeting to the pulmonary endothelium, carcinogenicity and potential global affects of gene alteration are limiting factors for this gene therapy approach. Despite this, there have also

been many ways to overcome these drawbacks including using progenitor and mesenchymal stem cells as gene delivery vehicles as well as endothelial promoters inserted into the viral genome, such as *flt-1* (VEGFR1) and bi-specific conjugates which mask viral tropism and target to the pulmonary endothelium [134].

7.4.1 *BMPR2 Replacement Therapy*

Previously, Reynolds *et al* have delivered BMPR2 to the pulmonary endothelium using targeted Ad vector technology [29]. The BMPR2 gene is inserted in to the genome of the Ad vector, this is incubated with a bi-specific conjugate (FAB-9B9), where one end is specific for the knob domain on the Ad virus and the other is specific for angiotensin converting enzyme (ACE), which is highly expressed in the lung, particularly in individuals with PAH [135]. This approach has been used in two PAH rat models, the hypoxia and monocrotaline models (MCT) and a BMPR2 mutation transgenic mouse model with success in ameliorating PAH [29, 136]. Whilst the therapeutic outcomes are positive, the molecular mechanisms of how this is achieved are still yet to be determined. Nevertheless, this is a useful strategy to not only study potential therapies for PAH, but also examine the molecular pathogenesis and changes in the disease.

CONCLUSION

Pulmonary arterial hypertension is a complex and devastating disease. Though classified as a rare disease, for those individuals diagnosed, quality of life is severely reduced and despite a recent era of therapeutics, survival remains poor. Current treatments do not have the ability to reverse the pathological changes that occur, such as vessel remodelling, formation of plexiform lesions and right ventricular hypertrophy. The causal link between mutations in *BMPR2* and PAH make this disease an ideal candidate for gene and cell therapy. Reduced *BMPR2* expression is seen not only in familial PAH, but other primary and secondary forms of PH, demonstrating that *BMPR2* modulation as a potential therapy has a broader application for all PAH patients, not only those with the mutation. Importantly, only 20% of individuals with a *BMPR2* mutation develop the phenotype, suggesting that they require a 'second hit' or 'trigger' to develop the disease. This leads to the notion that they only require a 'reversal trigger' to potentially reprogram the abnormal cellular behaviour that occurs and prevent further development of the disease, potentially reversing it.

The complex molecular pathology of PAH lends to many cell types typically being involved and interaction between cells is a critical mechanism for pathogenesis and disease severity. Endothelial and smooth muscle cells are found to be dysfunctional and are critical in the recruitment of chemokines, cytokines and other inflammatory cells. Therefore, targeting therapy towards the pulmonary endothelium with the view that this can alter not only the behaviour of ECs, but this will also have an impact on how these cells cross-talk to surrounding cells and have an influence on their activity. In PAH patients, EPCs are also dysfunctional and are reduced in number.

Therefore, they are not only an ideal candidate to package desired genes such as BMPR2 safely to the pulmonary endothelium, as well as being a potential therapeutic target themselves.

BMPR2 replacement therapy is aimed at restoring BMPR2 to normal levels. Previously, Reynolds *et al* have succeeded in delivering BMPR2 to the pulmonary endothelium using a targeted Adenoviral vector system, showing an attenuation of PAH [29]. However, the precise mechanism of how this occurs remains unknown, and the limiting factors of viral vector systems are yet to be overcome.

Herein, I look to assess the cellular signalling that is altered following our Ad-vector gene delivery of BMPR2, identify any novel mediators of disease reversal or therapeutic targets and develop a BMPR2 cell therapy to overcome the known limitations of Ad-vector technology. Specifically, I aim to:

1. obtain a better understanding of the molecular pathways involved in PAH pathogenesis and/ or the reversal of PAH;
2. identify novel targets for PAH therapy; and
3. develop and assess an effective and clinically applicable cell therapy for PAH

Part II

GENERAL METHODOLOGY

The methodology, materials and reagents used for all experiments in this study are described herein.

METHODS AND MATERIALS

9.1 CELL CULTURE

HEK-293 and A549 cells were grown in Dulbecco's Modified Eagle's Medium (DMEM) with HEPES buffer: Nutrient Mixture F12 (50:50) (Gibco, Invitrogen Corporation, Grand Island, NY), with 10% FCS, L-glutamine (2mM), Penicillin (100 µg/mL) and Gentamycin (50 µg/mL). CHO and CHO-2C2 cells were grown in Nutrient Mixture F12 medium (Gibco, Invitrogen Corporation, NY, USA) with 10% FCS, supplemented as above, with G418 (100 µg/mL) for CHO-2C2 cells. All cells were grown in a 5% CO₂-atmosphere at 37°C.

9.2 ADENOVIRAL VECTOR PREPARATION

9.2.1 *Virus Amplification*

AdCMVBMPR2myc, a replication-incompetent serotype 5 adenovirus vector, previously created and described [137] was used with control virus, AdTrackLuc, AdCMVGFP or AdCMVLuc. These contain the cytomegalovirus promoter, which drives the expression of the gene of interest (BMPR2), reporter gene luciferase (Luc) or green fluorescent protein (GFP).

To amplify these viruses, HEK-293 cells were seeded onto 20 x 150 cm² culture plates for 3 days and then infected with the relevant virus in 2% FCS DMEM/F12 medium. After 4-5 h incubation, medium was supplemented with 1.5 mL FCS. After four days of incubation, the virus was harvested and collected as a batch for purification.

9.2.2 Cesium Chloride Purification of Virus

Cesium chloride (CsCl) centrifugation and dialysis was used to purify each virus. The viral amplification batch including the cells is freeze/thawed three times at -20°C (dry ice) and 37°C (water bath). The batch is then pelleted by centrifugation at 3000 $\times g$ at 4°C for 20 mins. The supernatant containing the virus is removed for the CsCl purification. This is done by loading 4 mL of 1.33 CsCl (454.2 g CsCl/mL in 5 mM HEPES, pH 7.8) into an Ultraclear polycarbonate 12 mL tube (Beckman Coulter, Lane Cove, Australia). This is underlayered with 4 mL of 1.45 CsCl (609.0 g CsCl/mL in 5 mM HEPES pH 7.8). The viral supernatant is drop-wise added to the top of the layered CsCl, and centrifuged at 18,000 rpm for 2.5 h at 4°C . The tubes were then carefully erected on a tort stand, and using a 19 G needle, a hole was created in the bottom of the tube so that the liquid can only drip at a slow rate out of the tube for collection of the bottom viral band only [Figure 23](#). A second round of CsCl gradients was made with the collected virus placed drop-wise on top, and topped up with cold PBS. These were centrifuged at 25,000 rpm overnight at 4°C . Collection of the bottom (main) band was repeated as stated above [Figure 23](#). CsCl was then removed via dialysis, where the virus was diluted to 1 mL in the dialysis buffer (10% glycerol, 10 mM HEPES, 1 mM MgCl_2) and added to a SlideALyzerTM dialysis cassette (ThermoFisher Scientific, Scoresby, Australia), which was then submerged 600 mL of dialysis buffer for 1 h with gentle stirring at 4°C . This was repeated 3 times with fresh dialysis buffer, and on the third change the cassette was left overnight with gentle stirring at 4°C . Following dialysis, the virus was removed carefully from the cassette, aliquoted and stored in -70°C .

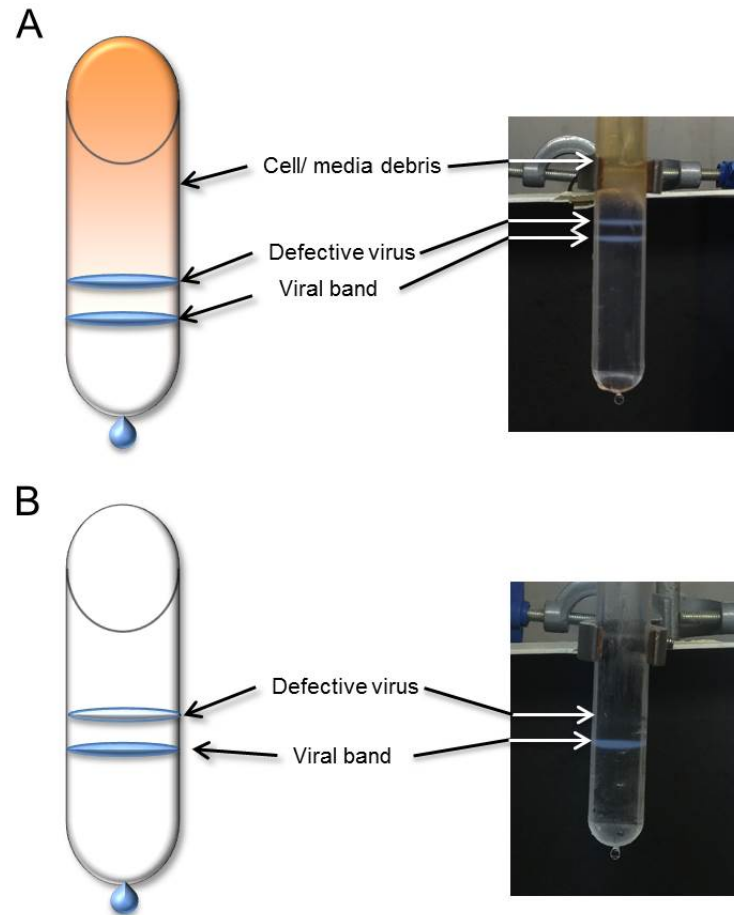


Figure 23: Cesium chloride centrifugation purification method. A. Separation of viral band (lower blue band) from defective virus (upper blue band) and cell/ media debris (yellow). Collection of the viral band is performed by creating a hole in the bottom of the tube for the liquid to slowly drip out into a collection vessel; and B. For further purification, a second centrifugation step is used to separate the viral band (lower band) and left over defective virus (upper, faint blue band), the lower blue band is again collected for dialysis.

9.2.3 Particle and Infectious Titre

Particle titre was determined by optical density at 260 nm (OD₂₆₀) using a spectrometer. The infectious titre was obtained by conducting a 50% tissue culture infectious dose (TCID₅₀) assay [138]. Briefly, HEK-293 cells were seeded into 2 x 96 well plates at 1×10^5 cells/mL. Serial dilutions were made of the virus and placed on the plates from 10^{-6} to 10^{-13} Figure 24. Following 10 days of incubation, each well was examined for cytopathic effects (CPE), where the cell morphology is changed due to the virus infect-

ing the cell. Calculation of how many wells contain CPE gives the viral titre in plaque forming units (pfu)/mL.

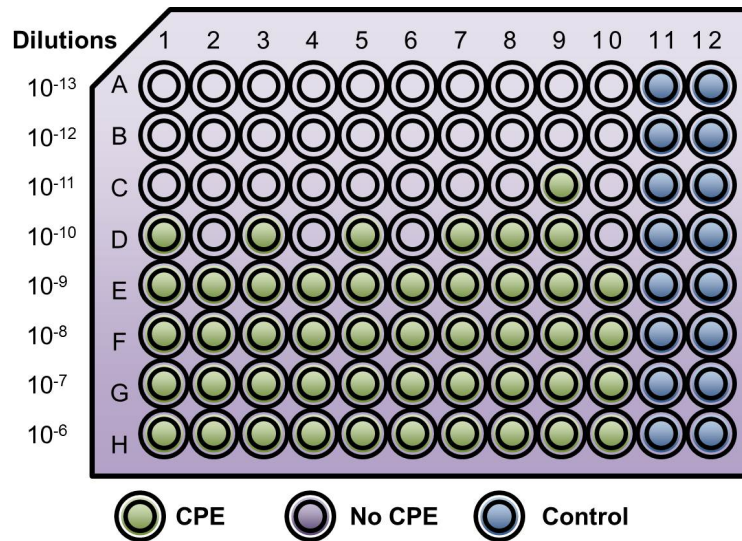


Figure 24: TCID₅₀ Assay layout, including typical dilutions and results.

9.3 RAT DERIVED EPC ISOLATION AND CHARACTERISATION

9.3.1 *Extraction, Isolation and Culture of Rat derived EPCs*

Rats were sacrificed with CO₂ and an incision was made in the lower lumbar area to the tip of the knee. The skin was separated from the connective tissue and the overlaying muscle was cut to expose the femur. Once the bone was free from muscle and tissue, it was cut from the hip and knee joints and placed in EGM-2MV (Lonza, Walkerville, USA) media with antibiotic/ antimycotic agents. The bone was flushed out by cutting off the epiphyses to expose the bone marrow cavity, and using a 10 mL syringe and a 25 G needle the bone marrow was flushed out with the seeding media EGM-2MV (Lonza) and 20% FCS, and seeded into a T₇₅ flask. Cells were grown in a 5% CO₂-atmosphere at 37°C. Media changes were started 72 h post-seeding, and then every 48 h. Following 6 days of culture, cells were washed with HEPES buffer (Lonza), lifted with trypsin/ EDTA and

treated with Trypsin Neutralising Solution (Lonza) and counted using a hemocytometer. Viability was obtained using Trypan Blue (Sigma, St Louis, MO, USA) staining.

9.3.2 *Rat derived EPC characterisation*

Rat derived EPCs (r-EPCs) are characterised in two ways:

(1) *Morphologically*: via fluorescence microscope stained with phalloidin-Alexa 488 to label F-actin and TO-PRO-3-nuclear counter-stain.

(2) *Flow cytometry*: where cells are stained with **Primary Antibodies**: Sheep anti-CD34, CD106, CD31; and **Secondary Antibodies**: donkey anti sheep FITC and goat anti rabbit PE to confirm endothelial like properties. Performed on the Canto II, Becton Dickinson Biosciences, Franklin Lakes, NJ, USA.

Analysis was performed on FACS – Diva™ (BD). Analysis was performed by looking for a positive staining shift of stained cells when compared to an unlabelled control. A shift in a histogram peak to the right of the plot is considered to be positive staining and increased fluorescence. This technique was used due to the homogeneous nature of the cell population.

9.3.3 *Flow Cytometry*

All cytometric analyses were optimised and performed on a Canto II flow cytometer (BD). Cells were washed with HEPES (Lonza), then lifted with trypsin/ EDTA (Lonza) and, once lifted the trypsin is neutralised with Trypsin Neutralising Solution (TNS) (Lonza). Cells were pelleted and

washed with PBS via centrifugation at 2500 rpm for 2 mins. Cells were re-suspended in FACS buffer (1% Bovine Serum Albumin (BSA) in PBS), blocked with IgG for 10 mins, and then incubated with: mouse anti CD31 (BD Pharmingen, BD Biosciences), sheep anti CD34 (R&D Systems, Minneapolis, MN, USA), and rabbit anti CD106 (AbCam, Cambridge, UK) primary antibodies for another 10 mins at RT. Cells were then washed in 2 mL FACS buffer at 2500 rpm for 2 mins. The supernatant was discarded and the cell pellet was re-suspended in 1 drop of FACS buffer. Tubes are thoroughly mixed before they are loaded onto the flow cytometer.

9.3.4 *Rat derived EPC AdCMVGFP Transduction Studies*

r-EPCs and A549 cells, a known readily infected cell line as the control, were seeded onto a 24 well plate at 5×10^4 cells/well. Cells were infected with AdCMVGFP at 0, 10, 100 and 200 pfu/cell. After 48 h of incubation, cells were viewed under a confocal microscope (Nikon C1-Z Confocal Microscope, Tokyo, Japan) to assess the proportion of cells positive for GFP.

9.3.5 *Rat derived EPC Transduction with AdCMVBMPR2myc*

r-EPCs were seeded in T₇₅ flasks for animals studies (1×10^6 cells/flask) and in triplicate in 6 well plates for the validation studies (1×10^5 cells/well) and grown for 2 days. Cells were infected at 200 pfu/cell with AdCMVBMPR2myc or AdTrackLuc or media only. Cells were quiesced in EGM-2 MV containing 0.05% FCS for 24 h, stimulated with 50 ng/mL of BMP7 (R&D Systems, Minneapolis, MN) for 90 mins before lysing. Cells were washed with ice cold HEPES buffer (Lonza) and lysed with Takahashi lysis buffer [139] with protease (Roche Diagnostics, Indianapolis, IN, USA) and Halt phosphatase inhibitor cocktails (ThermoScientific, Rockford, IL, USA) 48 h post infection. Protein concentration was determined using the

detergent compatible Bio-Rad DC protein assay kit (Bio-Rad Laboratories, Hercules, CA, USA).

9.3.6 *Analysis of AdCMVBMPR2myc Transduction in r-EPCS*

BMPR2 and myc analysis was conducted via immunoblot. Protein samples (15µg) were combined with McKenzie Loading Buffer [140] and boiled at 95°C for 8 mins prior to being loaded into self-made 12% polyacrylamide/SDS gels, and Turbo-Transblotted to Trans-Blot Turbo Mini nitrocellulose membranes (BioRad). Membranes were blocked with Odyssey Blocking Buffer (OBB) (LI-COR, Lincoln, NA, USA) then incubated overnight at 4°C with goat anti BMPR2 (1:500) (Santa Cruz, Dallas, TX, USA) and rabbit anti myc (1:1000) (Cell Signaling, Boston, MA, USA) in OBB. Membranes were washed and incubated with donkey anti goat flouochrome 680 and goat anti-rabbit flouochrome 800CW secondary antibody (LI-COR). Immunodetection was performed via the Odyssey System including quantification (LI-COR Odyssey B446 System). All membranes were stripped with NewBlot Stripping Buffer (LI-COR) and re-probed with rabbit anti β-actin (Cell Signaling) (1:1000).

9.4 PHYSIOLOGICAL STUDIES

9.4.1 *Construction of Fab-9B9: ACE Targeted Gene Delivery Conjugate*

Construction and validation of Fab-9B9 has previously been described [141]. Briefly, Fab and MAbs 9B9 were derivatized with the bi-functional crosslinker N-succinimidyl 3-(2-pyridyldithio)propionate (SPDP) (Pierce, Rockford, IL, USA). SPDP was combined with 9B9 or Fab in PBS at a molar ratio of 4

SPDP:1 antibody and incubated with shaking at RT for 30 min. The pH of Fab was lowered by adding 0.1 vol of 1 M sodium acetate, pH 4.5, and then the Fab was reduced by adding 1 mg of dithiothreitol (Bio-Rad). After 5 min incubation, the reduced Fab was passed through a PD10 column (Pharmacia, Uppsala, Sweden), equilibrated in borate buffer, and then added immediately to the derivatized 9B9 and shaken at RT overnight. The conjugate mixture was purified by gel filtration (Superose 12 column; 2 Pharmacia) in borate buffer, pH 8.5. Monomeric Fab and 9B9 were discarded, and fractions larger than 150 kDa were assessed for specificity.

9.4.2 Validation of ACE Targeted Gene Delivery *in vitro* via Luciferase Assay

CHO cells and the high ACE expressing CHO-2C2 cells were seeded in a 24 well plate at 2.5×10^4 cell/ well. Chromatography fractions of Fab-9B9 conjugates were diluted (neat, 1/10, 1/100, 1/1000 & 1/10,000) and incubated with AdCMVLuc for 45 min at RT. Each dilution was added to infecting medium (2% FCS F12), cells were infected for 1 h, then washed with PBS and medium replaced with 10% FCS medium. Following 24 h of incubation a luciferase assay was performed with the Promega Luciferase System (Promega, Madison, WI, USA) on a Luminometer (Berthold, Moorebank, NSW, Aus). Samples were normalised to the amount of protein using the detergent compatible Bio-Rad DC protein assay kit (Bio-Rad). For validation results, see [Appendix A](#).

9.4.3 Validation of ACE Targeted Gene Delivery *in vivo* via Luciferase Assay

In vivo validation of Fab-9B9 has previously been described [141]. Briefly, AdCMVLuc (5×10^{10} pfu/cell/rat) was complexed with 7 μ g Fab-9B9 for

30 min at room temperature. The total volume was brought up to 150 μ L with sterile PBS. Rats were injected via the lateral tail vein, then sacrificed three days later. Lungs and livers were harvested into 50 mL polypropylene tubes and snap frozen in ethanol/dry ice.

For luciferase analysis, entire organs were ground to a fine powder using a mortar and pestle cooled in an ethanol/dry ice bath. 200 mg of organ powder was weighed and placed in a 1.5 mL polypropylene tube. Subsequent processing for luciferase activity was performed using a Promega luciferase assay system kit (Promega). Tissue powders were lysed in 300 μ L of cell lysis buffer, vortexed briefly and incubated at room temperature for 10 mins. Samples were then subjected to three freeze thaw cycles to ensure complete lysis. Tubes were centrifuged at 15,000 rpm at 4°C and supernatant analysed on a Luminometer (Berthold) for luciferase activity according to the manufacturer's instructions. The protein concentration of lysate was determined using a Bio-Rad detergent compatible (DC) protein assay kit (BioRad). For validation results, see: [Appendix A](#).

9.4.4 *Animals*

Animal protocols were approved by the SA Pathology/CAHLN and University of Adelaide Animal Ethics Committees. Experiments were performed on male Sprague-Dawley (SD) rats and housed at the SA Pathology Animal Care Facility. AEC approval: 2/13.

9.4.5 *Bio-Distribution Studies of Rat derived EPCs in Sprague-Dawley Rats*

r-EPCs were transduced as outline above with 200 pfu of AdTrackLuc for 48 h, washed, counted and re-suspended in 250 μ L of PBS. Rats aged 6 weeks, were IV injected with 7×10^7 cells/rat ($n=3$), with one rat uninjected.

1 h later, one rat was IP injected with *in vivo* grade luciferin (Promega). A time course was created with this first rat to ascertain the optimal scanning time for the peak of luminescence. Following the advice from Adelaide University Microscopy staff the first scan was 10 mins following injection, where the animal was placed in the IVIS Lumina XRMS Multi-species Optical and X-Ray imaging system (PerkinElmer, Waltham, MA, USA) and imaged every 5 mins until a peak was detected. After obtaining the peak luminescence, the animal was sacrificed, and the lungs and liver extracted for imaging separately. The other 3 rats were imaged over the optimised time period.

9.4.6 Protein Analysis: 1 hour post BMPR2-EPC injection

r-EPCs were transduced as outlined above with AdCMVBMPR2myc for 48 h at 200 pfu. Cells were lysed, washed, counted and re-suspended in 250 μ l PBS. Rats were injected IV with 7×10^7 cells/rat ($n=3$), and 1 h later, rats were humanly killed via CO₂ asphyxiation and lungs, heart, liver, spleen and kidneys were removed and snap frozen in dry ice. Right lung lobes were processed into powder using a mortar and pestle pre-cooled in dry ice. The powder was re-suspended in lysis buffer (Long *et al*) [5] and homogenised until homogeneous. Samples were placed on ice for 10 mins, and spun down at 40,000 g for 30 mins at 4°C. Protein concentration was obtained using the DC protein assay (BioRad).

Protein samples (20-35 μ g) were combined with McKenzie Loading Buffer [140] and boiled at 95°C for 8 mins prior to being loaded into self-made 10% polyacrylamide/SDS gels, and Turbo-Transblotted to Trans-Blot Turbo Mini nitrocellulose membranes (BioRad). Membranes were blocked with OBB (LI-COR) then incubated overnight at 4°C with rabbit anti p-Smad1/5/8, p-Smad3 (1:200), Smad3, (1:1000) (Cell Signaling) and goat anti BMPR2

1:1000 and rabbit anti Smad1/5/8 (1:1000) (Santa Cruz) in OBB. Membranes were washed and incubated with goat anti rabbit flouochrome 800CW and donkey anti goat 680 secondary antibodies (LI-COR). Immunodetection was performed via the Odyssey System including quantification (LI-COR Odyssey B446 System). All membranes were stripped with NewBlot Stripping Buffer (LI-COR) and re-probed with rabbit anti β -actin (Cell Signaling) (1:1000).

9.4.7 *Rat Monocrotaline Model*

Male SD rats (6 weeks) were given either a saline or MCT injection (60 mg/kg SC), subcutaneously to the left thigh. 10 days after this, rats were given tail vein injections of the relevant treatment or control injections via the lateral tail vein using 27 G insulin syringes (Terumo, Elkton, MD).

9.4.8 *AdBMPR2 Studies: 2 and 10-day time-points*

Male SD rats (290-430 g) were assigned to four groups (n=8/group): saline, MCT Only (60 mg/kg SC), MCT+irrelevant control virus (AdTrackLucFab-9B9) and MCT+treatment virus (AdBMPR2Fab-9B9). Rats were given MCT via subcutaneous injection and 10 days after, rats in the MCT+virus groups were given tail vein injections of the relevant virus+Fab-9B9 (5×10^{10} pfu/cell/rat). For each dose, the virus was incubated with 7 μ l Fab-9B9 for 30 min at RT before injection. The total volume was brought up to 250 μ l with sterile PBS. Injections were via the lateral tail vein using 27 G insulin syringes (Terumo, Elkton, MD).

9.4.8.1 2-day Time-point

2 days following viral injection the fulton index (FI) was assessed. FI is measured by removing the whole heart, taking the weight, and then cutting the right ventricle (RV) off and re-weighing the RV only. The left ventricle (LV) and septum (S) are then weighed. The FI is calculated by $RV/LV+S$. FI is technically simple and a robust measurement. Hemodynamic assessment of PAH was not performed for this time-point due to the expected changes to be minimal and thus, not technically robust.

9.4.8.2 10-day Time-point

10 days following viral injection, rats in each experimental group were anaesthetised with ketamine (100 mg/kg IP) and xylazine (20 mg/kg) IP and hemodynamic measurements were taken via left carotid arterial and right subclavian vein catheters [Figure 25](#). To do this, a small transverse incision was made in the left carotid artery [Figure 25](#) into which a PE50 catheter was inserted. The PE50 catheter was prepared with a rapid response, Teflon-coated, thermocouple (IT-21, Physitemp Instruments, Clifton, NJ), which was passed through the lumen of a Tuohy-Borst Adapter (Model TBA-6, William A. Cook Australia Pty. Ltd. Brisbane, Australia). The thermocouple was slowly advanced into the aortic arch to measure systemic pressure and arterial blood temperature. A second transverse cut was made in the proximal right subclavian vein [Figure 25](#) into which a PE10 catheter was placed (Portex, Kent, UK). A metal catheter is slid over this PE10 catheter, advanced over the collarbone and slowly advanced into the right ventricle and pulmonary artery to measure and record pressures [Figure 25](#). All catheters were attached to pressure transducers (Transpac IV, Abbot, Ireland) coupled to amplifiers (ADInstruments, Bella Vista, NSW, Australia). All signals were captured using a bio-amplifier and visualised using LabChart software (ADInstruments). FI is measured as outlined in **Section 9.4.8.1**.

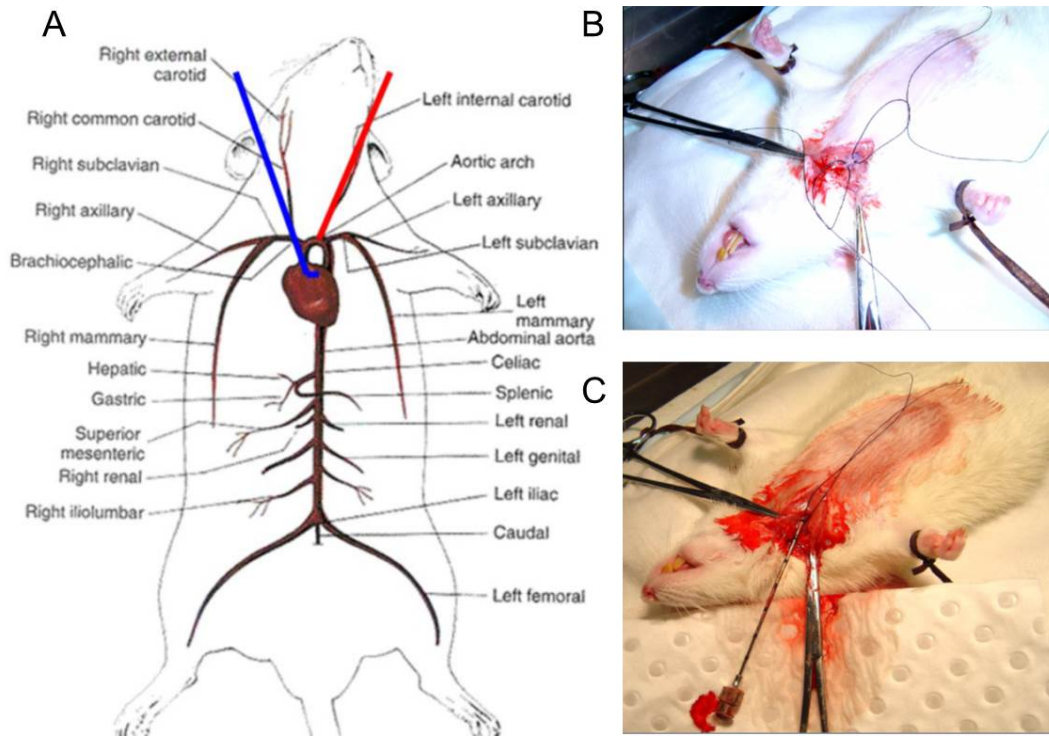


Figure 25: Placement of catheters in hemodynamic measurements. A. Schematic of catheter placement in the rat: left carotid artery (red) and right subclavian vein (blue); B. Isolation of the left carotid artery; and C. placement of metal catheter to access the right ventricle to obtain the right ventricular systolic pressure and mean pulmonary arterial pressure.

9.4.9 *AdBMP2-EPC Studies: 10-day Time-point*

Male SD rats (250-380 g) were assigned to three groups (n=8/group): MCT Only (60 mg/kg SC), MCT + EPCs and MCT + BMP2-EPCs (r-EPCs that have been transduced with AdBMP2 at 200 pfu/cell for 48 h). Rats were given MCT via SC injection and 10 days after, rats in the MCT + EPCs and MCT + BMP2-EPCs groups were given tail vein injections of the relevant EPC treatment (1×10^6 cells/rat). For each dose, the cells were prepared by being lysed, washed, counted and re-suspended in 250 μ l PBS. The total volume was brought up to 250 μ l with sterile PBS. Injections were via the lateral tail vein using 27 G insulin syringes (Terumo, Elkton, MD).

18-21 days following the MCT injection, the rats undergo hemodynamic assessment as outlined in **Section 9.4.8.2**.

9.5 ANIMAL TISSUE PROCESSING AND ANALYSIS

9.5.1 *Tissue Extraction and Preparation*

Following hemodynamic analysis, rats were humanely killed via CO₂ asphyxiation. A transverse cut is made at the base of the rib cage, and the chest cavity is opened with a cut from the xiphoid process, following the sternum to the apex of the ribcage. The chest cavity is opened with chest expanders and the dural lining around the heart is cut, exposing the heart. A 22 G IV catheter (BD) is inserted into the RV, a 5 mL syringe (BD) is used to collect as much blood as possible from the heart and lungs. Once the blood flow stops, catheter tubing with a 50 mL reservoir erected 40 cm above the animal on a torte stand is attached to the catheter. Heparin infused PBS is forced through the RV, and throughout the lungs. An incision is made in the LV for fluid to exit, allowing a steady flow through the heart and lungs. Following this perfusion, the right lobes are tied off with a suture, and the left lobe is perfused with 10 mL of 10% formalin (ACE Chemical Company, Adelaide, AUS). The catheter is taken out of the RV, and a cut is made in the neck of the rat, exposing the trachea. A suture is placed around the trachea, an incision is made in the trachea and the 22 G IV catheter is placed and secured with the suture down the trachea towards the lungs. The left lobe is then inflated with 20 mL of 10% formalin (ACE). Once fully inflated the left lobe is excised and placed in a 50 mL pot with 10% formalin (ACE), and left to fix overnight. The right lobes are excised and placed in either lysis buffer ([5]) or RNALater®. After 24 h the left lobe is cut from the apex to the base of the lung, into 3 sections and processed for *en bloc*.

Right lung lobes stored in lysis buffer were processed into powder using a mortar and pestle pre-cooled in dry ice. The powder was suspended in lysis buffer (Long *et al*) and homogenised until homogeneous. Samples were placed on ice for 10 mins, and spun down at 40,000 g for 30 mins at 4°C. Samples were aliquot and stored in -70°C until used for immunoblot analysis as outlined in **Section 9.5.6**.

9.5.2 *Smad and Non-Smad Pathway Analysis*

Protein samples (20-35 µg) were combined with McKenzie Loading Buffer [140] and boiled at 95°C for 8 mins prior to being loaded into self-made 10/12% polyacrylamide/SDS gels, and Turbo-Transblotted to Trans-Blot Turbo Mini nitrocellulose membranes (BioRad). Membranes were blocked with OBB (LI-COR) then incubated overnight at 4°C with rabbit anti p-Smad_{1/5/8}, p-Smad₂, p-Smad₃ (1:200), Smad₁, Smad₃, (1:1000), PI3K and p-p38 MAPK (1:1000) (Cell Signaling) in OBB. Membranes were washed and incubated with goat anti-rabbit flouochrome 800CW secondary antibody (LI-COR). Immunodetection was performed via the Odyssey System including quantification (LI-COR Odyssey B446 System). All membranes were stripped with NewBlot Stripping Buffer (LI-COR) and re-probed with rabbit anti β-actin (Cell Signaling) (1:1000).

Note: Antibody selection for Smad proteins were dependent upon varying availability and effectiveness against the intended target. Substituting p-Smad₂ with p-Smad₃ during tissue analysis was due to the release of a more reliable antibody. Furthermore, normalising with β-actin for p-Smad_{1/5/8} was super-seeded with the release of a total Smad_{1/5/8} antibody.

9.5.3 RNA extraction

RNA extraction and purification was performed using the Ambion mirVANA™ miRNA Isolation kit (ThermoFisher). Tissue was crushed in a pre-cooled mortar and pestle to a powder, re-suspended and homogenised in a pre-chilled Lysis/Binding Buffer. miRNA Homogenate Addition was added and following vortexing, the sample incubated on ice for 10 mins. Acid-Phenol: Chloroform was added, the sample was vortexed and centrifuged at 10,000 g for 5 mins. Following centrifugation, the upper aqueous phase was removed, 100% ethanol was added and samples are passed through a filter cartridge via centrifugation. Samples were then washed 3 times with wash buffers and eluted using the 95°C Elution solution. Samples were aliquot and frozen in -70°C freezer. The RNA concentration and purity ratio (A₂₆₀/A₂₈₀) was measured on a spectrometer (BioRad SmartSpec Plus).

9.6 MICROARRAY STUDIES

Following RNA extraction, samples were taken to the Adelaide Microarray Centre (University of Adelaide, Adelaide, Australia) and ran through a Bioanalyzer (Agilent Technologies Inc, Santa Clara, USA) to measure their RNA integrity score (RIN). From this, the best 4 samples (as defined by the highest RIN [Appendix B](#)) from each group were chosen for the Affymetrix® Rat Gene Array (Affymetrix, Santa Clara, CA, USA). In close consultation, preliminary analysis was conducted by the Adelaide Microarray Centre using Partek® Genomics Suite® (Helios, Singapore). The resultant list of significant genes are then given back for further pathways analysis.

9.6.1 *Ingenuity Pathway Analysis*

Results of the microarray are returned in the form of an excel spreadsheet containing a list of all genes which are differentially expressed between the groups of interest. This excel spreadsheet was uploaded into the Ingenuity Pathway Analysis (IPA) (Qiagen) software program. Analysis using IPA allows identification of canonical on non-canonical pathways that are significantly altered between the treatment groups. Single molecules and genes are identified as either significantly increased or decreased, as well as effects on known biological processes, for example angiogenesis, cell growth and death and cell migration. Signalling 'maps' are created by the program, and all are given in a full report.

9.7 STATISTICAL ANALYSIS

Data are expressed as mean \pm standard error (SEM). One-way ANOVA or 2-tailed *t*-test was used for between group analysis, when the *F* value indicated significance, the Student-Newman-Keuls multiple comparison test was used (GraphPad Prism, La Jolla, CA, USA). A value of $P < 0.05$ was considered to be statistically significant.

Part III

RESULTS

10.1 OVERVIEW

BMPR₂ expression in PAH is reduced, not only in subjects with a known BMPR₂ mutation, but also in primary and secondary PH, as well as in commonly used PH animal models. The rationale for up-regulating BMPR₂ via gene therapy is to restore BMPR₂ to functional levels, and thus reverse the disease. Using a targeted (Fab-9B9) Adenoviral vector, we were previously successful in delivering functional BMPR₂ to the pulmonary endothelium [134] and have shown amelioration of PAH in both the MCT and chronic hypoxia rat models [29]. Additionally, I have demonstrated in an *in vitro* model that up-regulation of BMPR₂ in human lung blood vessel derived microvascular endothelial cells (HMVEC-LBI) results in increased activation of the BMPR₂ mediated Smad_{1/5/8} pathway and a decrease in the TGF- β mediated Smad_{2/3} pathway [Figure 27](#) [142]. I hypothesise that similar changes in the Smad profiles will be seen in the *in vivo* model following our targeted gene delivery of BMPR₂.

PAH is induced in SD rats via SC injection of the toxin, MCT. As outlined in [Chapter 5](#), MCT causes severe PAH in these rats and is a widely used model for investigating suitable therapy options as well as molecular mechanisms of PAH. Ultimately, successful therapy is aimed at reversing the vascular remodelling that occurs in PAH, as well as showing an alleviation of increased pulmonary pressures, both hallmarks of human PAH. Key measurements are undertaken to assess successful reversal of PAH. The Fulton Index (FI) is the measurement of right ventricular hypertrophy (RVH) which is typically increased in PAH due to the increase in pulmonary vas-

cular resistance (PVR). By using an animal model such as the MCT-induced PAH model, FI is easily measured and expected to be reduced with PAH treatment. Other hemodynamic assessments such as right ventricular systolic pressure (RVSP) and mean pulmonary arterial pressure (mPAP) are increased in human PAH as well as in the MCT-induced PAH model and therefore are measured to assess if a decrease occurs following PAH treatment [Figure 26](#).

Experimental controls are essential when using an animal model to assess the effectiveness of a treatment. PAH models require hemodynamic assessment, and there are many factors which can impact on these measurements that need to be considered. Mean systemic arterial pressure (mSAP) and heart rate (HR) are important secondary measurements that are essential for ensuring consistency in animal health at the time of surgery. For example: if an animal's mSAP is low, the RVSP and mPAP will also be low, potentially giving a false impression of successful treatment if not accounted for. Body weight (BW) is another internal control as an indicator of animal health across all the treatment groups.

A variety of treatment groups is essential to ensure that you have the appropriate positive and negative controls in an animal model. In this model, saline treated animals are used as a reference 'normal' control to assess the efficacy of the AdBMP2 treatment and as a comparison to assess MCT induction of PAH. Saline animals have an SC injection of saline only at the same time as the other animals receive the MCT injection, thus these animals are not expected to develop PAH. Saline and MCT Only animals do not receive any subsequent treatments. Comparison of the saline and MCT animals allows positive identification of PAH induction or no induction, when comparing the FI, RVSP and mPAP between these groups.

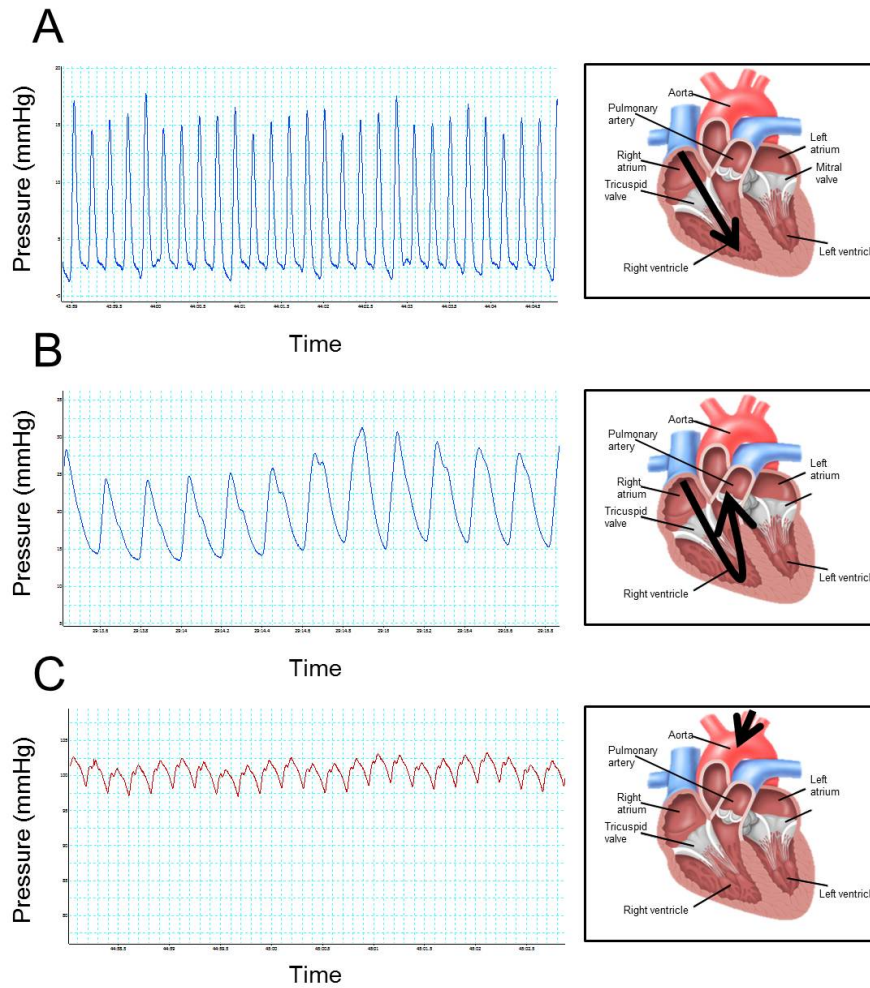


Figure 26: Example of hemodynamic pressure traces taken from a healthy rat via a catheter in the left carotid artery extended to the aortic arch and a second catheter in the right subclavian vein advanced into the right ventricle. A. Right ventricular systolic pressure with corresponding schematic showing catheter placement in the right ventricle; B. pulmonary arterial pressure with corresponding schematic showing catheter placement in the pulmonary artery; and C. systemic arterial pressure with corresponding schematic showing catheter placement in the aortic arch.

For this study, a viral vector was used as a vehicle for the gene therapy. Therefore, it is essential to include an irrelevant virus control group which has MCT induced PAH, and also treatment via IV injection of an Ad with an inserted gene that is irrelevant, which in this case, was Luciferase and GFP (AdTrackLuc). This is given at the same time-point as the gene therapy vector, AdBMP2, and also for consistency, is incubated with the ACE targeting conjugate Fab-9B9. The reasoning for including the control

Ad vector is that viral treatment itself may cause physiological changes, irrespective of what target gene the vector is carrying. Therefore, it is critical to rule out that these changes can influence the FI or hemodynamic measurements that are taken to assess the PAH in this model. Thus, MCT + AdTrackLucFab-9B9 is a negative control group for the PAH treatment group MCT + AdBM_{PR2}Fab-9B9, where it is expected that the viral control group does not show any decreases in the FI or hemodynamic pressures, and thus allowing the assessment that any changes in the AdBM_{PR2} treatment is due to the BM_{PR2} inserted gene, and not the viral vector itself. These two viral groups are the most robust comparisons in this animal model.

Consistency of treatment time-points are also critical for robust comparisons between each treatment groups. MCT SC injections were given in animals at the same age (6 weeks) and all subsequent IV viral treatments were given 10 days following MCT injection. This time-point was chosen as it is the most widely accepted time-point that guarantees that PAH pathological changes are occurring, and pulmonary vascular pressures are increasing [77, 74, 77, 75, 5]. 10-13 days following to the IV injection of the gene therapy vector, hemodynamic assessment is performed. The spread of analyses over these days is due to the time consuming nature and technical difficulty of the procedure, making it impossible to conduct analysis of all animals in each group in the one day. To avoid any systematic effect, analyses were conducted from some animals from each group on each day. This takes the duration of the MCT treatment to 17-21 days, and at this time-point MCT Only and MCT + AdTrackLucFab-9B9 animals are becoming increasingly unhealthy. To take these animals out to a longer time-point would not only make it difficult for hemodynamic analysis, but it would also be unethical. Additionally, the Ad-vectors used in this study have a known transgene expression of around 2 weeks [141]. Thus, the 10 day

post treatment time-point was chosen to as an optimal point to evaluate the therapeutic effect on AdBMP2 treatment in the rat MCT model of PAH.

Smad signalling is directly mediated via the activation of BMP2 by BMP ligands [Chapter 4](#). Therefore, I hypothesise that our success in ameliorating PAH in the PAH animals models is due to changes in the BMP2 mediated Smad signalling profiles. Following the delivery of BMP2 and the resulting increase in BMP2 expression [29], it is logical to assume that there would be an increase in Smad1/5/8 signalling, which is known to be decreased in PAH [5]. Furthermore, the TGF- β mediated Smad2/3 pathway is increased in PAH, and thus I examined this pathway to assess whether there is a decrease following the AdBMP2 treatment. I proposed that the AdBMP2 treatment shifts the BMP2/TGF- β signalling axis from Smad2/3 to Smad1/5/8 and this is a factor for why we see the attenuation of disease following our treatment.

Prior to commencing these studies, as part of my honours thesis, vector validation *in vitro* was performed, whereby transduction of HMVEC-LBI *in vitro* with AdBMP2 was shown to up-regulate pSmad1/5/8 expression and down-regulate TGF- β mediated pSmad3 expression [Figure 27](#). It was thus rational to proceed to the following *in vivo* studies.

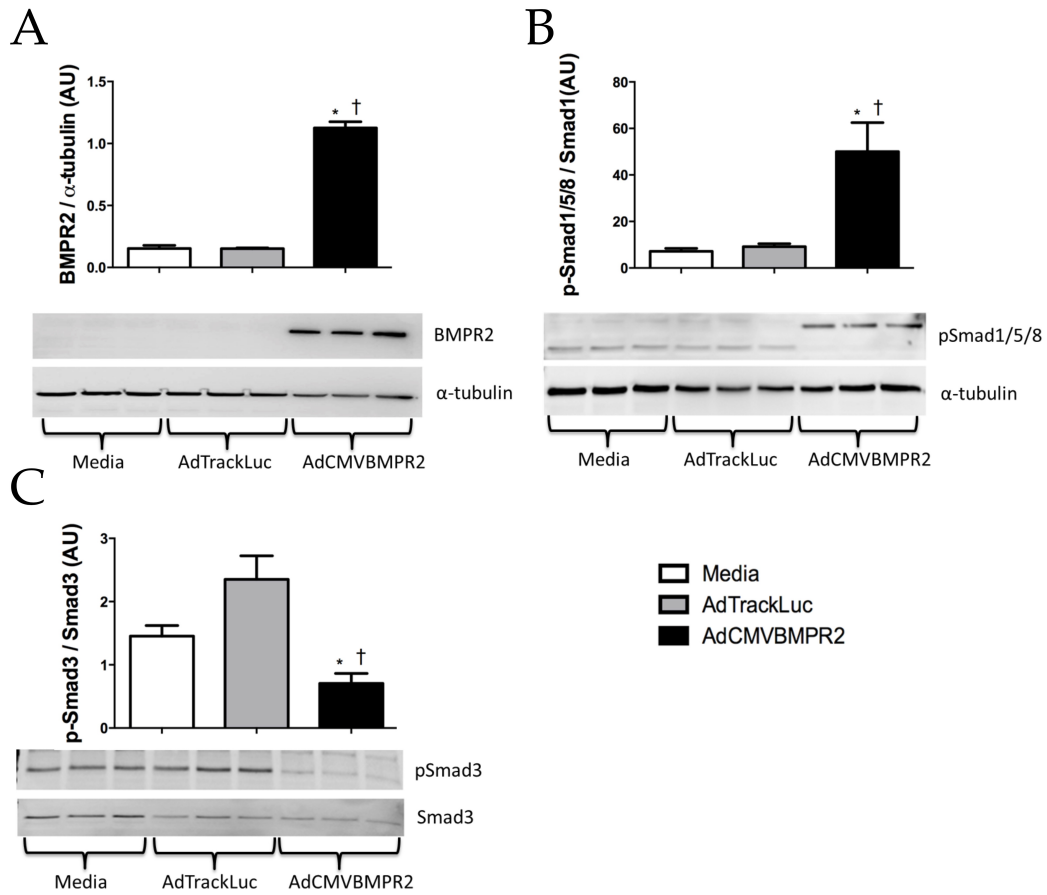


Figure 27: Up-regulation of BMPR2 mediated pSmad1/5/8 and down-regulation of pSmad3 following BMPR2 transduction of lung blood derived human microvascular endothelial cells. A. Immunoblot with quantification of increased BMPR2 expression; B. Immunoblot with quantification of increased phosphorylated-Smad1/5/8 expression; and C. Immunoblot and quantification of decreased phosphorylated-Smad3 expression. Values are mean \pm SEM for $n=3$. * compared with Media and \dagger compared with AdTrackLuc. $p < 0.05$.

10.2 AMELIORATION OF PAH: 10 DAYS FOLLOWING ADBMPR2 TREATMENT

This experiment comprised of the following groups: Saline as a healthy control, MCT Only as a disease only control, MCT + AdTrackLucFab-9B9 as the disease + irrelevant viral control and MCT + AdBMPR2Fab-9B9 as the disease + treatment.

Confirmation of PAH induction and reversal is via FI and hemodynamic assessment. This is an essential analytical step in every PAH *in vivo* model before commencing any additional analysis on the animal tissue. Assessment of PAH for this study involved FI, RVSP and mPAP analysis 17-21 days following MCT \pm viral treatment (along with HR, mSAP and BW).

The first assessment is to confirm PAH induction. This is demonstrated through increases in FI and hemodynamics of the MCT Only rats compared to the Saline rats. For the MCT Only group, their FI was significantly increased by 23.9% compared to the Saline group ($0.399 \text{ g} \pm 0.027$ vs $0.304 \text{ g} \pm 0.023$ SEM) as was their RVSP by 46.8% ($27.68 \text{ mmHg} \pm 2.192$ vs $14.71 \text{ mmHg} \pm 0.918$ SEM) and mPAP was increased by 43.8% ($15.14 \text{ mmHg} \pm 2.946$ vs $8.51 \text{ mmHg} \pm 0.704$ SEM) [Figure 28](#).

To assess the effectiveness of the AdBMPR2 treatment, the FI and hemodynamics of the MCT + AdBMPR2Fab-9B9 group was compared with the MCT Only and MCT + AdTrackLucFab-9B9 groups. Amelioration of PAH is seen through the significant 26.6% reduction of the FI of MCT + AdBMPR2Fab-9B9 ($0.293 \text{ g} \pm 0.007$ SEM) treated rats compared to the MCT Only rats ($0.399 \text{ g} \pm 0.027$ SEM) and a 23.9% reduction compared to MCT + AdTrackLucFab-9B9 ($0.385 \text{ g} \pm 0.033$ SEM). There was a 41.7% reduction in RVSP of MCT + AdBMPR2Fab-9B9 ($16.14 \text{ mmHg} \pm 0.413$ SEM) treated rats compared with

RAW HEMODYNAMIC DATA OBTAINED 10 DAYS FOLLOWING ADBMPR2 TREATMENT			
Treatment Group	FI	RVSP (mmHg)	mPAP (mmHg)
Saline	0.304 ± 0.023	14.71 ± 0.918	8.511 ± 0.704
MCT Only	0.399 ± 0.027	27.67 ± 2.192	15.14 ± 2.946
MCT + AdTrackLuFab-9B9	0.385 ± 0.033	29.06 ± 0.649	14.56 ± 1.471
MCT + AdBMPr2Fab-9B9	0.293 ± 0.007 * †	16.14 ± 0.413 * †	7.62 ± 0.376 * †

Table 5: Raw hemodynamic data obtained 10 days following AdBMPr2 treatment. Values are mean ± SEM. * compared with MCT Only and † versus AdTrackLucFab-9B9. $p < 0.05$

MCT Only (27.67 mmHg ± 2.192 SEM) and a 44.6% reduction compared with MCT + AdTrackLucFab-9B9 (29.06 mmHg ± 0.649 SEM). Additionally, the mPAP of MCT + AdBMPr2Fab-9B9 (7.62 mmHg ± 0.376 SEM) rats was reduced by 49.7% compared with MCT Only (15.14 mmHg ± 2.946 SEM) and 47.7% reduced compared with MCT + AdTrackLucFab-9B9 (14.56 mmHg ± 1.471 SEM) [Table 5](#) & [Figure 28](#).

There was no statistical difference between HR, mSAP and BW across all treatment groups, showing animal health was consistent at the time of surgery [Figure 29](#).

10.3 ACTIVATION OF SMAD PATHWAYS WAS INCONCLUSIVE 10-DAYS FOLLOWING ADBMPr2 TREATMENT

AdBMPr2 therapy is aimed at restoring BMPr2 expression to normal levels in PAH subjects. Patients with HPAH, also patients with idiopathic and secondary PH have reduced expression of BMPr2. Furthermore, BMPr2 is reduced in the chronic hypoxia and MCT *in vivo* models of PAH [5]. Once the AdBMPr2 treatment ameliorates PAH is established, the next logical step is to investigate the BMPr2 mediated Smad pathways.

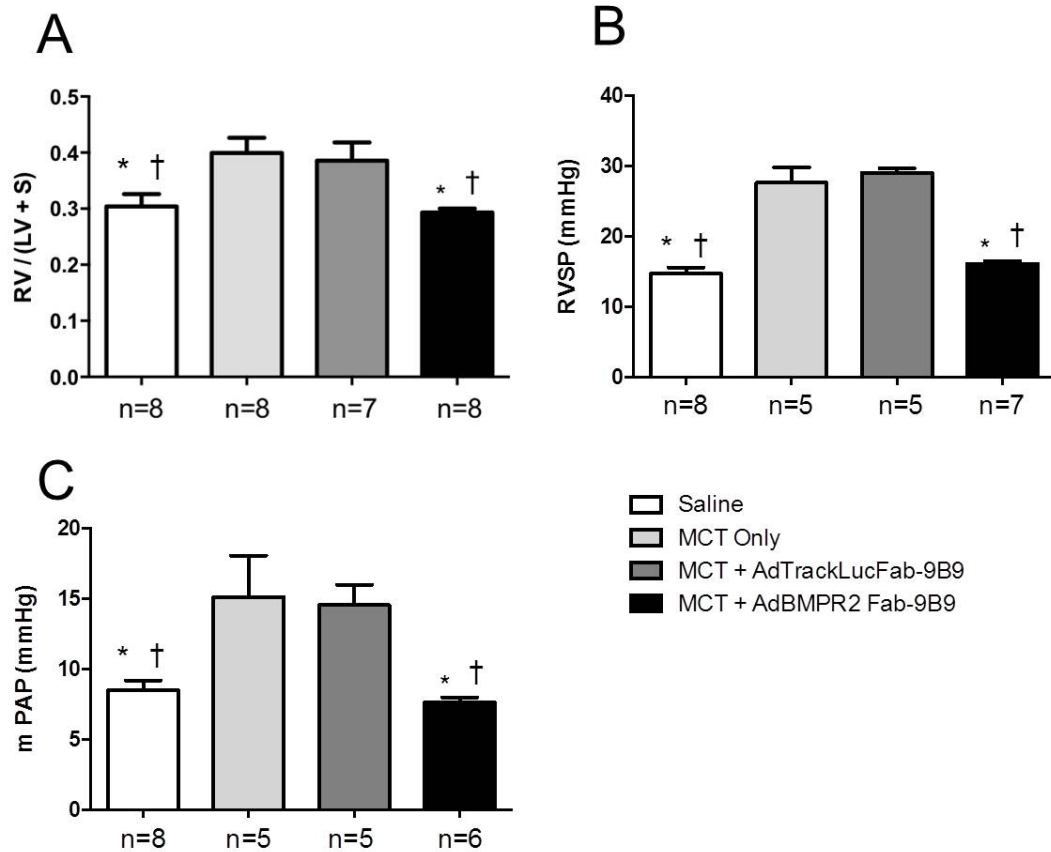


Figure 28: Effect of AdBMPR2Fab-9B9 treatment on the progression of MCT-induced PAH. A. Fulton Index (g); B. right ventricular systolic pressure (mmHg); and C. mean pulmonary arterial pressure (mmHg). Values are mean \pm SEM for $n=5-8$ rats/group. * compared with MCT Only and † compared with AdTrackLucFab-9B9. $p < 0.05$.

Protein analysis of whole rat lung tissue lysate was performed via immunoblot using the Odyssey system (LI-COR) outlined in [Chapter 9](#). Antibodies were selected due to their availability at the time of analysis (see [Chapter 9](#) for note on antibody selection).

Protein expression was analysed and is expressed as a percentage of the Saline group ($100\% \pm 29.730$). pSmad1/5/8 was significantly increased in the Saline group compared to all other groups [Figure 30](#). pSmad1/5/8 expression in the MCT Only ($31.8\% \pm 10.783$ SEM) had a 3.14-fold decrease compared to Saline ($100\% \pm 29.73$ SEM). MCT + AdTrackFab-9B9 (35.3%

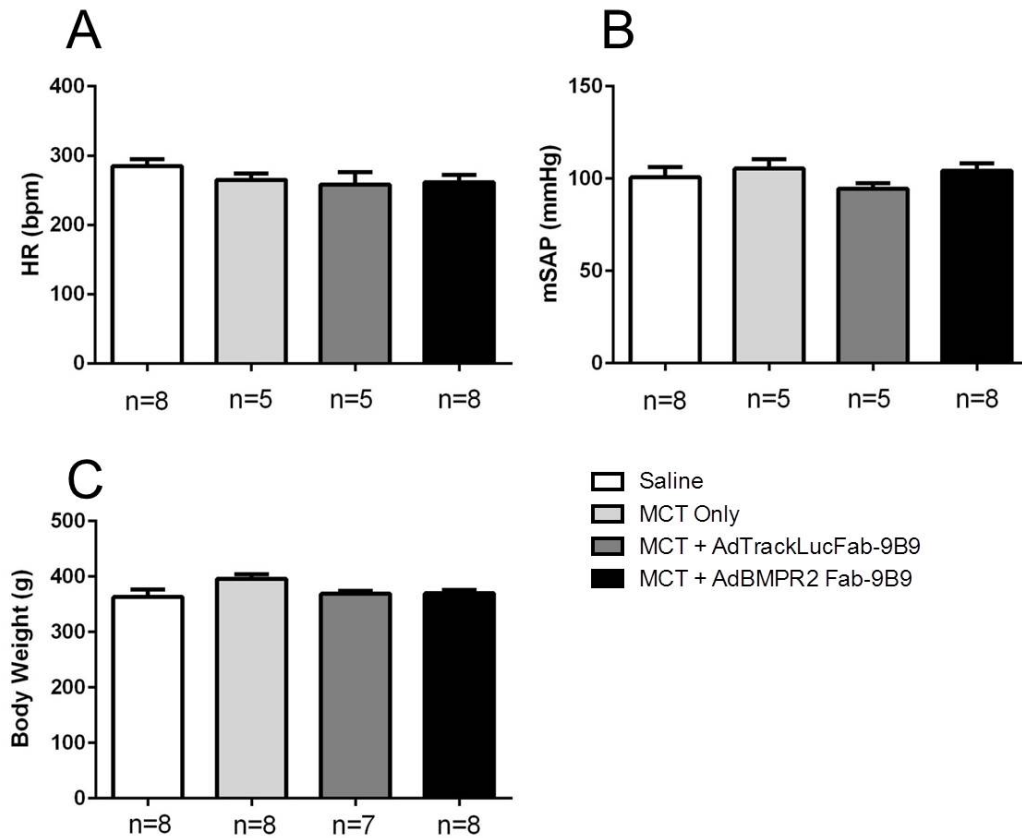


Figure 29: Consistency of animal health at the time of hemodynamic analysis. A. Heart rate (bpm); B. mean systemic arterial pressure (mmHg); and C. total body weight (g). Values are mean \pm SEM for $n=5-8$ rats/ group.

± 6.436 SEM) had a 2.83-fold decrease and MCT + AdBMPR2Fab-9B9 (21.8% ± 4.351 SEM) had a 4.58-fold decrease compared to the Saline group (100% ± 29.73 SEM) [Figure 30](#).

pSmad2 was significantly decreased in the Saline (100% ± 12.31 SEM) group compared to all other groups [Figure 31](#). MCT Only (173.4% ± 18.91 SEM) had a 1.73-fold increase compared to Saline (100% ± 12.3 SEM). MCT + AdTrackLucFab-9B9 (188.18% ± 13.44 SEM) had a 1.88-fold increase and MCT + AdBMPR2Fab-9B9 (171.29% ± 18.51 SEM) had a 1.71-fold increase compared to Saline (100% ± 12.31 SEM) [Figure 31](#).

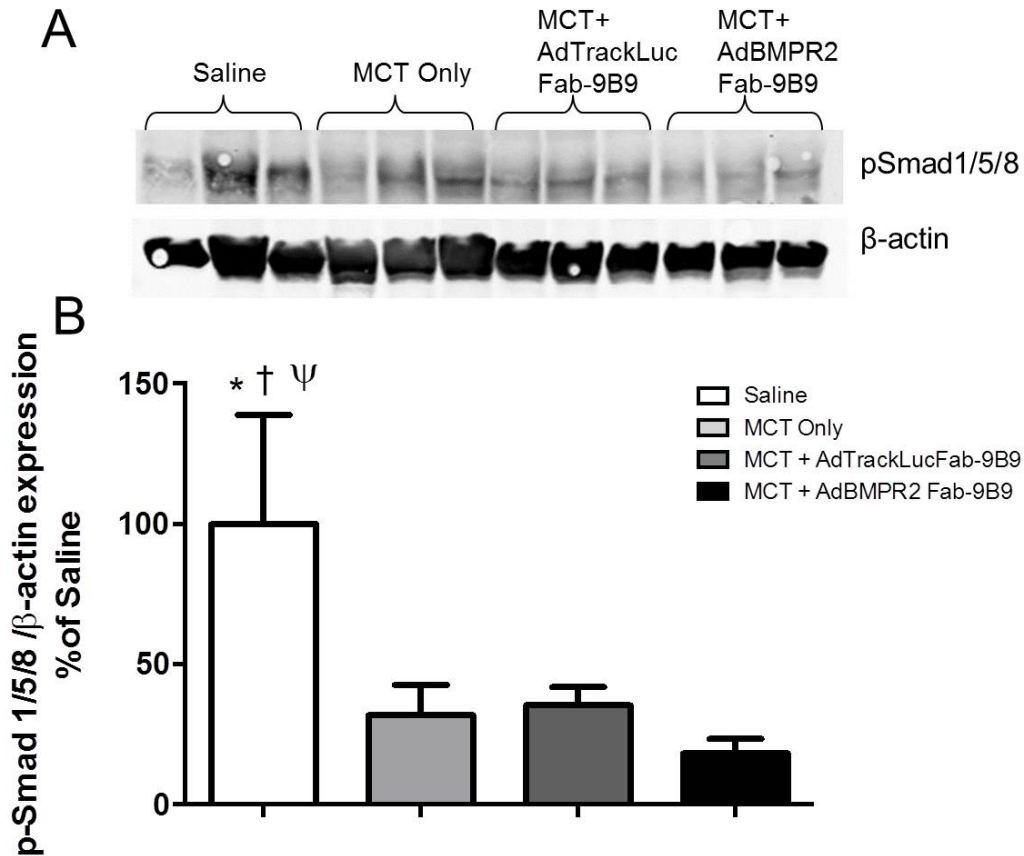


Figure 30: Immunoblot analysis of whole rat lung tissue 10 days post AdBMPR2 treatment. A. Representative immunoblot of 3 individual rats per group for pSmad1/5/8 and β -actin; and B. pSmad1/5/8 immunodetection results. Values are mean \pm SEM for $n=6$ rats/group. * compared with MCT + AdBMPR2 Fab-9B9, † compared with MCT Only and ψ compared with MCT + AdTrackLuc Fab-9B9. $p < 0.05$.

Analysis of BMPR2 mediated Smad signalling appears inconsistent with the physiological results at the 10-day time-point and unexpected given the previous *in vitro* results. A microarray study was conducted using RNA from tissue from this time-point in parallel with this protein analysis. Results from this microarray also did not show any significant differences in gene expression of the Smad pathways [Chapter 11](#). Therefore, I hypothesised that a peak signalling effect on the Smad pathways was being missed at the 10-day time-point and thus a shorter time-point of 2 days post AdBMPR2 treatment was examined.

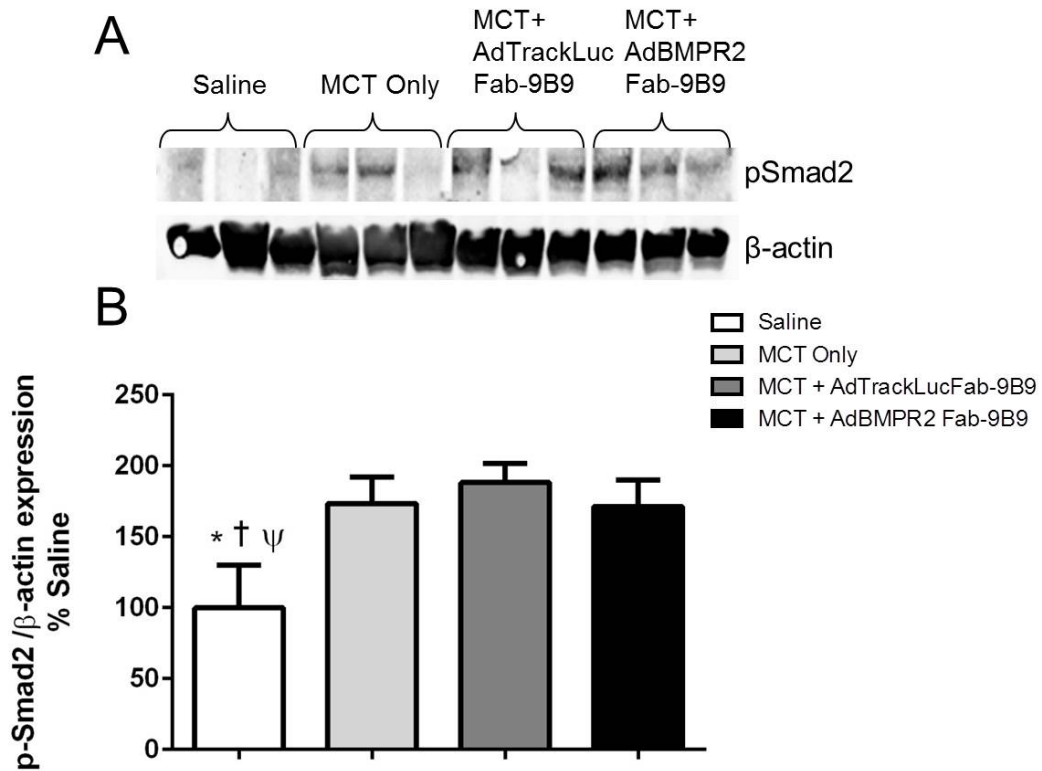


Figure 31: Immunoblot analysis of whole rat lung tissue 10 days post AdBMPR2 treatment. A. Representative immunoblot 3 individual rats per group for pSmad2 and β-actin; and B. pSmad2 immunodetection results. Values are mean ± SEM for $n=6$ rats/group. * compared MCT + AdBMPR2 Fab-9B9, † compared with MCT Only and ψ compared with MCT + AdTrackLuc Fab-9B9. $p < 0.05$.

10.4 REDUCTION IN RIGHT VENTRICULAR HYPERTROPHY IN MCT-INDUCED PAH RATS ONLY 2 DAYS POST ADBMPR2 TREATMENT

The treatment groups for the 2-day time-point were the same as the 10-day time-point. The Saline group as a healthy control, the MCT Only group as a disease only control, the MCT + AdTrackLuc Fab-9B9 group as the irrelevant viral control group and again, this is the most robust control for the treatment group, MCT + AdBMPR2 Fab-9B9.

The FI was the only disease induction and reversal assessment undertaken at the 2-day time-point post AdBMPR2 treatment. Changes in the

hemodynamic measurements of RVSP and mPAP were expected to be quite minimal, and thus due to the technically challenging nature of obtaining these measurements, they were deemed unlikely to be technically robust. The FI on the other-hand is a simple procedure that is easily reproducible, and thus was used for this study.

The induction of RVH was assessed by comparing the Saline ($0.294 \text{ g} \pm 0.018 \text{ SEM}$) and MCT Only ($0.397 \text{ g} \pm 0.025 \text{ SEM}$) groups. There was a 26.0% increase in RVH in the MCT Only group compared to Saline, as well as a 31.7% increase in the MCT + AdTrackLucFab-9B9 group ($0.431 \text{ g} \pm 0.045 \text{ SEM}$) compared with the Saline group ($0.294 \text{ g} \pm 0.018 \text{ SEM}$) [Figure 32](#).

Interestingly, reversal of the RVH was seen through a 23.2% decrease in FI of the MCT + AdBMPR2Fab+9B9 group ($0.304 \text{ g} \pm 0.025 \text{ SEM}$) compared to MCT Only and 29.4% reduction compared with the MCT + AdTrackLucFab-9B9 group ($0.431 \text{ g} \pm 0.045 \text{ SEM}$) [Figure 32](#). This unexpected early effect may be due to the release of vasodilatory mediators such as: eNOS [136, 106], after BMPR2 gene delivery.

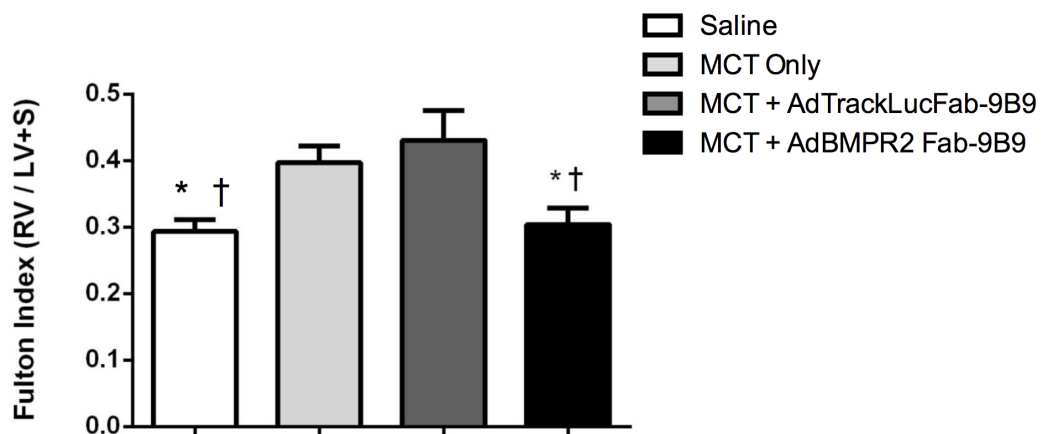


Figure 32: Reduction in FI 2 days post MCT + AdBMPR2Fab-9B9 treatment versus MCT Only and MCT + AdTrackLucFab-9B9. $n=8$ rats/group. Values are mean \pm SEM. * compared with MCT Only and † compared with AdTrackLucFab-9B9. $p < 0.05$.

Body weight of the animals was consistent across all groups at the time the FI was measured [Figure 33](#).

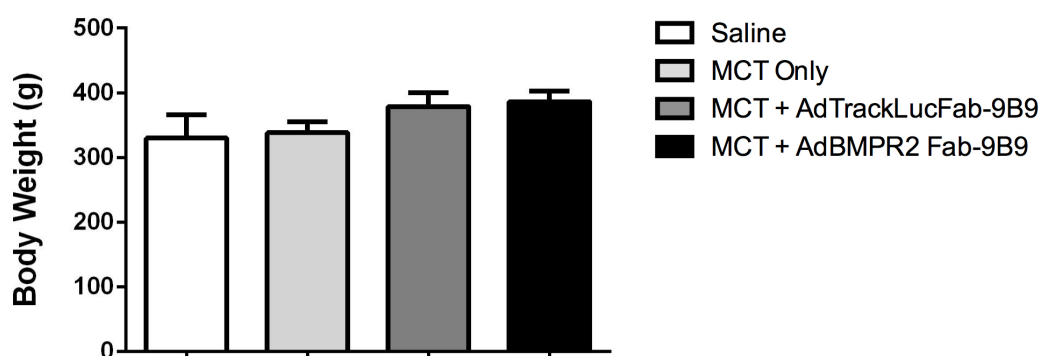


Figure 33: Body weight of animals at the time of Fulton Index measurement. $n=8$ rats/-group. Values are mean \pm SEM.

10.5 ACTIVATION OF SMAD1/5/8: 2 DAYS FOLLOWING ADBMPR2 TREATMENT

Following the positive FI results at the 2-day time-point it was hypothesised that BMPR2 mediated Smad signalling would be altered. Therefore, Smad1/5/8 and Smad2/3 signalling was investigated via immunoblot.

Results of the treatment groups were derived as a percentage of the Saline (100% \pm 17.19 SEM) treated animals. Both of the disease controls MCT Only (18.9% \pm 8.597 SEM) and MCT + AdTrackLucFab-9B9 (19.4% \pm 2.931 SEM) had a 5.29 & 5.15-fold respective decrease compared to Saline (100% \pm 17.19 SEM) [Figure 34](#).

The MCT + AdBMPR2Fab-9B9 group (55.0% \pm 10.42 SEM) had a significant 2.91-fold increase in p-Smad1/5/8 expression compared to MCT Only (18.9% \pm 8.597 SEM) and 2.83-fold increase compared to MCT + AdTrackLucFab-9B9 (19.43% \pm 2.931 SEM) [Figure 34](#).

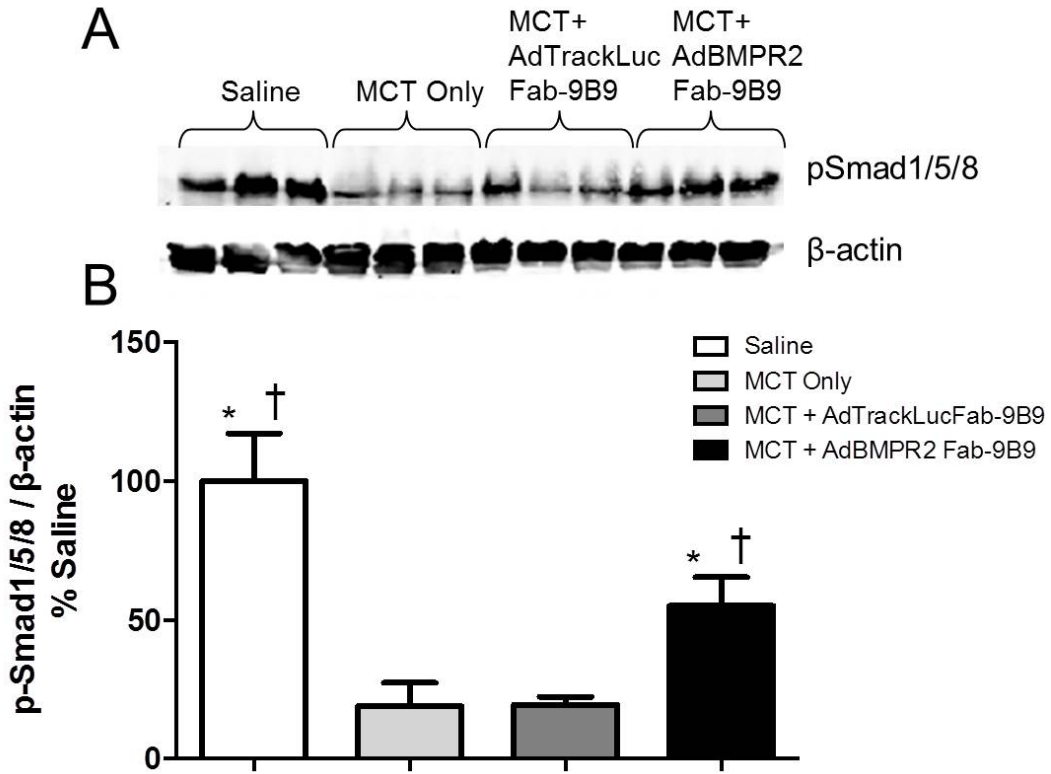


Figure 34: AdBMPR2 treatment activates the Smad_{1/5/8} pathway. A. Representative immunoblot of 3 individual rats per group for pSmad_{1/5/8} and βactin; and B. pSmad_{1/5/8} immunodetection quantification. *n*=6 rats/group. Values are mean ± SEM. * compared with MCT Only and † compared with MCT + AdTrackLucFab-9B9. *p* < 0.05.

10.6 EFFECT ON SMAD3 ACTIVATION: 2 DAYS FOLLOWING ADBMPR2 TREATMENT

Smad₃ was used to analyse the TGF-β mediated Smad_{2/3} pathway at this time-point. This differs from the Smad₂ protein analysed at the 10-day time-point. The change in antibody was due to the availability of a newly available pSmad₃ antibody variant with increased specificity and reliability.

Results of the treatment groups were derived as a percentage of the Saline (100% ±4.383 SEM) treated animals. MCT Only (682.0% ±138.1 SEM) had a 6.82-fold increase in pSmad₃ expression compared to Saline (100% ±4.383

SEM) and MCT + AdTrackLucFab-9B9 (788.9% ±160.5 SEM) had a 7.89-fold increase compared to the Saline control (100% ±4.383 SEM) [Figure 35](#).

Despite there being a clear trend of a decrease in the level of expression in the MCT + AdBMPR2Fab-9B9 group, p-Smad3 expression was not significantly decreased in the MCT+ AdBMPR2Fab-9B9 (541.5% ±64.59 SEM) treated rats compared with the MCT Only (682.0% ±138.1 SEM) and MCT+AdTrackLucFab-9B9 (788.9% ±160.5 SEM) treated rats [Figure 35](#).

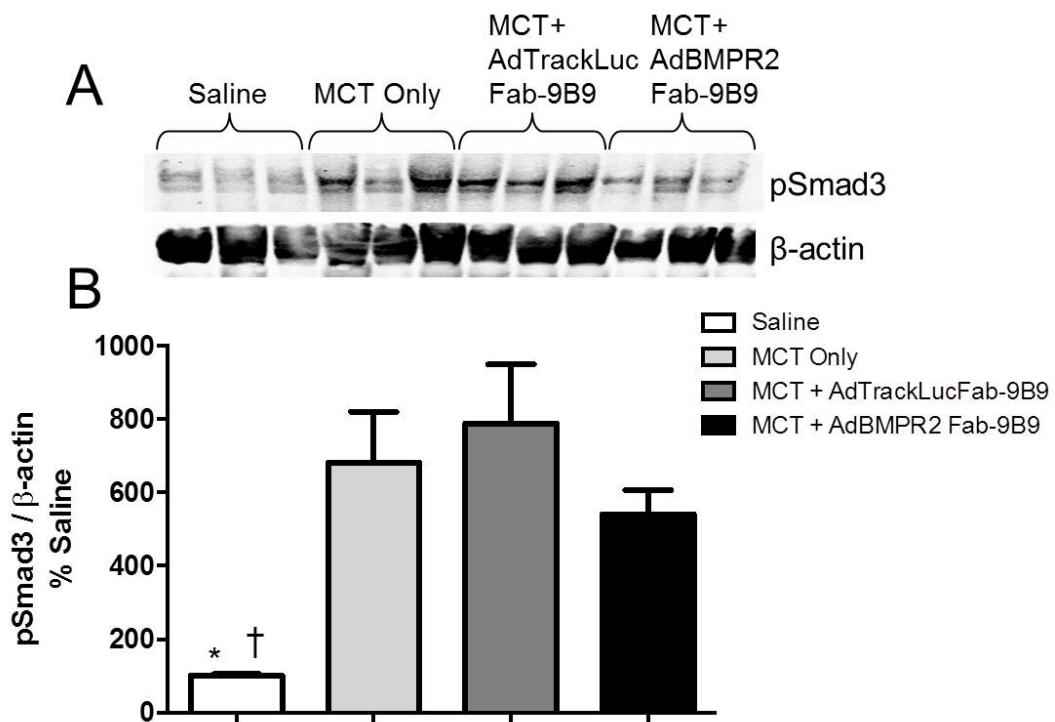


Figure 35: AdBMPR2 treatment caused a trending effect on Smad3 activation. A. Representative immunoblot of 3 individual rats per group for pSmad3 and βactin; and B. pSmad3 immunodetection quantification. *n*=6 rats/group. Values are mean ± SEM. * compared with MCT Only and † compared with MCT + AdTrackLucFab-9B9. *p* < 0.05.

10.7 DISCUSSION AND CONCLUSIONS

In this study, I have shown for the first time that up-regulation of functional BMPR2 ameliorates PAH 2 days post treatment. Furthermore, I have shown that this attenuation of disease may be attributed to the activation of BMPR2 mediated Smad1/5/8 signalling at this time-point and that this activation coincides with the likely down-regulation of the TGF- β mediated Smad2/3 signalling pathway. The IV injection of the targeted Ad-vector, AdBMPR2Fab-9B9 in SD rats with MCT-induced PAH surprisingly showed a significant reduction in the FI only 2 days post injection. This is an important physiological improvement, as RV function is a critical determinant of morbidity and mortality in PAH [143]. Activation of Smad1/5/8 and trending down-regulation of pSmad3 was shown through immunoblot protein analysis of whole lung tissue at this 2-day time-point.

Previously we have successfully up-regulated BMPR2 in the pulmonary endothelium of rats with MCT and chronic hypoxia induced PAH and attenuated the disease [29]. BMPR2 delivery was via a targeted Ad-vector, which has been extensively validated to target to the lungs with minimal sequestration to the liver [141]. The rationale for this treatment approach is to address the known down-regulation of BMPR2 in PAH by restoring it to functional levels. Following this successful proof-of-principle work, the subsequent work was to examine the effect of BMPR2 up-regulation on downstream signalling pathways. We have shown that increasing BMPR2 expression in pulmonary endothelial cells induces a return to the homeostatic BMPR2/ TGF- β signalling balance via Smad1/5/8 and Smad2/3 in HMVEC-L [142]. This study shows that this balance is also restored in our *in vivo* MCT induced rat model.

After the positive *in vitro* results, I moved into the *in vivo* setting looking specifically at the MCT model with our previously validated and described BMPR2 modulation system. Through MCT injections, I was able to induce PAH in male SD rats. The disease development is evidenced through the significant increase between the Saline and MCT Only treated rats of the FI as a measure of right ventricular hypertrophy (at 2 and 10 days post treatment), RVSP, and mPAP. The success of our model is shown in the reduction in these parameters following our AdBMPR2 treatment.

Surprisingly, I was unable to demonstrate any persisting impact of BMPR2 delivery on changes in Smad signalling at the 10-day time-point, despite the physiological findings. This analysis was performed in parallel with a microarray study on tissue from the same time-point, and this also did not show any gene expression differences in Smad proteins. I can only speculate that other, non-Smad mechanisms may have more of a role as the model response evolves, but this requires further studies. Gene expression profiles are more sensitive to change than protein analysis and the change in gene expression is generally larger. Thus, it is planned to extract the tissue at an earlier time-point to examine whether a peak signalling effect was being missed, and to get a more complete understanding of the Smad and non-Smad effects over time.

Encouraged by the positive FI results for the 2-day time-point, I proceeded to analyse the whole lung tissue. Induction of PAH was associated with reduced activated Smad1/5/8 and increased activated Smad3, consistent with published findings of decreased BMPR2 mediated Smad signalling and increased TGF- β mediated Smad signalling in this PAH model [5]. This Smad signalling axis was reversed with AdBMPR2 treatment.

Down-regulation of BMPR2 is seen not only in hereditary, but also secondary PH, as well as in the animals models of PAH [5]. Thus, the premise of our approach is to restore BMPR2 expression to a functional level, directly addressing this deficiency in PAH subjects. To date, therapeutics such as ERA's, PDE's and Prostacyclin have shown modest improvements for PAH patients, however the mortality of this disease is still likened to the worst cancers [1]. Unfortunately, current therapies when used singularly or in combination seem to have short-term positive effects, which diminish with time and don't result in a 'cure' of the disease. We hypothesise that BMPR2 therapy will have a long-term effect by addressing the reduced levels of expression, and changing the molecular consequences of this. Despite not being able to show persistent changes in Smad signalling at the 10-day time-point, I was able to show positive hemodynamic changes. Notwithstanding the technical limitations of this experiment, there may be two reasons for seeing these physiological changes: 1. The BMPR2 therapy acts as a 'reversal trigger' and restores the abnormal cellular signalling that occurs in PAH, however the up-regulation or over-expression of the BMPR2 mediated Smad signalling has subsided and thus difficult to quantify; and 2. the transgene effect has started to diminish and although the physiological changes remain, the pathology of PAH may be returning.

PAH is thought to be triggered by external factors such as hypoxia, inflammation or environmental influences, as only 20% of BMPR2 mutation carriers display the PAH phenotype [73]. This phenotype is the result of abnormal endothelial cellular signalling, specifically a shift in the BMPR2/TGF- β signalling axis [Chapter 4](#). Our BMPR2 therapy is aimed at rectifying this imbalance with the notion that this is sufficient to trigger a permanent reversal of the disease. However, the results indicate that the level of activated Smad1/5/8 expression in the MCT + AdBMPR2Fab-9B9 group is consistent with the two disease controls, suggesting that the AdBMPR2

therapy needs to have longer transgene expression. The use of older generation Ad-vectors with limited transgene expression (around 2 weeks) are a limitation of this study. Development of advanced generation vectors are under-way, however it is still in the initial phases of experimentation for delivering BMPR2 to the pulmonary endothelium. Despite this, Ad-vectors have other limiting factors, such as systemic inflammatory consequences and pre-existing immunity of the host, and this has prompted our studies to move towards a cell based approach [Chapter 14](#).

Technical limitations of this study arose in the protein analysis. The Smad proteins investigated are difficult to detect particularly when antibodies are continually being refined and replaced, as is the case with Smad antibodies. Additionally, there are difficulties with the sample being a whole lung lysate. The signal may be dampened as there are not just endothelial cell proteins in the sample to give a large enough signal in the immunoblot. This is the case as all proteins from other cells that make up the lung structure such as smooth muscle cells, epithelial cells, pericytes, alveolar type cells and resident macrophage are also in the lysate. To overcome this, micro-dissection of the blood vessels would make the investigation more specific to the cell populations and structure I wish to investigate. This was not pursued as an option due to the availability of equipment at the time.

Whilst this work demonstrates that BMPR2 modulation therapy attenuates PAH through restorative changes in the BMPR2/ TGF- β mediated Smad signalling axis, BMPR2 signalling is not limited to Smad proteins. A natural progression then is to explore any novel targets that are identified from a microarray study of each treatment group.

MICROARRAY STUDIES

11.1 OVERVIEW

Given the physiological changes seen 10 days following BMPR2 modulation in the MCT induced PAH rat model, I used this model to explore novel pathways that are either being directly or indirectly affected following our AdBMPR2 treatment.

A microarray study was conducted using RNA from lungs extracted at the 10-day time-point. This array was looking at the whole SD rat transcriptome and comparing all the treatment groups against each other for variances in gene expression. These studies were conducted with the aim of identifying any novel pathways in either the pathogenesis of PAH or the reversal of the disease following our AdBMPR2 treatment.

PAH is a complex disease involving many different systems, cell types and pathologies. Therefore, it is a difficult disease to study and despite increasing work and success in treatment development, there still remains an enormous gap in our knowledge of the precise cell signalling pathways that are integral to PAH pathogenesis, and furthermore, are critical in the reversal of the disease. Thus, the AdBMPR2 treatment in the MCT model is an ideal candidate to examine not only the pathways I hypothesise are crucial in PAH pathogenesis, but also to identify any novel pathways that are altered as a result of our effective treatment shown in [Chapter 10](#).

To do this, the whole rat gene transcriptome was examined using samples from our AdBMPR2 treatment model, at the 10-day time-point. Lung

tissue taken from SD rats treated as outlined in [Chapter 10](#) was processed to extract total RNA [Chapter 9](#). The microarray study was conducted using all treatment groups: Saline (healthy control), MCT Only (disease control), MCT + AdTrackLucFab-9B9 (irrelevant viral control) and MCT + AdBMP2Fab-9B9 (treatment group).

Samples were initially assessed for quality on a bioanalyzer (Agilent) [Appendix B](#). Following the recommendations from the experts at the University of Adelaide Microarray Core Facility, each treatment group had an $n=4$ for the microarray. Therefore the 4 samples with the highest quality based on the RNA integrity number (RIN) in each treatment group were chosen for the microarray.

Initial analysis identified if there were any significant gene expression variances between the treatment groups. Once this is ascertained and there were variances identified, the subsequent analysis involves extracting a list of the individual genes that were significantly different between the chosen treatment groups. This often results in an extensive list of thousands of genes, which is difficult to interpret and make use of. Thus, I utilised a software program that has been developed to handle the large amount of information generated from a microarray analysis. I utilised the analysis program: Ingenuity Pathway Analysis (IPA) (Qiagen), to identify novel pathways to further investigate. IPA utilises gene and protein databases of known cellular signalling pathways and networks to form network schematics of the microarray results.

By conducting this microarray in parallel with the protein analysis of the whole rat lung tissue [Chapter 10](#), I was able to examine if there were any variances in gene expression of the BMP2 mediated Smad proteins at the 10-day time-point. Further to this, the microarray could also identify any

novel cell signalling pathways that were altered following the AdBMPr2 treatment, leading to the identification of novel therapy targets or a better understanding of the pathogenesis of PAH.

11.2 GENE EXPRESSION PROFILES DIFFER BETWEEN TREATMENT GROUPS

Following the bioanalyzer analysis (shown in [Appendix B](#)) 4 samples were selected from each group to run on the microarray. Each sample represents an individual rat.

Initial analysis involves generating a false discovery rate (FDR) report for all group comparisons at 3 different significant levels: $p=0.01$, $p=0.02$ & $p=0.05$ [Table 6](#). This quantitative analysis immediately indicates whether there are any groups that have significant gene expression variances, and whether further analysis is viable. From this report, I was able to identify the most robust group comparisons for further pathways analysis.

Confirmation of the induction of PAH was shown through the significant differences between Saline and MCT Only groups. Additionally, there are significant differences between the Saline and MCT + AdTrackLucFab-9B9 groups [Table 6](#).

The effectiveness of the AdBMPr2 treatment is shown through the significant differences between the MCT + AdBMPr2Fab-9B9 and MCT Only groups. However, there was no significant differences between the MCT + AdBMPr2Fab-9B9 and MCT + AdTrackLucFab-9B9 groups at any level of significance [Table 6](#).

FALSE DISCOVERY RATE (FDR) REPORT OF MICROARRAY	
Groups	Significant p-values
$p=0.01$ total number of p-values = 29214	
Saline vs MCT Only	1123
Saline vs MCT + AdTrackLucFab-9B9	242
Saline vs MCT + AdBMPR2Fab-9B9	430
MCT + AdBMPR2Fab-9B9 vs MCT Only	1250
MCT + AdBMPR2Fab-9B9 vs MCT + AdTrackLucFab-9B9	0
MCT + AdTrackLucFab-9B9 vs MCT Only	3
$p=0.02$ total number of p-values = 29214	
Saline vs MCT Only	2248
Saline vs MCT + AdTrackLucFab-9B9	336
Saline vs MCT + AdBMPR2Fab-9B9	579
MCT + AdBMPR2Fab-9B9 vs MCT Only	5165
MCT + AdBMPR2Fab-9B9 vs MCT + AdTrackLucFab-9B9	0
MCT + AdTrackLucFab-9B9 vs MCT Only	741
$p=0.05$ total number of p-values = 29214	
Saline vs MCT Only	5143
Saline vs MCT + AdTrackLucFab-9B9	560
Saline vs MCT + AdBMPR2Fab-9B9	943
MCT + AdBMPR2Fab-9B9 vs MCT Only	11632
MCT + AdBMPR2Fab-9B9 vs MCT + AdTrackLucFab-9B9	0
MCT + AdTrackLucFab-9B9 vs MCT Only	9118

Table 6: False Discovery Rate Report of Microarray performed on whole lung tissue from the MCT-induced PAH: 10 days following AdBMPR2 treatment.

A principle components analysis (PCA) is performed to graphically show the variance in gene expression profiles of each treatment group. The main difference between a PCA and a FDR report is that the PCA considers each sample to be a variable, and the analysis creates a set of 'principle experiment components' which indicate features of the sample that best describes the gene behaviours they elicit [144]. Whereas the FDR report only gives a quantification of significant gene differences. Variance in gene profiles are shown through the physical separation of the groups on the PCA graph [Figure 36](#).

Again, successful induction of PAH is confirmed through the clear differences between the Saline and MCT Only groups and between the Saline and MCT + AdTrackLucFab-9B9 groups. The effect of AdBMP2 treatment is shown by the differences between the MCT Only and MCT + AdBMP2Fab-9B9 groups. Unfortunately, the gene profiles of MCT + AdBMP2Fab-9B9 and MCT + AdTrackLucFab-9B9 are very similar. This may be due to the global effects of viral vector delivery to the animals causing the up- and/or down-regulation of similar genes [Figure 36](#).

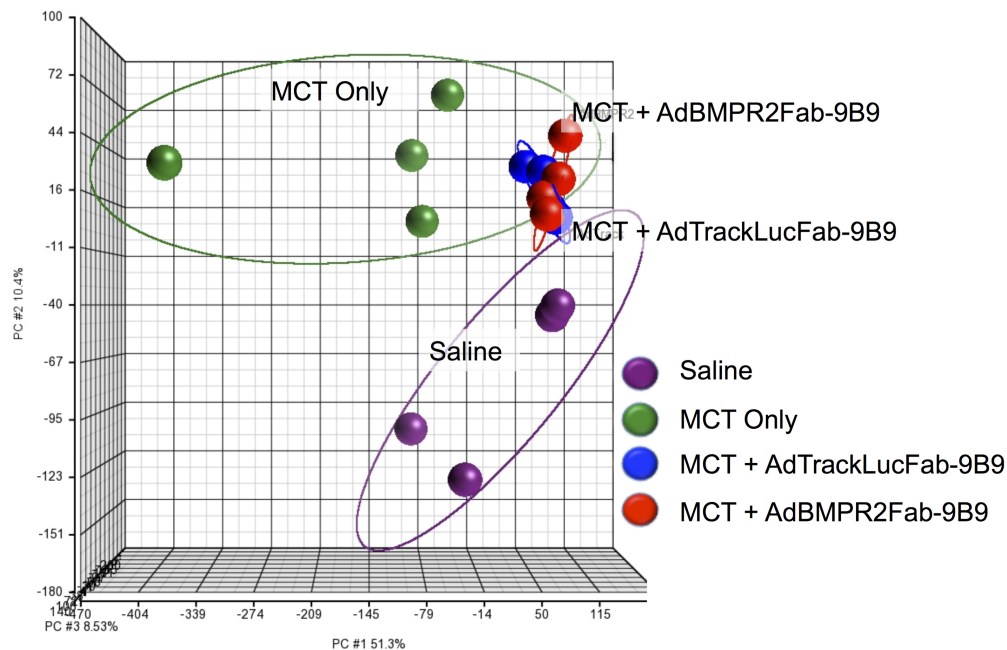


Figure 36: PCA analysis showing distinct differences in gene expression profiles between the Saline (purple) vs MCT Only (green); Saline and MCT + AdTrackLucFab-9B9 (blue) and MCT Only vs MCT + AdBMP2Fab-9B9 (red) groups. $n=4$ rats/group.

11.3 PRELIMINARY ANALYSIS

From the microarray results, it was identified that the best comparison for further pathway analysis was between the MCT Only and MCT + AdBMP2Fab-9B9 groups. A list of genes with significant expression differences was gen-

erated for the MCT Only vs MCT + AdBMPr2Fab-9B9 groups by **eliminating the exact same genes that were significant between MCT Only vs MCT + AdTrackLucFab-9B9 and MCT Only vs MCT + AdBMPr2Fab-9B9 groups** [Figure 37](#). This gave a list of genes that were exclusively different between MCT Only and MCT + AdBMPr2Fab-9B9.

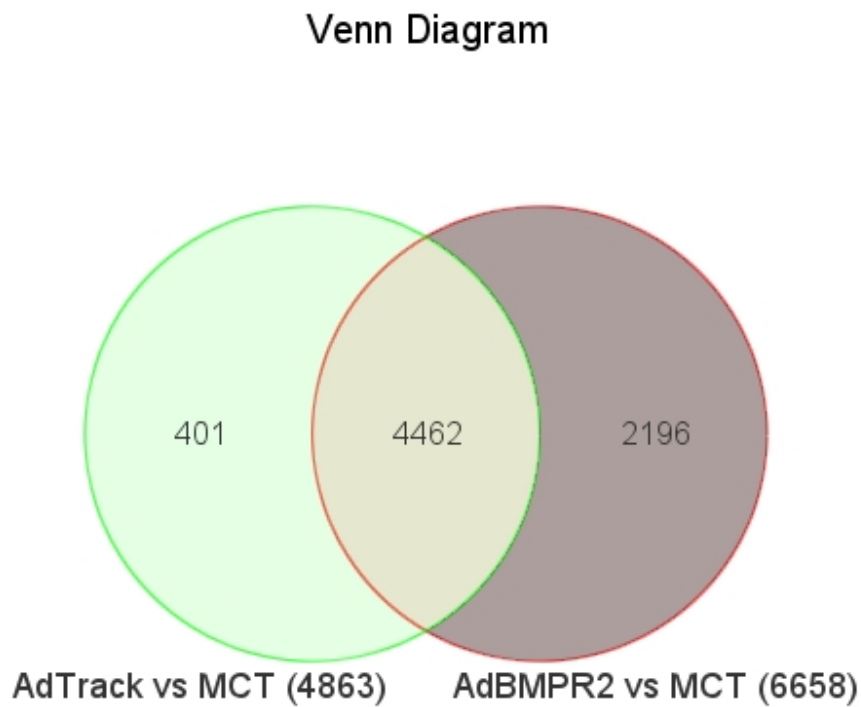


Figure 37: Venn diagram showing the exclusion of genes that are significantly different between the MCT Only vs MCT + AdTrackLucFab-9B9 groups that are also significantly different in the MCT Only vs MCT + AdBMPr2Fab-9B9 groups.

The resulting list of 2196 genes (see [Appendix B](#) for example of the list), with the fold change, was put through an IPA (Qiagen) analysis to identify any novel signalling pathways that are either critical to the reversal of PAH following our AdBMPr2 treatment or that could be secondary targets for therapy.

11.4 INGENUITY PATHWAY ANALYSIS: MAIN SUMMARY

The IPA (Qiagen) analysis produced a summary report which identified the top networks, canonical pathways, molecules, diseases and bio-functions that were changed between the MCT Only and MCT + AdBMPR2Fab-9B9 gene expression profiles [Table 7](#). This summary is a broad, general review of the microarray, and it gives a good indication of whether the therapy has achieved to reverse cellular processes that are known to be abnormal in PAH.

The summary identified top diseases and disorders that are relevant to PAH, such as: hereditary, haematological, and developmental disease / disorders, as well as cancer and inflammation. Furthermore, the top molecular and cellular functions that were identified: cell cycle changes, cellular movement, cell assembly and organisation, are associated with cellular migration, proliferation, apoptosis and organisation, all processes which are known to be abnormal in PAH [Table 7](#).

Affected systems such as the haematological system were identified as well as haematopoiesis, highlighting the vascular nature of the disease. Tissue morphology and connective tissue development are also part of the top systems affected by the treatment [Table 7](#), which may relate to the endothelial-to-mesenchymal transition (Endo-MT) that occurs in PAH.

The top canonical pathways affected were eukaryotic initiation factor-2 (EIF2) signalling, BRCA1, EIF4 and p70S6K signalling, as well as cell cycle control and homologous recombination [Table 7](#). All of these pathways are emerging as topical areas in PAH research.

IPA MAIN SUMMARY OF ANALYSIS

Top Networks*Associated Network Functions*

1. Post-translational modification, developmental disorder, hereditary disorder
2. Gene expression, protein synthesis, hereditary disorder
3. RNA post-transcriptional modification, RNA damage and repair, dermatological disease and conditions
4. Energy production, nucleic acid metabolism, small molecule biochemistry
5. DNA replication, recombination, and repair, energy production, nucleic acid metabolism

Top Diseases and Bio-functions*Disease and Disorders*

Developmental disorder
 Haematological disease
 Cancer
 Hereditary disease
 Inflammatory response

Molecular and Cellular Functions

Cell cycle
 Cellular assembly and organisation
 DNA replication, recombination and repair
 Cellular movement
 RNA post-transcriptional modification

Physiological System and Development Function

Nervous system development and function
 Haematological system development and function
 Haematopoiesis
 Tissue morphology
 Connective tissue development and function

Top Canonical Pathways

1. EIF2 signalling
2. Role of BRCA1 in DNA damage response
3. Cell Cycle control of chromosomal replication
4. Regulation of eIF4 and p70S6K signalling
5. DNA double-strand break and repair by homologous recombination

Table 7: IPA main summary of analysis including: Top networks, top disease and bio functions and top canonical pathways. Comparison between MCT Only gene expression profile against MCT + AdBMP2Fab-9B9 gene expression profile.

11.5 NON-SMAD PATHWAYS IDENTIFIED IN THE PATHWAY ANALYSIS

The IPA analysis utilised the list of genes generated from the microarray that were either up- or down-regulated in the MCT Only vs MCT + AdBMPR2Fab-9B9 treatments analysis to form schematics of the top cell signalling networks and molecules altered between the two treatment groups. This was done by utilising information stored online in a wide range of scientific literature and databases of known cellular signalling pathways.

BMPR2 mediated non-Smad pathways ERK1/2 [Figure 38](#) and p38 MAPK were identified [Figure 39](#). Additionally, known BMPR2 mediated molecules in those pathways such as Ras, PI3K and p38, were identified to be up-regulated (red) in the MCT + AdBMPR2Fab-9B9 group compared to MCT Only [Figure 39](#). The top canonical pathway was the eukaryotic initiation factor2 (eIF2) pathway, which also identified the molecules: Ras and PI3K as up-regulated [Figure 40](#).

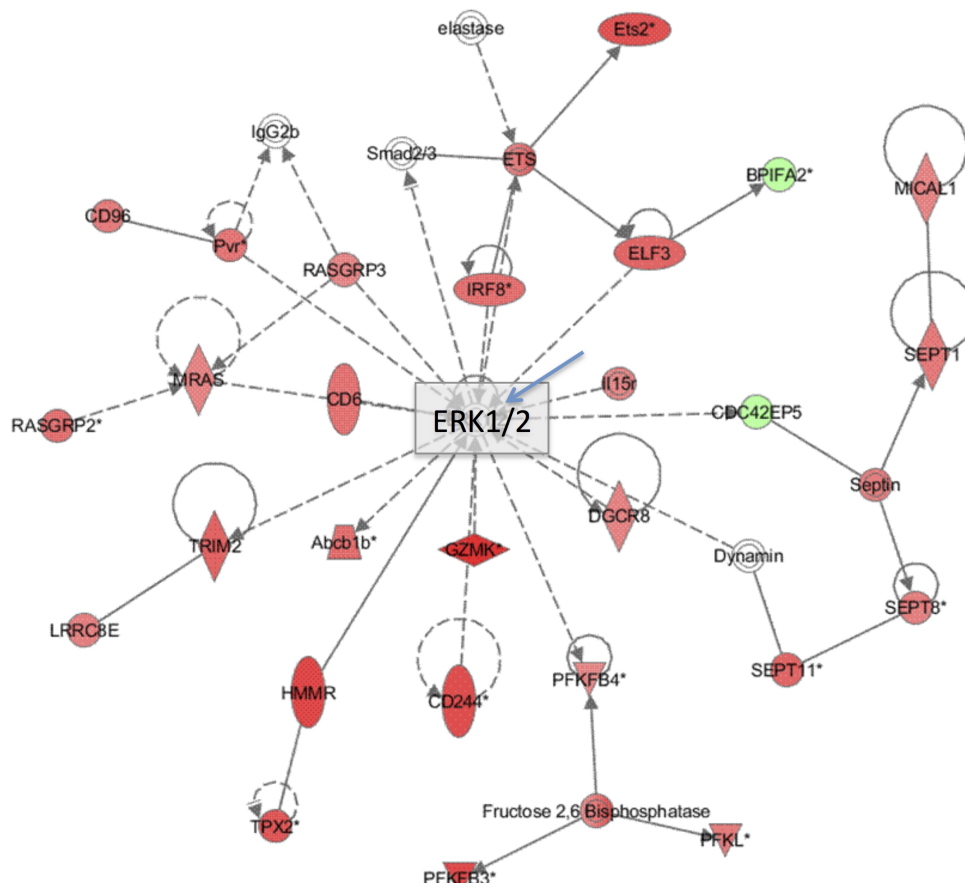


Figure 38: IPA analysis ERK1/2 (blue arrow) pathway schematic. Red = up-regulated, green = down-regulated in the MCT + AdBMPR2Fab-9B9 group vs MCT Only.

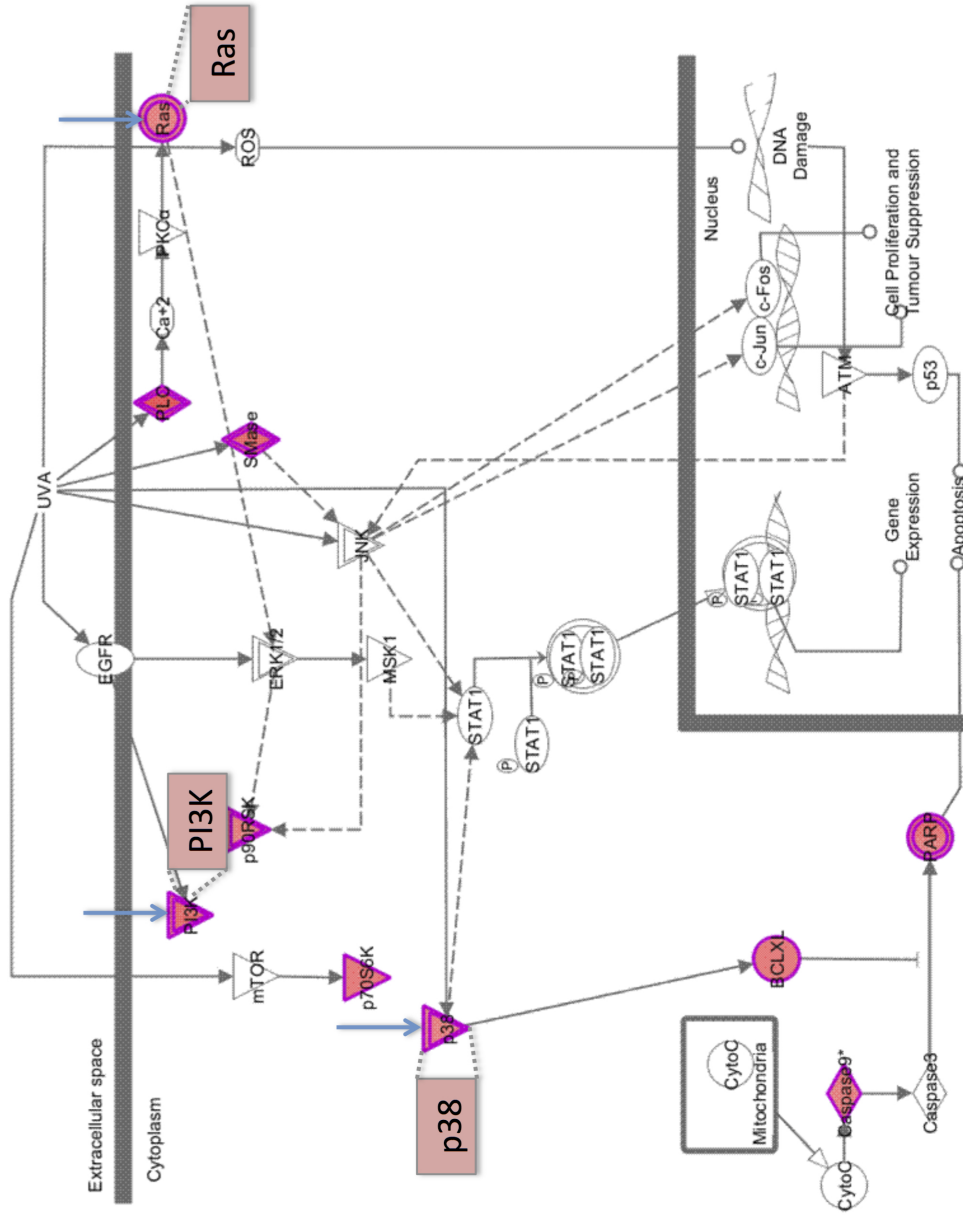


Figure 39: IPA analysis MAPK pathway schematic. Red = up-regulated, green = down-regulated in the AdBMPR2Fab-9B9 group vs MCT Only. Relevant non-Smad signalling molecules PI3K, Ras and p38 (blue arrows) are upregulated.

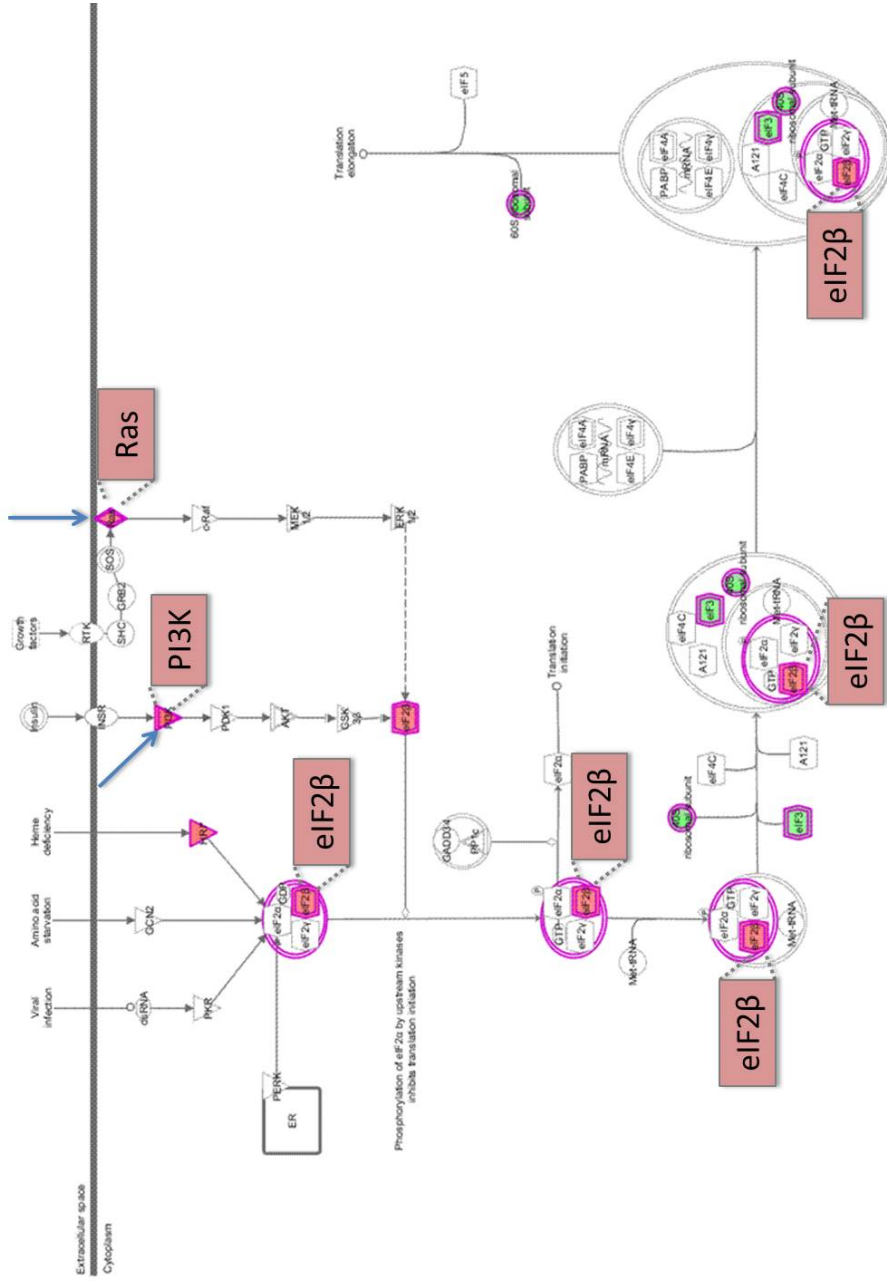


Figure 40: IPA analysis eIF2 pathway schematic. Red = up-regulated, green = down-regulated in the AdBMPR2Fab-9B9 group vs MCT Only. Relevant non-Smad signalling molecules PI3K and Ras (blue arrows) are upregulated.

11.6 DISCUSSION AND CONCLUSIONS

Following the success of the proof-of-concept AdBMP2 treatment in attenuating PAH in the rat MCT model, I was able to show that this may be due to or at least in part due to changes in BMP2 mediated Smad signalling [Chapter 10](#). However, PAH is a complex disease involving many cell types and signalling pathways. Therefore, I used RNA extracted from the *in vivo* MCT-induced PAH rat lung tissue, 10-days following AdBMP2 treatment, to conduct a microarray looking for any novel pathways that either contribute to the pathogenesis or reversal of PAH.

Unfortunately, the most robust comparison between the two viral treatment groups, MCT + AdTrackLucFab-9B9 and MCT + AdBMP2Fab-9B9 was not possible due to similarities in their gene expression profiles. This may be a result of the viral delivery in both groups, which may have dampened the genetic differences between the groups. Cellular and systemic responses due to the viral delivery would have been similar in both animal groups, and thus their gene expression profiles were not significantly different. However, the technical success of the experiment was shown through the significant differences in gene profiles between the Saline and MCT Only groups, as well as the MCT Only and MCT + AdBMP2Fab-9B9. Thus, it was pertinent to conduct a pathway analysis of MCT Only versus MCT + AdBMP2Fab-9B9 with the exclusion of matching significant genes that were identified between MCT Only and MCT + AdTrackLucFab-9B9 with the same significant genes that were identified between the MCT Only and MCT + AdBMP2Fab-9B9 groups. This layer of analysis eliminated those genes that were up- or down-regulated as a result of the viral delivery.

Pathway analysis of the resultant 2196 genes through the IPA system did not show any genetic differences in the Smad signalling pathways as ex-

pected. This has been speculated to be an issue with the time-point, and subsequent protein analysis of an earlier time-point (2 days post AdBMP2 treatment) was conducted. This protein analysis at the earlier time-point showed a significant increase in pSmad1/5/8 and a decrease in pSmad3 [Chapter 10](#). Thus, a peak signalling effect for the Smad pathways may be missed at the 10-day time-point, and therefore changes in the microarray for these Smad pathways are not seen.

Interestingly, non-Smad pathways were identified as altered and highly ranked in the analysis, along with eIF2 signalling as the top canonical pathway. eIF2 is essential for protein synthesis and involves PI3K, AKT, MEK, ERK1/2 and Ras molecules in its signalling pathways. All of these are well known molecules in BMP2 mediated non-Smad signalling. These molecules are involved in many cellular processes such as migration, differentiation, apoptosis, autophagy, extracellular matrix production and proliferation. Processes that have also been identified in PAH pathogenesis [145, 146, 147, 65]. Many of these non-Smad molecules have been implicated in tumorigenesis and other disease pathologies, usually exerting their control when increased [148]. However, their role in PAH needs to be further explored [147]. In this model, these molecules have been identified to be increased following AdBMP2 treatment, which seems to be counter-intuitive, however these molecules have varied roles depending upon the cell type and ligand stimulation [65]. For example, TGF- β mediated non-Smad signalling has been well characterised and is largely attributed to the pathogenesis of many diseases, as well as being essential for cellular homeostasis [68]. Thus, investigation of each of these molecules in the context of PAH needs to be undertaken to fully understand their role in the disease.

Other top canonical pathways such as the role of BRCA1, a gene well known for its mutational consequences in breast and ovarian cancer, is also emerging to be a novel target for PAH therapy [149]. Similarly, regulation of eIF4 and p70S6K signalling is a pathway that acts downstream of PI3K affecting cell proliferation and apoptosis [150]. These identified pathways all have been implicated in PAH pathogenesis, however, their role is yet to be fully elucidated [151]. Nevertheless, through examining these pathways, novel molecular targets for therapies can be identified.

The network functions analysis identified post-translational modification, developmental disorders, hereditary disorders, inflammatory response and energy production as the top associated network functions. All of these functions are known to be heavily disrupted in PAH pathogenesis. Disease and disorders that are highlighted reinforce the relevance of this PAH model. BMPR2 has a critical role in developmental biology, and developmental disorder is the top disordered network identified in the summary [152]. Similarly, mutations in BMPR2 are known to cause hereditary PAH [4]. Furthermore, plexiform lesions that are a hallmark of human disease are often described as "tumour-like" and thus very similar to cancer, with a high infiltration of inflammatory cells [35]. Furthermore, the identification of haematological disease networks is not surprising considering this is a disease that affects the pulmonary vascular system.

This microarray study determined that the BMPR2-mediated non-Smad pathways to be altered at the 10-day time-point. Whilst these pathways are known to be implicated in PAH pathogenesis, the therapeutic impact of key molecules in these pathways is unknown. Furthermore, the microarray identified novel targets such as eIFs and p70S6K amongst many more molecules that need to be further investigated in the context of this disease.

A microarray at the 2-day time point was not achievable within the time-frame of the project, however using these results from the 10-day time-point defined the scope of the non-Smad protein analysis of the 2-day time-point.

NON-SMAD SIGNALLING PROFILES ARE ALTERED FOLLOWING BMPR₂ MODULATION

12.1 OVERVIEW

The microarray studies at the 10-day time-point identified the importance of BMPR₂ mediated non-Smad signalling in the AdBMPR₂ treatment model [Chapter 11](#). Additionally, protein analysis of the 2-day time-point showed significant changes in the activation of the Smad signalling profiles [Chapter 10](#). Thus, further protein analysis was conducted of the 2-day time-point whole lung tissue, examining the non-Smad pathways identified with the microarray. I hypothesise that key non-Smad mediators identified in the microarray would also be altered in our protein analysis following our AdBMPR₂ treatment, contributing to the reversal of the disease.

BMPR₂ mediates both Smad and non-Smad signalling pathways [Chapter 4](#). Following the successful reversal of PAH following AdBMPR₂ treatment in the MCT induced PAH rat model and after showing an effect on the BMPR₂ mediated Smad pathways, I identified through a microarray that there are also effects on non-Smad signalling molecules in this study.

The AdBMPR₂ treatment study was initially conducted to assess both hemodynamic changes and lung tissue Smad protein expression, 10-days following the AdBMPR₂ treatment. However, despite replicating previously published positive hemodynamic results demonstrating a disease reversal at this time-point, I could not find any conclusive changes in Smad expression in the lung tissue following BMPR₂ up-regulation. Furthermore, the microarray analysis did not identify any Smad signalling pathways as

significantly changed at this time-point. It was hypothesised that a peak signalling effect was missed, and that an earlier time-point of 2 days post treatment would be better for the protein analysis. Following immunoblot studies of the whole rat lung tissue lysate at the 2-day time-point, I identified changes in pSmad1/5/8 and pSmad3. Thus, I have concluded that this time-point may be the best to examine protein expression in response to the early effect of BMPR2 gene delivery.

The microarray study did identify certain non-Smad molecules expression levels to be altered at the 10-day time-point, and thus these are the initial leads for protein analysis for non-Smad investigations at the 2-day time-point.

12.2 PI3K IS SIGNIFICANTLY INCREASED 2 DAYS FOLLOWING ADBMPR2 TREATMENT

Following the results in the BMPR2 mediated Smad molecules at the 2-day time-point [Chapter 10](#), it was logical to investigate the level of protein expression of the non-Smad molecules identified in the microarray. PI3K and p-p38 MAPK were investigated via immunoblot.

PI3K has been shown to be important in endothelial processes, particularly in angiogenesis [65] and this molecule was repeatedly identified in the IPA studies as altered in the MCT + AdBMPR2Fab-9B9 group compared to the disease control, MCT Only. Thus, analysis of this molecule may give an insight into what cellular signalling processes are being restored following our AdBMPR2 treatment in the rat MCT induced PAH model.

Protein analysis of whole rat lung tissue lysate, was performed via immunoblot using the Odyssey system (LI-COR) outlined in [Chapter 9](#). Antibodies were selected due to their availability at the time of analysis (see [Chapter 9](#) for note on antibody selection).

For the PI₃K analysis, results of the treatment groups were derived as a percentage of the Saline (100% ±19.39 SEM) treated animals. MCT Only (27.1% ±10.96 SEM) had a 3.68-fold decrease in PI₃K expression, and MCT + AdTrackLucFab-9B9 (43.1% ±7.880 SEM) had a 2.32-fold decrease compared to Saline (100% ±19.39 SEM) treated animals [Figure 41](#).

PI₃K expression in the MCT + AdBMPR2Fab-9B9 group was close to being fully restored to 95.1% (±7.357 SEM) of the Saline control group. MCT Only had a 3.50-fold decrease and MCT + AdTrackLucFab-9B9 had a 2.21-fold decrease compared to the MCT + AdBMPR2Fab-9B9 group [Figure 41](#).

12.3 DE-ACTIVATION OF P38 MAPK: 2 DAYS FOLLOWING ADBMPR2 TREATMENT

Phosphorylated-p38 MAPK (p-p38 MAPK) is a BMPR2 mediated non-Smad molecule. This molecule is important for cellular proliferation, is increased in tumours, and is also found to be increased in PAH plexiform lesions [145]. In addition to PI₃K, p-38 MAPK was repeatedly identified in the IPA studies as altered in the MCT + AdBMPR2Fab-9B9 group compared to the disease control, MCT Only.

For p-p38 MAPK analysis, results of the treatment groups were derived as a percentage of the Saline (100% ±10.91 SEM) treated animals. MCT Only (567.0% ±34.54 SEM) and MCT + AdTrackLucFab-9B9 (690.0% ±110.8 SEM)

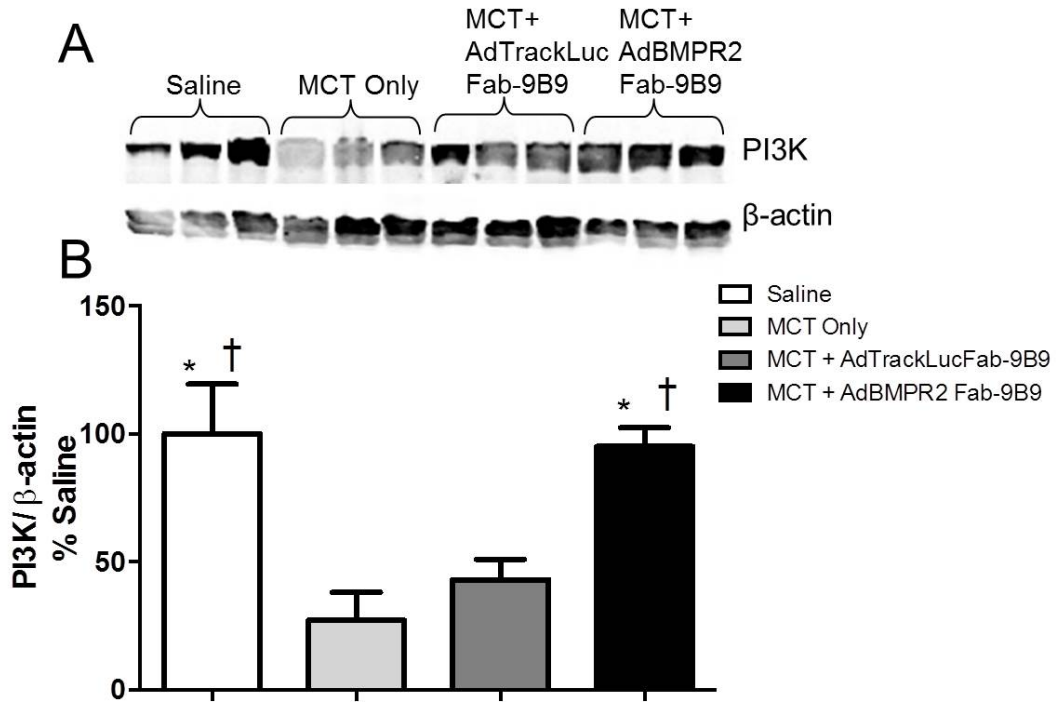


Figure 41: Immunoblot analysis of rat lung tissue 2 days post AdBMPR2 treatment. A. Immunoblot of 3 representative rats per group for PI3K and β -actin; and B. PI3K immunodetection results. $n=6$. Values are mean \pm SEM. * compared with MCT Only and † compared with MCT + AdTrackLucFab-9B9. $p < 0.05$.

groups had respective 5.67-fold and 6.90-fold increases compared to Saline (100% \pm 10.91 SEM) treated animals [Figure 42](#).

Activated p-p38 MAPK is decreased in the MCT + AdBMPR2Fab-9B9 (378.4% \pm 34.56 SEM) treatment group compared to the two disease controls, reflecting the lower level of expression seen in the Saline group [Figure 42](#). Both MCT Only (567.0% \pm 34.54 SEM) and MCT + AdTrackLucFab-9B9 (690.0% \pm 110.8 SEM) were significantly increased 1.50-fold & 1.82-fold, compared to MCT + AdBMPR2Fab-9B9 (378.4% \pm 34.556 SEM). However, despite the lower level of expression, the MCT + AdBMPR2Fab-9B9 treatment was still 3.78-fold higher than the Saline (100% \pm 10.91 SEM) group.

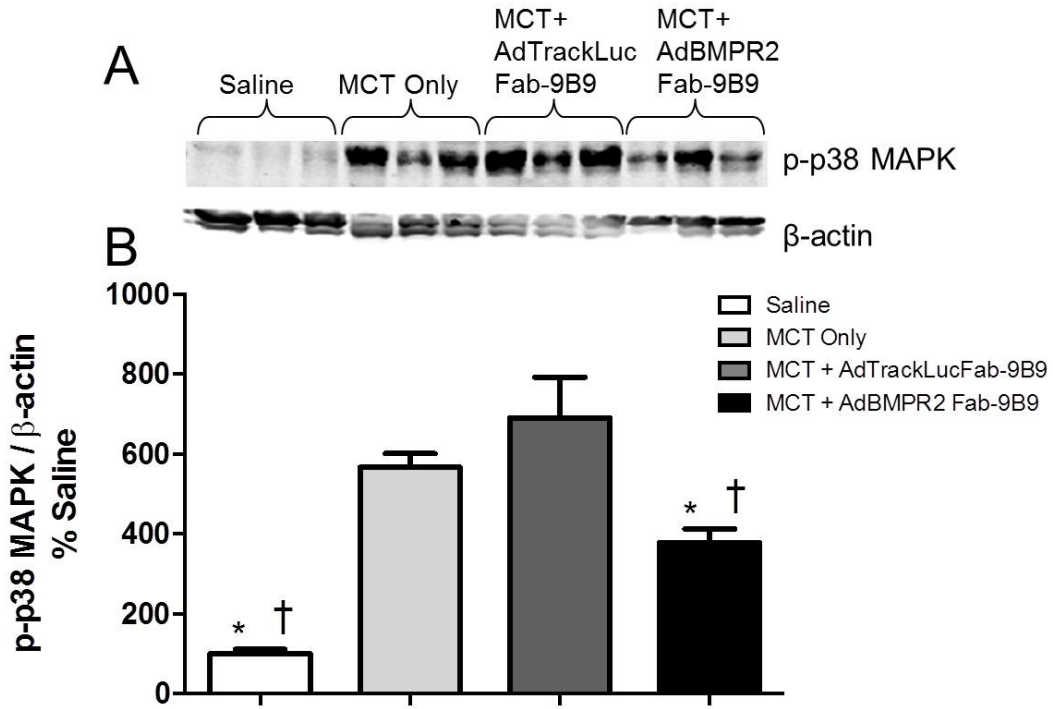


Figure 42: Immunoblot analysis of rat lung tissue 2 days post AdBMPR2 treatment. A. Immunoblot of 3 representative rats per group for p-p38 MAPK and β actin; and B. p-p38 MAPK immunodetection results. $n=6$. Values are mean \pm SEM. * compared with MCT Only and \dagger compared with MCT + AdTrackLucFab-9B9. $p < 0.05$.

12.4 DISCUSSION AND CONCLUSIONS

The attenuation of PAH following targeted delivery of BMPR2 to the pulmonary endothelium of rats with MCT-induced PAH has shown a restorative effect of the BMPR2/ TGF- β mediated Smad signalling axis [Chapter 10](#). Following a microarray analysis of the lung tissue from the 10-day time-point, it was apparent that the positive physiological responses to our therapy were not only due to these changes in Smad signalling, but also include changes in BMPR2 mediated non-Smad signalling pathways.

BMPR2 is known to mediate signalling pathways that do not involve Smad proteins. To date, known molecules in these pathways are PI₃K, ERK1/2, RhoA, Ras and p38 MAPK, however, these signalling mechanisms

are complex and under constant study [67]. The role of these pathways in PAH is not clear, certainly their role in the reversal of the disease is yet to be published. However, non-Smad pathways regulate apoptosis, cellular proliferation, migration and differentiation as well as exerting control over the Smad signalling pathways, thus it is not unreasonable to postulate that alteration of these pathways can contribute to the apoptotic resistant ECs, formation of plexiform lesions and the EndoMT changes seen in PAH.

Following the reversal of PAH in our MCT-induced PAH rat model, I have shown that PI3K is significantly reduced in the disease groups compare to the healthy Saline control group and the AdBMPR2 treatment group, PI3K is close to being fully restored to the same level of expression as the healthy control. The PI3K / AKT pathway regulates protein synthesis, apoptosis and cell proliferation [65, 147, 153]. Indeed, PI3K has been implicated in many different diseases, including many cancers. However, the role of PI3K is highly dependent on the cell type, the type of receptor and ligand that is activating the pathway. When activated by the BMP/ BMPR2 pathway, PI3K has been shown to have an essential role in normal angiogenic processes [65]. Furthermore, the PI3K / Akt pathway is a target of Adrenomedullin, a vasodilator peptide which decreases mPAP and RVH in hypoxic rats and has shown antiproliferative properties [150]. Thus, the classical pathway of PI3K / Akt may be pro-PAH pathogenesis, however, PI3K is involved in many non-canonical pathways which may indeed contribute to the reversal of PAH.

Another non-Smad pathway altered following our BMPR2 treatment is the p38 MAPK pathway. Activation of this pathway is significantly reduced in our BMPR2 treated animals compared to the two disease controls, approaching the normal levels shown in the healthy control. Phosphorylated-p38 MAPK is responsible for a plethora of cellular signalling processes,

such as proliferation, migration and apoptosis. Importantly, p38 MAPK signalling is retained in PAH with known BMPR2 mutation, suggesting that p38 MAPK is regulated in a BMPR2 independent manner, although still able to be activated through BMPs [150]. Furthermore, it has been shown that BMPR2 deficiency induces the activation of p38 MAPK in a TGF- β 1 dependent manner, contributing to PAH pathogenesis [48]. Thus, with the restoration of BMPR2 in our model the activation of p38 MAPK is decreased.

Despite the identification of these non-Smad molecules in the microarray at the 10-day time-point, there is difficulty showing protein expression changes at this time-point [Chapter 10](#). There may be physiological reasons for this as well as technical limitations of the protein analysis. The microarray pathway analysis that was conducted using IPA (Qiagen) utilises gene and protein databases to generate the significant list of molecules within a cellular signalling network that may be altered due to a gene being up- or down-regulated. Thus, this method of analysis is likened to a predictive model of cellular networks and whilst it gives a good indication of novel molecular targets to examine, it does not provide the level of expression of those molecules. Furthermore, genetic testing is significantly more sensitive than protein analysis, thus it was decided to analyse the earlier 2-day time-point which gave us the positive changes in the Smad protein analysis [Chapter 10](#).

The limited non-Smad molecules analysed is due to the technical limitations of the protein analysis, which makes it difficult to obtain clear results. The lysates are of the whole rat lung, and not of the pulmonary vessels, thus likely causing a dampening effect on what may be already a subtle change in expression. Additionally, the efficacy of these antibodies is somewhat low. These proteins are technically difficult to detect with immunoblot, and

required extensive optimisation. Further optimisation of other non-Smad molecules such as AKT, RAS, eIFs, BRCA1/2 and p70S6K are currently under way.

Through our targeted Ad vector technology we have previously restored BMPR2 expression in both the MCT and chronic hypoxia rat models of PAH [29]. Due to this BMPR2 modulation therapy, PAH was ameliorated. This current study demonstrates that attenuation of PAH is in part due to changes in Smad and non-Smad signalling pathways, reinforcing the notion that restoration of the BMPR2/ TGF- β signalling axis results in the reversal of PAH.

Our BMPR2 modulation therapy is useful for not only developing an alternative therapy for PAH, but also for studying the molecular process involved in this multifaceted disease. However, there are certain limitations to Ad vectors, such as systemic inflammation, targeting and length of transgene expression, and as such, I moved towards a cell-based approach to overcome these challenges.

GENE THERAPY USING ENDOTHELIAL PROGENITOR CELLS

13.1 OVERVIEW

To move our BMPR2 modulation model towards a more clinically applicable therapy, EPCs were used as a vehicle to deliver the BMPR2 to the pulmonary endothelium. For this proof-of-concept model, a method to extract bone marrow cells from rats, culture them in selective endothelial media to give EPCs, characterise them as EPCs, and transduce them with the Ad-vector containing BMPR2, was developed. Once this technique was established, these augmented cells could be used as a therapy in the rat MCT-induced PAH model.

Endothelial progenitor cells are becoming a widely studied cell type, not only for their involvement in recruitment and repair of vascular injury, but also because of their proliferative potential *in vitro*, which allows researchers to culture them, study their function and use them for potential therapies [154].

The therapeutic benefit of stem cells, as well as their role in pathogenesis has understandably become a popular area of research. This is due to their ability to self renew and differentiate into a wide range of cell types. There are two main reservoirs of stem cells: 1. embryonic, and 2. adult tissue. Embryonic stem cells (ESC) are pluripotent with the ability to self renew indefinitely and also differentiate into cells of all 3 germ layers, endoderm, ectoderm and mesoderm. Whilst stem cells resident in adult tissue have already undergone differentiation, they also have some capac-

ity to self renew [155]. Progenitor cells are the descendants of stem cells and whilst there is increasing study of these cells, their lineage is still quite contentious [22]. Progenitors are a subset of cells that have lost the ability to self-renew, however are able to divide in a clonogenic way and proliferate [155]. EPCs have been the most widely studied progenitor group since their discovery by Asahara *et al* [156] in 1997 and continue to be utilised in many different disease models as a potential therapy [157].

Due to recognised limitations of Ad-vectors in the *in vivo* setting, I have moved towards a cell based approach. EPCs not only contribute to neo-vascularisation and tissue recovery following injury, they also maintain vascular homoeostasis [156, 158, 128]. Furthermore, EPCs have natural lung homing abilities to areas of inflammation and stress [159]. EPCs however, have been implicated in many diseases, including PAH. Thus, these cells may not only be useful as a vehicle for therapy, but as target to be altered themselves.

These studies look to use bone marrow (BM) derived rat EPCs (r-EPCs) as a vehicle to deliver functional BMPR2 to the pulmonary endothelium. To achieve this, I devised a protocol to isolate and extract EPCs from the BM of male SD rats, and culture these cells until they are a purified, monoculture of proliferating EPCs. Once this was achieved, I looked to augment the cells by transducing them with AdCMVBMPR2myc for 48 h to over-express BMPR2. If up-regulation of BMPR2 in these cells is successful, then further studies to use them as a therapy for PAH could be conducted [Chapter 14](#).

Adapted from previous publications [160, 161], optimisation of the culture of r-EPCs involved many medium types (M199, RPMI and EBM), endothelial cell supplements (Lonza EC bullet-kit (EM & 2MV), and BD Endothelial Cell Growth Supplement (ECGS) and Heparin). FCS concentra-

tion has consistently been reported at 20% for human derived EPCs, and thus this was the concentration used in these experiments. M199 and RPMI (20%) with all EC supplements only gave rise to early out-growth r-EPCs, and these cells did not progress to colonies or proliferating r-EPCs. EBM with the 2MV supplement (Lonza) and 20% FCS was successful in producing colony forming, proliferating r-EPCs that were able to be cultured for 4 weeks and passaged.

Characterisation of the r-EPCs is the next essential step once the culture regime was optimised and successful. Methods for characterisation are under constant review and revision, however for this study I used morphological features and flow cytometry to confirm the r-EPC phenotype.

A transduction efficiency study was carried out to assess whether these cells could withstand the viral transduction and at what plaque forming unit (pfu) the viral transduction was most efficient. Both the r-EPCs and the positive control cell line A549 were transduced with an adenovirus with a GFP construct (AdCMVGFP) that is easily viewed under a fluorescent microscope. Once I established that these cells are capable of being transduced, I assessed AdBMPR2myc transduction capacity of the cells, as well as the positive up-regulation of BMPR2 from this transduction.

Development of the culture technique and augmentation of these r-EPCs to over-express BMPR2 allows the use of these cells as a potential therapy for PAH.

13.2 ISOLATION AND CHARACTERISATION OF RAT DERIVED EPCS

Bone marrow cells were successfully isolated from the femur of donor SD rats [Chapter 9](#). These cells were immediately cultured with the endothelial selective medium EGM-2MV (Lonza) in 20% FCS. Cells were undisturbed for 72 h to allow for maximum adherence of the EPCs. Media changes every 48 h over 6-8 days allowed the cells that were unable to grow and survive in the EC medium to be removed and the EPCs to remain. By day 6, a monoculture of cells appears.

Characterisation of EPCs continues to evolve as this field of study expands. However, there are several methods that are becoming widely accepted as the standard for positively characterising this cell population.

13.2.1 *Morphological Assessment*

Following seeding, cells were observed under the microscope for morphological changes. At day 4 post seeding, colonies appear, which continue to expand and by days 6-10, cells have the typical 'cobblestone' appearance and are ready to be passaged [Figure 43](#).

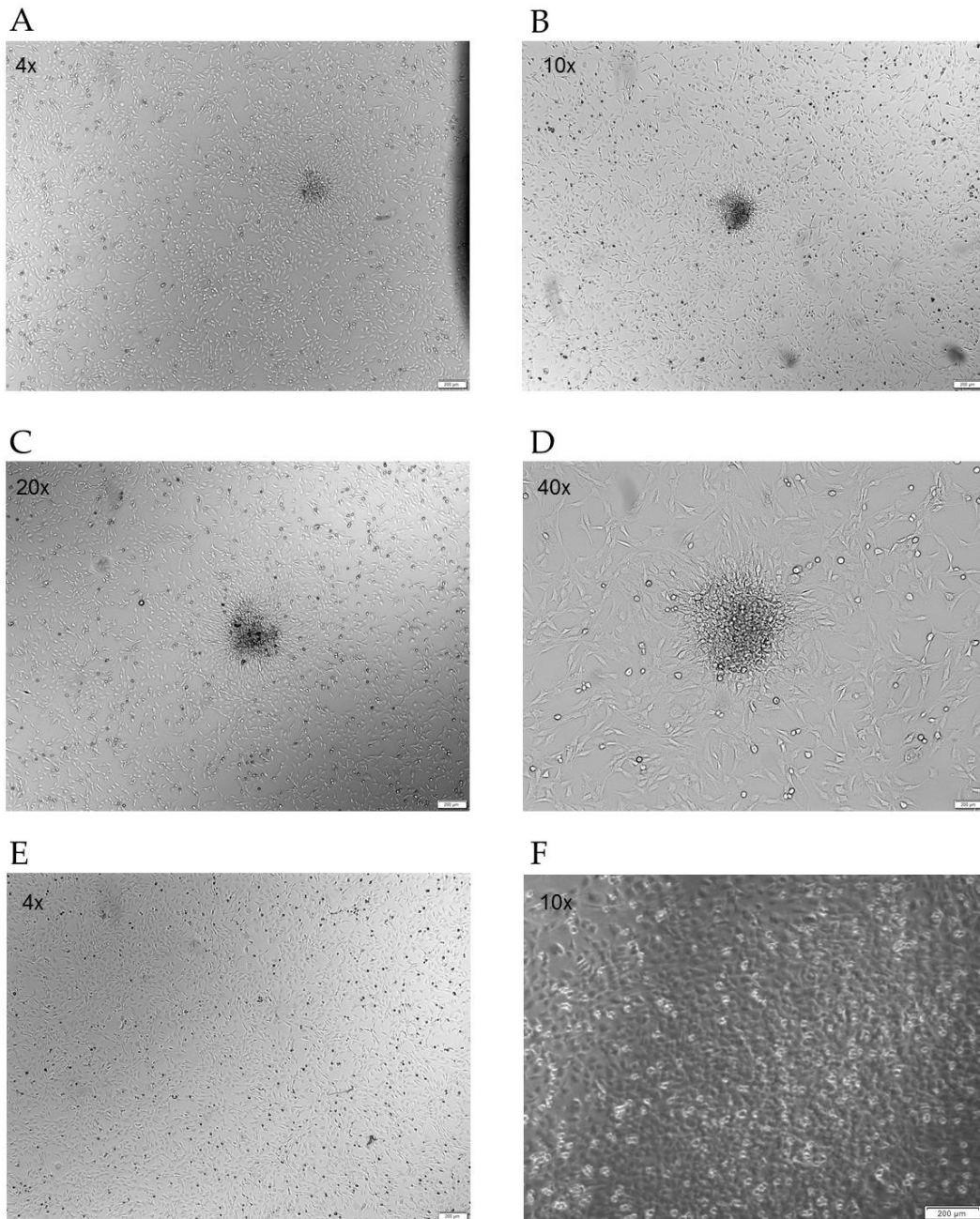


Figure 43: Phase contrast images of rat derived EPCs. A-D. Initial colony formation at day 3 under varying magnifications (4x, 10x & 20x) which give rise to proliferating EPCs; E. 4 days following seeding; and F. 10 days following seeding.

13.2.2 Flow cytometric analysis

Flow cytometry is regularly used to identify cell surface markers and thus is an ideal tool to assess the phenotype of the r-EPCs. However, there has been much debate in EPC literature as to what constitutes the phenotype of these cells, and what surface markers should and shouldn't be present on these cells. Added to this complication is the availability of rat species antibodies for analysis. Unfortunately, the availability of antibodies is limiting for this study, and thus only 3 antibodies were examined.

Flow cytometric analysis of the cells at day 6 show that they are VEGFR⁺, CD34⁺ and CD31⁻ [Figure 44](#). Compared to r-EPCs that are unlabelled, there is a clear shift in the peaks of cells that are labelled with pan-VEGFR and CD34. However, there is no shift in the cell population when labelled with CD31 [Figure 44](#).

13.3 EFFICIENT TRANSDUCTION OF RAT DERIVED EPCS

13.3.1 AdCMVGFP

Assessment of the transduction efficiency at the optimal viral load for r-EPCs was carried out. Cells were transduced with 0 pfu, 10 pfu, 100 pfu or 200 pfu for 48 h and then viewed under the confocal microscope. A549 cells, a readily transducible cell line was used as a positive control. Cells are transduced for 48 h as per previous *in vitro* studies which optimised transduction to a 48 h incubation. Transduction efficiency of the r-EPCs is shown with the positive GFP signal [Figure 45](#). Transduction is estimated to be around 90% at 200pfu.

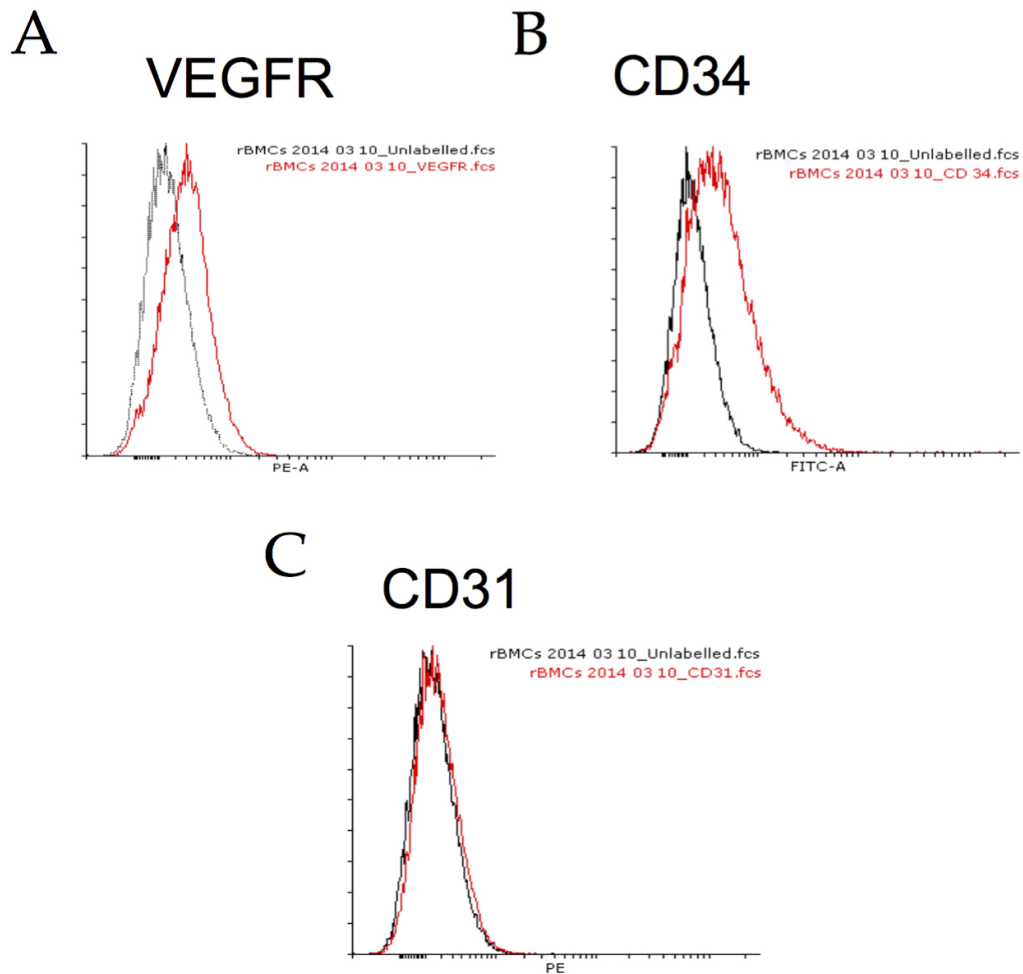


Figure 44: Flow cytometric analysis of rat derived EPCs: labelled (red) and unlabelled (black) 6 days following seeding. A. pan-VEGFR; B. CD34; and C. CD31.

13.3.2 *AdCMVLuc*

Further transduction studies looking at quantifying the production of the transgene expression in the r-EPCs was carried out using a luciferase assay system (Promega). Luciferase activity (RFU/ mg protein) was 1988-fold higher in the *AdCMVLuc* (1.66×10^8 RFU/ mg $\pm 3.143 \times 6$ SEM) transduced cells compared to r-EPCs treated with Media Only (83,328 RFU/ mg ± 24.03 SEM) [Figure 46](#).

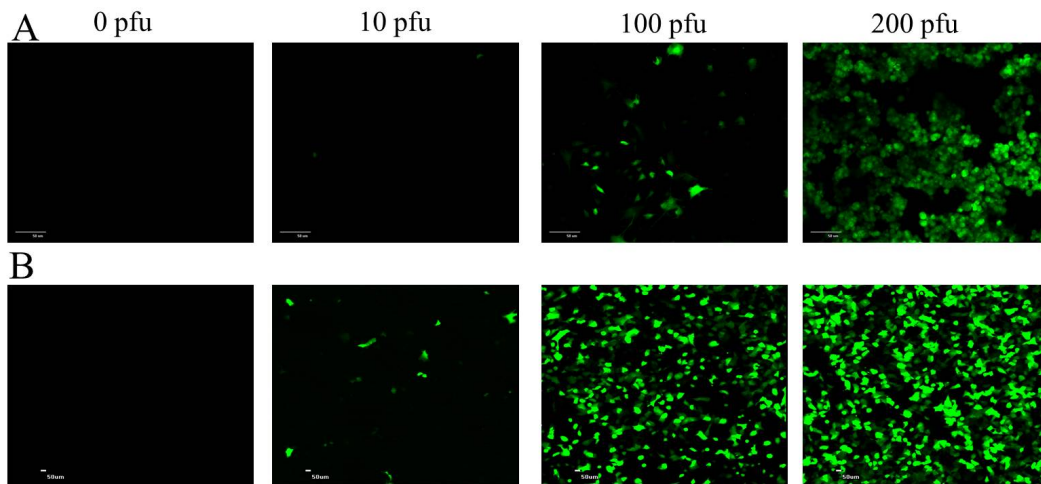


Figure 45: Assessment of transduction efficiency of AdCMVGFP in r-EPCs. Cells were transduced with 0 pfu, 10 pfu, 100 pfu or 200 pfu for 48 h and then viewed under the confocal microscope. A. r-EPCs; and B. A549.

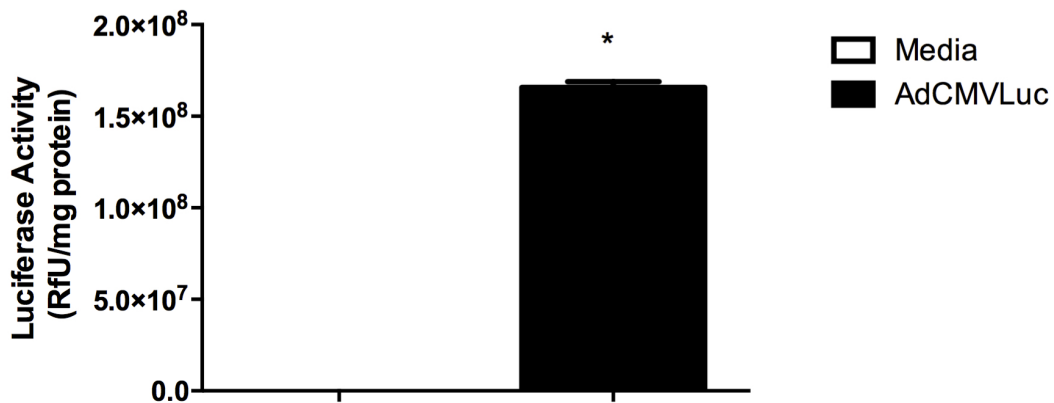


Figure 46: Quantification of the luciferase activity (RFU/mg protein) following AdCMVLuc transduction of r-EPCs for 48 h. Values are mean \pm SEM for $n=6$ /treatment. * compared with Media Only. $p < 0.0001$.

13.4 SUCCESSFUL BMPR2 UP-REGULATION IN RAT DERIVED EPCS

After assessing the r-EPCs ability to be transduced and optimising the viral load, r-EPCs were transduced with an Ad-vector containing the gene of interest, BMPR2. Thus, r-EPCs were transduced with AdCMVBMPR2myc at 200 pfu for 48 h. Samples were treated and analysed as per [Chapter 9](#). Briefly, cells were lysed and the protein lysate was analysed for total pro-

tein (DC Protein Assay, BioRad). 15 μ g of protein was loaded into each well, and ran in an SDS-Electrophoresis system. Proteins were transferred onto a nitrocellulose membrane and probed with goat anti BMPR2 (Santa Cruz).

Cells transduced with AdCMVBMPR2myc had a 12.6-fold increase in BMPR2 expression (0.067 I.I \pm 0.015 SEM) compared to Media Only (0.023 I.I \pm 0.004 SEM), and a 4.5-fold increase compared to AdTrackLuc (0.030 I.I \pm 0.008 SEM) **Figure 47**.

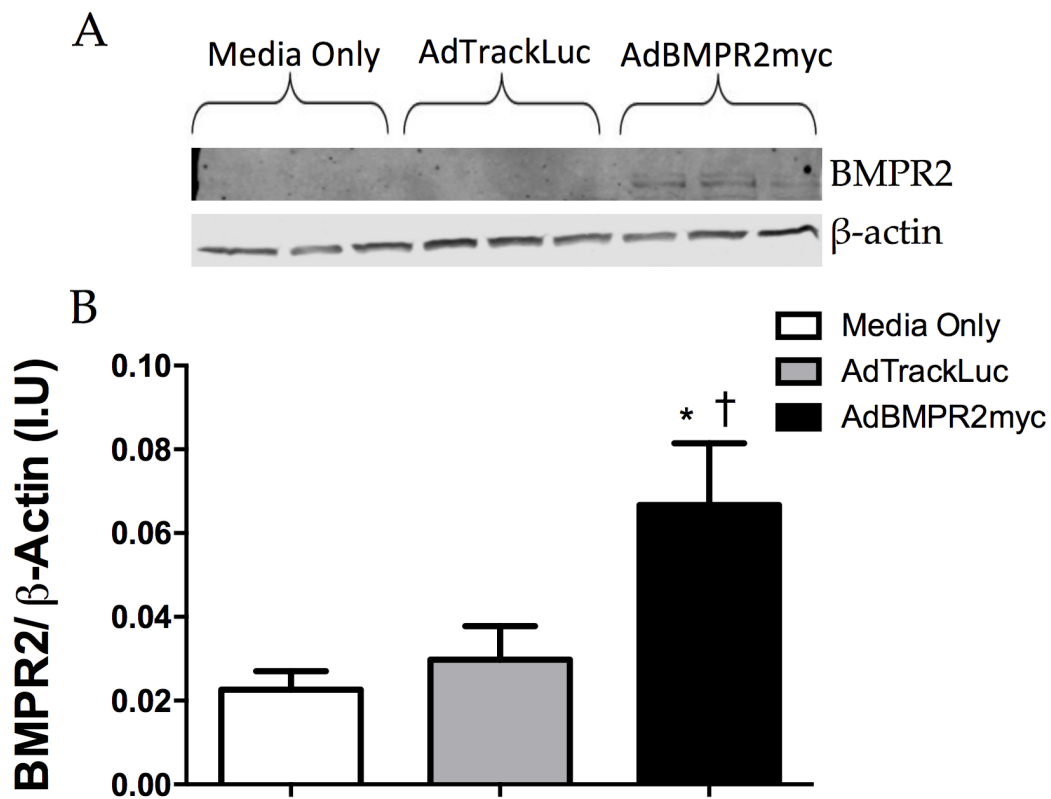


Figure 47: Immunoblot analysis of r-EPCs 48 h post AdCMVBMPR2myc transduction. **A.** Representative immunoblot of BMPR2 and β -actin; and **B.** BMPR2 immunodetection results. Values are mean \pm SEM for $n=3$ wells/treatment. * compared with Media Only and \dagger compare with AdTrackLuc. $p < 0.05$.

To confirm this up-regulation was indeed induced by the transduction of AdCMVBMPR2myc, samples were assessed for myc expression. There was a 8.32-fold increase in myc expression in cells treated with AdCMVBMPR2myc

(15.74 I.I \pm 4.270 SEM) compared to Media Only (1.893 I.I \pm 0.752 SEM), and a 15.65-fold increase in myc expression in the AdCMVBMPR2myc treated cells compared to the AdTrackLuc (1.006 I.I \pm 0.153 SEM) treated cells [Figure 48](#).

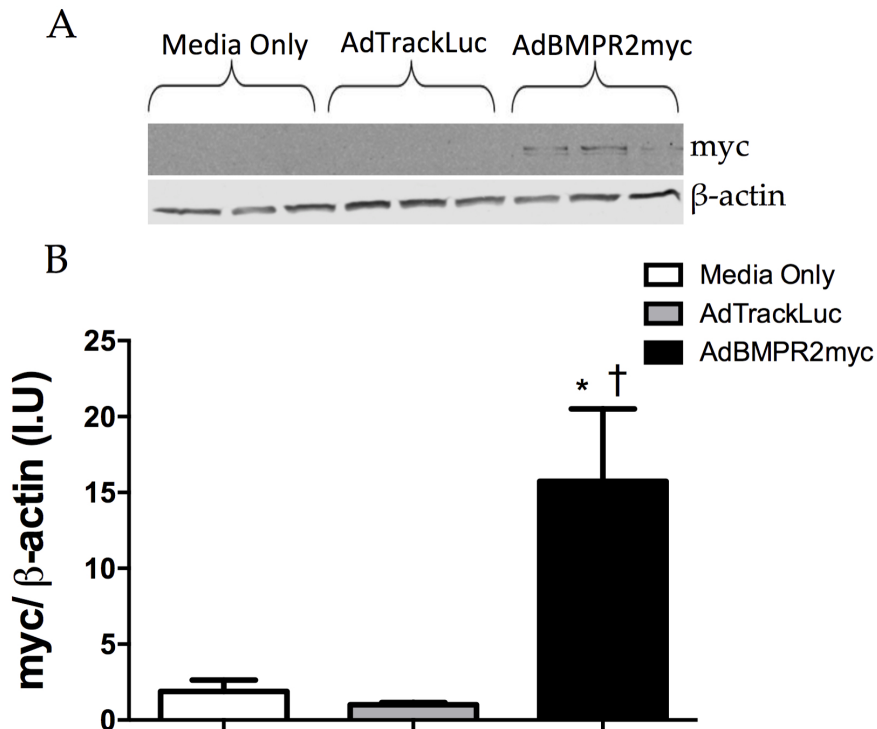


Figure 48: Immunoblot analysis of r-EPCs 48 h post AdCMVBMPR2myc transduction. A. Representative immunoblot of myc and β -actin; and B. myc immunodetection results. Values are mean \pm SEM for $n=3$ wells/treatment. * compared with Media Only and † compared with AdTrackLuc. $p < 0.05$.

13.5 DISCUSSION AND CONCLUSION

The use of EPCs in our BMPR2 modulation model would heighten this therapy's clinical applicability. Thus, deriving a method to isolate, culture, characterise and transduce these cell was imperative for this proof-of-concept model to be successful.

Our success in attenuating PAH following AdBMPR2 treatment using a targeted Ad-vector system has led to the development of a cell therapy, moving us towards a more clinical approach for treatment of PAH. Ad-vectors have recognised limitations: limited transgene expression, systemic inflammatory issues and potential 'off-target' effects. All of these issues, combined with the historical notion that Ad-viral delivery is unsafe for human subjects, makes the potential for this kind of therapy advancing to clinical trials as unlikely and limited. Cell therapy not only addresses these recognised pitfalls of Ad viral gene therapy, but is also perceived to be a safer approach for human therapy.

This study demonstrates a method to isolate r-EPCs from the bone marrow of SD rats [Chapter 9](#). These BMCs were seeded into an optimised endothelial selective medium, and following 6 days of culture, characterised as r-EPCs. These cells were proliferating and had the capability to be successfully passaged. Characterisation of these cells was conducted through morphological observation under microscope and flow cytometry. Limitations of this study arose from the availability of rat specific antibodies for flow cytometry. This resulted in only assessing 3 surface markers, though these are key in defining the r-EPC population. Nevertheless, with the increase in studies using rat derived EPCs, there will be an increase in development for antibodies to characterise these cells. The r-EPCs were positive for VEGFR and CD34, however they did not show any positive staining for CD31. Analysis of the r-EPCs was conducted at day 6, thus the cells were relatively 'young.' CD31 is a mature EC marker, and thus the cells may simply be not mature enough to display this on their surface.

Further functional characterisation of these cells have been undertaken by many other groups. EPCs ability to take-up Acetylated Low Density Lipoprotein (Ac-LDL), form tubes in Matrigel[®] and migrate *in vitro* as well

as form new vessels, integrate into existing vessels and improve existing vessels function *in vivo* have been extensively reported [162, 163, 164, 156].

Once the technique to isolate and culture the r-EPCs was established, the study moved towards establishing a BMPR2 augmentation method. Transduction efficiency of these cells was comparable to the readily transduced cell line, A549s. Furthermore, upon quantification, r-EPCs showed a significant increase in luciferase activity following AdTrackLuc transduction. Thus, through the transgene expression of GFP and luciferase this study demonstrated that these cells are able to be transduced with an Ad-vector with minimal cytoplasmic toxicity.

Following confirmation that these cells are transducible, they were transduced with AdCMVBMPR2myc, showing a significant increase in BMPR2 expression as well as myc expression. This is important for progressing this cell based gene therapy approach towards the *in vivo* model. Further BMPR2 mediated Smad and non-Smad analysis in these cells is currently under-way.

Endothelial progenitor cells have been used for many different therapy studies, mainly involving regeneration and repair of tissue [165, 166, 167]. Interestingly, the majority of these animal studies, and studies with human donors, use the r-EPCs without any augmentation. The rationale for this is that these cells naturally home to sites of damage and have the natural ability to exert therapeutic benefits. I hypothesise that by up-regulating BMPR2 in these cells, I am adding to these therapeutic properties and thus, boosting the potential for these cells to be a therapy for PAH.

Successful isolation and characterisation of the r-EPCs allows me to continue the pursuit to use these cells as a potential therapy for PAH. These

r-EPCs were easily transduced with the Ad vector containing the gene of interest, BMPR2, showing a significant increase in BMPR2 expression. This was the initial step in developing the r-EPCs as a vehicle to safely deliver BMPR2 to the pulmonary endothelium of rats with MCT induced PAH and is a logical progression from the *in vivo* studies with the Ad vector showing therapeutic efficacy. Ultimately however, a transfection strategy other than using Ad may prove to be more translatable for the '*ex vivo*' modulation of EPCs - high efficiency non-viral methods or integrative vectors such as lentivirus may be explored once the therapeutic principle of modified cell based therapy is established.

AMELIORATION OF PAH FOLLOWING BMPR₂ DELIVERY VIA AUGMENTED *EX VIVO* RAT DERIVED EPCS

14.1 OVERVIEW

Successful isolation, characterisation and up-regulation of BMPR₂ in rat bone marrow derived EPCs (r-EPCs) [Chapter 13](#) paved the way for a cell therapy model for PAH. In this pre-clinical study, I look to use these augmented r-EPCs to deliver BMPR₂ to the pulmonary endothelium of rats with MCT-induced PAH. I hypothesise that these cells will home to the lung, exert either direct or paracrine effects on the pulmonary endothelium and by doing this, PAH will be ameliorated.

Since the identification of endothelial progenitor cells (EPC) by Asahara *et al* in 1997 [156], the understanding of vasculogenesis in adults was revolutionised. Angiogenesis was once thought to be a process largely undertaken in embryogenesis and further vasculogenesis was carried out by endothelial cell (EC) precursors such as angioblasts [168]. Thus, this report gave strong evidence of post-natal angiogenesis as well as a cell population that can be isolated and cultured *ex vivo*. This was a pivotal step towards developing cell therapy for vascular diseases.

Endothelial progenitor cells have been used in many human trials and animal models as a therapy for a wide range of vascular diseases, including PAH, with varying results. Most cell therapies utilise the angiogenic potential of the EPCs alone to exert therapeutic effects, with a limited amount of studies augmenting the cells. Treatments have been autologous or with

donor cells, which leads to a need for cell banks to cater for the demand of treatments.

There are many advantageous characteristics which make EPCs an excellent candidate for cell therapy in the pulmonary vasculature. Firstly, these cells are the perfect size and shape to filter into the pulmonary arteries, particularly to the distal arteries where PAH lesions occur. Secondly, they are capable of being augmented to over-express a desired receptor, enzyme, ligand or molecules such as nitric oxide (NO) [169]. Thirdly, these cells naturally home to the site of injury and hypoxia. EPCs mobilise out of the BM when levels of hypoxia inducible factor-1 α (HIF-1 α), erythropoietin (EPO), VEGF or CXC chemokine ligand 12 (CXCL12) are produced [162]. All of which are elevated in the lungs in subjects with PAH. As part of this study, we examined the bio-distribution of r-EPCs following IV injection into SD rats. These cells were augmented with AdTrackLuc to over express luciferase and examined for biodistribution one hour following IV injection into the rats.

Following the positive bio-distribution results, I moved on to assess the immediate effects of BMPR2 transduced r-EPCs in rat lungs of healthy SD rats compared with untreated rats and rats with MCT-induced PAH. I examined BMPR2 expression and Smad1/5/8 signalling in whole rat lung lysates, taken from **healthy rats** 1 h following IV injection of BMPR2-EPCs, to initially assess whether the delivery of the BMPR2-EPCs had an immediate effect, if any, on Smad signalling in the lungs.

Following these studies, BMPR2 augmented r-EPCs were then IV injected into SD rats with MCT-induced PAH. Previously, we were successful in ameliorating PAH in our gene therapy proof-of-concept models [29], which involved delivering BMPR2 to the pulmonary endothelium via tar-

geted Adeno-viral technology. Thus, my rationale for this preclinical proof-of-concept model was to replicate this BMPR2 modulation therapy using augmented r-EPCs as the delivery vehicle.

This study involved three groups: 1. MCT Only; 2. MCT + EPCs; and 3. MCT + BMPR2-EPCs. A Saline group was not included in this study as we have an excessive amount of Saline animal data accumulated over the past 10 yrs and adding to this was deemed unnecessary. The MCT Only group is the disease control, allowing the assessment of the MCT inducement of PAH. The MCT + EPCs is the most robust control as the r-EPCs are used as the vehicle of BMPR2 delivery, and thus any physiological effects seen in the treatment group, MCT + BMPR2-EPCs must be compared to the MCT + EPCs group as it has been reported in the literature that EPCs alone can have a therapeutic effect in PAH models [110]. However, these reports are inconsistent as some studies have shown positive effects and others have shown no effects [159, 168, 22]. Thus, whilst the MCT + EPC group serves as a robust comparison for the MCT + BMPR2-EPC group, the potential result of that comparison was unpredictable before the study was conducted.

As outlined in [Chapter 10](#), physiological measurements are made of the animals to ascertain whether the PAH is attenuated following BMPR2-EPCs treatment. Briefly, these measurements are: FI as a measurement of the RVH, RVSP and mPAP. Again, measurements to ascertain the consistency of animal health were obtained, such as BW, HR and mSAP. The time-point for these was 10-days post treatment. This was chosen for consistency with our other treatment models as the effects of cell therapy has an unknown time-frame in the *in vivo* setting. Therefore, after obtaining positive hemodynamic results in our previous models at this time-point, I hypothesised that the 10-day time-point is the most relevant.

14.2 BIO-DISTRIBUTION OF RAT DERIVED EPCS

To assess the capacity for the IV injected r-EPCs to home to the lung, a bio-distribution study was conducted. For this study, r-EPCs were transduced consistently with the optimised method outlined in [Chapter 13](#). Briefly, the r-EPCs were isolated, cultured and transduced for 48 h at 200 pfu with Ad-TrackLuc. The cells were then lifted, washed and re-suspended in PBS for IV injection into SD rats. One hour after injection, the rats were given an IP injection of *in vivo* grade luciferin and viewed under the IVIS Lumina (PerkinElmer) to observe cell bio-distribution via luminescence intensity.

14.2.1 *In vivo* Luciferase Peak Signalling Time-curve

To establish the correct time of analysis post-luciferin injection in the live animals and thus to reduce the time animals are sedated and in the IVIS Lumina, a peak signalling curve was established. Following advice from the Adelaide University Microscopy staff, the first whole body scan proceeded 10 mins following luciferin injection, and every scan was conducted every 5 mins thereafter until a peak signal is recorded and subsequent luciferase signals were decreasing. For this study, a peak signal was recorded at 15 mins post luciferin injection [Figure 49](#).

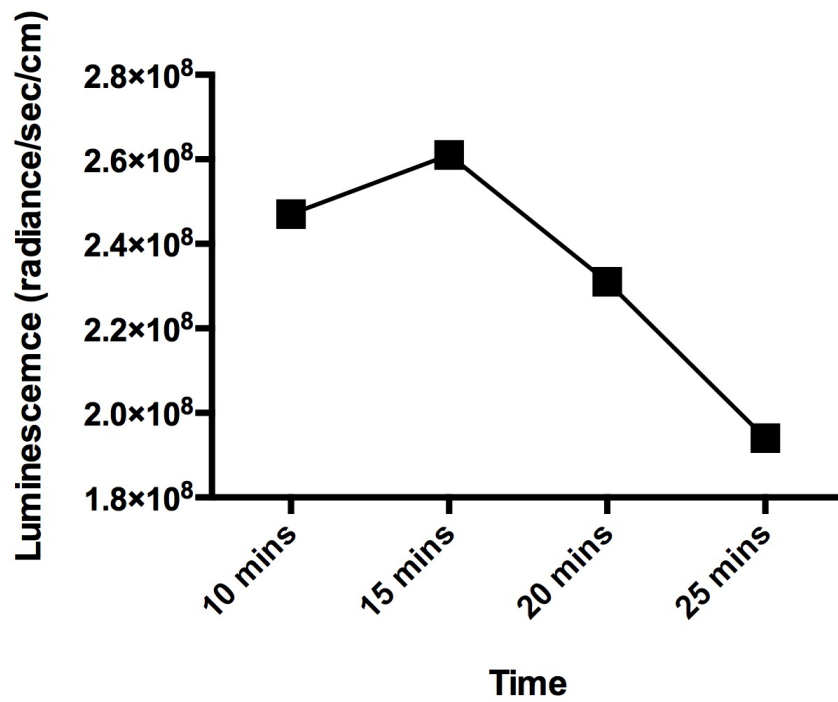


Figure 49: Luminescence time-curve in live rats post IV injection of AdTrackLuc transduced *ex vivo* r-EPCs. *n*=1 rat.

14.2.2 *R-EPCs home to the lung following IV injection*

Rat derived EPCs homing ability to the lung following IV injection was confirmed via luminescence full body scanning and *ex vivo* scanning of the lungs and liver [Figure 50](#). The average peak luminescence of the full body scan was 1.36×10^8 photons/sec ($n=3$ rats). No positive signal was detected outside of the lung region in the full body scan. The peak luminescence for the *ex vivo* lungs was 5.74×10^8 photons/sec ($n=1$) and the liver was 3.92×10^5 photons/sec ($n=1$) [Figure 51](#).

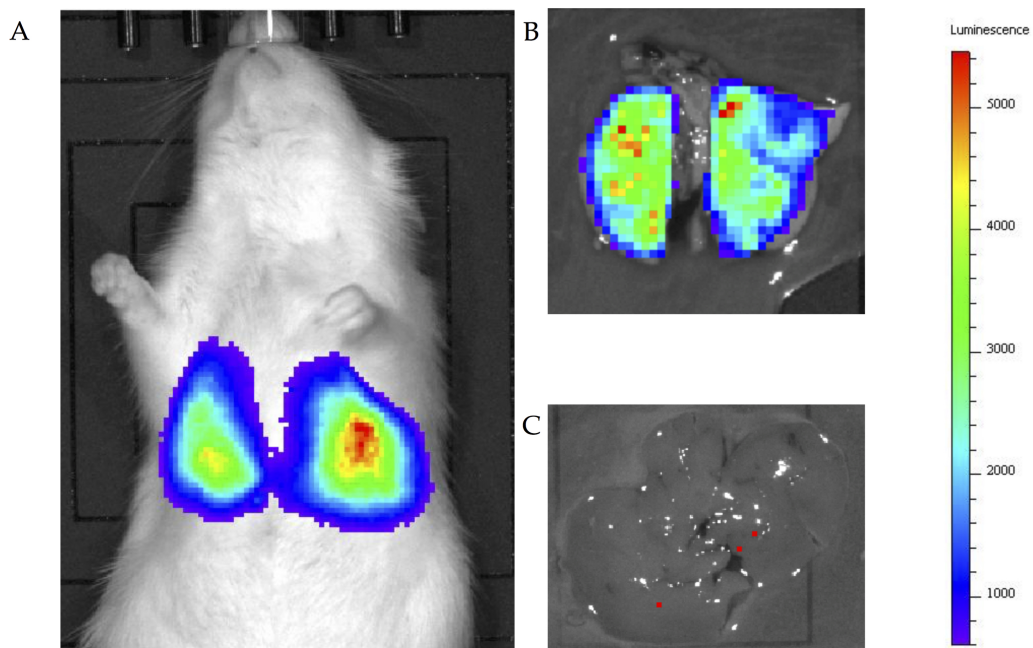


Figure 50: Luminescence scanning of rats 1 hour post IV injection of AdTrackLuc transduced r-EPCs. A. Full body scan. B. *Ex vivo* lung scan. C. *Ex vivo* liver scan. Colour on the images are representative of the amount of luminescence as indicated by the scale.

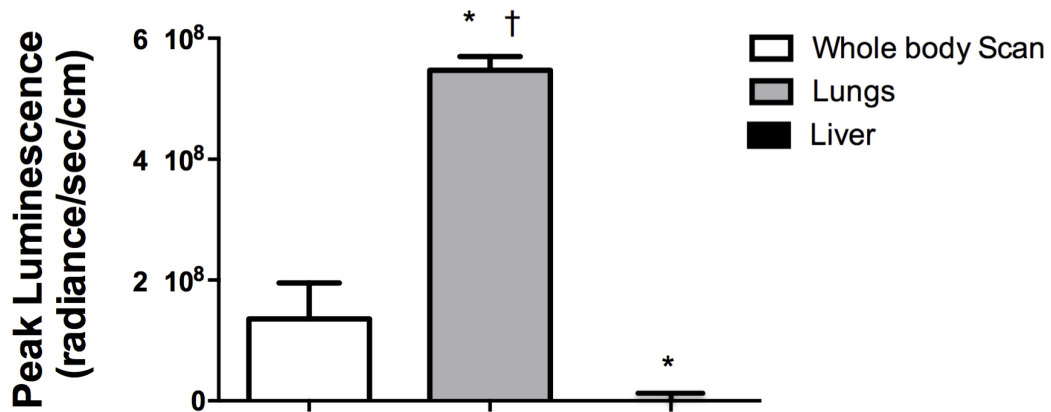


Figure 51: Quantification of luminescence scanning of rats 1 hour post IV injection of Ad-TrackLuc transduced r-EPCs. Values are mean \pm SEM. * compared with whole body scan and † compared with *ex vivo* liver. $p < 0.05$

14.3 BMPR2 UP-REGULATION 1 H FOLLOWING BMPR2-EPC TREATMENT

A lung biodistribution analysis of BMPR2-EPC treatment was undertaken. R-EPCs transduced with AdCMVBMPR2myc for 48 h were injected IV into healthy rats. After 1 h, the rats were humanely killed and the left lung lobe was not perfused to avoid washing out the cells in the vessels, however the lobe was inflated and processed into paraffin. The right lung lobes were snap frozen for protein analysis.

Initial immunohistochemical analysis was inconclusive. Auto-fluorescence from the red blood cells (RBC) in the pulmonary arteries made staining difficult. Therefore, protein was isolated from the frozen whole right lung lobes.

Protein analysis of lysate from whole rat lung tissue, was performed via immunoblot using the Odyssey system (Licor) as outlined in [Chapter 9](#). Antibodies were selected due to their availability, specificity and sensitivity (see [Chapter 9](#) for note on antibody selection).

Rats treated with BMPR2-EPCs were compared with Saline and MCT Only rats taken from the previous AdBMPR2 study. Saline rats were used a normal control, and MCT Only was used a 'negative' control.

BMPR2 expression in the BMPR2-EPC (1.9 I.I \pm 0.128 SEM) treated rats was increased 3.43-fold compared to Saline (0.55 I.I \pm 0.081 SEM) rats and increased by 7.55-fold compared with MCT Only (0.25 I.I \pm 0.087 SEM) rats [Figure 52](#). As expected, the MCT Only group had a 2.20-fold decrease in BMPR2 expression compared to the Saline rats.

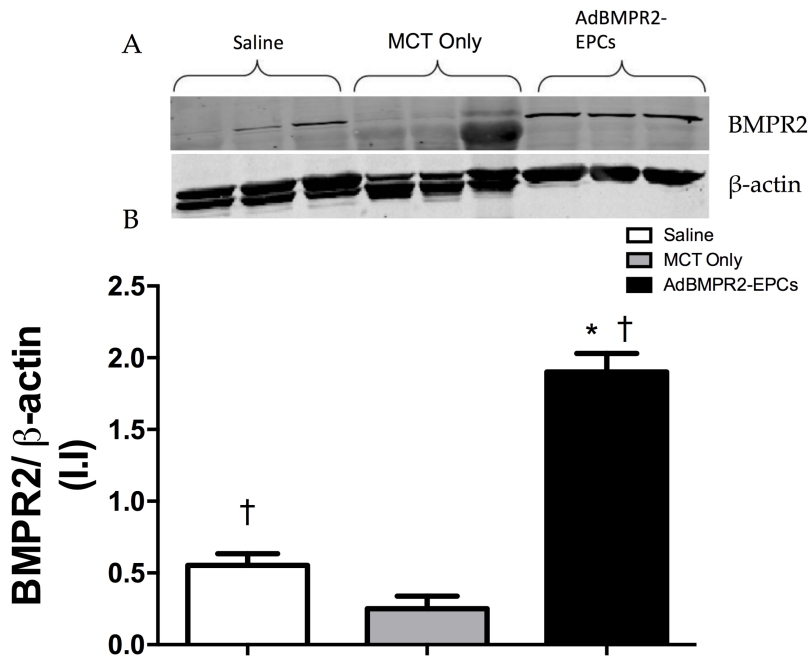


Figure 52: Immunoblot of a 1 h BMPR2-EPC treatment results in an immediate significant increase in BMPR2 expression. A. Representative immunoblot of 3 individual rats for BMPR2 and β -actin expression; and B. BMPR2 immunodetection quantification. $n=3$. Values are mean \pm SEM. * compared with Saline and † compared with MCT Only. $p < 0.05$.

14.4 ACTIVATION OF THE SMAD1/5/8 PATHWAY 1 H FOLLOWING BMPR2-EPC TREATMENT

Following BMPR2 analysis at the 1 h time-point, I proceeded to examine this tissue for changes in the BMPR2 mediated Smad1/5/8 pathway with the same controls, Saline and MCT Only.

Interestingly, p-Smad1/5/8 was increased 1.24-fold in the BMPR2-EPC (3.22 I.I ± 0.568 SEM) treated rats compared to Saline (2.59 I.I ± 0.640 SEM) and 4.49-fold compared to MCT Only (0.65 I.I ± 0.146 SEM) treated rats. pSmad1/5/8 was also significantly higher in the Saline group (2.59 I.I ± 0.640 SEM) by 3.99-fold compared to the MCT Only group (0.65 I.I ± 0.146 SEM) [Figure 53](#).

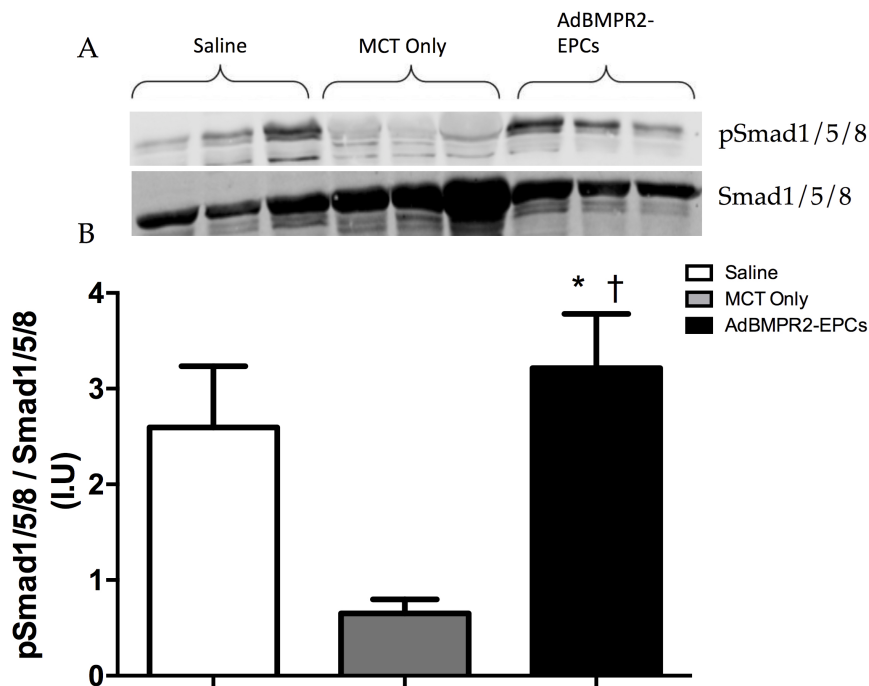


Figure 53: BMPR2-EPC treatment activates the Smad1/5/8 pathway. A. Representative immunoblot of 3 rats for pSmad1/5/8 and Smad1/5/8 expression; and B. pSmad1/5/8 immunodetection quantification. $n=3$. Values are mean ± SEM.* compared with Saline and † compared with MCT Only $p < 0.05$.

14.5 BMPR2 AUGMENTED RAT DERIVED EPCS AMELIORATES PAH IN THE RAT MCT MODEL

To assess the effectiveness of the BMPR2-EPC treatment in SD rats with MCT-induced PAH, physiological measurements were taken as outlined in [Chapter 9](#).

The induction of PAH by MCT is evidenced by the elevated FI, RVSP and mPAP in the MCT Only group compared to the Saline group from the previous AdBMPR2 study [Chapter 10](#). FI was significantly increased by 39.80% ($0.505 \text{ g} \pm 0.033$ vs $0.304 \text{ g} \pm 0.023$ SEM). The RVSP was increased by 80.64% ($76.00 \text{ mmHg} \pm 4.166$ vs $14.71 \text{ mmHg} \pm 0.918$ SEM) and mPAP was increased by 73.76% ($32.43 \text{ mmHg} \pm 3.254$ vs $8.51 \text{ mmHg} \pm 0.704$ SEM).

The amelioration of PAH is shown through the assessment of FI, RVSP and mPAP, 10 days following the EPC treatments. The FI was significantly reduced by 25.68% in the MCT + BMPR2-EPC ($0.375 \text{ g} \pm 0.017$ SEM) compared to the MCT Only ($0.505 \text{ g} \pm 0.033$ SEM) group, and despite there being no statistical significance, the MCT + BMPR2-EPC FI was reduced by 16.28% compared to the MCT + EPCs ($0.448 \text{ g} \pm 0.046$ SEM) group. The FI was also reduced in the MCT + EPCs by 11.24% compared to the MCT Only group, and this was also statistically insignificant [Table 8 Figure 54](#).

The amelioration of PAH following the BMPR2-EPC treatment is also shown by the significant reduction of the RVSP in the MCT + BMPR2-EPCs ($51.58 \text{ mmHg} \pm 4.284$ SEM) group by 32.89% compared to MCT Only ($76.00 \text{ mmHg} \pm 4.166$ SEM) and a 42.67% decrease in the mPAP ($18.60 \text{ mmHg} \pm 2.443$ SEM) compared to MCT Only ($32.43 \text{ mmHg} \pm 3.254$ SEM) [Table 8 Figure 54](#).

RAW HEMODYNAMIC DATA OBTAINED 10 DAYS FOLLOWING ADBMPR2 TREATMENT			
Treatment Group	FI	RVSP (mmHg)	mPAP (mmHg)
MCT Only	0.505 ± 0.033	76.00 ± 4.166	32.43 ± 3.254
MCT + EPCs	0.488 ± 0.046 *	77.73 ± 3.357 *	22.07 ± 1.366 *
MCT + BMPR2-EPCs	0.375 ± 0.017 * †	51.58 ± 4.283 * †	18.60 ± 2.443 * †

Table 8: Raw hemodynamic data obtained 10 days following AdBMPR2 treatment. Values are mean ± SEM. * compared with MCT Only and † compared with MCT + EPCs. p < 0.05

Interestingly, the MCT + BMPR2-EPCs group (51.58 mmHg ±4.283 SEM) had a 33.64% reduction in RVSP compared to MCT + EPCs (77.73 mmHg ±4.166 SEM) group and a 15.75% decrease in mPAP (18.60 mmHg ±2.443 SEM) compared to MCT + EPCs (22.07 mmHg ±1.366 SEM) group, which was not-statistically significant. However, the MCT + EPCs (22.07 mmHg ±1.366 SEM) had a 31.95% decrease in mPAP compared to MCT Only (32.43 mmHg ±3.254 SEM) group, despite there being no change in RVSP between these groups [Table 8](#). This finding warrants further confirmation, as the number of animals in which a technically satisfactory measurement of mPAP is achieved was low.

Consistency of animal health between the groups is assessed by the HR, mSAP and BW. Whilst there was no statistical difference between the groups for HR and mSAP, there was a significant increase of 10.01% in BW for the MCT + BMPR2-EPCs (383.15 g ±8.485 SEM) group compared to the MCT Only (348.3 g ±6.267 SEM) group and 18.27% increase compared to the MCT + EPCs (324.0 g ±5.420 SEM) group [Figure 55](#). This indicates that the MCT + BMPR2-EPCs group was healthier at the time of hemodynamic assessment.

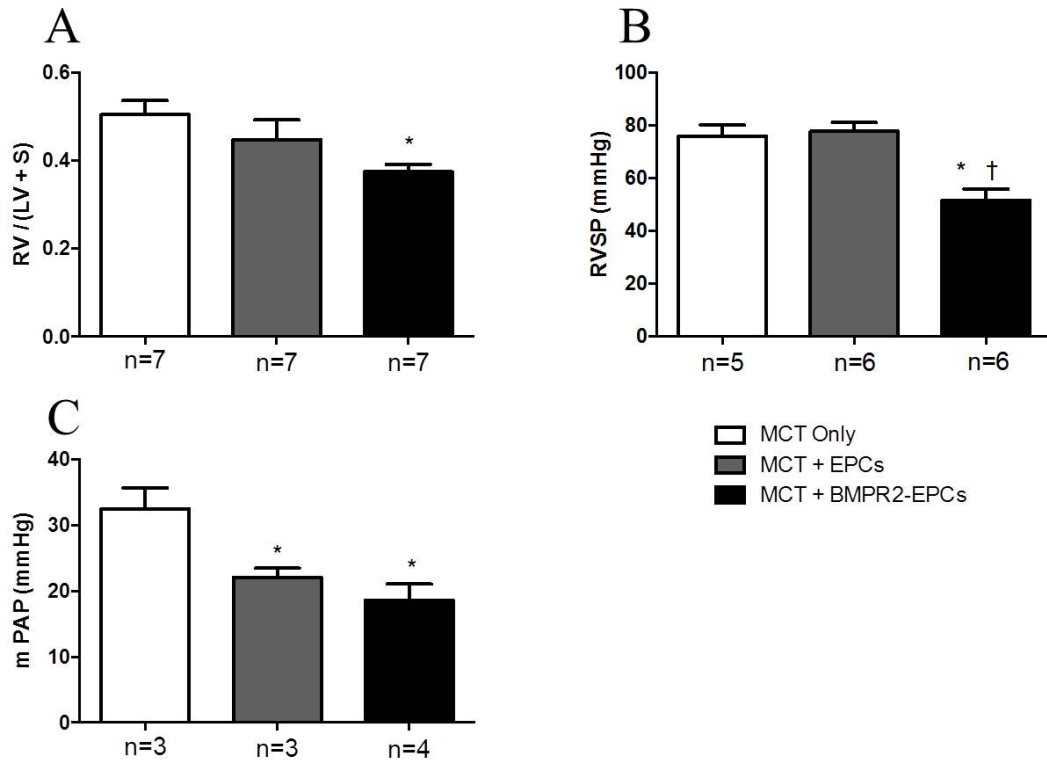


Figure 54: Effect of BMPR2-EPC treatment on the progression of MCT-induced PAH. A. Fulton Index (g); B. right ventricular systolic pressure (mmHg); and C. mean pulmonary arterial pressure (mmHg). Values are mean \pm SEM. * compared with MCT Only and † compared with MCT + EPCs. $p < 0.05$.

14.6 COMPARISON OF ADBMPR2 TREATMENT WITH BMPR2-EPCS TREATMENT: FI 10-DAYS FOLLOWING TREATMENT

To make a direct comparison between the AdBMPR2 treatment and the BMPR2-EPC treatment a secondary MCT- induced PAH SD rat study was conducted. The aim of this study was to re-confirm the previous findings of this cell therapy approach and also directly compare the Ad-vector treatment with the augmented r-EPCs treatment. Unfortunately, technical difficulties beyond any control were encountered and the only robust measurement obtained was the FI. Specifically, the housing for animals was changed by the animal facility, resulting in the oxygen and carbon dioxide levels be-

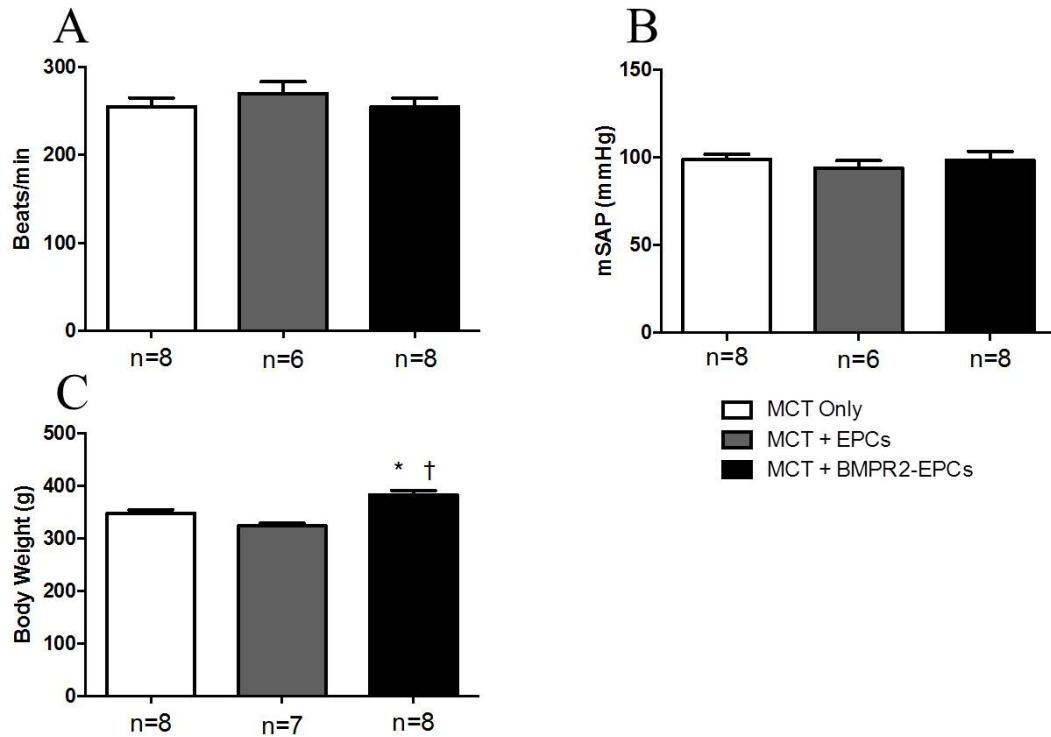


Figure 55: Consistency of animal health at the time of hemodynamic assessment. A. Heart rate (bpm); B. mean systemic arterial pressure (mmHg); and C. body weight (g). Values are mean \pm SEM. * compared with MCT Only and † compared with MCT + EPCs. $p < 0.05$.

ing altered within the housing.

Despite this, the FI findings were replicated showing that the BMPR2-EPCs treatment was effective in the rat MCT-induced PAH model, and that this was comparable to the FI changes induced with the AdBMPR2 treatment [Figure 56](#).

The successful reduction in the FI is shown with a 20.10% decrease in the MCT + AdBMPR2Fab-9B9 ($0.341 \text{ g} \pm 0.035 \text{ SEM}$) group and a 18.79% decrease in the MCT + BMPR2-EPCs ($0.347 \pm 0.029 \text{ SEM}$) compared to the MCT Only group ($0.427 \text{ g} \pm 0.019 \text{ SEM}$). MCT + AdBMPR2Fab-9B9 was also reduced by 16.95% and the MCT + BMPR2-EPCs group was reduced by 15.59% compared to the MCT + EPCs Only ($0.411 \text{ g} \pm 0.035 \text{ SEM}$) group,

though these comparisons were not statistically significant [Figure 56](#).

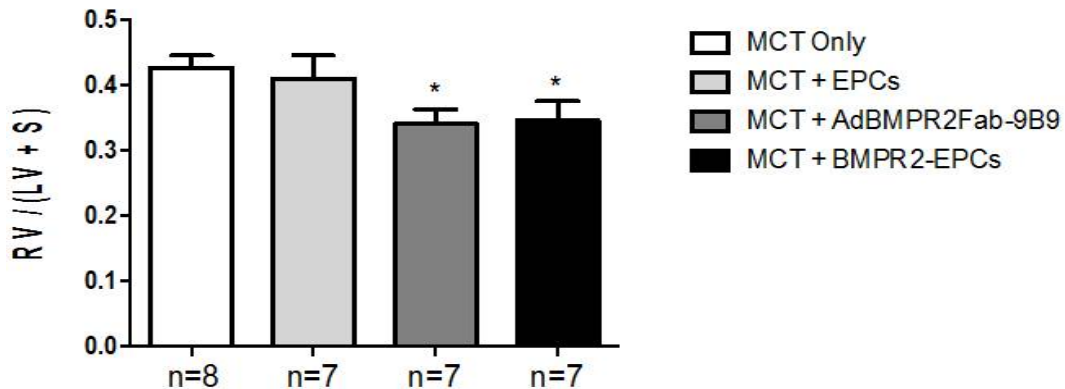


Figure 56: Fulton index measurement 10 days post BMPR2-EPC, EPC Only and AdBMPR2-Fab-9B9 treatments in SD rats with MCT induced PAH. Values are mean \pm SEM. * compared with MCT Only. $p < 0.05$.

14.7 DISCUSSION AND CONCLUSIONS

Previously we have successfully ameliorated PAH in both the rat MCT and chronic hypoxia models using a targeted Ad-vector system, which delivered functional BMPR2 to the pulmonary endothelium [141]. This proof-of-concept model is the first step towards developing a PAH therapy based on BMPR2 modulation. However, Ad-vectors pose their own challenges when used as a vehicle for introducing a therapeutic molecule *in vivo*. Thus, this study utilised cells as the vehicle for BMPR2 delivery to circumvent the limitations of Ad-vectors.

The limitations of Ad vectors when used *in vivo* include systemic inflammation, short-term transgene expression, acquired immunity issues and potential 'off-target' effects. Thus, to move this BMPR2 modulation model towards a more clinical approach, I have utilised r-EPCs as the vehicle to

deliver BMPR2 to the pulmonary endothelium.

BMPR2 augmented r-EPCs successfully ameliorated PAH in the rat MCT-induced PAH model. This was shown through the decrease in the FI, RVSP and mPAP. Interestingly, treatment with r-EPCs alone also showed a slight decrease in RVH and mPAP, however not a decrease in RVSP.

These findings are significant and a major step forward in developing a clinically applicable BMPR2 therapy for human subjects with PAH. As detailed below, there have been two clinical trials and several animal models that have utilised EPCs as a therapy for PAH [109, 110, 111, 112, 113, 114, 115]. The rationale for this is that EPCs are known to regulate angiogenesis where there is injury to the vasculature, as seen in PAH. However, these have had varying success. This may be due to the isolation and culture techniques of the varying groups or that the variability in severity of disease and time-points lead to inconsistent results. However, no group has augmented EPCs to deliver BMPR2 to the endothelium.

The first clinical study that utilised EPCs as a vehicle to deliver a molecule was conducted by Granton *et al* published in June 2015 (NCT00469027), which utilised EPCs to deliver eNOS to the pulmonary endothelium in patients with PAH [115]. In this study, EPCs were transfected with a pVAX1 plasmid containing the full cDNA for the human eNOS gene. Patients were given an escalating dose of eNOS-EPCs via a multi-path port into the right atrium. Despite being in its infancy, results of this clinical trial are encouraging in that transplantation of cells were tolerated well and resulted in a trend towards improved total PVR over the period of transfusion. Long-term outcomes measured by 6 minute walk distance (6MWD) also showed an improvement over a 6 month period following treatment. Despite these encouraging results, this study is limited by low numbers ($n=3$) and a lack

of hemodynamic measurements in the long-term follow-up. Nevertheless, this trial heralds a new beginning for cell therapy in PAH.

The advantage of this current study is the utilisation of BMPR2 gene delivery via EPCs. Mutations in this receptor have a causal link to PAH [170, 5]. Thus, BMPR2 plays a major role in the pathogenesis of PAH, and by addressing this lack of BMPR2 expression, we have shown that we can ameliorate PAH [29]. Whilst eNOS is a known vasodilator and can contribute to vascular repair and regeneration, it is not the gene that is mutated or down regulated, rather it is the production of nitric oxide (NO) that is reduced. Thus, there may be many contributing factors for the reduction in NO and contrary to our BMPR2 approach, increasing the expression of eNOS may not directly address these factors.

A unique aspect of this BMPR2 modulation approach is that EPCs have been transduced to express a membrane-bound receptor, rather than an enzyme that generates a secreted product (as for eNOS and NO). This raises the clear question as to how these cells are exerting their effect on the surrounding vascular milieu. I hypothesise that this is due to a secreted product of some sort, whether a soluble factor or microvesicles, and is now the subject of ongoing studies.

Further work needs to be undertaken to compare my cell therapy directly with the AdBMPR2 treatment. Despite external technical difficulties impacting on the viability of the secondary study, I was able to show in preliminary data, a clear reduction in the FI of both the AdBMPR2 and BMPR2-EPC treatment groups compared to the MCT Only group. This study however, needs to be repeated.

The usage of EPCs not only addresses the limitations of the Ad-vector technology, but also has practical utility. As these cells have become a focus point for therapy, the development of cell banks have emerged. The notion behind these is much like a blood bank, where patients who are in need of an EPC transplant have access to these cells as an off the shelf product. Furthermore, patients who are not in an acute need of cells can have EPCs isolated and cultured from their peripheral blood and undergo an autologous transplant at a later date when or if needed.

This study is highly novel and bears great significance for PAH therapy. This is the first application of BMPR2 modulated EPCs for the treatment of PAH in an animal model. Subsequent studies now look at the impact on BMPR2 mediated Smad signalling.

SMAD SIGNALLING PROFILES ARE ALTERED FOLLOWING BMPR₂ MODULATED EX VIVO EPC DELIVERY

15.1 OVERVIEW

Following the success in ameliorating PAH with the BMPR₂-EPC therapy in the rat MCT-induced PAH model, BMPR₂ mediated Smad_{1/5/8} signalling was assessed and found to be significantly altered following AdBMPR₂ treatment, and I hypothesise that this pathway is also significantly altered following the BMPR₂-EPC treatment.

Endothelial progenitor cells themselves have therapeutic benefits, as they are attributed to angiogenesis, tissue repair and vascular homeostasis [162]. However, EPCs have also been shown to be altered in PAH in both the number of circulating EPCs and their function [108]. Therefore by targeting these cells and augmenting them, we may be altering their role in PAH pathogenesis. In addition to the therapeutic benefits of these cells, they naturally home to the lungs following IV injection, as shown in [Chapter 14](#).

BMPR₂ mediated Smad signalling controls cellular processes such as proliferation, migration, differentiation and apoptosis in endothelial cells (ECs) and to a lesser extent, smooth muscle cells (SMCs) [Chapter 4](#). Smad_{1/5/8} signalling has been shown to be decreased and TGF- β mediated Smad_{2/3} signalling is increased in PAH [171, 5, 150]. This is not surprising given that BMPR₂ expression is reduced in HPAH, primary and secondary PH and animals models of PAH [170, 5].

Following the positive results of the BMPR2-EPC treatment of ameliorating PAH in the MCT-induced PAH model [Chapter 14](#), the current study assessed BMPR2 expression and Smad_{1/5/8} signalling in the MCT + BMPR2-EPC rat lungs at the 10-day time-point. I hypothesise that there will be altered Smad signalling in the whole rat lung lysate following the BMPR2-EPC treatment.

15.2 BMPR2 EXPRESSION IS INCREASED 10-DAYS FOLLOWING EPC AND BMPR2-EPC TREATMENT

Following the increased expression of BMPR2 and pSmad_{1/5/8} 1 h post IV injection of BMPR2-EPCs in the healthy rats [Chapter 14](#), whole rat lung lysates were assessed from the MCT-induced PAH model 10-days following BMPR2-EPCs treatment, using the Odyssey system (LI-COR) as outlined in [Chapter 9](#). Antibodies were selected due to their availability at the time of analysis (see [Chapter 9](#) for note on antibody selection).

BMPR2 expression following MCT + BMPR2-EPC (0.290 I.I \pm 0.030 SEM) treatment had a 3.00-fold increase compared to the MCT Only (0.096 \pm 0.012 SEM) group. Interestingly, the MCT + BMPR2-EPCs group did not have a significant increase in BMPR2 expression compared to the MCT + EPCs (0.302 I.I \pm 0.025 SEM) group. However, there was a 3.12-fold increase in the MCT + EPC group compared to MCT Only [Figure 57](#). This finding was not expected and raises the possibility that EPCs alone, even in the absence of BMPR2 transduction, are influencing BMPR2 expression, and may explain some of the therapeutic effects reported.

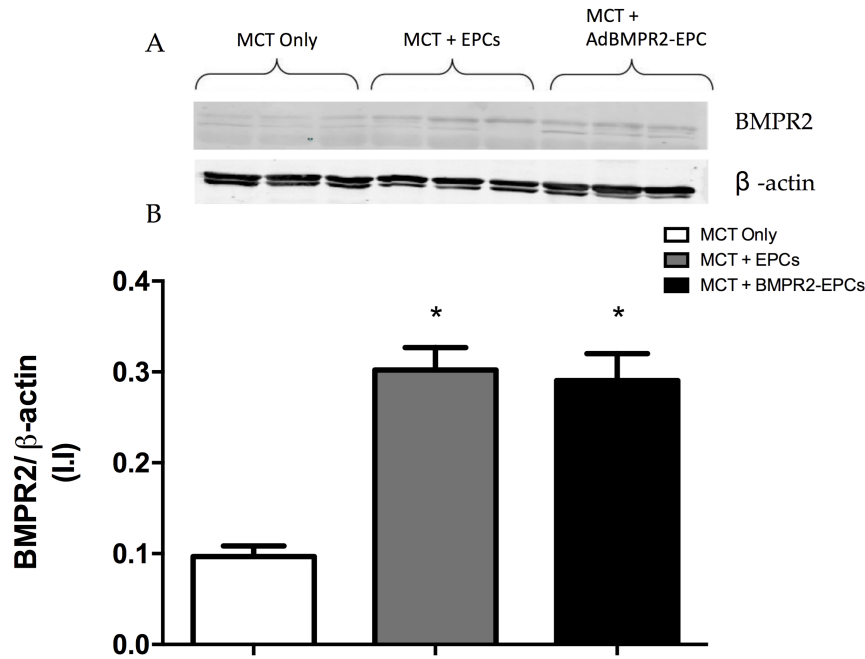


Figure 57: BMPR2 expression following EPC only and BMPR2-EPC treatment in the MCT-induced rat model. A. Representative immunoblot of 3 individual rats for BMPR2 and β -actin expression; and B. BMPR2 immunodetection quantification. $n=6$. Values are mean \pm SEM.* compared with MCT Only. $p < 0.05$.

15.3 ACTIVATION OF THE SMAD1/5/8 PATHWAY 10-DAYS FOLLOWING BMPR2-EPC TREATMENT

BMPR2 mediated Smad1/5/8 signalling was investigated via immunoblot. pSmad1/5/8 was significantly increased by 2.34-fold in the MCT + BMPR2-EPCs ($0.163 \text{ I.I} \pm 0.027 \text{ SEM}$) group compared to MCT Only ($0.077 \text{ I.I} \pm 0.013 \text{ SEM}$) treatment. Interestingly, pSmad1/5/8 was also significantly increased by 2.96-fold in the MCT + EPCs ($0.196 \text{ I.I} \pm 0.013$) treatment group compared to the MCT Only [Figure 58](#). These results are consistent with the findings for BMPR2 expression.

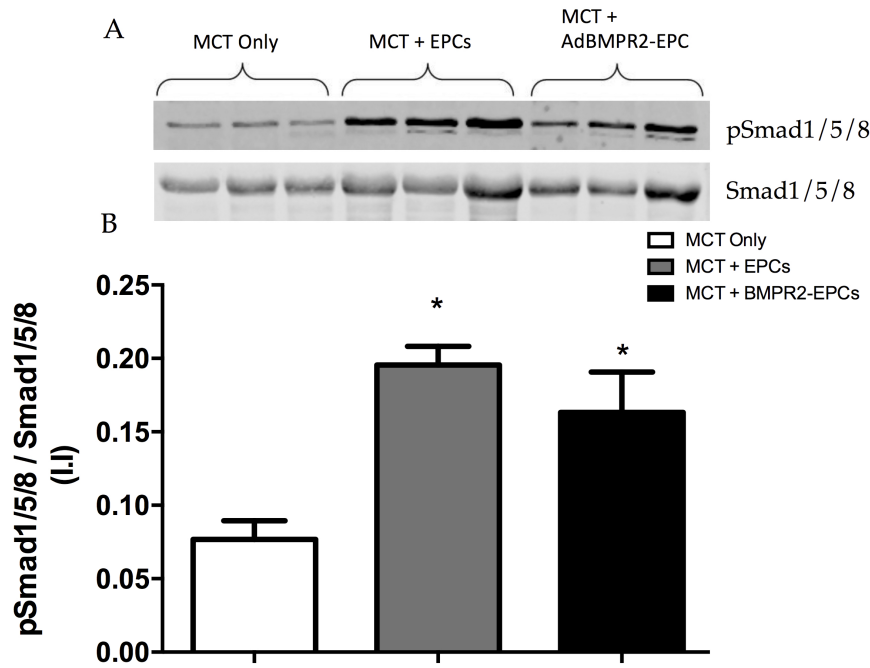


Figure 58: BMPR2-EPC treatment activates the Smad_{1/5/8} pathway. A. Representative immunoblot of 3 individual rats for pSmad_{1/5/8} and Smad_{1/5/8} expression; and B. pSmad_{1/5/8} immunodetection quantification. $n=6$. Values are mean \pm SEM. * compared with MCT Only. $p < 0.05$.

15.4 DECREASE IN ACTIVATED SMAD3 10-DAYS FOLLOWING BMPR2-EPC TREATMENT

TGF- β mediated Smad_{2/3} signalling was examined via immunoblot. p-Smad₃ expression was significantly decreased by 1.73-fold in the MCT + BMPR2-EPC (0.412 I.I. ± 0.108 SEM) treated rats compared with MCT Only (0.713 I.I. ± 0.185 SEM) and by 2.53-fold compared with MCT + EPC (1.043 I.I. ± 0.216 SEM) treated rats. Interestingly, there was a 1.45-fold increase in pSmad₃ expression in the MCT + EPCs group compared to the MCT Only, though this was not statistically significant [Figure 59](#).

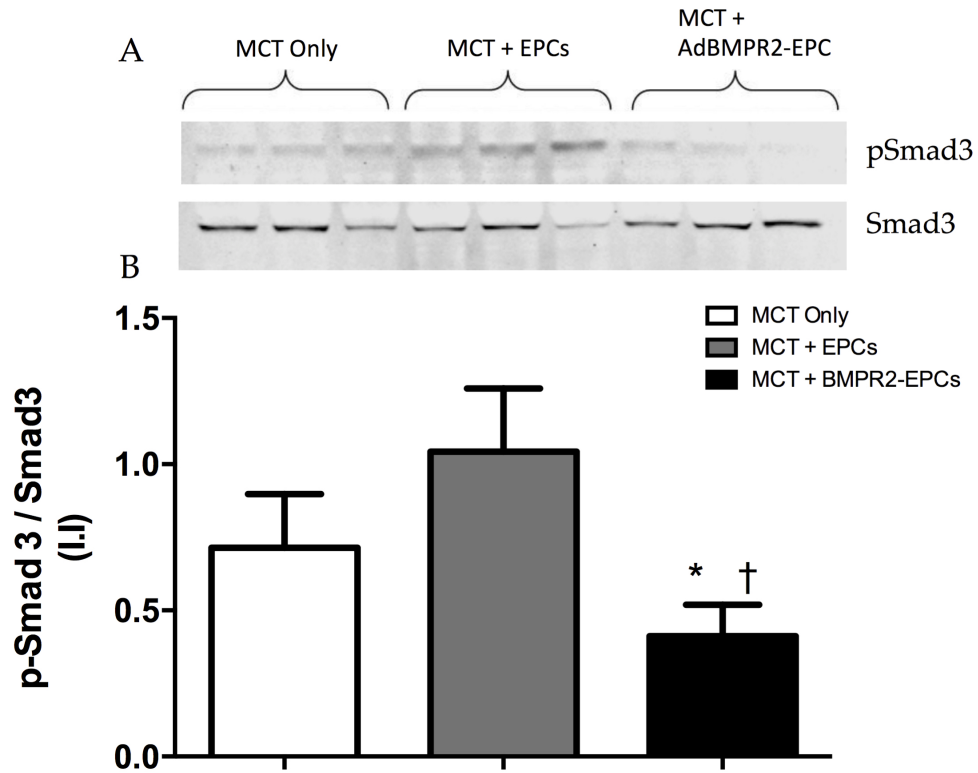


Figure 59: BMPR2-EPC treatment caused a decrease in Smad3 activation. A. Representative immunoblot of 3 individual rats for pSmad3 and Smad3 expression; and B. pSmad3 immunodetection quantification. $n=6$. Values are mean \pm SEM. * compared with MCT Only and † compared with MCT + EPCs. $p < 0.05$.

15.5 DISCUSSION AND CONCLUSIONS

Moving towards a more clinical approach from our Ad-vector BMPR2 delivery system, r-EPCs were used to deliver BMPR2 to the pulmonary vasculature of rats with MCT-induced PAH [Chapter 14](#). This proof-of-concept model is the first treatment of this nature to demonstrate that this treatment successfully ameliorates PAH in the MCT-induced PAH rat model.

In [Chapter 10](#), I demonstrated that the attenuation of PAH following AdBMPR2 treatment may be due to changes in BMPR2 mediated Smad_{1/5/8} and TGF- β Smad_{2/3} signalling pathways. Furthermore, augmented r-EPCs 1 h following intravenous injection, track to the lungs of rats with very little or no distribution to other organs.

In this current study, healthy untreated rats were used to examine if there were any immediate effects following IV injection of BMPR2 modulated r-EPCs. Healthy rats were used as there was no need for MCT treatment to see an effect on BMPR2 or Smad_{1/5/8} expression. Saline and MCT Only treated rats were used as comparative controls. Assessment of immediate BMPR2 and pSmad_{1/5/8} p expression post BMPR2-EPC treatment in healthy rats was made to examine how early these injected cells can mediate any effect in the lungs. I was able to show increased expression of BMPR2 in the lungs compared to Saline treated rats and also compared to rats with MCT Only treatment, only 1 h following IV injection. This increase was coupled with an immediate increase in activated Smad_{1/5/8} signalling only 1 h following BMPR2-EPC treatment compared to MCT Only and Saline treated rats.

These positive results lead directly to the assessment of BMPR2, Smad_{1/5/8} and Smad_{2/3} expression in the lungs in the MCT-induced PAH rat model,

10-days post MCT + BMPR2-EPC treatment. Once again, there was an increase in BMPR2 expression, not only in rats with the MCT + BMPR2-EPCs treatment, but also in rats treated with the MCT + EPCs treatment. This finding was not initially expected but may in part explain the success of EPC alone as a treatment option in many different diseases and animal models, including PAH [158, 169]. Zhou *et al* [110] used EPCs to treat Fisher-344 rats with MCT induced PAH, and showed that this treatment was able to prevent further progression of the disease, and they also used eNOS augmented EPCs which showed significant reversal of the disease. In this study, EPCs were derived from the bone marrow of healthy SD rats, and thus have normal expression levels of BMPR2. Thus, EPC treatment alone may provide increased expression of BMPR2 in the pulmonary endothelium of rats which have reduced BMPR2 expression due to the inducement of PAH.

Smad1/5/8 activation was also significantly increased following MCT + BMPR2-EPCs and MCT + EPCs treatments compared to the MCT Only. Again, it is an interesting finding that the rats treated with MCT + EPCs have an increased expression of pSmad1/5/8. This also may be due to the increase in BMPR2 expression in these rats.

TGF- β mediated Smad3 had reduced activation in rats treated with MCT + BMPR2-EPCs compared to MCT + EPCs and MCT Only. Interestingly, pSmad3 expression was **increased** in the MCT + EPCs group compared to both the MCT + BMPR2-EPCs and MCT Only treatments. This may possibly explain why the RVSP and FI were not significantly reduced with this treatment shown in [Chapter 14](#) despite the increase in BMPR2 and pSmad1/5/8 expression shown in this study.

These findings correlate well with the hemodynamic results shown in [Chapter 14](#), where there is a slight decrease in the FI and a significant decrease in the mPAP in the MCT + EPCs group compared with MCT Only. Whilst the FI is a robust measurement, the mPAP is a very difficult measurement to obtain due to the technical requirements of this measurement, thus the significant decrease seen in this measurement may be exaggerated and the changes would be more accurately reflected in the small decrease seen in the FI. Zhao *et al* reported in their study, hemodynamic assessment 3 weeks following treatment, and that the EPCs alone treatment stopped disease progression but did not reverse the disease. Whereas the augmented EPCs at 3 weeks showed significant disease reversal [110]. These results are consistent with the results in this study, where the MCT + EPCs treatment 10-days following IV injection are showing moderate positive effects on both the hemodynamics and BMPR2 mediated Smad1/5/8 signalling, but not in the TGF- β mediated Smad2/3 signalling. Indicating that either the positive effects are starting to diminish, or that reversal of the disease will not be achieved with treatment by EPCs without augmentation.

The BMPR2 augmented EPCs however, showed significant disease reversal and changes in BMPR2 expression, Smad1/5/8 and Smad2/3 expression at the 10-day time-point. Further, the early changes shown 1 h after injection may mean that the transduced cells are having a greater immediate impact. Transduction strategies other than Ad which possibly enable longer and higher level expression than Ad may further improve the differential between the transduced and untransduced EPCs. A limitation to this study is that assessment of this reversal is limited to the 10-day time-point. A longitudinal study would be required to assess whether this treatment was permanent or will diminish with time.

This study is highly novel and is the first step towards developing a clinically applicable BMPR2 therapy for PAH. This approach is also an excellent tool for investigating PAH biology and the impact of BMPR2 modulation in the context of PAH.

Part IV

CONCLUSIONS AND FUTURE WORK

CONCLUSIONS

16.1 CONCLUSIONS

The studies undertaken in this dissertation have emulated the novelty and applicability of BMPR2 modulation therapy for PAH. These studies have focussed on two main delivery systems: targeted Ad-vector and BMPR2 transduced EPCs. Both approaches not only ameliorate PAH, but are excellent tools for studying PAH biology and the role of BMPR2 therapy for PAH.

In summary, the studies undertaken were:

- Confirmation that targeted AdBMPR2 delivery to the pulmonary endothelium ameliorated PAH 10-day post treatment, with the novel finding that there is a significant reduction in right ventricular hypertrophy only 2-day post targeted AdBMPR2 therapy [Chapter 10](#);
- Assessment of BMPR2 mediated Smad1/5/8 and TGF- β mediated Smad2/3 signalling in whole rat lungs following targeted AdBMPR2 delivery to the pulmonary endothelium in a MCT-induced PAH rat model: 10 and 2-day post treatment. Significant changes in both activated Smad1/5/8 and Smad3 were seen at the 2-day time-point [Chapter 10](#);
- Microarray study of whole rat lungs 10-days following targeted AdBMPR2 delivery, resulting in the identification of the potential role of non-Smad signalling in the reversal of PAH, as well as other molecules

with known roles in either PAH or other relevant diseases. These were BRCA1, eIFs and p70S6K [Chapter 11](#);

- Assessment of non-Smad signalling in whole rat lungs 2-days following the targeted delivery of AdBMPR2 to the pulmonary endothelium, showing a near restoration of PI3K expression and reduced phosphorylated p38 MAPK expression [Chapter 12](#);
- Successful development of a method to isolate, culture and characterise rat bone marrow derived EPCs (r-EPCs) to use in a PAH cell therapy model [Chapter 13](#);
- Transduction efficiency studies in r-EPCs to obtain transduction capabilities of these cells and optimal transduction concentrations [Chapter 13](#);
- Assessment and confirmation of BMPR2 up-regulation in r-EPCs following AdCMVBMPR2myc transduction and confirmation that it was the AdBMPR2 treatment causing the increased expression through the assessment of increased myc expression;
- r-EPC biodistribution studies, where r-EPCs were augmented to express luciferase and injected IV into SD rats. Lung targeting by the r-EPCs was seen through the positive luciferase activity in the chest cavity of rats during a whole body scan with minimal or no activity seen in any other organ. Targeting was also seen through luciferase activity in scans of *ex vivo* lungs and no luciferase activity was in scans of the liver [Chapter 14](#);
- Assessment of the immediate effects in the lungs following BMPR2-EPCs delivery was assessed in healthy rats 1 h following IV injection. BMPR2 and pSmad1/5/8 expression was significantly increased in the whole lung lysates of these rats compared to untreated rats and rats with MCT-induced PAH;

- Successful PAH reversal 10-days following BMPR2-EPCs delivery via IV injection in the MCT-induced PAH rat model [Chapter 14](#); and
- BMPR2 expression, Smad1/5/8 and Smad2/3 signalling was assessed via immunoblot in whole rat lungs after the successful amelioration of PAH, 10-days following BMPR2-EPCs delivery. There was a significant increase in BMPR2 expression as well as Smad1/5/8 activation, with a significant decrease in Smad3 activation [Chapter 15](#)

The limited success of current therapeutics for patients with PAH (survival of 54.9% at three years [1]) shows a need to develop alternative methods of treatment. Additionally, BMPR2 mutation is causally linked to PAH and is reduced in PAH patients in the absence of mutation, and those who have secondary PH as well as in the animal models of PAH [5, 170]. Thus, reduced expression of BMPR2 is somehow contributing to the abnormal behaviour of endothelial (EC) and smooth muscles cells (SMC) which are the main contributors to the pathogenesis seen in PAH. Reduced expression of BMPR2 is also coupled with an increased expression of TGF- β [5]. By restoring BMPR2 expression in the pulmonary endothelium, we are hoping to restore this abnormal balance of the BMPR2 / TGF- β axis and reverse the disease.

This study confirms previous findings that BMPR2 modulation ameliorates PAH in both the rat MCT and chronic hypoxia models [29]. These reversal studies have provided an excellent model to study the cellular signalling pathways that are altered following this treatment. I hypothesised that changes in BMPR2 mediated Smad and non-Smad signalling is associated with the amelioration of the disease.

Assessment of Smad signalling did not show a significant change in response to BMPR2 gene delivery in whole rat lungs taken 10-day following AdBMPR2 treatment, indicating that a peak signalling effect may have been

missed. Confirmation of this was shown in the microarray study, where pathway analysis did not indicate any changes in Smad signalling. Thus, I looked at an earlier time-point post targeted AdBMPR2 treatment. Interestingly, there were significant changes in the FI only 2-days post AdBMPR2 treatment. Hemodynamic studies were not undertaken on the premise that there would be minimal disease reversal at this earlier time-point. Subsequent Smad analysis at the earlier time-point was able to show that there was a significant increase in the activation of the BMPR2 mediated Smad1/5/8 signalling, and a decrease in the activation of the TGF- β mediated Smad3 signalling. Confirming the hypothesis that the success of our BMPR2 therapy is associated with changes in Smad signalling.

The microarray analysis of RNA extracted from whole rat lungs taken 10-days following AdBMPR2 therapy indicated a potential role for non-Smad signalling in the reversal of PAH. Therefore examination of known BMPR2 mediated non-Smad signalling molecules by assessing whole rat lung protein lysates taken from rats with the 2-day AdBMPR2 treatment time-point via immunoblot was carried out. There were significant changes in PI3K and activated p38 MAPK. The microarray analysis also identified other key molecular pathways such as BRCA1, p70S6K and eIFs, which are beginning to emerge as important molecules/ gene in the field of PAH research [149, 172, 173, 150]. These are also identified in abnormal signalling pathways in other diseases such as breast cancer and lung cancer. This gives us the opportunity to investigate pre-existing therapies as well as an opportunity to develop therapies that are not isolated to the one disease pathology. Other interesting and current areas of study in PAH such as the role of metabolism and energy production in the development of the disease, were also identified in the top associated network functions of the microarray. Highly proliferative ECs found in PAH subjects have been shown to have a high rate of glycolysis which indicates impaired mitochondrial func-

tion [35]. There has also been a link between impaired metabolic functions and inflammation in PAH as well as the impaired serotonin metabolism seen in FH rats which are susceptible to PAH in altitude [35]. Thus, there were many identified networks, cellular functions, bio-functions and pathways that were identified in our microarray study which are already current areas of research within the PAH field as well as other well known diseases. This demonstrates the relevance of our study and also the utility of our pre-clinical model as a tool for studying PAH biology before and after disease reversal.

BMPR2 mediated Smad and non-Smad signalling pathways control cellular proliferation, apoptosis, migration and differentiation. These cellular processes are disrupted in EC and SMCs of the pulmonary vasculature, contributing to the pathogenesis of PAH. The formation of plexiform lesions is due to apoptotic resistant ECs and the intimal thickening is due to unchecked proliferation and migration of SMCs. The formation of extracellular matrix results from ECs undergoing endothelial to mesenchymal transition (EndoMT), where ECs differentiate into fibrotic/ mesenchymal-like cells. The decrease in BMPR2 mediated Smad1/5/8 signalling and the increase in the TGF- β mediated Smad2/3 signalling in PAH may be associated with these abnormal cellular events, thus by reversing this axis via our BMPR2 therapy, we are driving a reversal of this abnormal cellular behaviour.

Despite these promising pre-clinical results, gene therapy does have disadvantages in the human clinical setting. These limitations lie largely in the vector technology used for gene delivery. Previous studies have used aerosol as a potential form of delivery of the vector to vascular smooth muscle, however this did not succeed in reducing PAH in the MCT model [174]. Our approach of targeting the endothelium has been more successful, but

improvements in vector technology will be needed for clinical application. These improvements should lead to greater transduction efficiency and specificity, and will also need to address issues of immunological responses to the vector itself, as well as improvements in the duration of transgene expression. Highly modified "helper dependant" Ad vectors, which generate much lower immunological responses than first generation agents and have shown up to seven years of transgene expression in non-human primates, and may prove useful in this regard [175]. In addition to this, the use of alternate serotypes of Ad, including Simian derived Ads, can be used to circumvent pre-existing immunity, should that be an issue. However, there still remains the potential for hepatotoxicity and sequestration to the liver by Kupfer cells. Cell based therapies are directed at overcoming these issues that are inherent in the viral vectors.

Cell based therapy has emerged as a viable and clinically applicable mode of therapy for a wide range of diseases, particularly for vascular diseases, including PAH. With the identification of EPCs in adults by Asahara and colleagues [156] in 1997, there was a paradigm shift in how EPCs utility was perceived, moving away from embryogenesis and towards adult tissue vascular repair and angiogenesis as well as maintaining vascular homeostasis [162]. EPCs have natural homing abilities to tissue that requires repair and or tissue that is under hypoxic stress, and in addition to this, they tend to accumulate in the pulmonary circulation due to entrapment, thus making them an ideal candidate for cell therapy in PAH. Additionally, EPCs overcome most limitations that Ad-vectors possess, such as immunological responses, up-take by the liver and hepatotoxicity. These cells can also be augmented to over-express a desired gene and coupled with their ability to home to the lungs upon intravenous injection, they are an ideal candidate for BMPR2 PAH cell therapy. Currently, human trials are underway utilising EPCs alone [176] or EPCs that have been augmented to over-

express eNOS [115] with positive results. However, no study to date has addressed the BMPR2 deficiency that is the hallmark of PAH as well as being the mediator of the cell signalling that is directly linked to disease progression.

My BMPR2-EPC study is a highly novel cell therapy approach looking to address the decreased expression of BMPR2 in PAH with a clinically applicable therapy. This study was able to show that IV injected r-EPCs home to the lung, with little or no expression in any other organs, specifically the liver. Using this, I demonstrated that augmented r-EPCs within 1 h of injection, stimulates or mediates a significant increase in BMPR2 expression as well as BMPR2 mediated Smad1/5/8 activation. This is consistent with the findings in the 2-day time-point for the AdBMPR2 treatment model. Importantly, using this BMPR2-EPC treatment I was able to ameliorate PAH in the MCT-induced rat PAH model. This pre-clinical model demonstrated significant reductions in the RVSP, mPAP and FI following the BMPR2-EPC therapy. These findings are undoubtedly a pivotal step towards advancing studies to the clinic.

Whilst the BMPR2-EPC treatment gave the most conclusive results, the EPC Only treatment also showed an effect. This was not unexpected as previous studies have shown therapeutic benefits of not only EPCs [177, 109, 110] but also mesenchymal stem cells and also microvesicles (MVs) from those cells [114, 178, 179]. EPCs have been shown to provide therapeutic benefits for a wide range of diseases, however they have also been implicated in the pathogenesis of PAH. Therefore, by transplanting 'normal EPCs' into an *in vivo* setting with existing PAH, there may be an initial therapeutic benefit. However, the duration of this therapy is unknown. Through this Smad pathway analysis of these BMPR2-EPC reversal studies, I was able to show that in the whole lung tissue analysis, BMPR2 mediated ac-

tivation of Smad1/5/8 was increased in both the BMPR2-EPC and r-EPCs only treatments compared to the MCT Only, however, the TGF- β mediated Smad3 activation was significantly reduced in the BMPR2-EPC treatment but not altered in the the disease group receiving the r-EPCs only treatment. On balance, the findings suggest that the r-EPC only treatment is not as effective as the BMPR2-EPCs. This was also reflected in the RVSP and FI results, where there was minimal reduction in the r-EPCs only treatment for the FI, and no reduction in the RVSP following this treatment at the 10-day time-point.

It is unknown how long the enhanced BMPR2 expression is needed to achieve a therapeutic outcome. It is known that in the context of BMPR2 mutation-related PAH that the presence of the mutation alone only leads to disease in around 20% of subjects, thus the need for a 'second hit' to produce the PAH phenotype has been largely accepted. Whether a 'less than permanent' restoration of BMPR2 signalling can restore the BMPR2 / TGF- β balance that existed before the 'second hit,' and can have a lasting clinical benefit is unknown, but at least is plausible. Since our initial findings demonstrating a therapeutic role for BMPR2 up-regulation in PAH, other research groups, using conventional pharmacological agents, have extended the concept. Spiekerkoetter et al [106] used high through-put technology to determine that tacrolimus causes an up-regulation in BMPR2 signalling, and then subsequently showed a therapeutic impact in pre-clinical models. Whether either conventional or gene-based approaches will ultimately prove useful clinically remains to be seen, however the utility of cell based therapy has already progressed to human trials with positive outcomes [115]. My latest findings provide rationale for further development of this approach.

A very important advantage of BMPR2 modulation therapy is that BMPR2 up-regulation is unlikely to cause systemic issues. By introducing the receptor *in vivo* there is still the requirement of this to be activated by the ligand for there to be any effect. In PAH, it is BMPR2 that is down-regulated, not the BMP ligands that activate it. Thus, with restoration of BMPR2 expression to normal levels in the lungs, there still remains normal levels of BMP ligands available to activate it. There is no risk of BMPR2 to be over activated in this model. Recently, a seminal report was published using the ligand, BMP9 as a therapy [180]. Whilst this group up-regulated BMP9 in the pulmonary endothelium, there is still the potential that the ligand can act systemically on BMPR2 expressed in other organs with unknown effects. Thus, from my perspective, BMPR2 therapy is a safer option as it addresses the BMPR2 deficiency that we know is a hallmark feature of PAH, whereas this BMP9 therapy approach results in an over-expression of only the ligand used by this receptor.

This study confirms previous findings that BMPR2 modulation ameliorates PAH, and that this is associated with changes in both Smad and non-Smad signalling [Chapter 10](#) [Chapter 12](#). We know that this amelioration is achieved using either *in situ* endothelial transduction or via engineered EPCs. We propose that there are two ways that this is achieved:

1. **Direct repair:** where the endothelium is directly transducing the introduced viral vector carrying the BMPR2 gene or the EPCs are directly embedding into the pulmonary endothelium. However, we know there is only around 20% transduction efficiency in the pulmonary endothelium [134] and that other studies have shown very little amount of cells actually embed into the pulmonary endothelium [181].
2. **Paracrine effect:** where the small amount of ECs that were directly transduced or the injected EPCs emit soluble factors and / or MVs

with important miRNA's and proteins that have a global effect on the pulmonary endothelium.

These effects could be additive or synergistic, and importantly, there may be the potential for these therapies to be used in combination. Additionally, it raises the potential for MVs as a therapy, either independently or in combination with the AdBMP2 and / or BMP2-EPC treatments.

All of my findings provide further rationale for the development of therapies targeting BMP2 and downstream mediators. My pre-clinical cell based model has taken us one step closer to developing and trialling BMP2 modulation therapy in human subjects.

16.2 FUTURE WORK

These pre-clinical models of PAH therapy are an excellent tool for studying PAH biology before and after disease reversal. I have been able to explore many different cell signalling pathways that are altered following the successful therapy, and embark upon different analysis methods to discover novel mediators and targets for therapy. In particular, my microarray studies identified a plethora of networks, pathways and molecules that should be further investigated. Additionally, the success of the cell based therapy paves a way for further development of other cell derived components to be used in isolation or in combination with the cell therapy. Thus, there are many streams of investigation that can stem from these current studies to extend our PAH research.

Improvements in vector technology include advancing the Ad technology to improved vectors such as helper dependent, hexon modified (to reduce liver uptake) and the use of alternate Ad serotypes. This would reduced im-

mune responses, hepatic sequestration and transduction, with the potential to reduce hepatotoxicity. Furthermore, these vectors have longer transgene expression, with helper dependent vectors showing up to 7 years of transgene expression [175]. A myeloid-cell binding vector (AdMBP) has been created which targets to myeloid cells in the blood and by doing so, reduces the opportunity for Kupffer cells to sequester the virus to the liver. These leukocyte cells circulate through the pulmonary arteries, allowing for the cells to 'off-load' the virus to the pulmonary endothelial cells [130]. Currently, we are testing the efficiency and viability of an AdMBP with the BMPR2 transgene inserted in EPCs, looking to reduce any possible toxicity that our older generation Ad-vectors may cause. Additionally, the AdMBPBMPR2 vector may have a great specificity for transduction in our EPCs. This may become particularly important if the cell therapy moves to utilising human EPCs which seem to be more difficult to augment using viral vectors. In addition, we will explore the use of lentiviral vectors to achieve longer term transduction of EPCs *ex-vivo* as well as electroporation methods.

Further investigation of the identified molecules from the microarray studies: BRCA1, p70S6K and eIF may open our model to other therapeutic targets and give us a better understanding of how we are achieving the disease reversal in the *in vivo* PAH models. BRCA1 & 2 are well characterised oncogenic factors in breast cancer. Therefore there may be pre-existing studies that target these genes which may prove useful in PAH. p70S6K is a key molecule in the mTOR/PI3K/AKT cell proliferation, migration and survival pathway. It has been characterised as a mediator in many different cancers such as lung cancer, leukaemia and several carcinomas [151]. p70S6K also regulates eIF4, which is also involved in PI3K/AKT/p38MAPK/Ras signalling pathways. Investigating these molecules in the context of PAH may not only present a novel target for therapy, but may also provide new

insight into how these pathways contribute to the development of cancer.

Expanding on the current cell therapy approach may be achieved by isolating and characterising EPC-derived MV's as a therapy, either independently or in combination with EPCs. MVs from mesenchymal stem cells have shown positive results in pre-clinical PAH models [114], thus there is the potential that these may provide a further benefit if packaged with BMPR2 and delivered to the pulmonary vasculature. Furthermore, the role of MVs in exerting a potential 'paracrine effect' following EPC transplant should be investigated. Particularly looking at what these MVs are packaging which may be causing the positive effects on the surrounding ECs. Currently there are many published methods for isolating MVs [114, 182], however as the field is still emerging, there remains a debate on what is the best technique. Whilst MV isolation is emerging to be a simple process, visualisation of the resulting product is difficult. In our current studies looking at isolating MVs from peripheral blood, we have encountered difficulty in visualising MVs by electron microscopy (EM). Isolation involves centrifugation, and unfortunately the resulting sample is 'dirty' with cell debris, making it difficult to visualise and confirm successful isolation of the MVs using the EM. Once these difficulties are overcome and we can confirm we have isolated the MVs, we will be able to move towards using these as a potential vehicle for BMPR2 therapy. Additionally, there is the opportunity to study isolated MV's from blood samples taken from the animals in our AdBMPR2 and BMPR2-EPCs therapy models. This can give us more of an insight into the potential paracrine effects that are taking place in these therapy models.

Following the success of the BMPR2-EPCs therapy study, longitudinal studies of injected EPCs is important to conduct. These studies will be investigating specifically how long these cells stay in the lungs and how this

translates to the period of time BMPR2 and Smad1/5/8 expression is increased. Furthermore, a longitudinal study of our BMPR2-EPC treatment is needed to ascertain whether there is a lasting effect of this treatment or if the disease persists after a period of time, indicating whether there needs to be follow-up doses or even escalating doses. These studies are a critical step towards translating this therapy to the clinic. Further understanding of how long these cells remain in pulmonary vasculature allows us to ascertain the safety and efficacy of the treatment, as well as whether there are any potential long term immunological effects. Additionally, EPC dosage experiments are also required to progress this therapy to the clinic. Specifically looking at the number of cells required for an effective dose and the method of dosage, whether this be a 'once-off' dose, an escalating dose or course of treatment over a period of time.

Further to this initial BMPR2-EPCs study, we need to test our BMPR2-EPC therapy in other PAH animal models, such as the sugen chronic hypoxia and transgenic mouse models. Whilst the MCT PAH model is robust and a good model for PAH, there are features that limit the model, as well as having the propensity to show disease reversal for many treatments [79]. Human PAH has varying pathological features, and no one animal model is a perfect fit, therefore trialling this treatment in a variety of models is the most robust examination of the therapy. Furthermore, the more studies that are conducted and successful, the closer we are to trialling this therapy in a human population.

Ultimately, our goal is to progress this BMPR2-EPC therapy to clinical trials. More studies are required to fully evaluate their role in PAH pathophysiology, what are effective dosages, and how long they persist in the lungs, as well as looking at the effects of up-regulating BMPR2 in human derived EPCs. Initial studies indicate that AdCMVBMPR2myc transduction is possi-

ble in these cells [Appendix C](#) and I have successfully isolated, cultured and characterised cells from the left ventricle of patients with PAH [Appendix C](#). Clinical trials utilising cells therapies are currently under-way in Australia, and cooperative research centres are currently developing strategies to up-scale production of ECs, which give us a unique opportunity to utilise a 'bank' of expanded EPCs for clinical application.

The development of therapies for PAH is critical. Despite current available therapeutics, survival is still very poor and can be likened to some of the worst cancers. BMPR2 therapy is a novel therapeutic strategy which address the well known underlying pathology of BMPR2 deficiency that occurs not only in hereditary PAH, but secondary PAH and most PAH animal models. The success of our pre-clinical BMPR2 therapy models may lead the way for further development of BMPR2 therapies, as well as give significant insight into the pathophysiology of this devastating disease.

APPENDICES

ACE TARGETING

A.1 ACE TARGETING *in vitro* RESULTS

Fab-9B9 fractions were assessed *in vitro* for their targeting ability [Figure 60](#). Using CHO and the high expressing CHO-2C2 cells, we are able to assess what fractions have the best targeting and at what concentration [Chapter 9](#).

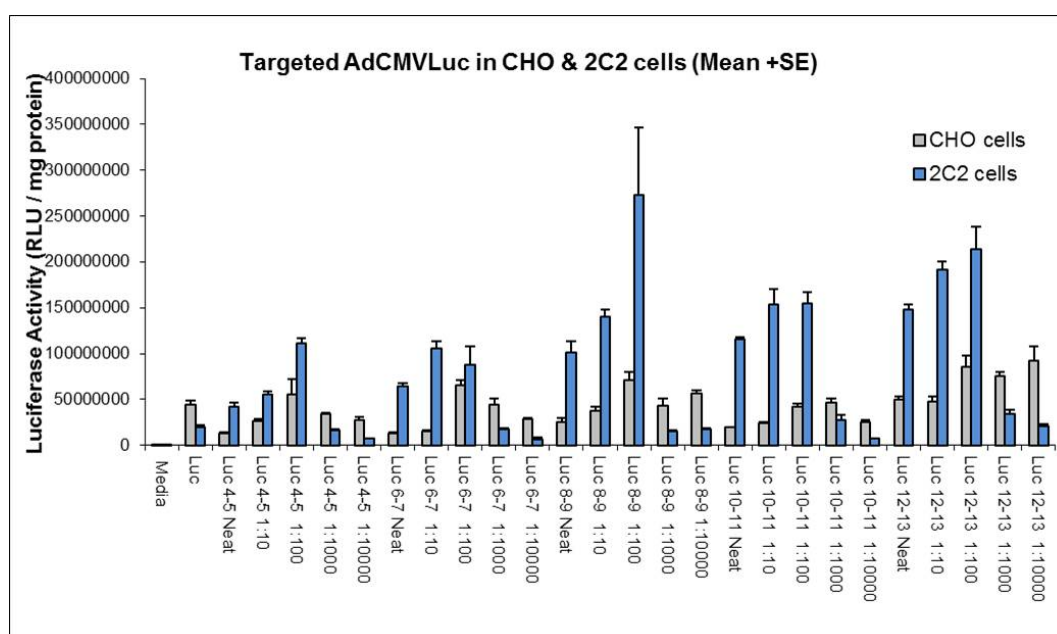


Figure 60: Luciferase assay of CHO and CHO-2C2 cells to assess the targeting ability of Fab-9B9 fractions *in vitro*.

A.2 ACE TARGETING *in vivo* RESULTS

In vivo validation of the best Fab-9B9 fractions ascertained in the textititn vitro studies was performed [Figure 61](#). Assessment is made via a luciferase assay of lung and livers from the treated animals [Chapter 9](#).

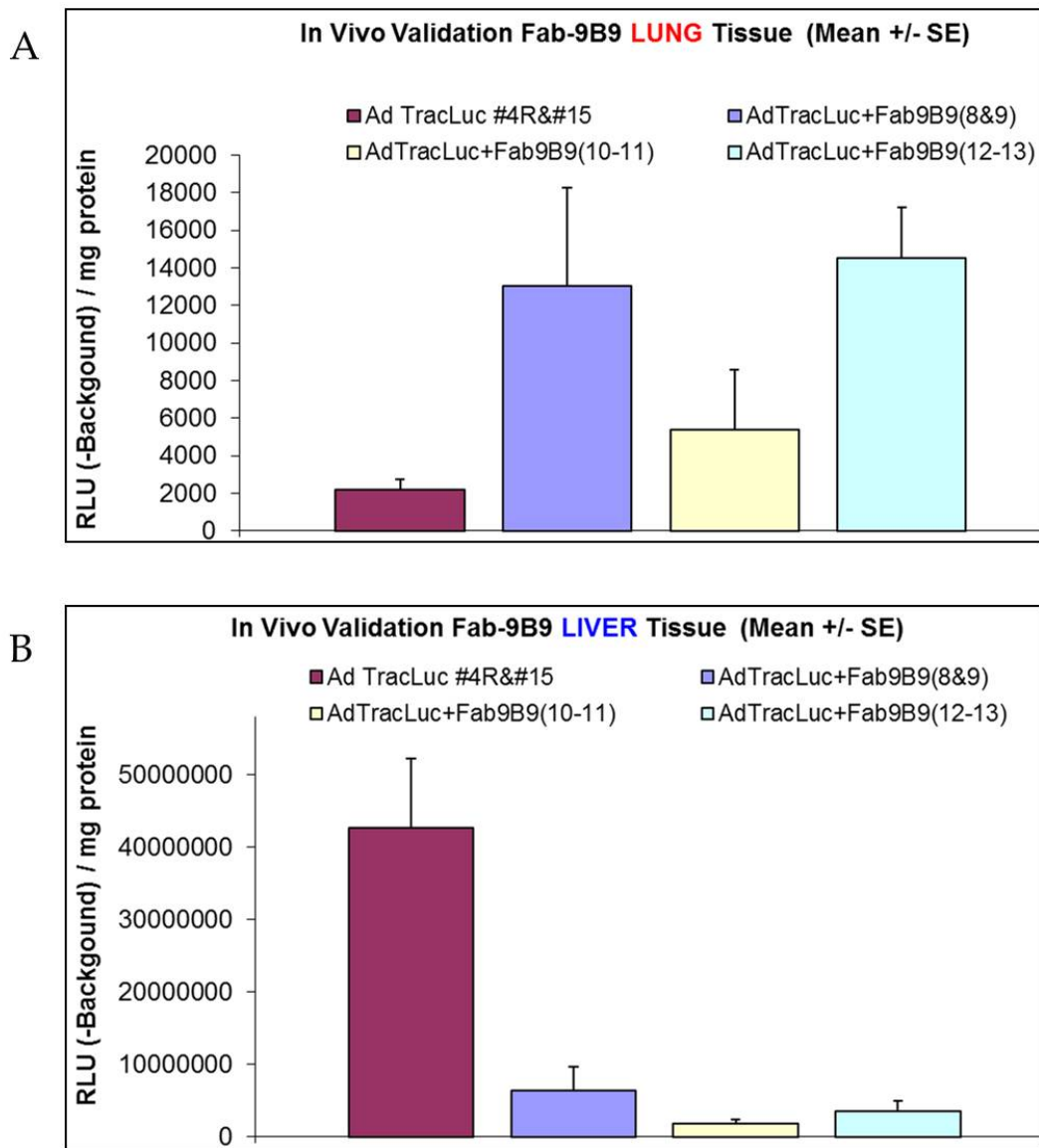


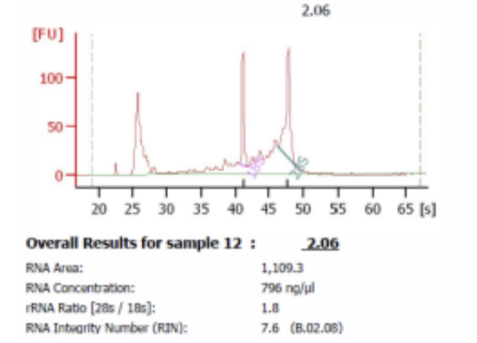
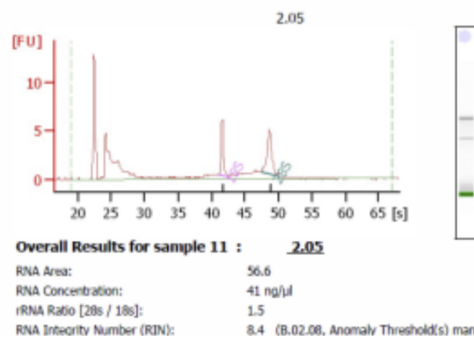
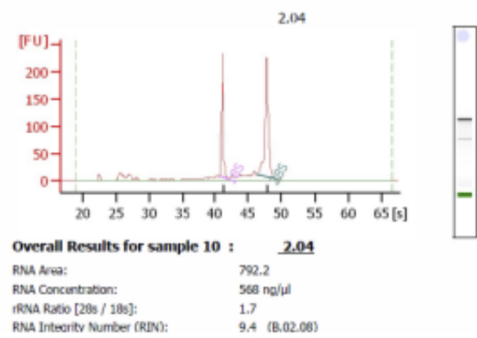
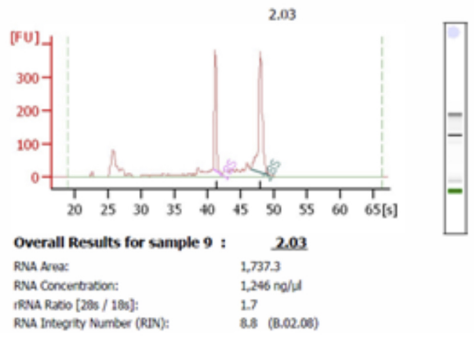
Figure 61: Luciferase assay of lung and liver tissue to assess the targeting ability of Fab-9B9 fractions *in vivo*. A. Lung tissue analysis; and B. Liver tissue analysis.

MICROARRAY

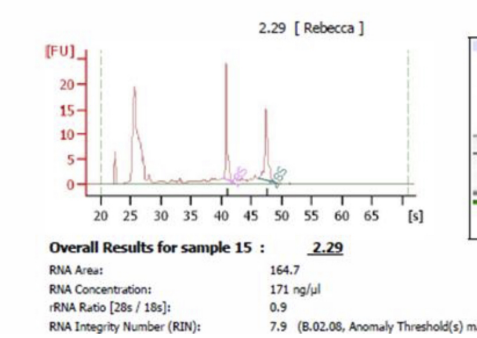
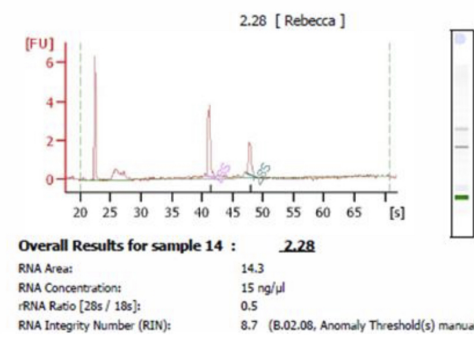
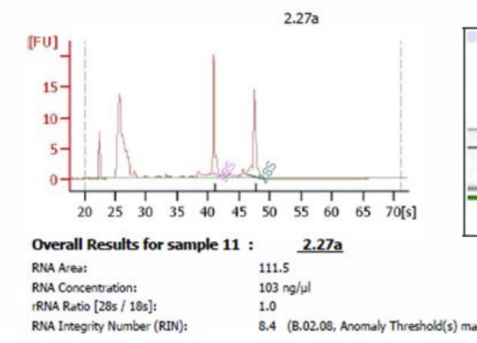
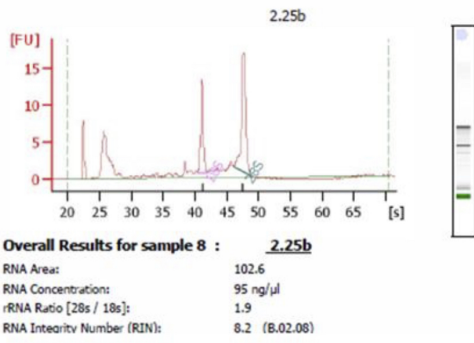
B.1 BIOANALYZER RESULTS

RNA samples were given to the Adelaide Microarray Centre for analysis via a BioAnalyzer (Agilent) [Figure 62](#).

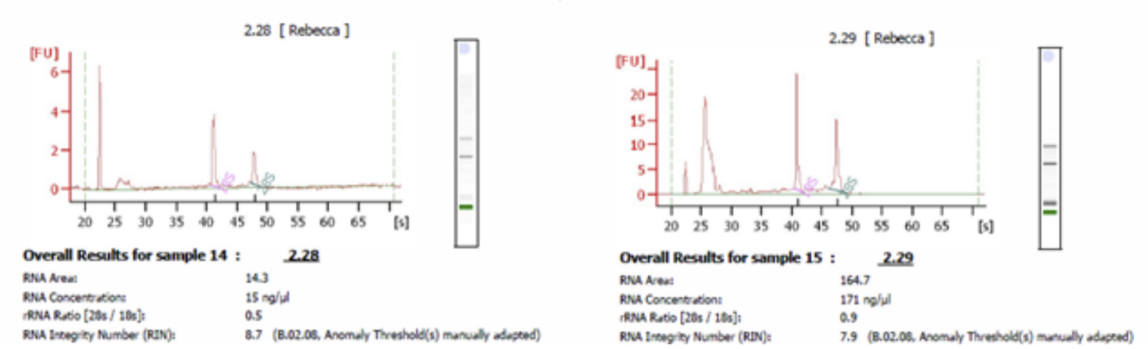
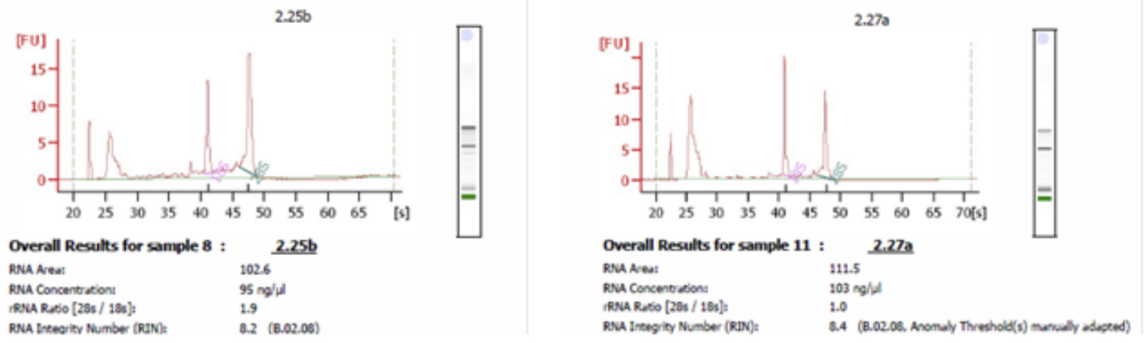
A



B



C



D

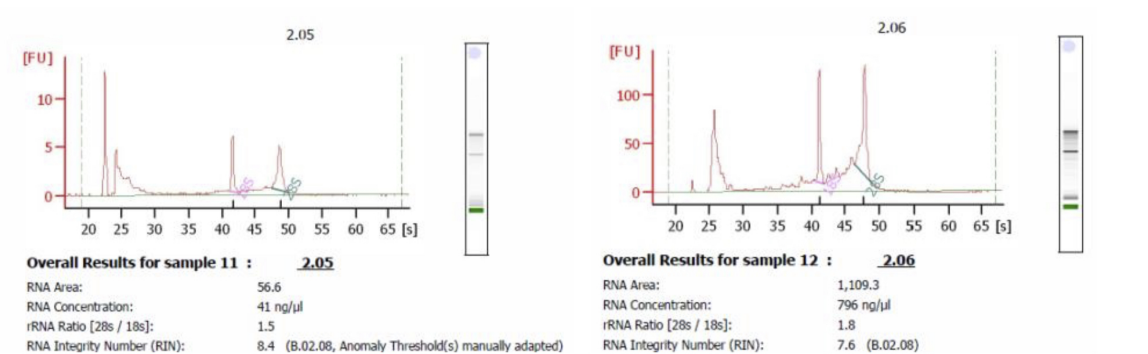
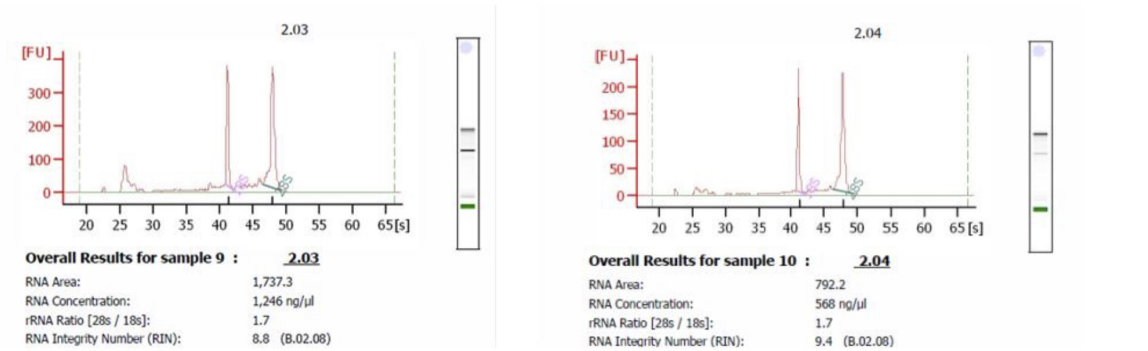


Figure 62: Chosen samples for microarray. (A) MCT+AdTrackLucFab-gB9; (B) MCT+AdCMVBMPr2Fab-gB9

B.2 SAMPLE LIST OF SIGNIFICANT GENES FROM MCT ONLY VS MCT + ADBMPR2FAB-9B9 COMPARISON

From the microarray results, it was identified that the best comparison for further pathway analysis was between the MCT Only and MCT + AdBMPr2Fab-9B9 groups. A list of genes with significant expression differences was generated for the MCT Only vs MCT + AdBMPr2Fab-9B9 by eliminating the exact same genes that were significant between MCT Only vs MCT + AdTrackLucFab-9B9 and MCT Only vs MCT + AdBMPr2Fab-9B9 [Figure 37](#). Thus, this analysis gave a list of genes that were exclusively different between MCT Only and MCT + AdBMPr2Fab-9B9. An example of this list is below: [Figure 63](#)

gene_assignment	Gene Symbol	RefSeq	p-value (Raw)	stepup(p-value)	Ratio	Fold-Change	Fold-Change (Description)
XM_575496 // Spty2d1 // SPT2, Suppressor of Ty, domain containing 1 (S. cerevisiae) //	Spty2d1	XM_575496	0.00000	0.002	1.68	7.32	AdBMPR2 up vs MCT
NM_212525 // Tyrobp // Tyro protein tyrosine kinase binding protein // 1q21 // 361537 /	Tyrobp	NM_212525	0.00000	0.003	0.64	6.15	AdBMPR2 down vs MCT
NM_001106454 // Ttf2 // transcription termination factor, RNA polymerase II // 2q34 //	Ttf2	NM_001106454	0.00000	0.003	1.60	4.18	AdBMPR2 up vs MCT
NM_001107678 // Dhx36 // DEAH (Asp-Glu-Ala-His) box polypeptide 36 // 2q31 // 310461 //	Dhx36	NM_001107678	0.00000	0.003	1.68	3.71	AdBMPR2 up vs MCT
NM_001107847 // Golga3 // golgin A3 // 12q16 // 312077 // ENSRN0000056656 // Golga3	Golga3	NM_001107847	0.00000	0.003	1.52	3.19	AdBMPR2 up vs MCT
NM_031691 // Itgad // integrin, alpha D // 1q36 // 64350 // ENSRN0000026855 // Itga	Itgad	NM_031691	0.00000	0.004	1.63	3.00	AdBMPR2 up vs MCT
NM_001107847 // Golga3 // golgin A3 // 12q16 // 312077 // ENSRN0000056656 // Golga3	Golga3	NM_001107847	0.00000	0.004	1.54	2.81	AdBMPR2 up vs MCT
NM_001105990 // Kif21b // kinesin family member 21B // 13q13 // 289397	Kif21b	NM_001105990	0.00000	0.004	1.83	2.78	AdBMPR2 up vs MCT
NM_001126096 // Lyrm2 // LYR motif containing 2 // 5q21 // 690354 // ENSRN0000006592	Lyrm2	NM_001126096	0.00000	0.004	1.92	2.74	AdBMPR2 up vs MCT
NM_017151 // Rps15 // ribosomal protein S15 // 7q11 // 29285 // ENSRN0000029791 //	Rps15	NM_017151	0.00000	0.004	0.60	2.74	AdBMPR2 down vs MCT
ENSRN0000013538 // Lgals1 // lectin, galactoside-binding, soluble, 1 // 7q34 // 5664	Lgals1	ENSRN0000013538	0.00000	0.005	0.61	2.66	AdBMPR2 down vs MCT
NM_001105853 // Recq5 // RecQ protein-like 5 // 10q32.3 // 287834 // ENSRN0000000072	Recq5	NM_001105853	0.00001	0.005	1.60	2.65	AdBMPR2 up vs MCT
NM_031687 // Uba52 // ubiquitin A-52 residue ribosomal protein fusion product 1 // 16p1	Uba52	NM_031687	0.00001	0.005	0.56	2.63	AdBMPR2 down vs MCT
NM_001126094 // Mrps21 // mitochondrial ribosomal protein S21 // 2q34 // 689432 // ENS	Mrps21	NM_001126094	0.00001	0.005	0.63	2.62	AdBMPR2 down vs MCT
NM_001191802 // Zfp445 // zinc finger protein 445 // 8q32 // 301076 // ENSRN0000000034	Zfp445	NM_001191802	0.00001	0.005	1.52	2.61	AdBMPR2 up vs MCT
ENSRN00000035338 // Dgkd // diacylglycerol kinase, delta // 9q35 // 368088 // FQ2187	Dgkd	ENSRN00000035338	0.00001	0.005	1.68	2.60	AdBMPR2 up vs MCT
NM_001107469 // Zc3h12d // zinc finger CCH type containing 12D // 1p13 // 308266 // E	Zc3h12d	NM_001107469	0.00001	0.005	1.85	2.59	AdBMPR2 up vs MCT
ENSRN00000038919 // RGD1565131 // similar to ribosomal protein L15 // 12p11 // 498143	RGD1565131	ENSRN00000038919	0.00001	0.005	0.56	2.58	AdBMPR2 down vs MCT
---	---	---	0.00001	0.005	0.63	2.52	AdBMPR2 down vs MCT
NM_012618 // S100a4 // S100 calcium-binding protein A4 // 2q34 // 24615 // ENSRN000000	S100a4	NM_012618	0.00018	0.008	0.62	2.48	AdBMPR2 down vs MCT
ENSRN00000002795 // Bmp2k // BMP-2 inducible kinase // 14p22 // 498333 // BC103651 //	Bmp2k	ENSRN00000002795	0.01039	0.034	1.69	2.48	AdBMPR2 up vs MCT

Figure 63: Example list of significant genes resulting from the microarray analysis following AdBMPR2 treatment in the MCT induced PAH: 10-day time-point study. Genes are significant in change between the MCT Only vs MCT + AdBMPR2Fab-9B9 groups.

HUMAN EPCS

C.1 HUMAN DERIVED ENDOTHELIAL PROGENITOR CELLS

I have progressed to endothelial progenitor cell (h-EPC) studies involving human subjects. For these studies, my aims are:

1. Isolate, culture and characterise EPCs from a human adult blood sample taken from the right and left ventricle;
2. Evaluate the transduction efficiency of h-EPCs; and
3. Transduce the h-EPCs with AdCMVBMPR2myc to up-regulated BMPR2

c.1.1 Isolation, Culture and Characterisation of h-EPCs from the peripheral blood

Blood was taken from the right and left ventricles of a PAH subject. Cells were isolated using Lymphoprep® cultured on gelatin coated 24 well plates in Endothelial Growth Medium-2MV (EGM-2MV) (Lonza, Walkersville, MD, USA) with 20% FCS [Figure 64](#). Cells were characterised as early endothelial cells (EPCs) after one week of culture. They were then characterised as late EPCs following 3-4 weeks in culture, in two ways:

1) Morphologically, via microscope, looking for the typical 'cobblestone' appearance of endothelial cells [Figure 65](#).

2) By flow cytometry, where cells will be stained with:
vWF & CD144 FITC, CD133 APC, CD31 PE Cy7, CD146 & VEGFR PE and CD45 V450 to confirm endothelial like properties.

EPCs were confirmed by their cell surface expression of vWF⁺, CD144⁺, CD146⁺, VEGFR2⁺, CD133⁻ and CD45^{dim} Figure 66.

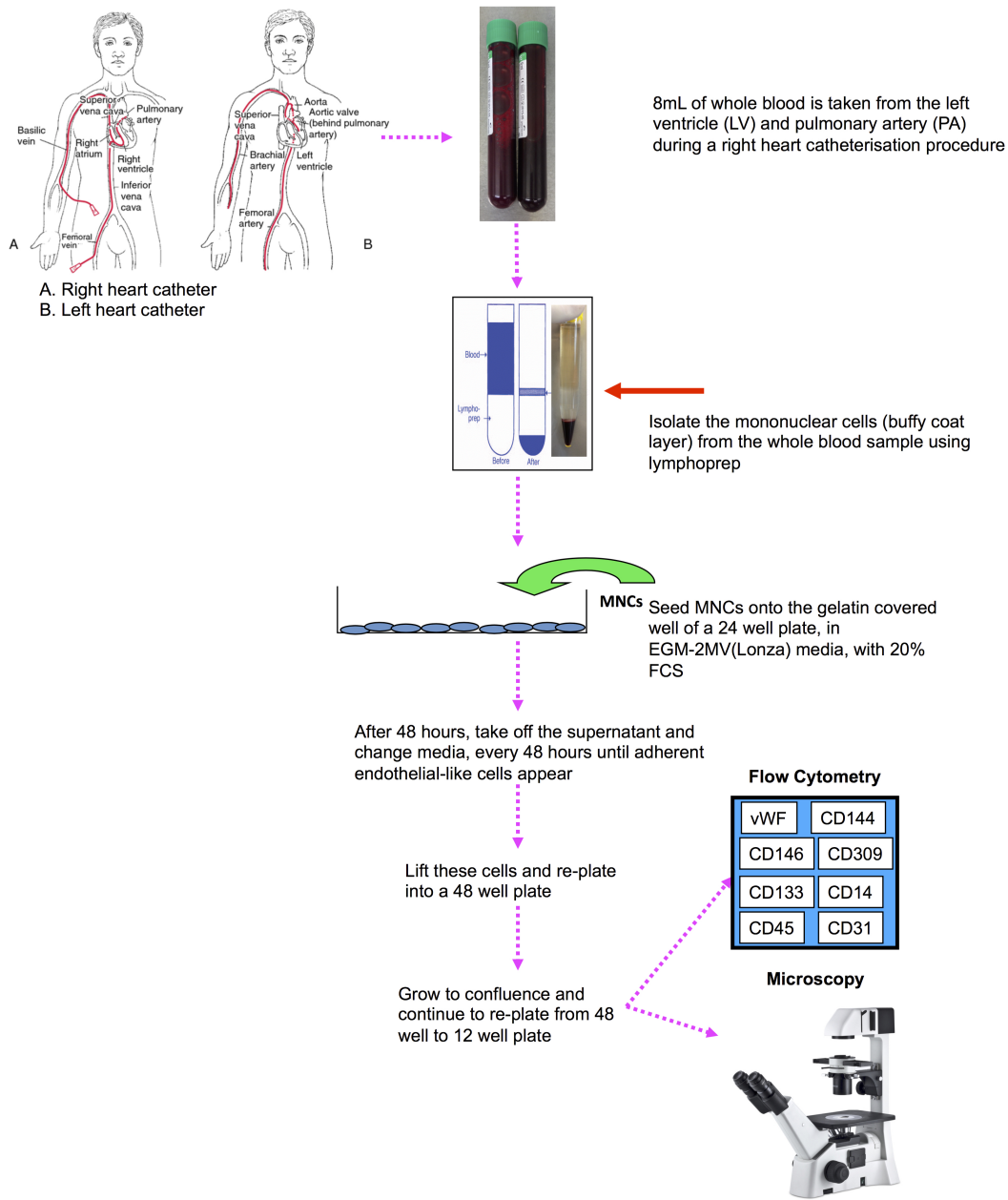


Figure 64: Isolation, culture and characterisation technique of h-EPCs. Blood samples were taken from the right and left ventricles. Mononuclear cells were isolated using Lymphoprep® and seeded onto 24 well plates coated with gelatin. Cells are cultured till the appearance of endothelial colonies, and then they are lifted and transferred to a 48 well plate. Cells are continued to be cultured until they are stable and capable of being culture in larger volumes. After 4 weeks, cells are assessed for morphological features and surface markers via flow cytometry.

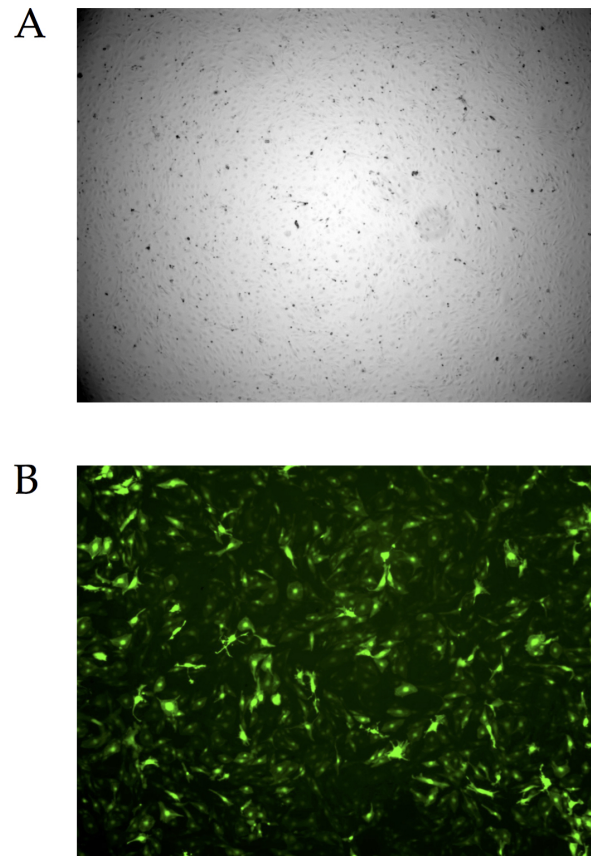


Figure 65: Phase contrast and fluorescent images of h-EPCs. A. Typical 'cobblestone' appearance of h-EPCs following 4 weeks of culture; and B. GFP expression in h-EPCs following 48 h incubation 200 pfu of AdCMVGFP.

Note: Cells isolated from the right ventricle did not culture. Further assessments of this are ongoing.

c.1.2 Transduction of h-EPCs with AdCMVGFP

H-EPCs derived from adult peripheral blood and provided by C S Bonder and colleagues were assessed for Adenoviral transduction capacity.

Due to the difficulty in culturing h-EPCs and the limited amount of cells obtained in an adult sample, cells were transduced initially with 200 pfu of AdCMVGFP for 48 h. This concentration of virus was used following the

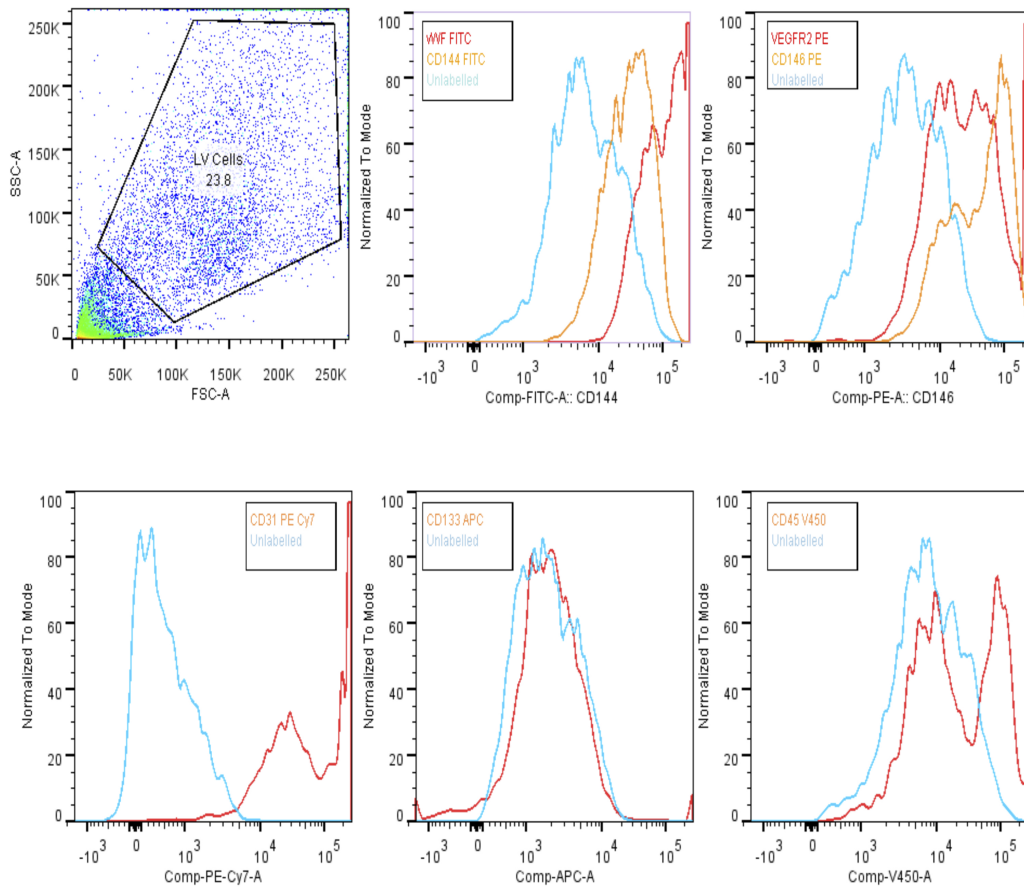


Figure 66: Flow cytometric analysis of h-EPCs derived from the left ventricle. EPCs were confirmed by their cell surface expression of vWF^+ , $CD144^+$, $CD146^+$, $VEGFR2^+$, $CD133^-$ and $CD45^{dim}$.

positive results for the r-EPCs [Chapter 13](#) at 200 pfu.

H-EPCs successfully transduced AdCMVGFP at 200 pfu with minimal cytotoxicity [Figure 65](#).

c.1.3 Transduction of h-EPCs with AdCMVBMPR2myc

Following the positive transduction of h-EPCs, we moved on to assess Ad-CMVBMPR2myc transduction in these cells via immunoblot. BMPR2 was significantly upregulated in the h-EPCs as seen in the representative immunoblot [Figure 67](#).

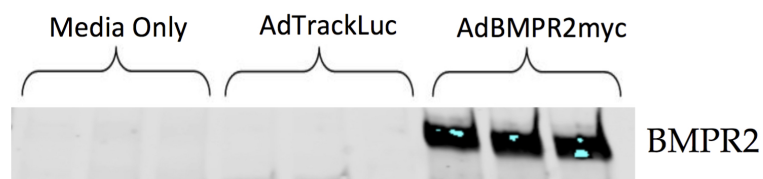


Figure 67: Immunoblot image of BMPR2 up-regulation in h-EPCs following Ad-CMVBMPR2myc transduction.

BIBLIOGRAPHY

- [1] Humbert, M., Sitbon, O., Chaouat, A., Bertocchi, M., Habib, G., Gressin, V., Yaici, A., Weitzenblum, E., Cordier, J., Chabot, F., Dromer, C., Pison, C., Reynaud-Gaubert, M., Haloun, A., Laurent, M., Hachulla, E., Cottin, V., Degano, B., Jais, X., Montani, D., Souza, R., and Simonneau, G., Survival in patients with idiopathic, familial, and anorexigen-associated pulmonary arterial hypertension in the modern management era. *Circulation*, 122(2):156–163, 2010.
- [2] Frost, A. E., Badesch, D. B., Barst, R. J., Benza, R. L., Elliott, C. G., Farber, H. W., Krichman, A., Liou, T. G., Raskob, G. E., Wason, P., Feldkircher, K., Turner, M., and McGoon, M. D., The changing picture of patients with pulmonary arterial hypertension in the united states: How reveal differs from historic and non-us contemporary registries. *Chest*, 139(1):128–137, 2011.
- [3] Sikirica, M., Iorga, S., Bancroft, T., and Potash, J., The economic burden of pulmonary arterial hypertension (pah) in the us on payers and patients. *BMC Health Serv. Res.*, 14(1):676, 2014.
- [4] Deng, Z., Morse, J. H., Slager, S. L., Cuervo, N., Moore, K. J., Venetos, G., Kalachikov, S., Cayanis, E., Fischer, S. G., and Barst, R. J., Familial primary pulmonary hypertension (gene pph1) is caused by mutations in the bone morphogenetic protein receptor-ii gene. *Am. J. Hum. Genet.*, 67(3):737–744, 2000.
- [5] Long, L., Crosby, A., Yang, X., Southwood, M., Upton, P. D., Kim, D. K., and Morrell, N. W., Altered bone morphogenetic protein and transforming growth factor-beta signaling in rat models of pul-

- monary hypertension: Potential for activin receptor-like kinase-5 inhibition in prevention and progression of disease. *Circulation*, 119(4):566, 2009.
- [6] McLaughlin, V. V. and McGoon, M. D., Pulmonary arterial hypertension. *Circulation*, 114(13):1417, 2006.
- [7] D'Alonzo, G. F., Barst, R. J., Ayres, S. M., Bergofsky, E. H., Brundage, B. H., Detre, K. M., Fishman, A. P., Goldring, R. M., Groves, B. M., Kernis, J. T., Levy, P. S., Pietra, G. G., Reid, L. M., Reeves, J. T., Rich, S., Vreim, C. E., Williams, G. W., and Wu, M., Survival in patients with primary pulmonary hypertension. *Ann. Intern. Med.*, 115(5):343, 1991.
- [8] Fishman, A. P., Clinical classification of pulmonary hypertension. *Clin. Chest Med.*, 3(22):385–91, 2001.
- [9] Simonneau, G., Gatzoulis, M. A., Adatia, I., Celermajer, D., Denton, C. P., Ghofrani, A., Gomez Sanchez, M. A., Krishna Kumar, R., Landzberg, M., Machado, R. F., Olschewski, H., Robbins, I. M., and Souza, R., Updated clinical classification of pulmonary hypertension. *J. Am. Coll. Cardiol.*, 62(25, Supplement):D34–D41, 2013.
- [10] Hoeper, M. M., Huscher, D., Ghofrani, A. H., Delcroix, M., Distler, O., Schweiger, C., Grunig, E., Staehler, G., Rosenkranz, S., Halank, M., Held, M., Grohe, C., Lange, T. J., Behr, J., Klose, H., Wilkens, H., Filusch, A., Germann, M., Ewert, R., Seyfarth, H.-J., Olsson, K. M., Opitz, C. F., Gaine, S. P., Vizza, C. D., Vonk-Noordegraaf, A., Kaemmerer, H., Gibbs, S. J. R., and Pittrow, D., Elderly patients diagnosed with idiopathic pulmonary arterial hypertension: Results from the compera registry. *Int. J. Cardiol.*, 168(2):871–880, 2013.

- [11] Mathai, S. C., Suber, T., Khair, R. M., Kolb, T. M., Damico, R. L., and Hassoun, P. M., Health-related quality of life and survival in pulmonary arterial hypertension. *Ann. ATS*, 13(1):31–39, 2015.
- [12] Humbert, M., Sitbon, O., and Simonneau, G., Treatment of pulmonary arterial hypertension. *N. Eng. J. Med.*, 351(14):1425–1436, 2004.
- [13] Townsley, M. I., *Structure and Composition of Pulmonary Arteries, Capillaries, and Veins*, vol. 2, pp. 675–709, John Wiley and Sons, Inc., American Physiological Society, 2011.
- [14] Reid, L., The angiogram and pulmonary artery structure and branching (in the normal and with reference to disease). *Proceed. Royal Soc. Med.*, 58(9):681–684, 1965.
- [15] Inc, M.-H. E., *Medical education: Anatomy*, 2015.
- [16] Toshima, M., Ohtani, Y., and Ohtani, O., Three-dimensional architecture of elastin and collagen fiber networks in the human and rat lung. *Arch. Hist. Cyt.*, 67(1):31–40, 2004.
- [17] Jain, R. K., Molecular regulation of vessel maturation. *Nat. Med.*, 9(6):685–693, 2003.
- [18] McLaughlin, V. and Humbert, M., *Pulmonary Hypertension*, book section 74, pp. 1682–1702, Elsevier Inc., Saunders, 10 ed., 2015.
- [19] Xin, M., Olson, E. N., and Bassel-Duby, R., Mending broken hearts: cardiac development as a basis for adult heart regeneration and repair. *Nat. Rev. Mol. Cell. Biol.*, 14(8):529–541, 2013.
- [20] Naeije, R., Brimiouille, S., and Dewachter, L., Biomechanics of the right ventricle in health and disease (2013 grover conference series). *Pulm. Circ.*, 4(3):395–406, 2014.

- [21] Reynolds, A. M., Holmes, M. D., Morrell, N. W., Danilov, S., and Reynolds, P. N., Gene delivery of bone morphogenic protein receptor type-2 attenuates established hypoxic and monocrotaline-induced pulmonary hypertension. *Am. J. Respir. Crit. Care Med.*, 181:A6333, 2010.
- [22] Bautch, V. L., Stem cells and the vasculature. *Nat. Med.*, 17(11):1437–1443, 2011.
- [23] Sumpio, B. E., Timothy Riley, J., and Dardik, A., Cells in focus: endothelial cell. *Int. J. Biochem. Cell Biol.*, 34(12):1508–1512, 2002.
- [24] Crosby, J. R., Kaminski, W. E., Schatteman, G., Martin, P. J., Raines, E. W., Seifert, R. A., and Bowen-Pope, D. F., Endothelial cells of hematopoietic origin make a significant contribution to adult blood vessel formation. *Circ. Res.*, 87(9):728–730, 2000.
- [25] Alberts, B., Johnson, A., Lewis, J., Raff, M., Roberts, K., and Walter, P., *Blood Vessels and Endothelial Cells*, Molecular Biology of the Cell, Garland Science, New York, 4 ed., 2002, 1464 pp.
- [26] Arnaoutova, I. and Kleinman, H. K., In vitro angiogenesis: endothelial cell tube formation on gelled basement membrane extract. *Nat. Protocols*, 5(4):628–635, 2010.
- [27] Tuder, R. M., Abman, S. H., Braun, T., Capron, F., Stevens, T., Thistlethwaite, P. A., and Haworth, S. G., Development and pathology of pulmonary hypertension. *J. Am. Coll. Cardiol.*, 54(1 Suppl. S):S3–9, 2009.
- [28] Pfeiffer, F., Kumar, V., Butz, S., Vestweber, D., Imhof, B. A., Stein, J. V., and Engelhardt, B., Distinct molecular composition of blood and lymphatic vascular endothelial cell junctions establishes specific functional barriers within the peripheral lymph node. *Euro. J. Immun.*, 38(8):2142–2155, 2008.

- [29] Reynolds, A. M., Holmes, M., Danilov, S. M., and Reynolds, P. N., Targeted gene delivery of *bmpr2* attenuates pulmonary hypertension. *Euro. Resp. J.*, 39:329–343, 2012.
- [30] Zeisberg, E. M., Tarnavski, O., Zeisberg, M., Dorfman, A. L., McMullen, J. R., Gustafsson, E., Chandraker, A., Yuan, X., Pu, W. T., and Roberts, A. B., Endothelial-to-mesenchymal transition contributes to cardiac fibrosis. *Nat. Med.*, 13(8):952–961, 2007.
- [31] Medici, D., Shore, E. M., Lounev, V. Y., Kaplan, F. S., Kalluri, R., and Olsen, B. R., Conversion of vascular endothelial cells into multipotent stem-like cells. *Nat. Med.*, 16(12):1400–1406, 2010.
- [32] Tuder, R., Marecki, J., Richter, A., Fijalkowska, I., and Flores, S., Pathology of pulmonary hypertension. *Clin. Chest Med.*, 28(1):23–42, 2007.
- [33] Heath, D. and Edwards, J. E., The pathology of hypertensive pulmonary vascular disease: A description of six grades of structural changes in the pulmonary arteries with special reference to congenital cardiac septal defects. *Circulation*, 18(4):533–547, 1958.
- [34] Heath, D., Smith, P., Gosney, J., Mulcahy, D., Fox, K., Yacoub, M., and Harris, P., The pathology of the early and late stages of primary pulmonary hypertension. *Brit. Heart J.*, 58(3):204–213, 1987.
- [35] Rabinovitch, M., Molecular pathogenesis of pulmonary arterial hypertension. *J. Clin. Invest.*, 122(12):4306–4313, 2012.
- [36] Tuder, R. M., Groves, B. M., Badesch, D. B., and Voelkel, N. F., Exuberant endothelial cell growth and elements of inflammation are present in plexiform lesions of pulmonary hypertension. *Am. J. Pathol.*, 144(2):275–285, 1994.

- [37] Yeager, M. E., Halley, G. R., Golpon, H. A., Voelkel, N. F., and Tuder, R. M., Microsatellite instability of endothelial cell growth and apoptosis genes within plexiform lesions in primary pulmonary hypertension. *Circ. Res.*, 88(1):e2–11, 2001.
- [38] Cool, C. D., Stewart, J. S., Werahera, P., Miller, G. J., Williams, R. L., Voelkel, N. F., and Tuder, R. M., Three-dimensional reconstruction of pulmonary arteries in plexiform pulmonary hypertension using cell-specific markers: Evidence for a dynamic and heterogeneous process of pulmonary endothelial cell growth. *Am. J. Path.*, 155(2):411–419, 1999.
- [39] Balabanian, K., Foussat, A., Dorfmueller, P., Durand-Gasselin, I., Capel, F., Bouchet-Delbos, L., Portier, A., Marfaing-Koka, A., Krzysiek, R., Rimaniol, A., Simonneau, G., Emilie, D., and Humbert, M., Cx3c chemokine fractalkine in pulmonary arterial hypertension. *Am. J. Respir. Crit. Care Med.*, 165(10):1419–1425, 2002.
- [40] Savai, R., Pullamsetti, S. S., Kolbe, J., Bieniek, E., Voswinckel, R., Fink, L., Scheed, A., Ritter, C., Dahal, B. K., Vater, A., Klussmann, S., Ghofrani, H. A., Weissmann, N., Klepetko, W., Banat, G. A., Seeger, W., Grimminger, F., and Schermuly, R. T., Immune and inflammatory cell involvement in the pathology of idiopathic pulmonary arterial hypertension. *Am. J. Respir. Crit. Care Med.*, 186(9):897–908, 2012.
- [41] Hassoun, P. M., Mouthon, L., Barber, J. A., Eddahibi, S., Flores, S. C., Grimminger, F., Jones, P. L., Maitland, M. L., Michelakis, E. D., Morrell, N. W., Newman, J. H., Rabinovitch, M., Schermuly, R., Stenmark, K. R., Voelkel, N. F., Yuan, J. X. J., and Humbert, M., Inflammation, growth factors, and pulmonary vascular remodeling. *J. Am. Coll. Cardio.*, 54(1 Supplement 1):S10–S19, 2009.
- [42] Kherbeck, N., Tamby, M. C., Bussone, G., Dib, H., Perros, F., Humbert, M., and Mouthon, L., The role of inflammation and autoimmunity in

- the pathophysiology of pulmonary arterial hypertension. *Clinic. Rev. Allerg. Immunol.*, 2011.
- [43] Sanchez, O., Marcos, E., Perros, F., Fadel, E., Tu, L., Humbert, M., Dartevelle, P., Simonneau, G., Adnot, S., and Eddahibi, S., Role of endothelium-derived cc chemokine ligand 2 in idiopathic pulmonary arterial hypertension. *Am. J. Respir. Crit. Care Med.*, 176(10):1041–1047, 2007.
- [44] Taraseviciene-Stewart, L., Kasahara, Y., Alger, L., Hirth, P., McMahon, G., Waltenberger, J., Voelkel, N. F., and Tudor, R. M., Inhibition of the vegf receptor 2 combined with chronic hypoxia causes cell death-dependent pulmonary endothelial cell proliferation and severe pulmonary hypertension. *The FASEB J.*, 15(2):427–438, 2001.
- [45] Sakao, S., Taraseviciene-Stewart, L., Lee, J. D., Wood, K., Cool, C. D., and Voelkel, N. F., Initial apoptosis is followed by increased proliferation of apoptosis-resistant endothelial cells. *The FASEB J.*, 2005.
- [46] Morrell, N. W., Adnot, S., Archer, S. L., Dupuis, J., Lloyd Jones, P., MacLean, M. R., McMurtry, I. F., Stenmark, K. R., Thistlethwaite, P. A., Weissmann, N., Yuan, J. X. J., and Weir, K. E., Cellular and molecular basis of pulmonary arterial hypertension. *J. Am. Coll. Cardiol.*, 54(1 Suppl. S):S20–31, 2009.
- [47] Dickens, F. and Warburg, O., *Uber Den Stoffwechsel Der Tumoren. The Metabolism of Tumours. Investigations from the Kaiser Wilhelm Institute for Biology*, Kaiser Wilhelm-Institut fur Biologie, Berlin- London, 1930, 327 pp., (BERLIN).
- [48] Nasim, M. T., Ogo, T., Chowdhury, H. M., Zhao, L., Chen, C., Rhodes, C., and Trembath, R. C., Bmpr-2 deficiency elicits pro-proliferative and anti-apoptotic responses through the activation of tgfbeta -tak1-mapk pathways in pah. *Human Mol. Gen.*, 21(11):2548–2558, 2012.

- [49] Harrison, R. E., Flanagan, J. A., Sankelo, M., Abdalla, S. A., Rowell, J., Machado, R. D., Elliott, C. G., Robbins, I. M., Olschewski, H., McLaughlin, V., Gruenig, E., Kermeen, F., Laitinen, T., Morrell, N. W., and Trembath, R. C., Molecular and functional analysis identifies *alk-1* as the predominant cause of pulmonary hypertension related to hereditary haemorrhagic telangiectasia. *J. Med. Gen.*, 40(12):865–871, 2003.
- [50] Chaouat, A., Coulet, F., Favre, C., Simonneau, G., Weitzenblum, E., Soubrier, F., and Humbert, M., Endoglin germline mutation in a patient with hereditary haemorrhagic telangiectasia and dexfenfluramine associated pulmonary arterial hypertension. *Thorax*, 59(5):446–448, 2004.
- [51] Nasim, M. T., Ogo, T., Ahmed, M., Randall, R., Chowdhury, H. M., Snape, K. M., Bradshaw, T. Y., Southgate, ., Lee, G. J., Jackson, I., Lord, G. M., Gibbs, S. R. J., Wilkins, M. R., Ohta-Ogo, K., Nakamura, K., Girerd, B., Coulet, F., Soubrier, F., Humbert, M., Morrell, N. W., Trembath, R. C., and Machado, R. D., Molecular genetic characterization of smad signaling molecules in pulmonary arterial hypertension. *Hum. Mut.*, 32(12):1385–1389, 2011.
- [52] Austin, E. D., Ma, L., LeDuc, C., Berman Rosenzweig, E., Borczuk, A., Phillips, J. A., Palomero, T., Sumazin, P., Kim, H. R., Talati, M. H., West, J., Loyd, J. E., and Chung, W. K., Whole exome sequencing to identify a novel gene (*caveolin-1*) associated with human pulmonary arterial hypertension. *Circ. Cardiovas. Gen.*, 5(3):336–343, 2012.
- [53] Ma, L., Roman-Campos, D., Austin, E. D., Eyries, M., Sampson, K. S., Soubrier, F., Germain, M., Tregouet, D. A., Borczuk, A., Rosenzweig, E. B., Girerd, B., Montani, D., Humbert, M., Loyd, J. E., Kass, R. S., and Chung, W. K., A novel channelopathy in pulmonary arterial hypertension. *N. Eng. J. Med.*, 369(4):351–361, 2013.

- [54] Beppu, H., Kawabata, M., Hamamoto, T., Chytil, A., Minowa, O., Noda, T., and Miyazono, K., Bmp type 2 receptor is required for gastrulation and early development of mouse embryos. *Dev. Biol.*, 221(1):249–258, 2000.
- [55] Hassel, S., Eichner, A., Yakymovych, M., Hellman, U., Knaus, P., and Souchelnytskyi, S., Proteins associated with type 2 bone morphogenetic protein receptor (bmpr-2) and identified by two-dimensional gel electrophoresis and mass spectrometry. *Proteom.*, 4(5):1346–1358, 2004.
- [56] Gamez, B., Rodriguez-Carballo, E., and Ventura, F., Bmp signaling in telencephalic neural cell specification and maturation. *Front. Cell. Neurosci.*, 7, 2013.
- [57] Gamer, L. W., Tsuji, K., Cox, K., Capelo, L. P., Lowery, J., Beppu, H., and Rosen, V., Bmpr-2 is dispensable for formation of the limb skeleton. *Gen.*, 49(9):719–724, 2011.
- [58] Upton, P. D., Davies, R. J., Trembath, R. C., and Morrell, N. W., Bone morphogenetic protein (bmp) and activin type 2 receptors balance bmp9 signals mediated by activin receptor-like kinase-1 in human pulmonary artery endothelial cells. *J. Biol. Chem.*, 284(23):15794, 2009.
- [59] Cogan, J. D., Vnencak-Jones, C. L., Phillips Iii, J. A., Lane, K. B., Wheeler, L. A., Robbins, I. M., Garrison, G., Hedges, L. K., and Loyd, J. E., Gross bmpr2 gene rearrangements constitute a new cause for primary pulmonary hypertension. *Genet. Med.*, 7(3):169–174, 2005.
- [60] Machado, R. D., Aldred, M. A., James, V., Harrison, R. E., Patel, B., Schwalbe, E. C., Gruenig, E., Janssen, B., Koehler, R., and Seeger, W., Mutations of the tgf type ii receptor bmpr2 in pulmonary arterial hypertension. *Hum. Mutat.*, 27(2):121–132, 2006.

- [61] Humbert, M., Morrell, N. W., Archer, S. L., Stenmark, K. R., MacLean, M. R., Lang, I. M., Christman, B. W., Weir, E. K., Eickelberg, O., Voelkel, N. F., and Rabinovitch, M., Cellular and molecular pathobiology of pulmonary arterial hypertension. *J. Am. Coll. Cardio.*, 43(12, Supplement 1):S13–S24, 2004.
- [62] Yang, J., Davies, R. J., Southwood, M., Long, L., Yang, X., Sobolewski, A., Upton, P. D., Trembath, R. C., and Morrell, N. W., Mutations in bone morphogenetic protein type ii receptor cause dysregulation of Id gene expression in pulmonary artery smooth muscle cells: Implications for familial pulmonary arterial hypertension. *Circ. Res.*, 102(10):1212–1221, 2008.
- [63] NCBI, Chromosome mapping, 2015.
- [64] Waite, K. A. and Eng, C., From developmental disorder to heritable cancer: it's all in the bmp/tgf-beta family. *Nat. Rev. Genet.*, 4(10):763–773, 2003.
- [65] Guzman, A., Femiak, M. Z., Boergemann, J. H., Paschkowsky, S., Kreuzaler, P. A., Fratzl, P., Harms, G. S., and Knaus, P., Smad versus non-smad signaling is determined by lateral mobility of bone morphogenetic protein (bmp) receptors. *J. Biol. Chem.*, 287(47):39492–39504, 2012.
- [66] Nohe, A., Keating, E., Knaus, P., and Petersen, N. O., Signal transduction of bone morphogenetic protein receptors. *Cell. Sig.*, 16(3):291–299, 2004.
- [67] Derynck, R. and Zhang, Y. E., Smad dependent and smad independent pathways in tgfb family signalling. *Nature*, 425:577–585, 2003.
- [68] Zhang, Y., Wen, G., Shao, G., Wang, C., Lin, C., Fang, H., Balajee, A. S., Bhagat, G., Hei, T. K., and Zhao, Y., Tgfb1 deficiency predisposes mice to spontaneous tumor development. *Cancer Res.*, 69(1):37 – 44, 2009.

- [69] Machado, R. D., James, V., Southwood, M., Harrison, R. E., Atkinson, C., Stewart, S., Morrell, N. W., Trembath, R. C., and Aldred, M. A., Investigation of second genetic hits at the *bmpr2* locus as a modulator of disease progression in familial pulmonary arterial hypertension. *Circulation*, 111(5):607–613, 2005.
- [70] Austin, E. D., Phillips, J. A., Cogan, J. D., Hamid, R., Yu, C., Stanton, K. C., Phillips, C. A., Wheeler, L. A., Robbins, I. M., and Newman, J. H., Truncating and missense (*bmpr2*) mutations differentially affect the severity of heritable pulmonary arterial hypertension. *Respir. Res.*, 10:87, 2009.
- [71] Morse, J. H., Jones, A., Barst, R. J., Hodge, S. E., Wilhelmsen, K. C., and Nygaard, T. G., Mapping of familial primary pulmonary hypertension locus (*pph1*) to chromosome 2q31-q32. *Circulation*, 95(12):2603, 1997.
- [72] Nicholls, M. G., Richards, A. M., and Begg, E. J., Hypertension and heart failure. *Adv. Exp. Med. Biol.*, 432:273, 1997.
- [73] Newman, J. H., Wheeler, L., Lane, K. B., Loyd, E., Gaddipati, R., Phillips, J. A., and Loyd, J. E., Mutation in the gene for bone morphogenetic protein receptor ii as a cause of primary pulmonary hypertension in a large kindred. *N. Engl. J. Med.*, 345(5):319, 2001.
- [74] Ryan, J. J., Marsboom, G., and Archer, S. L., *Rodent Models of Group 1 Pulmonary Hypertension*, vol. 218 of *Handbook of Experimental Pharmacology*, book section 5, pp. 105–149, Springer Berlin Heidelberg, 2013.
- [75] Wagner, J. G., Petry, T. W., and Roth, R. A., Characterisation of monocrotaline pyrrole-induced dna cross-linking in pulmonary artery endothelium. *Am. J. Physiol. Lung Cell Mol. Physiol.*, 5(256):L517–522, 1993.

- [76] Huang, J., Wolk, J. H., Gewitz, M. H., and Mathew, R., Progressive endothelial cell damage in an inflammatory model of pulmonary hypertension. *Exp. Lung. Res.*, 36(1):57–66, 2010.
- [77] Rosenberg, H. C. and Rabinovitch, M., Endothelial injury and vascular reactivity in monocrotaline pulmonary hypertension. *Am. J. of Physiol. Heart Circ. Physiol.*, 255(6):H1484–H1491, 1988.
- [78] Dumitrascu, R., Koebrich, S., Dony, E., Weissmann, N., Savai, R., Pulamsetti, S. S., Ghofrani, H. A., Samidurai, A., Traupe, H., Seeger, W., Grimminger, F., and Schermuly, R., Characterization of a murine model of monocrotaline pyrrole-induced acute lung injury. *BMC Pulm. Med.*, 8(1):25, 2008.
- [79] Stenmark, K. R., Meyrick, B., Galie, N., Mooi, W. J., and McMurtry, I. F., Animal models of pulmonary arterial hypertension: the hope for etiological discovery and pharmacological cure. *Am. J. Physiol. Lung Cell. Mol. Physiol.*, 297(6):L1013–L1032, 2009.
- [80] Burke, D. L., Frid, M. G., Kunrath, C. L., Karoor, V., Anwar, A., Wagner, B. D., Strassheim, D., and Stenmark, K. R., Sustained hypoxia promotes the development of a pulmonary artery-specific chronic inflammatory microenvironment. *Am. J. Physiol. Lung Cell. Mol. Physiol.*, 297(2):L238–L250, 2009.
- [81] Moreno-Vinasco, L., Gomberg-Maitland, M., Maitland, M. L., Desai, A. A., Singleton, P. A., Sammani, S., Sam, L., Liu, Y., Husain, A. N., Lang, R. M., Ratain, M. J., Lussier, Y. A., and Garcia, J. G. N., Genomic assessment of a multikinase inhibitor, sorafenib, in a rodent model of pulmonary hypertension. *Physiol. Genom.*, 33(2):278–291, 2008.
- [82] Humbert, M. and Ghofrani, H. A., The molecular targets of approved treatments for pulmonary arterial hypertension. *Thorax*, 2015.

- [83] Galie, N., Corris, P. A., Frost, A., Girgis, R. E., Granton, J., Jing, Z. C., Klepetko, W., McGoon, M. D., McLaughlin, V. V., Preston, I. R., Rubin, L. J., Sandoval, J., Seeger, W., and Keogh, A., Updated treatment algorithm of pulmonary arterial hypertension. *J. Am. Coll. Cardiol.*, 62(25, Supplement):D60–D72, 2013.
- [84] Ghofrani, H. A. and Humbert, M., The role of combination therapy in managing pulmonary arterial hypertension. *Euro. Respir. Rev.*, 23(134):469–475, 2014.
- [85] Takaoka, S., Faul, J. L., and Doyle, R., Current therapies for pulmonary arterial hypertension. *Sem. Cardio. Vas. Anesth.*, 11(2):137–148, 2007.
- [86] Sitbon, O., Humbert, M., Jais, X., Ioos, V., Hamid, A. M., Provencher, S., Garcia, G., Parent, F., Herve, P., and Simonneau, G., Long-term response to calcium channel blockers in idiopathic pulmonary arterial hypertension. *Circulation*, 111(23):3105–3111, 2005.
- [87] Cacoub, P., Dorent, R., Nataf, P., Carayon, A., Riquet, M., Noe, E., Piette, J. C., Godeau, P., and Gandjbakhch, I., Endothelin-1 in the lungs of patients with pulmonary hypertension. *Cardiovas. Res.*, 33(1):196–200, 1997.
- [88] Sitbon, O., Badesch, D. B., Channick, R. N., Frost, A., Robbins, I. M., Simonneau, G., Tapson, V. F., and Rubin, L. J., Effects of the dual endothelin receptor antagonist bosentan in patients with pulmonary arterial hypertension: A 1-year follow-up study. *Chest*, 124(1):247–254, 2003.
- [89] Rubin, L. J., Badesch, D. B., Barst, R. J., Galie, N., Black, C. M., Keogh, A., Pulido, T., Frost, A., Roux, S., Leconte, I., Landzberg, M., and Simonneau, G., Bosentan therapy for pulmonary arterial hypertension. *N. Eng. J. Med.*, 346(12):896–903, 2002.

- [90] Simonneau, G., Galie, N., Jansa, P., Meyer, G. M. B., Al-Hiti, H., Kusic-Pajic, A., Lemarie, J. C., Hoeper, M. M., and Rubin, L. J., Long-term results from the early study of bosentan in who functional class ii pulmonary arterial hypertension patients. *Int. J. Cardiol.*, 172(2):332–339, 2014.
- [91] McLaughlin, V. V., Sitbon, O., Badesch, D. B., Barst, R. J., Black, C., Galie, N., Rainisio, M., Simonneau, G., and Rubin, L. J., Survival with first-line bosentan in patients with primary pulmonary hypertension. *Eur. Respir. J.*, 25(2):244–249, 2005.
- [92] Barst, R. J., Langleben, D., Badesch, D. B., Frost, A., Lawrence, C. E., Shapiro, S., Naeije, R., and Galie, N., Treatment of pulmonary arterial hypertension with the selective endothelin-a receptor antagonist sitaxsentan. *J. Am. Coll. Cardiol.*, 47(10):2049–2056, 2006.
- [93] Benza, R. L., Barst, R. J., Galie, N., Frost, A., Girgis, R. E., Highland, K. B., Strange, C., Black, C. M., Badesch, D. B., Rubin, L. J., Fleming, T. R., and Naeije, R., Sitaxsentan for the treatment of pulmonary arterial hypertension: A 1-year, prospective, open-label observation of outcome and survival. *Chest*, 134(4):775–782, 2008.
- [94] Clapp, L. H., Finney, P., Turcato, S., Tran, S., Rubin, L. J., and Tinker, A., Differential effects of stable prostacyclin analogs on smooth muscle proliferation and cyclic amp generation in human pulmonary artery. *Am. J. Respir. Cell Mol. Biol.*, 26(2):194–201, 2002.
- [95] Moncada, S., Gryglewski, R., Bunting, S., and Vane, J. R., An enzyme isolated from arteries transforms prostaglandin endoperoxides to an unstable substance that inhibits platelet aggregation. *Nature*, 263(5579):663–665, 1976.

- [96] Higenbottam, T., Wells, F., Wheeldon, D., and Wallwork, J., Long-term treatment of primary pulmonary hypertension with continuous intravenous epoprostenol (prostacyclin). *Lancet*, 323(8385):1046–1047, 1984.
- [97] Hanson, K. A., Ziegler, J. W., Rybalkin, S. D., Miller, J. W., Abman, S. H., and Clarke, W. R., Chronic pulmonary hypertension increases fetal lung cgmp phosphodiesterase activity. *Am. J. Physiol.*, 275(5):L931–L941, 1998.
- [98] Rubin, L. J., Badesch, D. B., Fleming, T. R., Galie, N., Simonneau, G., Ghofrani, H. A., Oakes, M., Layton, G., Serdarevic-Pehar, M., McLaughlin, V. V., and Barst, R. J., Long-term treatment with sildenafil citrate in pulmonary arterial hypertension: The super-2 study. *Chest*, 140(5):1274–1283, 2011.
- [99] Fox, B. D., Shimony, A., and Langleben, D., Meta-analysis of monotherapy versus combination therapy for pulmonary arterial hypertension. *Am. J. Cardiol.*, 108(8):1177–1182, 2011.
- [100] Simonneau, G., Rubin, L. J., Galie, N., Barst, R. J., Fleming, T. R., Frost, A. E., Engel, P. J., Kramer, M. R., Burgess, G., Collings, L., Cossons, N., Sitbon, O., and Badesch, D. B., Addition of sildenafil to long-term intravenous epoprostenol therapy in patients with pulmonary arterial hypertensiona randomized trial. *Ann. Intern. Med.*, 149(8):521–530, 2008.
- [101] McLaughlin, V. V., Oudiz, R. J., Frost, A., Tapson, V. F., Murali, S., Channick, R. N., Badesch, D. B., Barst, R. J., Hsu, H. H., and Rubin, L. J., Randomized study of adding inhaled iloprost to existing bosentan in pulmonary arterial hypertension. *A. J. Respir. Crit. Care Med.*, 174(11):1257–1263, 2006.
- [102] Hassoun, P. M., Zamanian, R. T., Damico, R. L., Lechtzin, N., Khair, R., Kolb, T. M., Tedford, R. J., Hulme, O. L., Houston, T., Pisanello,

- C., Sato, T., Pullins, E. H., Corona-Villalobos, C. P., Zimmerman, S. L., Gashouta, M. A., Minai, O. A., Torres, F., Girgis, R. E., Chin, K., and Mathai, S. C., Ambrisentan and tadalafil up-front combination therapy in scleroderma-associated pulmonary arterial hypertension. *Am. J. Respir. Crit. Care Med.*, 192(9):1102–1110, 2015.
- [103] Ghofrani, H. A. and Grimminger, F., Soluble guanylate cyclase stimulation: an emerging option in pulmonary hypertension therapy. *Euro. Respir. Rev.*, 18(111):35–41, 2009.
- [104] Ghofrani, H. A., D'Armini, A. M., Grimminger, F., Hoeper, M. M., Jansa, P., Kim, N. H., Mayer, E., Simonneau, G., Wilkins, M. R., Fritsch, A., Neuser, D., Weimann, G., and Wang, C., Riociguat for the treatment of chronic thromboembolic pulmonary hypertension. *N. Eng. J. Med.*, 369(4):319–329, 2013.
- [105] Thompson, A. W., Bonham, C. A., and Zeevi, A., Mode of action of tacrolimus (fk506): molecular and cellular mechanisms. *Ther. Drug Monit.*, 17(6):584–591, 1995.
- [106] Spiekerkoetter, E., Tian, X., Cai, J., Hopper, R. K., Sudheendra, D., Li, C. G., El-Bizri, N., Sawada, H., Haghghat, R., Chan, R., Haghghat, L., de Jesus Perez, V., Wang, L., Reddy, S., Zhao, M., Bernstein, D., Solow-Cordero, D. E., Beachy, P. A., Wandless, T. J., ten Dijke, P., and Rabinovitch, M., Fk506 activates bmpr2, rescues endothelial dysfunction, and reverses pulmonary hypertension. *J. Clin. Invest.*, 123(8):3600–3613, 2013.
- [107] Chow, K., Fessel, J. P., Kaorilhida, S., Schmidt, E. P., Gaskill, C., Alvarez, D. F., Graham, B., Harrison, D. G., Wagner, D. H., Nozik-Grayck, E., West, J. D., Klemm, D. J., and Majka, S. M., Dysfunctional resident lung mesenchymal stem cells contribute to pulmonary microvascular remodeling. *Pulm. Circ.*, 3(1):31–49, 2013.

- [108] Toshner, M., Voswinckel, R., Southwood, M., Al-Lamki, R., Howard, L., Marchesan, D., Yang, J., Suntharalingam, J., Soon, E., Exley, A., Stewart, S., Hecker, M., Zhu, Z., Gehling, U., Seeger, W., Pepke-Zaba, J., and Morrell, N. W., Evidence of dysfunction of endothelial progenitors in pulmonary arterial hypertension. *Am. J. Respir. Crit. Care Med.*, 180(8):780–787, 2009.
- [109] Wang, X. X., Zhang, F. R., Shang, Y. P., Zhu, J. H., Xie, X. D., Tao, Q. M., Zhu, J. H., and Chen, J. Z., Transplantation of autologous endothelial progenitor cells may be beneficial in patients with idiopathic pulmonary arterial hypertension: A pilot randomized controlled trial. *J. Am. Coll. Cardiol.*, 49(14):1566–1571, 2007.
- [110] Zhao, Y. D., Courtman, D. W., Deng, Y., Kugathasan, L., Zhang, Q., and Stewart, D. J., Rescue of monocrotaline-induced pulmonary arterial hypertension using bone marrow derived endothelial-like progenitor cells. *Circ. Res.*, 96(4):442–450, 2005.
- [111] Kalka, C., Masuda, H., Takahashi, T., Kalka-Moll, W. M., Silver, M., Kearney, M., Li, T., Isner, J. M., and Asahara, T., Transplantation of ex vivo expanded endothelial progenitor cells for therapeutic neovascularization. *Proc. Nat. Acad. Sci.*, 97(7):3422–3427, 2000.
- [112] Luan, Y., Zhang, X., Kong, F., Cheng, G. H., Qi, T. G., and Zhang, Z. H., Mesenchymal stem cell prevention of vascular remodeling in high flow-induced pulmonary hypertension through a paracrine mechanism. *Int. Immunopharm.*, 14(4):432–437, 2012.
- [113] Berra, L., Pinciroli, R., Stowell, C. P., Wang, L., Yu, B., Fernandez, B. O., Feelisch, M., Mietto, C., Hod, E. A., Chipman, D., Scherrer-Crosbie, M., Bloch, K. D., and Zapol, W. M., Autologous transfusion of stored red blood cells increases pulmonary artery pressure. *Am. J. Respir. Crit. Care Med.*, 190(7):800–807, 2014.

- [114] Chen, J., Tang, H., Sysol, J. R., Moreno-Vinasco, L., Shioura, K. M., Chen, T., Gorshkova, I., Wang, L., Huang, L. S., Usatyuk, P. V., Sammani, S., Zhou, G., Raj, J. U., Garcia, J. G. N., Berdyshev, E., Yuan, J. X. J., Natarajan, V., and Machado, R. F., The sphingosine kinase 1/sphingosine-1-phosphate pathway in pulmonary arterial hypertension. *Am. J. Respir. Crit. Care Med.*, 190(9):1032–1043, 2014.
- [115] Granton, J., Langleben, D., Kutryk, M. J., Camack, N., Galipeau, J., Courtman, D., and Stewart, D. J., Endothelial no-synthase gene-enhanced progenitor cell therapy for pulmonary arterial hypertension: the phacet trial. *Circ. Res.*, 2015.
- [116] Zhou, L., Chen, Z., Vanderslice, P., So, S., Ruan, K., Willerson, J. T., and Dixon, R. A. F., Endothelial-like progenitor cells engineered to produce prostacyclin rescue monocrotaline-induced pulmonary arterial hypertension and provide right ventricle benefits. *Circ.*, 128(9):982–994, 2013.
- [117] Unknown, The 2007 revised national statement on ethical conduct in human research, 2015.
- [118] Wirth, T., Parker, N., and Yla-Herttuala, S., History of gene therapy. *Gene*, 525(2):162–169, 2013.
- [119] Alloway, J. L., The transformation in vitro of r pneumococci into s forms of different specific types by the use of filtered pneumococcus extracts. *J. Exp. Med.*, 55(1):91–99, 1932.
- [120] Alloway, J. L., Further observations on the use of pneumococcus extracts in effecting transformation of type in vitro. *J. Exp. Med.*, 57(2):265–278, 1933.
- [121] Griffith, F., The significance of pneumococcal types. *J. Hyg.*, 27(2):113–159, 1928.

- [122] Temin, H. M., Mixed infection with two types of rous sarcoma virus. *Virology*, 13(2):158–163, 1961.
- [123] Szybalska, E. H. and Szybalski, W., Genetics of human cell lines, iv. dna-mediated heritable transformation of a biochemical trait. *Proc. Natl. Acad. Sci. U S A.*, 48(12):2026–2034, 1962.
- [124] Rogers, S. and Pfuderer, P., Use of viruses as carriers of added genetic information. *Nature*, 219(5155):749–751, 1968.
- [125] Blaese, M. R., Culver, K. W., Miller, A. D., Carter, C. S., Fleisher, T., Clerici, M., Shearer, G., Chang, L., Chiang, Y., Tolstoshev, P., Greenblatt, J. J., Rosenberg, S. A., Klein, H., Berger, M. M., Mullen, C. A., Ramsey, W. J., Muul, L., Morgan, R. A., and Anderson, W. F., T lymphocyte-directed gene therapy for ada- scid: Initial trial results after 4 years. *Science*, 270(5235):475–480, 1995.
- [126] Descamps, D. and Benihoud, K., Two key challenges for effective adenovirus-mediated liver gene therapy: innate immune responses and hepatocyte-specific transduction. *Curr. Gene Ther.*, 9(2):115–127, 2009.
- [127] Lemarchand, P., Jones, M., Yamada, I., and Crystal, R. G., In vivo gene transfer and expression in normal uninjured blood vessels using replication-deficient recombinant adenovirus vectors. *Circ. Res.*, 72(5):1132–8, 1993.
- [128] Suen, C. M., Mei, S. H. J., Kugathasan, L., and Stewart, D. J., *Targeted Delivery of Genes to Endothelial Cells and Cell- and Gene-Based Therapy in Pulmonary Vascular Diseases*, John Wiley and Sons, Inc., 2011.
- [129] Reynolds, P. N., Gene therapy for pulmonary hypertension: prospects and challenges. *Biol. Theory*, 11(2):133–143, 2011.

- [130] Alberti, M. O., Deshane, J. S., Chaplin, D. D., Pereboeva, L., Curiel, D. T., and Roth, J. C., A myeloid cell-binding adenovirus efficiently targets gene transfer to the lung and escapes liver tropism. *Gene Ther*, 20(7):733–741, 2013.
- [131] Leboulch, P., Gene therapy: Primed for take-off. *Nature*, 500(7462):280–282, 2013.
- [132] Aiuti, A., Biasco, L., Scaramuzza, S., Ferrua, F., Cicalese, M. P., Baricordi, C., Dionisio, F., Calabria, A., Giannelli, S., Castiello, M. C., Bosticardo, M., Evangelio, C., Assanelli, A., Casiraghi, M., Di Nunzio, S., Callegaro, L., Benati, C., Rizzardi, P., Pellin, D., Di Serio, C., Schmidt, M., Von Kalle, C., Gardner, J., Mehta, N., Neduva, V., Dow, D. J., Galy, A., Miniero, R., Finocchi, A., Metin, A., Banerjee, P. P., Orange, J. S., Galimberti, S., Valsecchi, M. G., Biffi, A., Montini, E., Villa, A., Ciceri, F., Roncarolo, M. G., and Naldini, L., Lentiviral hematopoietic stem cell gene therapy in patients with wiskott-aldrich syndrome. *Science*, 341(6148), 2013.
- [133] Rincon, M. Y., VandenDriessche, T., and Chuah, M. K., *Gene therapy for cardiovascular disease: advances in vector development, targeting and delivery for clinical translation*, 2015.
- [134] Reynolds, P. N., Zinn, K. R., Gavrilyuk, V. D., Balyasnikova, I. V., Rogers, B. E., Buchsbaum, D. J., Wang, M. H., Miletich, D. J., Grizzle, W. E., Douglas, J. T., Danilov, S., and Curiel, D. T., A targetable, injectable adenoviral vector for selective gene delivery to pulmonary endothelium in vivo. *Mol. Ther.*, 2(6):562–578, 2000.
- [135] Jeffery, T. K. and Morrell, N. W., Molecular and cellular basis of pulmonary vascular remodeling in pulmonary hypertension. *Prog. Cardiovasc. Dis.*, 45(3):173–202.

- [136] Feng, F., Harper, R. L., and Reynolds, P. N., Bmpr-2 gene delivery reduces mutation-related pah and counteracts tgf-beta mediated pulmonary cell signalling. *Resp. Res.*, 2015.
- [137] Reynolds, A. M., Xia, W., Holmes, M. D., Hodge, S. J., Danilov, S., Curiel, D. T., Morrell, N. W., and Reynolds, P. N., Bone morphogenetic protein type 2 receptor gene therapy attenuates hypoxic pulmonary hypertension. *Am. J. Physiol. Lung Cell. Mol. Physiol.*, 292(5):L1182, 2007.
- [138] Qbiogene, *AdEasy Vector System*, Q BIO gene, Carlsbad, CA, USA, 1.4 ed., 61 pp.
- [139] Takahashi, H., Goto, N., Kojima, Y., Tsuda, Y., Morio, Y., Muramatsu, M., and Fukuchi, Y., Downregulation of type ii bone morphogenetic protein receptor in hypoxic pulmonary hypertension. *Am. J. Physiol. Lung Cell. Mol. Physiol.*, 290(3):L450–L458, 2006.
- [140] Mckenzie, A. J. and Strauss, P. R., A quantitative method for measuring protein phosphorylation. *Analyt. Biochem.*, 313(1):9–16, 2003.
- [141] Reynolds, P. N., Nicklin, S. A., Kaliberova, L., Boatman, B. G., Grizzle, W. E., Balyasnikova, I. V., Baker, A. H., Danilov, S. M., and Curiel, D. T., Combined transductional and transcriptional targeting improves the specificity of transgene expression in vivo. *Nat. Biotechnol.*, 19:838–842, 2001.
- [142] Harper, R. L., Reynolds, A. M., and Reynolds, P. N., Bmpr2 gene therapy for pah acts via smad and non-smad signalling. *Resp. Res.*, 2015.
- [143] Bogaard, H. J., Abe, K., Vonk Noordegraaf, A., and Voelkel, N. F., The right ventricle under pressure: Cellular and molecular mechanisms of right-heart failure in pulmonary hypertension. *Chest*, 135(3):794–804, 2009.

- [144] Raychaudhuri, S., Stuart, J. M., and Altman, R. B., Principal components analysis to summarize microarray experiments: Application to sporulation time series. *Pacific Symposium on Biocomputing*, pp. 455–466, 2000.
- [145] Patel, M., Predescu, D., Tandon, R., Bardita, C., Pogoriler, J., Bhorade, S., Wang, M., Comhair, S., Ryan-Hemnes, A., Chen, J., Machado, R. D., Husain, A., Erzurum, S., and Predescu, S., A novel p38 mitogen-activated protein kinase/elk-1 transcription factor-dependent molecular mechanism underlying abnormal endothelial cell proliferation in plexogenic pulmonary arterial hypertension. *J. Biol. Chem.*, 288(36):25701–25716, 2013.
- [146] Bajaj, A., Zheng, Q., Adam, A., Vincent, P., and Pumiglia, K., Activation of endothelial ras signaling bypasses senescence and causes abnormal vascular morphogenesis. *Cancer Research*, 70(9):3803–3812, 2010.
- [147] Wu, J., Yu, Z., and Su, D., Bmp4 protects rat pulmonary arterial smooth muscle cells from apoptosis by pi3k/akt/smad1/5/8 signaling. *Int. J. Mol. Sci.*, 15(8):13738–54, 2014.
- [148] Ikushima, H. and Miyazono, K., Cellular context-dependent "colors" of transforming growth factor-beta signaling. *Cancer Sci.*, 101(2):306 – 312, 2010.
- [149] Li, M., Vattulainen, S., Aho, J., Orcholski, M., Rojas, V., Yuan, K., Helenius, M., Taimen, P., Myllykangas, S., De Jesus Perez, V., Koskenvuo, J. W., and Alastalo, T. P., Loss of bone morphogenetic protein receptor 2 is associated with abnormal dna repair in pulmonary arterial hypertension. *Am. J. Respir. Cell. Mol. Biol.*, 50(6):1118–1128, 2014.

- [150] Archer, S. L., Weir, K. E., and Wilkins, M. R., Basic science of pulmonary arterial hypertension for clinicians: New concepts and experimental therapies. *Circulation*, 121(18):2045–2066, 2010.
- [151] Bahrami, F., Pourgholami, M. H., Mekkawy, A. H., Rufener, L., and Morris, D. L., Monepantel induces autophagy in human ovarian cancer cells through disruption of the mtor/p70s6k signalling pathway. *Am. J. Can. Res.*, 4(5):558–571, 2014.
- [152] Broege, A., Pham, L., Jensen, D., Emery, A., Huang, T. H., Stemig, M., Beppu, H., Petryk, A., O'Connor, M., Mansky, K., and Gopalakrishnan, R., Bone morphogenetic proteins signal via smad and mitogen-activated protein (map) kinase pathways at distinct times during osteoclastogenesis. *J. Biol. Chem.*, 288(52):37230–37240, 2013.
- [153] Graupera, M., Guillermet-Guibert, J., Foukas, L. C., Phng, L. K., Cain, R. J., Salpekar, A., Pearce, W., Meek, S., Millan, J., Cutillas, P. R., Smith, A. J. H., Ridley, A. J., Ruhrberg, C., Gerhardt, H., and Vanhaesebroeck, B., Angiogenesis selectively requires the p110 isoform of pi3k to control endothelial cell migration. *Nature*, 453(7195):662–666, 2008.
- [154] Yoder, M. C., Differentiation of pluripotent stem cells into endothelial cells. *Curr. Opin. Hematol.*, 22(3):252–257, 2015.
- [155] Firth, A. L., Choi, I. W., and Park, W. S., Animal models of pulmonary hypertension: Rho kinase inhibition. *Prog. Biophys. Mol. Biol.*, 109(3):67–75, 2012.
- [156] Asahara, T., Murohara, T., Sullivan, A., Silver, M., van der Zee, R., Li, T., Witzenbichler, B., Schatteman, G., and Isner, J., Isolation of putative progenitor endothelial cells for angiogenesis. *Science*, 275(5302):964–966, 1997.
- [157] Yeager, M. E., Frid, M. G., and Stenmark, K. R., Progenitor cells in pulmonary vascular remodeling. *Pulm. Circ.*, 1(1):3–16, 2011.

- [158] Diller, G., Thum, T., Wilkins, M. R., and Wharton, J., Endothelial progenitor cells in pulmonary arterial hypertension. *Trends Cardiovas. Med.*, 20(1):22–29, 2010.
- [159] Firth, A. L. and Yuan, J. X. J., Identification of functional progenitor cells in the pulmonary vasculature. *Pulm. Circ.*, 2(1):84–100, 2012.
- [160] Bonder, C. S., Sun, W. Y., Matthews, T., Cassano, C., Li, X., Ramshaw, H. S., Pitson, S. M., Lopez, A. F., Coates, T. P., Proia, R. L., Vadas, M. A., and Gamble, J. R., Sphingosine kinase regulates the rate of endothelial progenitor cell differentiation. *Blood*, 113(9):2108–2117, 2009.
- [161] Penko, D., Mohanasundaram, D., Sen, S., Drogemuller, C., Mee, C., Bonder, C. S., Coates, P. T. H., and Jessup, C. F., Incorporation of endothelial progenitor cells into mosaic pseudoislets. *Islets*, 3(3):73–79, 2011.
- [162] Sen, S., McDonald, S. P., Coates, T. P., and Bonder, C. S., Endothelial progenitor cells: novel biomarker and promising cell therapy for cardiovascular disease. *Clin. Science*, 120:263–283, 2011.
- [163] Fadini, G. P., Losordo, D., and Dimmeler, S., Critical reevaluation of endothelial progenitor cell phenotypes for therapeutic and diagnostic use. *Circ. Res.*, 110(4):624–637, 2012.
- [164] Ingram, D. A., Mead, L. E., Tanaka, H., Meade, V., Fenoglio, A., Mortell, K., Pollok, K., Ferkowicz, M. J., Gilley, D., and Yoder, M. C., Identification of a novel hierarchy of endothelial progenitor cells using human peripheral and umbilical cord blood. *Blood*, 104(9):2752–2760, 2004.
- [165] Chen, B., Bo, C. J., Jia, R. P., Liu, H., Wu, R., Wu, J., Ge, Y. Z., and Teng, G. J., The renoprotective effect of bone marrow derived endothelial progenitor cell transplantation on acute ischemia-reperfusion injury in rats. *Transplantation Proceedings*, 45(5):2034–2039, 2013.

- [166] Seebach, C., Henrich, D., Schaible, A., Relja, B., Jugold, M., Bonig, H., and Marzi, I., Cell-based therapy by implanted human bone marrow derived mononuclear cells improved bone healing of large bone defects in rats. *Tissue Eng.*, 21(9-10):1565–1578, 2015.
- [167] Zhang, S., An, Q., Li, Q., Huang, J., Chen, X., Chen, X., Zhang, J., Wang, Y., Yang, G. Y., and Zhu, W., Therapeutic benefit of bone marrow derived endothelial progenitor cell transplantation after experimental aneurysm embolization with coil in rats. *PLoS ONE*, 9(2):e90069, 2014.
- [168] Foster, W. S., Suen, C. M., and Stewart, D. J., Regenerative cell and tissue-based therapies for pulmonary arterial hypertension. *Can. J. Cardiol.*, 30(11):1350–1360, 2014.
- [169] Stewart, D. J. and Mei, S. H. J., Cell-based therapies for lung vascular diseases. *Proceedings ATS*, 8(6):535–540, 2011.
- [170] Atkinson, C., Stewart, S., Upton, P. D., Machado, R. D., Thomson, J. R., Trembath, R., and Morrell, N. W., Primary pulmonary hypertension is associated with reduced pulmonary vascular expression of type II bone morphogenetic protein receptor. *Circulation*, 105(14):1672–1678, 2002.
- [171] Yang, X., Long, L., Southwood, M., Rudarakanchana, N., Upton, P. D., Jeffery, T. K., Atkinson, C., Chen, H., Trembath, R. C., and Morrell, N. W., Dysfunctional smad signaling contributes to abnormal smooth muscle cell proliferation in familial pulmonary arterial hypertension. *Circ. Res.*, 96(10):1053–1063, 2005.
- [172] Wang, Y., McKay, J. D., Rafnar, T., Wang, Z., Timofeeva, M. N., Broderick, P., Zong, X., Laplana, M., Wei, Y., Han, Y., Lloyd, A., Delahaye-Sourdeix, M., Chubb, D., Gaborieau, V., Wheeler, W., Chatterjee, N., Thorleifsson, G., Sulem, P., Liu, G., Kaaks, R., Henrion, M., Kinnersley,

- B., Vallee, M., LeCalvez-Kelm, F., Stevens, V. L., Gapstur, S. M., Chen, W. V., Zaridze, D., Szeszenia-Dabrowska, N., Lissowska, J., Rudnai, P., Fabianova, E., Mates, D., Bencko, V., Foretova, L., Janout, V., Krokan, H. E., Gabrielsen, M. E., Skorpén, F., Vatten, L., Njolstad, I., Chen, C., Goodman, G., Benhamou, S., Vooder, T., Valk, K., Nelis, M., Metspalu, A., Lener, M., Lubinski, J., Johansson, M., Vineis, P., Agudo, A., Clavel-Chapelon, F., Bueno-de Mesquita, H. B., Trichopoulos, D., Khaw, K., Johansson, M., Weiderpass, E., Tjønneland, A., Riboli, E., Lathrop, M., Scelo, G., Albanes, D., Caporaso, N. E., Ye, Y., Gu, J., Wu, X., Spitz, M. R., Dienemann, H., Rosenberger, A., Su, L., Matakidou, A., Eisen, T., Stefansson, K., Risch, A., Chanock, S. J., Christiani, D. C., Hung, R. J., Brennan, P., Landi, M. T., Houlston, R. S., and Amos, C. I., Rare variants of large effect in *brca2* and *chek2* affect risk of lung cancer. *Nat. Genet.*, 46(7):736–741, 2014.
- [173] Tsai, C. L., Tsai, C. N., Lin, C. Y., Chen, H. W., Lee, Y. S., Chao, A., Wang, T. H., Wang, H. S., and Lai, C. H., Secreted stress-induced phosphoprotein 1 activates the *alk2-smad* signaling pathways and promotes cell proliferation of ovarian cancer cells. *Cell Reports*, 2(2):283–293, 2012.
- [174] McMurtry, M. S., Moudgil, R., Hashimoto, K., Bonnet, S., Michelakis, E. D., and Archer, S. L., Overexpression of human bone morphogenetic protein receptor 2 does not ameliorate monocrotaline pulmonary arterial hypertension. *Am. J. Physiol. Lung Cell. Mol. Physiol.*, 292(4):L872–L878, 2007.
- [175] Brunetti-Pierri, N., Ng, T., Iannitti, D., Cioffi, W., Stapleton, G., Law, M., Breinholt, J., Palmer, D., Grove, N., Rice, K., Bauer, C., Finegold, M., Beaudet, A., Mullins, C., and Ng, P., Transgene expression up to 7 years in nonhuman primates following hepatic transduction with

- helper-dependent adenoviral vectors. *Hum. Gene Ther.*, 24(8):761–765, 2013.
- [176] Zhao, J., Bolton, E. M., Ormiston, M. L., Bradley, J. A., Morrell, N. W., and Lever, A. M., Late outgrowth endothelial progenitor cells engineered for improved survival and maintenance of function in transplant-related injury. *Trans. Int.*, 25(2):229–241, 2012.
- [177] Stewart, D. J. and Mei, S. H. J., Cell-based therapies for lung vascular diseases. *Proceedings ATS*, 8(6):535–540, 2011.
- [178] Deng, W., Bivalacqua, H. C., Champion, H. C., Hellstrom, W. J., Murthy, S. N., and Kadowitz, P. J., Gene therapy techniques for the delivery of endothelial nitric oxide synthase to the lung for pulmonary hypertension. *Free Radicals and Antioxidant Protocols: Methods Mol. Biol.*, 2010.
- [179] Hansmann, G., Fernandez-Gonzalez, A., Aslam, M., Vitali, S. H., Martin, T., Mitsialis, A. S., and Kourembanas, S., Mesenchymal stem cell-mediated reversal of bronchopulmonary dysplasia and associated pulmonary hypertension. *Pulm. Circ.*, 2(2):170–181, 2012.
- [180] Long, L., Ormiston, M. L., Yang, X., Southwood, M., Graf, S., Machado, R. D., Mueller, M., Kinzel, B., Yung, L. M., Wilkinson, J. M., Moore, S. D., Drake, K. M., Aldred, M. A., Yu, P. B., Upton, P. D., and Morrell, N. W., Selective enhancement of endothelial *bmpr-ii* with *bmp9* reverses pulmonary arterial hypertension. *Nat. Med.*, advance online publication, 2015.
- [181] Noiseux, N., Gnechi, M., Lopez-Illasaca, M., Zhang, L., Solomon, S. D., Deb, A., Dzau, V. J., and Pratt, R. E., Mesenchymal stem cells overexpressing akt dramatically repair infarcted myocardium and improve cardiac function despite infrequent cellular fusion or differentiation. *Mol. Ther.*, 14(6):840–850, 2006.

- [182] Quesenberry, P. J., Goldberg, L. R., Aliotta, J. M., Dooner, M. S., Pereira, M. G., Wen, S., and Camussi, G., Cellular phenotype and extracellular vesicles: Basic and clinical considerations. *Stem Cells Develop.*, 23(13):1429–1436, 2014.